Diagnostic Reference Levels for digital mammography in Australia

Mo'ayyad E. Suleiman
BSc Applied Physics
Master of Information Technology

A thesis submitted in fulfilment of the requirements for the degree of Doctor of Philosophy

Discipline of Medical Radiation Sciences

Faculty of Health Sciences

University of Sydney

June 2018

Supervisor's statement

As primary supervisor of Mo'ayyad E. Suleiman's doctoral work, I, Mark McEntee, certify that I consider his thesis "Diagnostic Reference Levels for digital mammography in Australia" suitable for examination.

……26 June 2018

Associate Professor Mark F. McEntee
Discipline of Medical Radiation Sciences
Faculty of Health Sciences
The University of Sydney
Date 26-06-2018

Candidate statement

I, Moayyad E. Suleiman, hereby declare that this dissertation is my own work. As the primary investigator, I was responsible for data collection, analysis, and interpretation of the findings. I was also responsible for the writing of the content of this dissertation. The co-authors of the publications included therein are either supervisor of the studies and/or assisted at different stages of the work as well as appraisal of the manuscript drafts. I acknowledge that this dissertation contains no material previously published or written by another person except where acknowledged. I also declare that this dissertation does not contain materials that have been accepted or under consideration for the award of another degree.

……. 26/6/2018

Moayyad E. Suleiman

Discipline of Medical Radiation Sciences

Faculty of Health Sciences

The University of Sydney

Date 26-06-2018

Abstract

Aims: The optimisation of radiation in screening mammography aims to reduce women's exposure to radiation. In three phases, this thesis explores radiation doses delivered to women undergoing screening mammography, methods used to estimate the mean glandular dose (MGD), and the use of mammographic breast density (MBD) in the calculation of MGD. Firstly, it examines Diagnostic Reference Levels (DRLs) for digital mammography in Australia as a trigger for optimisation for radiation doses delivered in screening mammography in Australia, with novel focus on whether compressed breast thickness and detector technologies should be used as a guide when determining patient derived DRLs. Secondly, it analyses the agreement between Organ Dose estimated by different digital mammography units and calculated MGD for clinical data. Thirdly, it explores a novel method of including MBD in MGD calculations, suggesting a new dose estimation called the actual glandular dose (AGD), and compares MGD to AGD.

Methods: In phase one, anonymised mammograms (52,405) were retrieved from a central database, and DICOM headers were extracted using third party software. Women with breast implants; breast thicknesses outside 20-110 mm; and images with incomplete exposure or quality assurance (QA) data where excluded. Exposure and QA information were utilised to calculate the mean glandular dose (MGD) for 45,055 mammograms from 61 units representing four manufacturers using methods by Dance et al. The median, 75th and 95th percentiles were calculated across MGDs obtained for all included data and according to compressed breast thickness (CBT) from 20 – 110 mm with 10 mm increment ranges, average CBT for the population, and for three different detector technologies. ANOVA with Tukey's post hoc was used to test the significance of the difference between MGDs for different CBT ranges. In phase two, Organ Dose values were extracted from the DICOM headers of the study population, and MGD was calculated using the methods published by Dance et al., Sobol and Wu, and Boone et al. Bland-Altman analysis and regression were used to study the agreement and correlation between Organ Dose and MGD calculated using the three methods. In phase three, LIBRA software was utilised to estimate MBD for mammograms of women screened using GE and Hologic systems. MBD values were then imported into Dance et al. method to calculate AGD for the 31,097 mammograms

(7728 women). Bland-Altman analysis and regression were used to study the agreement and correlation between MGD and AGD.

Results: In phase one, the overall median image MGD, minimum, maximum were 1.39 mGy, 0.19 mGy and 10.00 mGy respectively. The 75^{th} and 95^{th} percentiles across all units; median image MGD for 60 ± 5 mm compressed breast thickness were 2.06 mGy and 2.69 mGy respectively. Median, minimum, maximum, 75th and 95th MGD percentiles were presented for nine compressed breast thickness ranges. DRLs for NSW are suggested for the compressed breast thickness range of 60 ± 5 mm for the whole study and three detector technologies CR, DR, and photon counting to be 2.06, 2.22, 2.04, and 0.79 mGy respectively. In phase two, Bland-Altman analysis showed statistically significant bias between organ and calculated doses. The bias differed for different unit makes and models. Philips had the lowest bias overestimating Dance et al. method by 0.03 mGy. GE had the highest bias overestimating Sobol and Wu method by 0.20 mGy. Hologic Organ Dose underestimated Boone et al. method by 0.07 mGy, and Fuji Organ Dose underestimated Dance et al. method by 0.09 mGy. In phase three, both MGD and AGD showed skewed distributions with medians of 1.53 and 1.62 mGy respectively. Dance et al. method MGD underestimated dose at lower CBTs (below 80mm) compared to AGD by up to 10%.

Conclusions: This thesis has recommended DRLs for mammography in Australia and shows that MGD is dependent upon compressed breast thickness and detector technology. The work also shows wide variation in Organ Dose and dose calculation methodologies across mammography vendors. Organ doses reported by vendors vary from that calculated using established methodologies. Data produced also show that the use of MGD calculated using standardised glandularities underestimates radiation risk. Finally, AGD was proposed; it considers differences in breast composition for individualised radiation-induced risk assessment.

Executive summary

This thesis examines digital mammography dosimetry from several perspectives. The work is divided into four parts: the first part reviewed the literature on Diagnostic Reference Levels (DRLs) established around the world and the methods used to establish DRLs. The second part analysed data from BreastScreen NSW to propose DRLs for digital mammography for Australian screening services. The third part compared different dosimetry methods used for calculating Mean Glandular Dose (MGD) and tested the consistency of the Organ Dose recorded in the Digital Imaging and Communication in Medicine (DICOM) header. It also examined whether the Organ Dose in the DICOM header can be used to establish DRLs. The final study proposed a new method for calculating individualised glandular dose for better estimation of radiation-induced breast cancer risk from mammography. The proposed method involved the integration of Mammographic Breast Density (MBD) in the calculations of Actual Glandular Dose (AGD).

Acknowledgments

I would like to express my gratitude to everyone who supported me during this journey, it has been long and uneasy, for that I say thank you.

For this accomplishment, I would like to first and foremost express my deepest regards and appreciation to my primary supervisor Associate Professor Mark McEntee, whom without I would not have reached this stage. Your experience, patience and understanding have been the source of my ongoing inspiration and progress. I am forever grateful for your guidance and mentorship.

To my co-supervisor, Professor Patrick Brennan, I say thank you. Your support and constructive timely feedback are greatly appreciated. I am also appreciative of your encouragement and confidence in my skills, and the opportunity you have given me. I feel privileged to have you as a mentor.

I would also like to extend my deepest appreciation to my secondary supervisors, Dr Peter Kench and Dr Ernest Ekpo, for the time spent reviewing my work, invaluable comments, and patience. Your experience and feedback have shaped my work. Also, a special thank you to Dr Jennifer Diffey and Ms Lucy Cartwright; your experience, help and feedback at the beginning of this journey have laid down the strong base-work on which my studies stood strong.

My sincerest gratitude goes to my family; mom, for your prayers and encouragement; and my brothers for your support and understanding.

Finally, to my wife Marwa and daughters, Lilac and Cataleya I say, you are the light at the end of the tunnel, your love and patience gives me the strength to go on.

Publications and presentation

The research presented in this dissertation has been published, and/or presented in the following forms:

Peer Reviewed Journal Articles:

1. Suleiman, M., Brennan, P., McEntee, M. (2015). *Diagnostic reference levels in digital mammography: A systematic review*. Radiation Protection Dosimetry, 167(4), 608-619.
2. Suleiman, M., McEntee, M., Cartwright, L., Diffey, J., Brennan, P. (2017). *Diagnostic reference levels for digital mammography in New South Wales*. Journal of Medical Imaging and Radiation Oncology, 61(1), 48-57.
3. Suleiman, M., Brennan, P., McEntee, M. (2017). *Mean glandular dose in digital mammography: a dose calculation method comparison*. Journal of Medical Imaging, 4(1), 013502-1-013502-6.
4. Suleiman ME, Brennan PC, Ekpo E, Kench P., McEntee MF. (2018). *Integrating mammographic breast density in glandular dose calculation*. Br J Radiol. 2018 M. ay;91(1085):20180032. doi: 10.1259/bjr.20180032.

Conference Proceedings:

1. Suleiman, M. E., Brennan, P. C., McEntee, M. F. (2016). *DICOM organ dose does not accurately represent calculated dose in mammography*. Proc. SPIE 9783, Medical Imaging 2016: Physics of Medical Imaging, 97832L (22 March 2016); doi:10.1117/12.2216698

Presentations:

1. Suleiman, M. E., Brennan, P. C., McEntee, M. F. *Diagnostic reference levels in mammography: a systematic review of methods and values*. The University of Sydney higher degree research students' symposium. Sydney, Australia, 2014.
2. Suleiman, M. E., Brennan, P. C., McEntee, M. F. *DICOM organ dose does not accurately represent calculated dose in mammography*. Proc. SPIE 9783-96, Medical Imaging 2016: Physics of Medical Imaging, 97832L (22 March 2016); doi:10.1117/12.2216698.

3. Suleiman ME, Brennan PC, Kench P., Diffey J., Cartwright L., McEntee MF. *Diagnostic reference levels for digital mammography; time for a new paradigm.* EPSM O100, Sydney, Australia, 2016.
4. Suleiman ME, Brennan PC, Kench P, McEntee MF. *Radiation doses received by women attending BreastScreen NSW in 2014.* ECR B-663, Vienna, Austria, 2017.
5. Suleiman ME, Brennan PC, Kench P, McEntee MF. *Diagnostic reference levels for digital mammography in NSW.* BIG meeting Queenstown, NZ, 2017.

Table of Contents

List of tables

List of Figures

Chapter one

Background to the thesis

Breast cancer is the most common cancer in women world-wide, representing 30% of all cancers in women [1]. The 2012 worldwide breast cancer incidence rate (age-standardised per 100,000 women) was 43.1 ranging from 27 in Middle Africa and Eastern Asia to 92 in North America [2]. The 2017 Australian breast cancer expected incidence rate (age standardised per 100,000 women) was 124.2 [3], almost 44% higher than the 2012 incidence rate (86 per 100,000 women) [2]. Breast cancer is the fifth most common cause of cancer-related deaths in the developed world, accounting for 14.3% of the total deaths from cancer [2]. Breast cancer is the second most common cause of cancer death in women in developing countries accounting for 15.4% of the total deaths from cancer [2]. Nonetheless, breast cancer death rates continue to drop worldwide as the early detection of the disease has been shown to reduce mortality by 25-40% [4-6].

1.1 Breast Screening

Screening is defined as "the presumptive identification of unrecognised disease or defect by the application of tests, examinations, or other procedures which can be applied rapidly. Screening tests sort out apparently well persons who probably have a disease from those who probably do not" [7]. In theory, early detection of cancer is commonly believed to be beneficial, however in practice there is a delicate balance to be maintained between benefits and risks. Therefore, ten screening principles were defined in 1968 [8], which until now are being utilised by the World Health Organisation (WHO) as a guide in the selection of diseases that are suitable for organised population-based screening.

Organised population-based screening programs have proven to be the most effective approach for the early detection of breast cancer [5]. The success of the initial screening programs in Sweden in 1977 [9], which resulted in a 31% reduction in mortality from breast cancer [10], led to the introduction of screening programs in many other countries. Australian breast screening programs target women aged 50-74 years for biennial screening mammograms to aid the detection of unsuspected breast cancer in asymptomatic women in order to reduce mortality and morbidity from the disease [3]. Knowledge of the existence of lesions, its characteristics, and extent can help with treatment planning in the early stages of the disease, thereby increasing

survival rates [3]. However, there are still controversies about the benefits and risks of screening mammography [11-15]. The following sections provide an overview of the benefits and risks of screening mammography and a rationale for inclusion of radiation dose in the risk assessment.

1.2 Breast Screening: Benefits versus harms

Although early detection of breast cancer through screening improves the treatment outcomes for patients with the disease [3], mammography screening programs have been the focus of ongoing debate [11-15]. The benefits vs. harms of screening mammography have been examined since screening was introduced on a national level in Sweden in 1977 [9]. The evidence for the benefits offered by screening mammography [16-23] was challenged in 2000, and it was suggested that the methods utilised in the assessment of the benefit and risk were scientifically flawed [24, 25]. At the time, the International Agency for Research on Cancer (IARC) reported a 35% reduction in mortality for screening mammography participants aged 50-69 years [26]. In 2015, the IARC revisited this evidence and an analysis of all published peer reviewed literature to date revealed that mammography screening is still effective in reducing breast cancer mortality by up to 40% with a substantial reduction for women aged 70-74 [5]. Three years prior to this, an independent review was commissioned in the UK to examine the benefits and harms of breast cancer screening [27]. The review panel looked at three major results from the reviewed Randomised Controlled Trials (RCTs):

First, the relative mortality benefit, the panel found a 20% reduction in mortality from breast cancer for women offered screening compared to women not offered screening. They acknowledged three sources of uncertainties involved in this estimation, 1. the 95% confidence intervals of the relative reduction in mortality being 11-27%, 2. bias in the sources of information such as the cause of death, and 3. the applicability of the RCTs reviewed and how it relates to the new technologies in screening mammography. Nonetheless, the panel concluded that a 20% reduction in mortality was the most reasonable estimate of mortality benefit in the UK.

Second, the absolute mortality benefit, being the number of lives saved among women invited to screening. The panel found a 20-fold difference in the absolute mortality

benefit, mainly caused by age factors. Nonetheless, concluded that the absolute mortality benefit being one saved life for every 250 women invited to screening.

Third, overdiagnosis, in which its consequences were deemed important as 19% of women diagnosed during screening were subjected to cancer treatment unnecessarily, leading to psychological and quality of life effects. The panel weighed the benefits of cancer mortality reduction of 20%, against overdiagnosis (11%) and other harms affecting screened women and concluded that screening programs save lives and should continue as the benefits outweighed the harms [27].

Risks arising from mammography are two-fold: 1. radiologists' errors such as overdiagnosis, false positive, and false negative outcomes; 2. radiation induced cancer risk arising from exposing the radio-sensitive breast to X-rays [15]. Educational and technological interventions are continuously being explored to mitigate radiologist-related errors. However, although some consideration is given to the impact of radiation dose, it is frequently thought of as a comparatively insignificant risk. However, as this work will describe later, it is not insignificant, and it is critical to explore approaches to keep radiation doses to the breast as low as reasonably achievable (ALARA) whilst maintaining image quality standards. It is important though to acknowledge here that the estimates of radiation induced cancer risk are based on averages established from epidemiological studies, not on the basis of risk to the actual individual. Modern cellular biology adds a different picture to the traditional model of risk.

The risk of radiation damage is related to organ radio-sensitivity. A comparison between ICRP 60 and ICRP 103 tissues weighting factors (Table 1.1) indicates that the traditional priority given to the gonads should be shared with the breasts. Evidence demonstrates that the breast tissue is one of the most radio-sensitive tissue in the body [28]. The difference in tissue weighting factor for the breast between ICRP 60 and ICRP 103 is due to the different definition of detriment used for the calculation of tissue weighting factors. ICRP 60 calculated the detriment based on the mortality risk [29] while ICRP 103 detriment was based on the incidence risk [30]. It is evident that breast cancer incidence have increased and continue to increase [31] while mortality continues to decline [30], hence the increased priority to breast protection from ionising radiations.

Table 1.1: Tissue weighting factors in ICRP 26, 60, and 103 [28].

Organ	ICRP 26	ICRP 60	ICRP 103
Gonads	0.25	0.20	0.08
Bone marrow	0.12	0.12	0.12
Lung	0.12	0.12	0.12
Breast	0.15	0.05	0.12
Thyroid	0.03	0.05	0.04
Bone Surfaces	0.03	0.01	0.01
Remainder	**0.3**	**0.45**	0.51

The principles of radiation protection are summarised in three key words: Justification, optimisation, and dose limits [32]. However, dose limits are often replaced with Diagnostic Reference Levels (DRLs) in the area of diagnostic imaging, this is because a dose limit may affect the quality of images.

The ICRP identifies three levels of justification for the use of radiation in medical imaging. The first level, considers the use of radiation in medicine in general, in which it is accepted that the benefit outweighs the harm. The radiological procedure is the second level, where the procedure should provide necessary information about exposed individuals and improve diagnosis and treatment. In screening mammography, women with dense breasts are advised to undergo further screening using other modalities such as MRI, hence, the information facilitated by screening mammography has led to an improvement in diagnosis and treatment. Lastly, the application of the procedure should be justified on a patient level and have specific objectives to the exposure. Women who have higher risk of developing breast cancer are invited to screening mammography according to their age (50-74 years old), family history, in order to diagnose breast cancer at its early stages, hence meeting the objectives of screening mammography [33].

Optimisation does not necessarily involve the reduction of dose to the patient but relates to the optimisation of protection of patients from radiation harms. Optimisation entails the management of radiation dose to the patient to be balanced with the medical

purpose and produce a clinically optimal mammogram. Restrictions on the dose could prove harmful to the patient if the image quality does not serve the clinical needs. Optimisation processes in medical imaging are applied at the equipment design and procedural levels to ensure that the net benefit is maximised, and the dose is kept as low as reasonably achievable. In mammography, dose optimisation is achieved through many means including continuous advances in technology. For example, newer digital mammography systems use photon counting detectors that reduce patient dose and reject noise to improve image quality and thus cancer detection [34]. Furthermore, improvements in breast compression techniques reduce geometric blur in mammograms and allowing for less exposure time due to the reduction of breast thickness. Compression also produces more uniform exposure to the breast, hence eliminating over-exposure to the nipple area. DRL are discussed further in the next subsections, as it is the main theme in this thesis.

1.3 Diagnostic Reference Levels

The International Commission of Radiation Protection (ICRP) first mentioned the concept of DRLs in 1990, before expanding on it in 1996 [35]. The ICRP defines DRLs as:

> *"A form of investigation level, applied to an easily measured quantity, usually the absorbed dose in air, or tissue-equivalent material at the surface of a simple phantom or a representative patient [35]."*

DRLs are a dose auditing tool that usually provides medical physicists with the median dose received by patients for each X-ray unit. As population characteristics and facilities differ, the ICRP has recommended that DRLs be established at local, regional, and/or national levels to offer guidance for dose optimisation at each level. This is to encourage mammography centres whose median doses exceed the recommended DRLs to consider potential optimisation avenues. Thus, DRLs are not maximum penal doses that must not be exceeded; rather they are intended to provide standards for dose optimisation across facilities. DRLs have three main elements and are discussed in the following subsections.

1.3.1 **Investigation level**

The investigation level utilised for DRLs in mammography is taken as a certain percentile of the median mean glandular doses (MGDs) for each mammography unit included in the survey. The percentile value depends on the variation in median MGD between the mammography units. If a wide MGD variation exists, a rigorous percentile such as the 75^{th} is used to reduce the variation and establish DRLs. However, when there is less variation, the 90^{th} is used [36]. This is usually within well-established screening programs that are regularly monitored and assessed. Dose monitoring is performed in Australia by the Australian Radiation Protection and Nuclear Safety Agency (ARPANSA). This body recommends best practice on the use of ionizing radiation and is the primary authority on radiation protection and nuclear safety in Australia. ARPANSA collates data from individual medical imaging facilities to establish and update National DRLs (NDRLs). Australian medical imaging facilities utilise the NDRLs as a benchmark to compare their Facility Reference Levels (FRLs). ARPANSA has established NDRLs for some imaging modalities, however, NDRLs for mammography are yet to be set for Australia. Thus, there is a need to establish DRLs for mammography to facilitate dose monitoring and optimisation in Australia.

1.3.2 **Easily measured quantity:**

DRLs in mammography are established using one of two dose (or risk) descriptors recommended by the ICRP [35]: Entrance Surface Air Kerma (ESAK) or Mean Glandular Dose (MGD). ESAK describes the amount of radiation entering through the surface of the breast. It is an indicator of the amount of exposure to the surface of the breast. MGD on the other hand, estimates the dose absorbed by the glandular tissue of the breast [37]. MGD cannot be measured directly rather, it is estimated using Monte-Carlo simulations and standard assumptions that depend on breast characteristics and X-ray spectra [37]. Monte-Carlo techniques simulate the behaviour of X-rays penetrating a simple breast model to estimate the absorbed energy, and provide conversion factors that relate MGD to ESAK [37].

Monte-Carlo based MGD estimation methods support a wide range of X-ray spectra, breast thicknesses and breast glandularities [37-44]. MGD is based on a simple breast

model with homogeneous composition. The simplicity of the model contributes to errors in MGD estimation [45]. The use of heterogeneous breast compositions versus more accurate quantifications of glandular tissue results in up to 48% errors in the conversion factors [45], and up to 30% overestimation of dose [45, 46]. The high degree of error highlights the need to explore alternative and better models for MGD measurement.

The easily measured quantity described by the ICRP in 1996 was formulated to facilitate regular dose optimisation due to the lack of, or limited access to computing facilities at the time. Although technological advancement has shaped all aspects of modern life, MGD measurement has not evolved. In particular, the effect of glandular tissue in the breast on the screening process, as it is directly associated with the absorbed dose. Currently, only the model proposed by Dance et al. provides glandularity estimates that are related to age and compressed breast thickness (CBT). Even the use of age and CBT to define glandularity has limitations: first women of the same age and CBTs may have different glandularities; secondly, women of different ages may have similar CBTs or glandularities. Thus, if accurate measures of risk are to be established it is important that actual measures of glandularity be used for MGD measurement. Evidence shows that an "easily measured quantity" is a laudable concept, but the ease of measurement changes with time. Keeping the method constant is a flawed concept. In this work I emphasise the need to explore accurate methods made available through technological innovation. A description of MGD calculation methods and their limitations is detailed in chapter two. A newly developed MGD method that accounts for actual glandularity is also discussed in chapter five.

1.3.3 **Standard patient**

There are no standard patients. When it comes to a representative breast, this has been defined differently around the world with breast thickness and composition as the main criteria [47]. Researchers have used either the average breast thickness of the population [48], a set of breast thickness based on the quality assurance protocol followed [49] or the thicknesses that allow for a comparison with other established DRLs [50]. This raises the question of how truly representative and consistent a

definition might be given the diversity of women in the screening mammography population.

For the establishment of DRLs in other modalities such CT, Radiography, and Fluoroscopy, patients are grouped according to weight, and dose differences across weights have been reported. In paediatric radiography, patients are stratified by age or weight, whereas in mammography, DRLs are established for one standard CBT and glandularity [35]. This I argue, is a mistake.

MGD increases with CBT [51], however MGD is directly proportional to CBT in that one CBT cannot possibly represent an entire population, and breasts having similar CBT demonstrating differences in glandularities, the major determinant of radiation-induced risk [52]. The effect of CBT on DRLs is discussed further in chapter three. In addition, there is a direct relationship between the glandular component of the breast (breast density) and absorbed radiation dose, with breast density influenced by many confounding factors such as age, reproductive history, hormonal factors, and body mass index [53]. Furthermore, area-based and volumetric measures show that a significant proportion of the population demonstrates less than 50% glandularity [52, 54]. These limitations suggest that the assumptions made in MGD calculation models that the average glandularity is 50% are inaccurate. Therefore, if accurate measures of risk are to be established a solution that accounts for differences in breast composition is required.

1.4 Establishing mammography DRLs

Dose surveys are used to establish DRLs locally, regionally or nationally, and the ICRP recommends the use of patients or phantoms to establish DRLs [35]. The latest ICRP recommendations suggest that a random collection of medium to large sized centre be included in the dose survey. Such recommendation is to facilitate the collection of a random minimum sample of 50 standard size patients per mammography unit [35]. Patient surveys (compared to phantom surveys) are a closer representation of the actual population of women and provide a more accurate reflection of the status of absorbed dose in screening mammography and the factors affecting it [35].

Phantom surveys on the other hand, are good indicators of mammography unit status and can be used for quick dose surveys. They have the advantage of less variability, with fewer measurements needed to calculate the absorbed dose [54]. To establish the MGD for a mammography unit a certain standard size phantom is used across all units. Once the median MGD has been established for each unit surveyed (whether it is phantom, or patient based), the 75th percentile of all units median MGDs is determined. This 75th percentile serves as the DRL value as recommended by the ICRP [35]. A less stringent value (95th percentile) maybe used when minimum variation is found between mammography units as stated earlier. Advances in dose-saving technology, such as photon counting detectors, and image processing algorithms, such as contrast enhancement algorithms, have influenced dose values [34, 55]. Therefore, DRLs values are not static, leading to recommendations by the ICRP for regular update every three to five years to ensure that dose reduction is consistent with advances in technology.

1.5 Thesis aims:

The following subsections detail the aims of this study shown as they appear in each chapter, together with a short rationale for each aim.

1.5.1 Chapter one and two

To review the literature associated with DRLs in mammography.

1.5.2 Chapter three

- ***To recommend DRLs for digital mammography in Australia***

DRLs have been established for mammography in many countries; however, no DRLs exist for optimisation of mammography in Australia. A phantom DRLs study was published in 2011 [56], however since phantom studies are not very representative of the population, the outcome of this phantom study was not adopted as national DRLs. No work has established DRLs for mammography using patient data in Australia yet.

Our published study, presented in chapter three, should provide a proposal for DRLs for mammography dose optimisation in Australia using a large sample of patients from BreastScreen NSW, which can be used as a representative sample of Australian women.

- ***To explore whether DRLs should be stratified by compressed breast thickness.***

CBT has been used as the key element in selecting conversion factors required for the estimation of MGD within the three main calculation methods (Dance et al., Wu et al. and Boone) [36-43], as it has been shown that MGD is dependent upon CBT. While the standard size breast is acceptable for establishing DRLs, it does not reflect the status of the whole population, especially when thicker breasts require different X-ray spectra to produce a good quality image. Therefore, the use of one standard CBT for establishing DRLs may not provide optimum results for a given mammography unit. Chapter three explores the stratification of DRLs according to CBT.

- ***To explore the effect of different detector technologies on the effectiveness of DRLs and whether DRLs should be stratified by detector technology.***

Dose levels are influenced by exposure parameters and detector technology. As the use of new detector technologies in mammography such as the photon-counting detectors in Phillips mammography units has proven to require the lowest MGD to produce an effective mammogram [57]. To generate DRLs, it is critically important to account for the effect of these technological factors on dose in order to establish DRLs that are representative of current detector technology. Further to this, I examined the impact of detector technology on DRLs and whether DRLs should be stratified by detector technology in chapter three.

1.5.3 **Chapter four**

- ***To verify the consistency of Organ Dose provided by different mammography vendors.***

The use of DRLs as an optimisation tool becomes more effective when it is easily measured. Given variability in screened population and technologies utilised for

screening, the stratification of DRLs according to breast thickness and detector technologies may complicate this process.

Organ Dose is a readily available value stored within the digital mammogram DICOM header. As such, the use of Organ Dose will substantially reduce the complexity of establishing DRLs. However, Organ Dose is estimated differently among different vendors, such variation, may reduce the applicability of DRLs in accordance with radiation risk estimations. Hence, there is a need to verify the consistency of Organ Dose calculation before it is applied to DRLs. In chapter four, I tested the consistency of the Organ Dose, and compared it to MGD calculated using three other calculation methods utilised by the vendors, namely: GE medical systems utilise Wu et al. method [42], Phillips (Sectra) and Fujifilm systems utilise Dance et al. method [36, 39, 40], while Hologic systems utilise a method by Boone et al. [37, 38, 58].

1.5.4 **Chapter five**

- ***To propose the use of Mammographic Breast Density (MBD) in the calculation of Actual Glandular Dose (AGD).***

The estimation of MGD has been built upon simple phantom models and such models assume a homogenous composition of 50% glandularity within the breast [36-43, 58]. Nonetheless, all calculation methods highlight the need for a better model for the breast. It has been established that the average breast glandularity within the female population is almost half the suggested glandularity of the simple 50:50 phantom model [51]. The integration of an individualised breast density measure within the dose estimation methods can be achieved as new technologies provide automated tools to assess MBD (the representation of glandularity on a mammogram) from mammograms in raw or post processed formats. In chapter five, I presented a new method integrating MBD in the calculation of MGD, providing an individualised dose descriptor I call "Actual Glandular Dose" (AGD) to facilitate accurate radiation-induced risk assessment.

1.6 Thesis structure

This thesis is with publications, structured around the published work.

- Chapter one introduces the topic and briefly describes issues in the literature on DRLs that require consideration.
- Chapter two provides a detailed review of mammography and dosimetry and systematic review of the literature on DRLs.
- In chapter three, DRLs were established for BreastScreen NSW services, and a new method to stratifying DRLs according to CBT and detector technologies introduced.
- In chapter four, the accuracy and consistency of Organ Dose was evaluated and compared to other MGD calculation methods to test whether Organ Dose can be used to establish DRLs.
- Chapter five introduces a new method for integrating MBD in the calculation of AGD, comparing MGD with AGD. It also examines the effect of MBD on glandular dose estimation.
- Finally, chapter six provides a holistic discussion integrating results from all original studies within the thesis. It also summarises the outcomes of the works and provides a conclusion on the dosimetry and optimisation methods used in mammography.

1.7 References

1. Tabar, L., et al., Swedish two-county trial: impact of mammographic screening on breast cancer mortality during 3 decades. Radiology, 2011. 260(3): p. 658-63.
2. Globocan. 2016 2016 [cited 2016 31 May]; Available from: http://globocan.iarc.fr/Pages/fact_sheets_population.aspx.
3. AIHW, Cancer in Australia 2017. Cancer series no.101.Cat. no. CAN 100. 2017, AIHW Canberra.
4. Glasziou, P. and N. Houssami, The evidence base for breast cancer screening. Prev Med, 2011. 53(3): p. 100-2.
5. Lauby-Secretan, B., et al., Breast-cancer screening—viewpoint of the IARC Working Group. New England Journal of Medicine, 2015. 372(24): p. 2353-2358.
6. Njor, S., et al., Breast cancer mortality in mammographic screening in Europe: a review of incidence-based mortality studies. J Med Screen, 2012. 19 Suppl 1: p. 33-41.
7. Illness, C.o.C., Preventive Aspects of Chronic Disease: Conference Proceedings, March 12-14, 1951, Chicago, Illinois. 1952: Health Publications Institute.
8. Wilson, J.M.G. and G. Jungner, Principles and practice of screening for disease, ed. W.H. Organization. 1968: World Health Organisation, Geneva, Switzerland.
9. Tabar, L. and A. Gad, Screening for breast cancer: the Swedish trial. Radiology, 1981. 138(1): p. 219-22.
10. Tabár, L., et al., REDUCTION IN MORTALITY FROM BREAST CANCER AFTER MASS SCREENING WITH MAMMOGRAPHY: Randomised Trial from the Breast Cancer Screening Working Group of the Swedish National Board of Health and Welfare. The Lancet, 1985. 325(8433): p. 829-832.
11. Berry, D., Breast cancer screening: Controversy of impact. Breast (Edinburgh, Scotland), 2013. 22(0 2): p. S73-S76.
12. Løberg, M., et al., Benefits and harms of mammography screening. Breast Cancer Research : BCR, 2015. 17(1): p. 63.
13. Otto, P.M. and C.B. Blecher, Controversies surrounding screening mammography. Mo Med, 2014. 111(5): p. 439-43.
14. Heyes, G.J., A.J. Mill, and M.W. Charles, Mammography - Oncogenecity at low doses. Journal of Radiological Protection, 2009. 29(2): p. A123-A132.
15. Yaffe, M.J. and J.G. Mainprize, Risk of radiation-induced breast cancer from mammographic screening. Radiology, 2011. 258(1): p. 98-105.
16. Chu, K.C., C.R. Smart, and R.E. Tarone, Analysis of breast cancer mortality and stage distribution by age for the health insurance plan clinical trial. Journal of the National Cancer Institute, 1988. 80(14): p. 1125-1132.

17. Miller, A.B., et al., Canadian National Breast Screening Study: 2. Breast cancer detection and death rates among women aged 50 to 59 years. CMAJ, 1992. 147(10): p. 1477-1488.

18. Miller, A.B., et al., Canadian National Breast Screening Study: 1. Breast cancer detection and death rates among women aged 40 to 49 years. CMAJ, 1992. 147(10): p. 1459-1476.

19. Bjurstam, N., et al., The Gothenburg breast screening trial: First results on mortality, incidence, and mode of detection for women ages 39-49 years at randomization. Cancer, 1997. 80(11): p. 2091-2099.

20. Frisell, J., et al., Followup after 11 years - Update of mortality results in the Stockholm mammographic screening trial. Breast Cancer Research and Treatment, 1997. 45(3): p. 263-270.

21. Tabar, L., et al., Efficacy of breast cancer screening by age. New results swedish two-county trial. Cancer, 1995. 75(10): p. 2507-2517.

22. Andersson, I., et al., Mammographic screening and mortality from breast cancer: The Malmo mammographic screening trial. British Medical Journal, 1988. 297(6654): p. 943-948.

23. Alexander, F.E., et al., 14 years of follow-up from the Edinburgh randomised trial of breast-cancer screening. Lancet, 1999. 353(9168): p. 1903-1908.

24. Olsen, O. and P.C. Gotzsche, Cochrane review on screening for breast cancer with mammography. Lancet, 2001. 358(9290): p. 1340-2.

25. Gøtzsche, P.C. and O. Olsen, Is screening for breast cancer with mammography justifiable? The Lancet, 2000. 355(9198): p. 129-134.

26. IARC, IARC handbooks of cancer prevention. Vol. 10. 2005: IARC.

27. Marmot, M.G., et al., The benefits and harms of breast cancer screening: an independent review: A report jointly commissioned by Cancer Research UK and the Department of Health (England) October 2012. British Journal of Cancer, 2013. 108(11): p. 2205-2240.

28. Obed, R.I., G.I. Ogbole, and S.B. Majolagbe, Comparison of the ICRP 60 and ICRP 103 Recommendations on the Determination of the Effective Dose from Abdominopelvic Computed Tomography. International Journal of Medical Physics, Clinical Engineering and Radiation Oncology, 2015. 4(02): p. 172.

29. Hamada, N. and Y. Fujimichi, Classification of radiation effects for dose limitation purposes: history, current situation and future prospects. Journal of Radiation Research, 2014. 55(4): p. 629-640.

30. Valentin, J., The 2007 recommendations of the international commission on radiological protection. 2007: Elsevier Oxford.

31. Torre, L.A., et al., Global Cancer Incidence and Mortality Rates and Trends—An Update. Cancer Epidemiology Biomarkers & Prevention, 2016. 25(1): p. 16-27.

32. ICRP, The 2007 Recommendations of the International Commission on Radiological Protection,ICRP publication 103. Ann. ICRP, 2007. 37(2.4): p. 1-332.

33. Malone, J., et al., Justification of diagnostic medical exposures: some practical issues. Report of an International Atomic Energy Agency Consultation. The British Journal of Radiology, 2012. 85(1013): p. 523-538.

34. Weigel, S., et al., Digital Mammography Screening with Photon-counting Technique: Can a High Diagnostic Performance Be Realized at Low Mean Glandular Dose? Radiology, 2014. 271(2): p. 345-355.

35. Vañó, E., et al., ICRP Publication 135: Diagnostic Reference Levels in Medical Imaging. Annals of the ICRP, 2017. 46(1): p. 1-144.

36. Seeram, E. and P.C. Brennan, Diagnostic reference levels in radiology. Radiologic Technology, 2006. 77(5): p. 373-384.

37. Dance, D., Monte-Carlo calculation of conversion factors for the estimation of mean glandular breast dose. Physics in mediine and biology, 1990. 35(9): p. 1211.

38. Boone, J.M., Glandular breast dose for monoenergetic and high-energy X-ray beams: Monte Carlo assessment. Radiology, 1999. 213(1): p. 23-37.

39. Boone, J.M., Normalized glandular dose (DgN) coefficients for arbitrary X-ray spectra in mammography: computer-fit values of Monte Carlo derived data. Med Phys, 2002. 29(5): p. 869-75.

40. Dance, D.R., et al., Additional factors for the estimation of mean glandular breast dose using the UK mammography dosimetry protocol. Physics in Medicine and Biology, 2000. 45(11): p. 3225-3240.

41. Dance, D.R., K.C. Young, and R.E. van Engen, Further factors for the estimation of mean glandular dose using the United Kingdom, European and IAEA breast dosimetry protocols. Phys Med Biol, 2009. 54(14): p. 4361-72.

42. Sobol, W.T. and X. Wu, Parametrization of mammography normalized average glandular dose tables. Med Phys, 1997. 24(4): p. 547-54.

43. Wu, X., G.T. Barnes, and D.M. Tucker, Spectral dependence of glandular tissue dose in screen-film mammography. Radiology, 1991. 179(1): p. 143-148.

44. Wu, X., et al., Normalized average glandular dose in molybdenum target-rhodium filter and rhodium target-rhodium filter mammography. Radiology, 1994. 193(1): p. 83-89.

45. Dance, D.R., et al., Breast dosimetry using high-resolution voxel phantoms. Radiation Protection Dosimetry, 2005. 114(1-3): p. 359-363.

46. Hernandez, A.M., J.A. Seibert, and J.M. Boone, Breast dose in mammography is about 30% lower when realistic heterogeneous glandular distributions are considered. Med Phys, 2015. 42(11): p. 6337-48.

47. Suleiman, M.E., P.C. Brennan, and M.F. McEntee, Diagnostic reference levels in digital mammography: A systematic review. Radiat Prot Dosimetry, 2014: p. ncu365.

48. Asada, Y., et al., Results of a 2011 national questionnaire for investigation of mean glandular dose from mammography in Japan. Journal of radiological protection : official journal of the Society for Radiological Protection, 2014. 34(1): p. 125-132.

49. Young, K.C., A. Burch, and J.M. Oduko, Radiation doses received in the UK Breast Screening Programme in 2001 and 2002. British Journal of Radiology, 2005. 78(927): p. 207-218.

50. O'Leary, D. and L. Rainford, A comparison of mean glandular dose diagnostic reference levels within the all-digital Irish National Breast Screening Programme and the Irish Symptomatic Breast Services. Radiat Prot Dosimetry, 2013. 153(3): p. 300-8.

51. Young, K.C. and J.M. Oduko, Radiation doses received in the United Kingdom breast screening programme in 2010 to 2012. The British Journal of Radiology, 2016. 89(1058): p. 20150831.

52. Yaffe, M.J., et al., The myth of the 50-50 breast. Medical Physics, 2009. 36(12): p. 5437-5443.

53. Ekpo, E.U., et al., Relationship Between Breast Density and Selective Estrogen-Receptor Modulators, Aromatase Inhibitors, Physical Activity, and Diet: A Systematic Review. Integr Cancer Ther, 2016. 15(2): p. 127-44.

54. Suleiman, M.E., et al., Integrating mammographic breast density in glandular dose calculation. Br J Radiol, 2018: p. 20180032.

55. Tang, J., X. Liu, and Q. Sun, A Direct Image Contrast Enhancement Algorithm in the Wavelet Domain for Screening Mammograms. IEEE Journal of Selected Topics in Signal Processing, 2009. 3(1): p. 74-80.

56. Thiele DL, Irvine M, Want D, Bernardo M (2011) Diagnostic reference levels for mammography in BreastScreen Queensland. Australas Phys Eng Sci Med 34 (3):415-418. doi:10.1007/s13246-011-0078-0

57. McCullagh, J.B., P. Baldelli, and N. Phelan, Clinical dose performance of full field digital mammography in a breast screening programme. Br J Radiol, 2011. 84(1007): p. 1027-33.

58. Boone, J.M., T.R. Fewell, and R.J. Jennings, Molybdenum, rhodium, and tungsten anode spectral models using interpolating polynomials with application to mammography. Med Phys, 1997. 24(12): p. 1863-74.

Chapter two

Introduction

Section 2.6 of this chapter has been published as:

Suleiman, M. E., Brennan, P. C., & McEntee, M. F. (2015). ***Diagnostic reference levels in digital mammography: a systematic review.*** **Radiation Protection Dosimetry, 167(4), 608-619. doi:10.1093/rpd/ncu365**

[Published copy is available in Appendix 7.1]

I had had substantial contribution to this work. I designed the study, collected and analysed the data, was the primary author, wrote and edited each draft of the manuscript.

The following sections present background information on mammography relevant to the aims of the thesis. A brief history of breast cancer screening and the development of mammography is presented. Methods employed for mammographic dosimetry are discussed, with focus on the evolution of measurement and the rationales behind using different dose and risk estimates in mammography. The chapter also explores breast composition and the effect of glandularity on dosimetry as well as radiation-induced risk of cancer. Approaches to radiation risk management are introduced, and a detailed exposition of the literature on DRLs for mammography established around the world is presented.

2.1 Development of mammography

Since their discovery in 1895 X-rays have given scientists a robust tool for the examination of the human body. In 1913, Albert Salomon first explored the use of X-ray to visualise breast tumours [1]. Thereafter, many scientists and researchers attempted breast radiography as a diagnostic method to breast pathologies [2-5]. In the 1950s, Gershen-Cohen et al. were able to demonstrate palpable tumours on roentgenograms and described asymptomatic lesions, suggesting the possibility of the early breast cancer detection with X-rays [6]. Later, Raul Leborgne became the first to report a significant association between radiographically detectable microcalcifications and breast carcinoma. These discoveries set the stage for diagnostic and screening mammography [7]. However, despite these discoveries, it was only in the late 1950s that a specific method for the examination of the breast was refined, when Robert L. Egan demonstrated the use of high milli-amperage, low-voltage coupled with an industrial film and a fine-grain intensifying screen to provide clearer images [8]. A reproducibility study that aimed to test mammography as a diagnostic aid using Egan's method, showed a 79% true-positive rate for the detection of lesions. The study confirmed the usefulness of mammography as a diagnostic tool given that radiologists had the time to learn Egan's technique and become familiar with it [9]. In the 1960s, many large-scale clinical trials that demonstrated the efficacy of mammography for breast examinations as a diagnostic tool were published [10-14]. Mammography gained momentum afterwards as a screening tool and the most effective method for the early detection of breast cancer [15, 16].

Significant advances were seen in mammography in the 1960s and 1970s, with the use of xeromammography units, however, the first dedicated breast imaging X-ray units were introduced in 1965 [17]. Film screen mammography methods were refined in the 1970s, producing sharper images with fast processing times. However, the conical shape of the breast meant that the narrow end would be overexposed to produce clinically optimised image of the thick back of the breast. The introduction of uniform breast compression helped overcome many issues related to breast imaging using film screen mammography; breast compression moves the breast away from the chest wall allowing all the breast tissue to be imaged and produce more uniform thickness that allowed for more uniform exposure. Also, breast compression reduced blur due to reduced geometrical unsharpness, and less breast motion [18]. Thinner breast and reduced motion allowed for less exposure time, consequently, resulting in a significant reduction of radiation dose [19].

Earlier mammographic systems produced radiographic images on films, which were time consuming and inefficient for storage and particularly archiving [20]. Film certainly had advantages particularly with excellent spatial resolution characteristics, however, data management was a huge constraint. In 1973, George Luckey a research scientist at Kodak filed a patent entitled 'apparatus and method for producing images corresponding to patterns of high energy radiation' [21]. The idea was to use phosphor or thermo-luminescent material to store radiation image information on the phosphoric plate, which can then be scanned by another source of radiation, emitting the initial image information as a third type of radiation. The latter can be converted to electrical energy and digitised to form an image [21]. Luckey's patent was approved in 1975; consequently, many companies followed Luckey's invention opening the way for many patents referencing his original work leading to the first commercial computed radiography (CR) system being released by Fuji (AC-1) in 1983. The turn of the century showed revolutionary technological advancements driven by the world's insatiable demand for computerised systems and connectivity through the World Wide Web. This was reflected on mammography by the introduction the FCR 5000M CR system specifically for mammography and of Full Field Digital Mammography (FFDM) that was approved first by the Food and Drug Administration (FDA) in 2000. Digital systems (digital radiography [DR] and CR) use flat panel or photon counting detectors to capture X-rays and digitise the image so that it can be read directly on a

computer. The difference between DR and CR is the signal conversion method, being more direct for DR, or more indirect (for CR) [22].

Today the three technologies: Screen Film Mammography (SFM), CR and DR coexist around the world, however, many countries are in the processes of transitioning into DR systems. SFM is a limited technology; once films are processed, the image contrast cannot be enhanced or adjusted. Furthermore, films are expensive, labour intensive, use harmful chemicals for processing, can be easily lost or accidentally misfiled. They are not compatible with the Picture Archiving and Communication Systems (PACS) unless scanned by a digitiser [23]. DR systems on the other hand, are PACS compatible allowing for better management of images and dose reduction researchers have demonstrated up to 40% dose reduction for DR when compared to SFM [24-26]. Furthermore, the ACR Imaging Network Digital Mammography Imaging Screening Trial (ACRIN DMIST) found an average 22% dose reduction for DR systems compared to SFM, albeit, this was dependent on the digital detector design, as it was also found that Hologic Selenia systems had 18% higher dose than SFM systems. The higher dose was attributed to the AEC setting on the system (allowing more manual exposure settings) and the use of molybdenum anode/filter combination (Mo/Mo), which produced softer, lower energy, beam quality, resulting in a higher absorbed dose but better subjective contrast. Nonetheless, the ACRIN DMIST concluded that DR produces doses that are comparable or less than SFM systems on average [27]. Furthermore, the ACRIN DMIST trial concluded that the overall diagnostic accuracy of digital and film mammography was similar for breast screening, however, digital mammography producing more accurate results for women under the age of 50 years, women with radiographically dense breasts, and premenopausal or perimenopausal women.

2.2 Screening mammography

The first breast cancer screening trial was conducted between 1963-1966 by Strax and Shapiro [11]. This trial referred to as the Health Insurance Plan of New York randomised study (HIP) showed a reduction in breast cancer mortality rate by up to 30% for women aged 50-64 years, however this evidence was inconclusive for women

aged 40-49 years [28, 29]. A second randomised controlled trial was conducted in 1977 in two counties in Sweden to assess the impact of screening mammography on mortality rates among women aged 40 years or more [30]. The results of this trial agreed with the HIP results, showing a 30% reduction in mortality rate from breast cancer in women aged 50-74 years, with no benefit seen for women under 50 due to the higher density and resulting reduced sensitivity [31].

As a result of the evidence provided by the screening trials, many countries started to establish national breast screening programs. The European Council (EC) recommended mammography screening pilot programs to its states in 1986 [32]. The UK, Sweden and the Netherlands had already decided to establish national screening programs, the pilot programs were established in Belgium, Denmark, France, Greece, Ireland, Luxemburg, Portugal, and Spain [33]. By 1995, the Australian breast screening program was introduced; all states tribes and territories in the United States of America were included in the National Breast and Cervical Cancer Early Detection Program (NBCCEDP) [34, 35]. However, less developed countries did not adopt national screening programs at that period. High cost, cultural beliefs, and traditional medicines among other factors were the reasons for delaying the development of national screening programs.

The transition to digital mammography was not embraced directly due to the high initial setup costs and the new processes associated with it. Subsequently, comparisons between film-screen and digital mammography began, with the most well-known being the ACRIN DMIST [36]. The DMIST was a multi-institutional study run by ACRIN comparing analogue to digital mammography at 33 screening sites in the United Stated and Canada. The DMIST resulted in a similar overall diagnostic accuracy for screening for breast cancer, however, digital mammography proved more accurate for women under 50 years, premenopausal women, and women with heterogeneously dense or extremely dense breasts [37]. Furthermore, subgroup analysis revealed a less accurate diagnostic sensitivity in digital mammography for older women with fatty breasts [38]. Nonetheless, current advances in mammography have overcome this weakness. The transition to digital mammography revealed more benefits to screening programs such as integrated medical systems, better management of images, and lower radiation dose [23].

Radiation dose from mammography contributes to a relatively small percentage of the lifetime accumulated dose from all radiation sources including medical imaging. However, the fact that breast tissue is considered to be amongst the most sensitive to radiations in the body [39] highlights the need to further explore the risk of carcinogenesis from repeated bilateral multi-view mammography on the breast and other body parts. Most models exploring risk vs. benefits of screening mammography fail to account for the risk from radiation exposure [40, 41]. However, a recent study estimating the effective lifetime radiation risk from screening mammography to the breast and other body parts have concluded that lifetime risk should be considered as a performance indicator for mammography screening programs [42]. To better establish the risk from radiation exposure in mammography, accurate estimation of dose absorbed by the breast is required.

2.3 Dosimetry in mammography

Radiation dosimetry is the quantitative assessment of the energy absorbed in a medium due to interactions with ionizing radiation. The early days of mammography revealed complexity in the determination of the energy absorbed by the breast and the associated risk. Early dosimetry instigations measured air exposure at the position of the entrance surface of the breast as a risk descriptor [43, 44]. In 1976, a US survey revealed wide variations in the entrance surface exposure values to a medium size breast [45]. Also, the relationship between entrance surface exposure and absorbed dose to the tissue at risk had to be established before accurate risk estimations can be made [46]. Hence, a more reliable value of the absorbed energy was needed to quantify the radiation risk in mammography.

Other risk-related measures of dose were explored in the 1970s, and mid-breast dose was adopted as a descriptor of risk [46-48]. Breslow et al. estimated mid-breast dose to be 20% of the skin dose, which was estimated to be 20 mGy for a two-view mammogram [47]. However, mid-breast dose did not take into account the distribution of tissue within the breast. Another risk-related measure was the total energy absorbed in the breast [49], and this estimation assumed all tissue in the breast to have equal risk from radiation. It was not until 1976, that Karlsson suggested dose be estimated to the glandular tissue of the breast because it is most sensitive to radiation [50]. This

conclusion is reasonable and generally supported as the fibroglandular tissue of the breast contains high concentrations of epithelial cells lining the milk ducts of the mammary glands. Epithelial cells are susceptible to radiation because they pass through the mitotic phases more frequently and have a high risk of developing radiation induced cancer [51]. The glandular dose cannot be measured directly on patients or equivalent material; however, incident air kerma (IAK) is an exposure measure that can be gauged directly at the surface of the irradiated object. Hence, conversion factors have been measured [46, 52] or estimated using Monte-Carlo techniques [53-56] to relate glandular dose to IAK. Monte-Carlo techniques simulate radiation interactions with breast tissues to estimate conversion factors that relate IAK to the glandular dose, which are dependent upon breast thickness, breast density and X-ray beam quality [54].

Many scientists have proposed methods of estimating radiation-induced risk to the breast. The following subsections discuss these methods in detail and their shortfalls. The rationale for exploring a more accurate estimation of dose absorbed by the breast in mammography is also provided.

2.3.1 **Hammerstein et al., 1979**

Due to the uncertainties in the estimates relating exposure to depth dose, Hammerstein et al. proposed a simplified model for the breast to study the mid-breast dose and the total energy absorbed in the breast. The breast model consisted of three phantoms made from material (used as tissue substitute) to imitate the radiation interaction properties of water, adipose, and 50% water- 50% adipose. Each phantom consisted of six 10 mm thick D shape disks. Each disk consisted of homogeneous sections of tissue substitutes and cavities at different depths to insert the Thermo-luminescent dosimeters (TLDs) to study exposure as a function of depth. The authors concluded that none of the above-mentioned dose descriptors were appropriate to reflect carcinogenic risk from mammographic radiation. Mid-breast dose did not account for the distribution of tissue (glandular tissue) in the breast at high risk, and the total energy absorbed by the breast over-estimated the risk. All tissue types were included when only the glandular tissue is considered at high risk of developing radiation induced cancer. Consequently, Hammerstein et al. introduced the “average breast”

glandular dose, which describes the energy absorbed by the glandular tissue of an average breast (6 cm thick with a uniform 50% glandular and 50% adipose composition). The "average breast" glandular dose represented a possible comparison tool between different imaging systems, however, to be considered as a risk measure a detailed individualised analysis of glandular compositions should be integrated to the calculation method [46].

Hammerstein et al. presented a method to estimate the "average breast" glandular dose for four radiation qualities, three of which were W/Al with different filter thicknesses and the last was Mo/Mo with 0.03mm filter thickness. Work was needed to cover more radiation qualities that were used in film and film-screen mammography. David Dance's work in 1980 presented results for a series of monoenergetic beams that can be integrated over any desired X-ray spectrum [53]. This is discussed in the next subsection.

2.3.2 **Dance, 1980**

In 1980, Dance estimated the absorbed dose within the breast using a similar breast model to that of Hammerstein et al. [46]. However, Dance estimated the absorbed dose within the breast in xeromammography using Monte-Carlo technique, developed to simulate the interactions of radiations with breast tissues. Furthermore, Dance presented results of absorbed dose as a function of breast thickness (2, 4, 6 and 8 cm), and beam quality (HVL). Data were also presented for absorbed dose within the glandular tissue of the breast [53]. Dance also reported that the use of Aluminium filters to reduce the dose to the breast did not affect the clinical quality of the mammograms.

Breast composition varies across women, and glandular dose is related to the amount of glandular tissue in the breast. Dance's work is limited in that it estimated the "average breast" glandular dose to one breast composition. Thus, further work accounting for the differences in breast composition was required to provide more accurate dose estimates. Stanton et al. acknowledged the need for a simple model to estimate the dose to the breast, however they stated that the use of such model was to be for the purposes of comparing mammography techniques only and not to be used for risk analysis purposes. Stanton et al., presented factors for extrapolating dose from

the simple model to other breast compositions [52]. The Stanton et al. work is discussed next.

2.3.3 **Stanton et al., 1984**

Stanton et al. developed a phantom based on the "average breast" glandular dose proposed by Hammerstein et al. [46]. This phantom was made of synthetic material to match the linear attenuation coefficient of a 50% glandular-50% adipose breast composition (BR12). The phantom was semi-circular in shape with a 150 mm diameter. Using experimental data and data from Hammerstein et al. [46], the authors developed working curves to estimate the average glandular and whole breast dose ($\overline{D_g}$ and $\overline{D}$) per view in mammography. $\overline{D_g}$ and $\overline{D}$ values could be derived from the working curves using HVL and breast thickness for different mammography techniques using the following equations:

$$\overline{D} = \overline{D_N}.X_a \quad (1.1)$$

$$\overline{D_g} = \overline{D_{gN}}.X_a \quad (1.2)$$

Where $\overline{D_{gN}}$ and $\overline{D_N}$ are the average dose per view to the whole breast and the average glandular dose per view normalised to unit incident exposure in air, respectively. X_a is the incident exposure in air.

The authors also studied the variation of average glandular dose for compositions other than the reference BR12 composition and computed conversion factors for different breast compositions. Finally, the authors suggested the average glandular dose as the preferred index of radiation risk in mammography [52]. Thereafter, in 1987 the International Commission of Radiological Protection (ICRP) recommended the use of the Average or Mean Glandular Dose (MGD) as the determinant of radiation risk in mammography [57].

2.3.4 **Rosenstein et al., 1985**

In 1985, Rosenstein et al. [55] used Monte-Carlo techniques and working curves, developed by Stanton et al. [52], to develop a handbook of conversion factors. Rosenstein's handbook facilitated the calculation of the glandular dose to the breast

for a variety of imaging scenarios (equations 1.1 and 1.2), depending on beam quality (HVL, 0.2-2.4 mm Al), breast thickness (3-8 cm), breast view (Craniocaudal or Mediolateral) breast compression (firm or moderate), target material (Molybdenum, Molybdenum-Tungsten alloy, and Tungsten), and glandular tissue content (5%, 25%, 50%, 75%, and 100%).

Although adopted by the National Council on Radiation Protection (NCRP) [58], Stanton working curves did not cover a wide range of breast thicknesses; it was missing data for 3, 7, and 8 cm CBTs. Furthermore, the Stanton et al. data was based on depth dose estimation and did not account for lateral variation of dose within the breast. The Rosenstein et al. glandular dose conversion factors however, were versatile and covered more imaging scenarios and breast sizes than Stanton et al. Nonetheless, they were lacking data on different breast thicknesses with firm compression [54]. This gap led to the development of conversion factors for the estimation of MGD by Wu et al. [56, 59, 60], Boone [61-63] and Dance et al. in 1990 [54, 64, 65]; these methods are explained in the next subsections.

2.3.5 **Wu et al., 1991-1997**

Wu et al. used a different simulation model to that utilised by Dance et al. [54]. The phantom was similar to the FDA phantom (semi-elliptical, homogeneous composition enclosed with a 4 mm skin layer), one anode/filter combination (Mo/Mo), and tabulated depending on tube potential (kVp), HVL and breast thickness for 0%, 50% and 100% glandularity initially. Wu's model used the normalised average glandular dose (D_{gN}) the average glandular dose per unit entrance surface air kerma. This is different to that of Dance [54] as D_{gN} incorporates all the variables used for the calculation of MGD while Dance et al. [54, 64] utilised more than one conversion factor in their calculations. Following the initial publication, Wu et al. published tables to include another two anode/filter combinations (Mo/Rh, Rh/Rh) [60]. In 1997 Sobol and Wu created mathematical equations to parameterise D_{gN} tables and match D_{gN} values within predefined uncertainties [59]. These equations can be used to calculate D_{gN} values for arbitrary breast composition depending on tube potential, HVL, and breast thickness. Wu et al. and Sobol and Wu methods are limited to three anode/filter combinations and do not account for the type widely used in digital imaging, the

tungsten anode with Al or Ag filters. Wu et al. method is utilised in the ACR optimisation protocol for film-screen mammography [66], however, the new manual utilises Dance et al. method because it has been updated to include more breast thicknesses and all spectra used in digital mammography [67].

2.3.6 **Boone et al., 1997-2002**

In 1999, Boone extended earlier work on D_{gN} calculations [54, 56, 60] to include higher energies (up to 120 keV), thicker breasts (up to 12 cm), and more anode/filter combinations (Mo/Mo, Mo/Rh, Rh/Rh, W/Rh, W/Pd, W/Ag). Boone's work on higher energy beams was motivated by his interest in dual energy mammography, where higher than conventional X-ray beam energies are used, as well as the introduction of digital mammography at the time where it was expected to utilise higher energy spectra. Monte-Carlo codes simulated one million photons interactions through a cylindrical shaped phantom. The rationale behind the use of a cylindrical shape was to account for the backscattered radiation due to the presence of tissue outside the radiation field. This is different from the semi-circular D-shaped phantom utilised earlier [54, 56]. Nonetheless, same breast composition from Hammerstein et al. [46] work was used. A wide range of mono-energetic, poly-energetic and mammographic X-ray spectra was covered in his work; hence, average glandular dose can be calculated for modalities other than mammography [61]. In response to the introduction of digital mammography, Boone published computer-fit equations for the calculation of interaction-specific corrected conversion factors for a range of breast thicknesses, breast glandularities, tube potentials, HVL, and X-ray spectra [62]. Although Boone's method accounted for all X-ray spectra and different CBTs, it did not include estimates of different glandularities. This led to the Dance et al. method being proposed.

2.3.7 **Dance et al. 1990, 2000 &2009**

Dance et al. conversion factors were tabulated according to HVL for compressed breast thicknesses in the range of 2-8 cm with 50% glandularity for a variety of X-ray spectra from molybdenum (Mo) and tungsten (W) targets with Mo, rhodium (Rh), or palladium (Pd) filters. Dance et al. estimated MGD using the following equation:

MGD = K.p.g (1.3)

Where: K is the entrance air kerma without backscatter; ‘g’ is the K to MGD conversion factor for the standard breast phantom (4.2 cm thick with 50% glandular composition). ‘p’ converts K for the phantom used in their experiments (4 cm thick with 50% glandular composition) to K for a standard breast phantom. The new p conversion factor enabled the use of inexpensive and convenient material such as PolyMethyl MethAcrylate (PMMA) to create phantoms and converts the results for standard material and sizes [54].

Dance et al. continued to update their method to include new technologies; in 2000 a new equation was published with tables that covered more breast thicknesses (2-11 cm) and added a conversion factor to account for different glandularities and spectra.

MGD = K.g.c.s (1.4)

Where **K** is the incident air kerma measured on top of the breast without backscatter. **g** converts K to MGD. **c** corrects for differences in breast composition from the 50% glandularity original assumption. **s** corrects for the use of different X-ray spectra [64].

Different X-ray spectra are achieved by changing the anode, filter or kVp combinations in a mammography system. Changes in these parameters significantly influence image quality and radiation dose. Different anode-filter combinations are available in different mammographic systems. Molybdenum (Mo) and rhodium (Rh) combination is used to produce optimal X-ray spectrum specific to the imaged breast, the choice depends on the size and density of the breast, thicker more dense breasts require harder beam quality (i.e. Rh/Rh) to penetrate the dense tissue, while fatty breasts require softer beam quality (i.e. Mo/Mo) to produce high quality images and low dose [68]. The advancements in digital mammography technologies, and the use of new anode/filter material sparked new research [65]. Further work was done on the s factor in equation 1.4 to account for new anode/filter combinations: tungsten/silver (W/Ag) and tungsten/aluminium (W/Al). The authors found that when W/Al was used, the estimation of equivalent breast thickness in PMMA depended on beam quality and breast thickness, causing up to 10% error. To account for this error, a new table was developed for s factors that depended on breast thicknesses and beam qualities (HVL) when W/Al anode/filter combination is used.

The inclusion of all variables affecting MGD and the continuous update on Dance et al. method resulted in it being adopted by the European protocol for quality assurance in breast cancer screening (EP) [69], the International Atomic Energy Agency (IAEA) [70-72], the Institute of Physics and Engineering in Medicine (IPEM) [73], and lately in American College of Radiology (ACR) [67]. Nonetheless, Dance method although calculates MGD taking into account MBD and parameters affecting exposure, it does not consider individual differences in MBD. Thus, Dance's method is limited in the calculation of Actual Glandular Dose (AGD), which better represents individualised dose estimates.

2.3.8 **Organ Dose**

The Digital Imaging and Communication in Medicine (DICOM) standard core application was to capture, store, and distribute medical images for almost all medical imaging modalities since its introduction in 1993. However, it was only in 2005 that radiation dose structured reports (RDSR) were developed within the DICOM standards to manage the already existing radiation dose information from imaging modalities. Mammography dose structured reports were developed in 2007, making it possible to add estimates of MGD within the DICOM header of a mammogram. Mammography vendors developed their own algorithms to estimate the MGD, adopting one of the three main methods of calculating MGD, Dance et al. [65], Sobol and Wu [59], or Boone [61-63]. The estimated MGD is displayed by the mammography system as a reference for radiographers as Organ dose. Although methods of MGD calculation vary between vendors, such reference could be beneficial for quick dose audits on the systems in question, given that Organ Dose accuracy is verified. Chapter four provides a comparison between Organ Dose and MGD estimated using three dose calculation methods to test the consistency and accuracy of the Organ dose.

2.4 Bridging section

Individualised dose estimates should provide more accurate risk descriptors for patients undergoing mammography examinations. Accurate estimation of risk benefit

analysis for screening mammography is an important factor to consider if we are to maintain the Basic Safety Standards (BSS) in medical imaging. Justification, optimisation and DRLs constitute the BSS for medical imaging, and for DRLs to be accurate, two factors should be considered.

Firstly, an accurate estimation of MGD is required, hence the need for an implementation of MBD in the calculations of MGD, this is explained further in chapter five.

Secondly, a worldwide standard method to establish DRLs should be agreed on. The next subsections detail the literature on DRLs in mammography and highlight the variation in the methods used to establish DRLs around the world.

The literature review was published as "Diagnostic reference levels in digital mammography: a systematic review". Since its publication, there have been several additions to the literature in the field. These are laid out below.

2.4.1 Additions to the literature on DRLs since publication

A review of the literature shows that different methods have been used for establishing DRLs worldwide. Variables such as the use of patient versus phantom data, breast thickness, phantom thickness, phantom type, breast glandularity, reported age, calculation methods and percentiles used were inconsistent across published work (Figure 2.1).

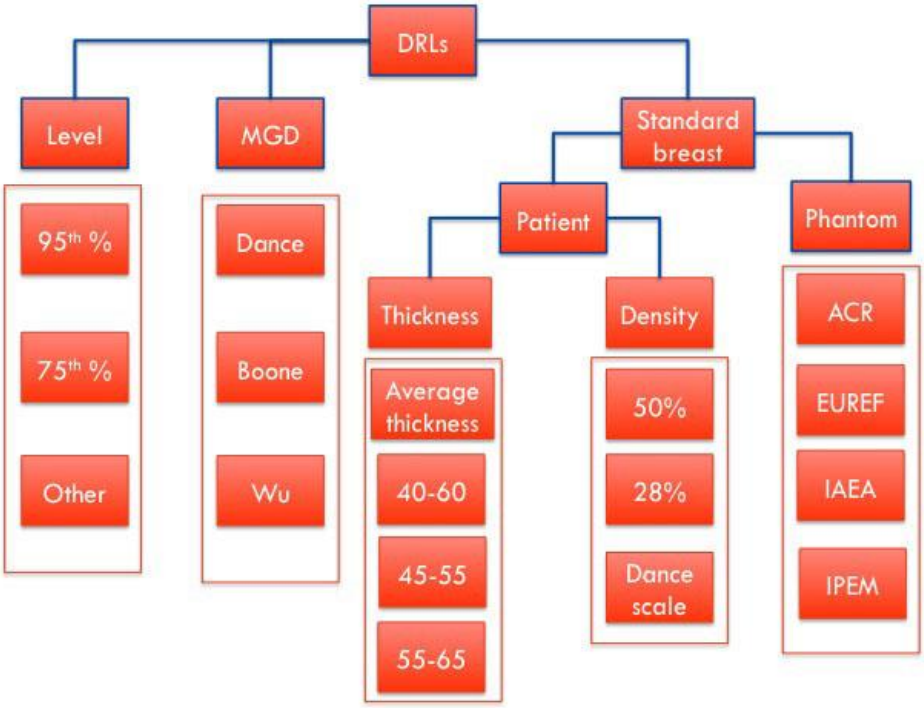

Figure 2.1: The different methods utilised internationally to establish Diagnostic Reference Levels (DRLs) for digital mammography.

Twenty-three studies were analysed, 8 of which utilised phantom data and 15 utilised patient data. The use of phantom or patient data for dose audits and DRLs can be debated in either side, a phantom study provides the advantage of eliminating patient variability for rapid examinations of equipment and quick update of DRLs. it also provides the basis of a standard patient [74]. Patient studies on the other hand, are a better representative of the women population screened in mammography and have the advantage of studying the variability in women breasts and the resultant effect on the dose delivered during a screening mammogram. Nonetheless, phantom based MGD estimates could carry up to 30% difference in either direction from patient based MGD [75]. Hence, the new ICRP publication on DRLs recommends the use of patient data to establish DRLs for mammography [76].

Different phantoms were used in the studies included, the ACR phantom which is 45 mm thick that simulates the X-ray attenuation to a 42 mm compressed breast with a 50% glandularity (Figure 2.1). A 45 mm PMMA phantom that simulates a 53 mm compressed breast with a 50% glandularity, a 40 mm BR12 phantom that simulates a 45 mm compressed breast with 50% glandularity, and a 45 mm RMI phantom that

simulates a 42 mm compressed breast with 50% glandularity. This variation in phantoms utilised eliminates the idea of standardisation and makes dose and DRLs comparisons difficult. In patient studies, average CBT of the study population was used to establish DRLs. Nonetheless, a few studies have used a certain range of breast thickness, and others used a few ranges of breast thickness for the purpose of comparison. Moreover, glandularity varied depending on the method of MGD calculation, sliding-scale, 50%, or an average estimation of the population glandularity were utilised for the calculations of MGD.

Two calculation methods were utilised for the estimation of MGD. The Dance method, which provides a utility to include variations in anode/filter combinations, breast thickness and glandularity and the Wu method, which provides tabulated values of normalised glandular dose per unit ESAK; in Australia, the ACPSEM recommends the Dance method for the calculation of MGD [77], however, work is in progress to change to Dance method. Since our review of the literature, two new studies that have been published (Table 2.1). Both utilised the 75^{th} percentile, however one used phantom data and the other used patient data. This only confirms the variability of methods used to establish DRLs. The next subsections present the published literature review titled: *Diagnostic reference levels in digital mammography: a systematic review*.

Note: The published article contained an error in section 2.6.4 first paragraph, last line. The number of articles should be 23 instead of 22. A note has been sent to the editor.

Table 2.1: Further studies that established DRLs for digital mammography.

Country	Authors (year)	Phantom /Patient	Conversion factors	Phantom type (Thickness /E-BCT/ G %) or Patients mean breast thickness	Average MGD mGy	DRLs mGy 75%
Chile	Leyton et al. (2015) [78]	Phantom	Dance et al. [64]	PMMA (20, 30, 40, 50, 60, 70 mm / 21, 32, 45, 53, 60, 75, 90 mm / Dance G [A])	0.85, 1.39, 2.21, 2.77, 3.33, 4.12, 6.26	0.90, 1.58, 2.46, 3.36, 4.17, 6.36
Ethiopia	Dellie et al. (2016) [79]	Patient	Dance et al. [64]	4.51 mm	2.57	2.37

ESAK : Entrance surface air kerma.
IAK : Incident air kerma.
E-BCT : Equivalent Breast compressed thickness
PMMA: Polymethyl-methacrylate.
CC : Cranio-caudal.
MLO : Mediolateral oblique.
G % : Glandularity.
[A] **:** Dance scale of glandularity

2.5 References

1. Salomon, A., Beiträge zur Pathologie und Klinik der Mammakarzinome. Arch Klin Chir, 1913. 101: p. 573-668.
2. Warren, S.L., A Roentgenologic Study of the Breast. Am. J. Roentgenol, 1930. 24: 113-124.
3. Lockwood, I.H., The Value of Breast Radiography. Radiology, 1934. 23(2): p. 202-207.
4. Menville, L.J. and H.P. Doub, Early diagnosis of breast carcinoma. Radiology, 1938. 30(2):258–259.
5. H, I. and G.-C. J, Comparative anatomy, pathology and roentgenology of the breast. Philadelphia, Pa: University of Pennsylvania Press, 1960.
6. Gershon-Cohen, J.J. and S.M. Berger, Detection of breast cancer by periodic x-ray examinations: A five-year survey. JAMA, 1961. 176(13): p. 1114-1116.
7. Ritvo, M., P.F. Butler, and E. O'Neil, Roentgen diagnosis of tumors of the breast. Journal of the American Medical Association, 1935. 105(5): p. 343-348.
8. Egan, R.L., Experience with Mammography in a Tumor Institution. Radiology, 1960. 75(6): p. 894-900.
9. Clark, R.L., et al., Reproducibility of the technic of mammography (egan) for cancer of the breast. The American Journal of Surgery, 1965. 109(2): p. 127-133.
10. Shapiro, S., Periodic screening for breast cancer: the HIP Randomized Controlled Trial. Health Insurance Plan. J Natl Cancer Inst Monogr, 1997(22): p. 27-30.
11. Shapiro, S., P. Strax, and L. Venet, Evaluation of periodic breast cancer screening with mammography: Methodology and early observations. JAMA, 1966. 195(9): p. 731-738.
12. Smith, R.A., et al., The randomized trials of breast cancer screening: what have we learned? Radiol Clin North Am, 2004. 42(5): p. 793-806, v.
13. Tabár, L., et al., REDUCTION IN MORTALITY FROM BREAST CANCER AFTER MASS SCREENING WITH MAMMOGRAPHY: Randomised Trial from the Breast Cancer Screening Working Group of the Swedish National Board of Health and Welfare. The Lancet, 1985. 325(8433): p. 829-832.
14. Tabar, L., et al., Swedish two-county trial: impact of mammographic screening on breast cancer mortality during 3 decades. Radiology, 2011. 260(3): p. 658-63.
15. Chamberlain, J., et al., VALIDITY OF CLINICAL EXAMINATION AND MAMMOGRAPHY AS SCREENING TESTS FOR BREAST CANCER. The Lancet, 1975. 306(7943): p. 1026-1030.
16. Shapiro, S., Evidence on screening for breast cancer from a randomized trial. Cancer, 1977. 39(6): p. 2772-2782.

17. Gold, R.H., The evolution of mammography. Radiol Clin North Am, 1992. 30(1): p. 1-19.

18. Murphy, F., et al., Compression force behaviours: An exploration of the beliefs and values influencing the application of breast compression during screening mammography. Radiography, 2015. 21(1): p. 30-35.

19. Brnic, Z. and A. Hebrang, Breast compression and radiation dose in two different mammographic oblique projections: 45 and 60 degrees. Eur J Radiol, 2001. 40(1): p. 10-5.

20. Faridah, Y., Digital versus screen film mammography: a clinical comparison. Biomedical Imaging and Intervention Journal, 2008. 4(4): p. e31.

21. Luckey, G. US3859527A- Apparatus and method for producing images corresponding to patterns of high energy radiation. 1975 [cited 2018 March 04]; Available from: https://patents.google.com/patent/US3859527.

22. Körner, M., et al., Advances in Digital Radiography: Physical Principles and System Overview. RadioGraphics, 2007. 27(3): p. 675-686.

23. Bansal, G.J., Digital radiography. A comparison with modern conventional imaging. Postgraduate Medical Journal, 2006. 82(969): p. 425-428.

24. Gennaro, G. and C. di Maggio, Dose comparison between screen/film and full-field digital mammography. European Radiology, 2006. 16(11): p. 2559-2566.

25. Juel, I.M., et al., Screen-film mammography versus full-field digital mammography in a population-based screening program: The Sogn and Fjordane study. Acta Radiol, 2010. 51(9): p. 962-8.

26. Hauge, I.H., et al., Patient doses from screen-film and full-field digital mammography in a population-based screening programme. Radiat Prot Dosimetry, 2012. 148(1): p. 65-73.

27. Bloomquist, A.K., et al., Quality control for digital mammography in the ACRIN DMIST trial: Part I. Medical Physics, 2006. 33(3): p. 737.

28. Shapiro, S., et al., Ten- to Fourteen-Year Effect of Screening on Breast Cancer Mortality. Journal of the National Cancer Institute, 1982. 69(2): p. 349-355.

29. Shapiro, S., et al., Selection, follow-up, and analysis in the Health Insurance Plan Study: a randomized trial with breast cancer screening. National Cancer Institute monograph, 1985. 67: p. 65-74.

30. Tabàr, L. and A. Gad, Screening for breast cancer: the Swedish trial. Radiology, 1981. 138(1): p. 219-222.

31. Tabár, L., et al., Swedish Two-County Trial: Impact of Mammographic Screening on Breast Cancer Mortality during 3 Decades. Radiology, 2011. 260(3): p. 658-663.

32. Resolution of the Council and the Representatives of the Governments of the Member States, meeting within the Council, of 7 July 1986, on a programme of action of the European Communities against Cancer. OJ C 184, 23.7.1986. p.19, R.o.t.G.o.t.M.S. Council of the European Union, Editor.

33. Biesheuvel, C., S. Weigel, and W. Heindel, Mammography Screening: Evidence, History and Current Practice in Germany and Other European Countries. Breast Care, 2011. 6(2): p. 104-109.

34. Smith-Bindman, R., et al., Comparison of screening mammography in the united states and the United Kingdom. JAMA, 2003. 290(16): p. 2129-2137.

35. Olver, I. and Roder D., History, development and future of cancer screening in Australia, 2017. Public Health Res Pract, 27(3). doi:10.17061/phrp2731725.

36. Pisano, E.D., et al., American College of Radiology Imaging Network Digital Mammographic Imaging Screening Trial: Objectives and Methodology. Radiology, 2005. 236(2): p. 404-412.

37. Pisano, E.D., et al., Diagnostic performance of digital versus film mammography for breast-cancer screening. N Engl J Med, 2005. 353(17): p. 1773-83.

38. Pisano, E.D., et al., Diagnostic Accuracy of Digital versus Film Mammography: Exploratory Analysis of Selected Population Subgroups in DMIST. Radiology, 2008. 246(2): p. 376-383.

39. ICRP, The 2007 Recommendations of the International Commission on Radiological Protection, ICRP publication 103. Ann. ICRP, 2007. 37(2.4): p. 1-332.

40. Vilaprinyo, E., et al., Cost-Effectiveness and Harm-Benefit Analyses of Risk-Based Screening Strategies for Breast Cancer. PLoS One, 2014. 9(2).

41. Marmot, M.G., et al., The benefits and harms of breast cancer screening: an independent review. The British Journal of Cancer, 2013. 108(11): p. 2205-40.

42. M.Ali, R.M.K., et al., Effective lifetime radiation risk for a number of national mammography screening programmes, 2018. Radiography. *24*(3), 240-246. doi:10.1016/j.radi.2018.02.001.

43. Rothenberg, L.N., R.L.A. Kirch, and R.E. Snyder, Patient Exposures from Film and Xeroradiographic Mammographic Techniques. Radiology, 1975. 117(3): p. 701-703.

44. Stanton, L., et al., Physical Aspects of Breast Radiography. Radiology, 1963. 81(1): p. 1-16.

45. Jensen, J.E. and P.F. Butler, Breast exposure: nationwide trends; a mammographic quality assurance program--results to date. Radiol Technol, 1978. 50(3): p. 251-7.

46. Hammerstein, G.R., et al., Absorbed radiation dose in mammography. Radiology, 1979. 130(2): p. 485-91.

47. Breslow, L., L.B. Thomas, and A.C. Upton, Final reports of the National Cancer Institute ad hoc Working Groups on Mammography in Screening for Breast Cancer and a summary report of their joint findings and recommendations. Journal of the National Cancer Institute, 1977. 59(2): p. 467-541.

48. Bailar, J.C., 3rd, Mammography: a contrary view. Annals Of Internal Medicine, 1976. 84(1): p. 77-84.

49. Boag, J.W., A.J. Stacey, and R. Davis, Radiation exposure to the patient in xeroradiography. British Journal of Radiology, 1976. 49(579): p. 253-261.

50. Karlsson, M., et al., Absorbed dose in mammary radiography. Acta Radiol Ther Phys Biol, 1976. 15(3): p. 252-8.

51. Yaffe, M.J. and J.G. Mainprize, Risk of radiation-induced breast cancer from mammographic screening. Radiology, 2011. 258(1): p. 98-105.

52. Stanton, L., et al., Dosage evaluation in mammography. Radiology, 1984. 150(2): p. 577-584.

53. Dance, D., The Monte Carlo calculation of integral radiation dose in xeromammography. Physics in Medicine and Biology, 1980. 25(1): p. 25.

54. Dance, D., Monte-Carlo calculation of conversion factors for the estimation of mean glandular breast dose. Physics in medicine and biology, 1990. 35(9): p. 1211.

55. Rosenstein, M., L.W. Anderson, and G.G. Warner, Handbook of glandular tissue doses in mammography. Final report March 1985. 1985: United States U6 - ctx_ver=Z39.88-2004&ctx_enc=info%3Aofi%2Fenc%3AUTF-8&rfr_id=info%3Asid%2Fsummon.serialssolutions.com&rft_val_fmt=info%3Aofi%2Ffmt%3Akev%3Amtx%3Ajournal&rft.genre=article&rft.title=Handbook+of+glandular+tissue+doses+in+mammography.+Final+report+March+1985&rft.au=Rosenstein%2C+M&rft.au=Anderson%2C+L.W&rft.au=Warner%2C+G.G&rft.date=1985-03-01&rft.externalDocID=5021739&paramdict=en-US U7 - Report.

56. Wu, X., G.T. Barnes, and D.M. Tucker, Spectral dependence of glandular tissue dose in screen-film mammography. Radiology, 1991. 179(1): p. 143-148.

57. ICRP, Protection of the Patient in Nuclear Medicine (and Statement from the 1987 Como Meeting of ICRP). ICRP Publication 52, 1987. Ann. ICRP 17(4).

58. National Council on Radiation, P., et al., Mammography--a user's guide: recommendations of the National Council on Radiation Protection and Measurements. 1986, The Council: Bethesda, MD.

59. Sobol, W.T. and X. Wu, Parametrization of mammography normalized average glandular dose tables. Med Phys, 1997. 24(4): p. 547-54.

60. Wu, X., et al., Normalized average glandular dose in molybdenum target-rhodium filter and rhodium target-rhodium filter mammography. Radiology, 1994. 193(1): p. 83-89.

61. Boone, J.M., Glandular breast dose for monoenergetic and high-energy X-ray beams: Monte Carlo assessment. Radiology, 1999. 213(1): p. 23-37.

62. Boone, J.M., Normalized glandular dose (DgN) coefficients for arbitrary X-ray spectra in mammography: computer-fit values of Monte Carlo derived data. Med Phys, 2002. 29(5): p. 869-75.

63. Boone, J.M., T.R. Fewell, and R.J. Jennings, Molybdenum, rhodium, and tungsten anode spectral models using interpolating polynomials with application to mammography. Med Phys, 1997. 24(12): p. 1863-74.

64. Dance, D.R., et al., Additional factors for the estimation of mean glandular breast dose using the UK mammography dosimetry protocol. Physics in Medicine and Biology, 2000. 45(11): p. 3225-3240.

65. Dance, D.R., K.C. Young, and R.E. van Engen, Further factors for the estimation of mean glandular dose using the United Kingdom, European and IAEA breast dosimetry protocols. Phys Med Biol, 2009. 54(14): p. 4361-72.

66. Hendrick, R., et al., Mammography quality control manual. Reston, Va: American College of Radiology, 1999.

67. Berns, E., J. Baker, and L. Barke, Digital mammography quality control manual. Reston, VA: American College of Radiology, 2016.

68. Desponds, L., et al., Influence of anode and filter material on image quality and glandular dose for screen-film mammography. Physics in Medicine & Biology, 1991. 36(9): p. 1165.

69. Perry, N., et al., European guidelines for quality assurance in breast cancer screening and diagnosis Fourth Edition. Luxembourg office for official publications of the European Communities, 2006.

70. IAEA, Dosimetry in diagnostic radiology: an international code of practice. 2007, International Atomic Energy Agency: Vienna.

71. IAEA, Quality Assurance Programme for Screen Film Mammography. Human Health Series. No. 2. 2009, Vienna: IAEA. 221.

72. IAEA, Quality Assurance Programme for Digital Mammography. Human Health Series. No. 17. 2011, Vienna: IAEA. 177.

73. Moore, A., The Commissioning and Routine Testing of Mammographic X-ray Systems: A Protocol Produced by a Working Party of the Diagnostic Breast Screening Quality Assurance Coordinating Group for Physics. 2005: Institute of Physics and Engineering in Medicine.

74. Seeram, E. and P.C. Brennan, Diagnostic reference levels in radiology. Radiologic Technology, 2006. 77(5): p. 373-384.

75. Kelaranta, A., et al., Conformance of mean glandular dose from phantom and patient data in mammography. Radiat Prot Dosimetry, 2015. 164(3): p. 342-53.

76. Vañó, E., et al., ICRP Publication 135: Diagnostic Reference Levels in Medical Imaging. Annals of the ICRP, 2017. 46(1): p. 1-144.

77. Heggie, J. C. P., Barnes, P., Cartwright, L., Diffey, J., Tse, J., Herley, J., . . . Collins, L. T. (2017). Position paper: recommendations for a digital mammography quality assurance program V4.0. *Australasian Physical and Engineering Sciences in Medicine, 40*(3), 491-543. doi:10.1007/s13246-017-0583-x

78. Leyton, F., et al., Mean glandular dose in six digital mammography services in Santiago, Chile: preliminary reference levels. Radiation Protection Dosimetry, 2015. 165(1-4): p. 115-120.

79. Dellie, S.T. and A.D.P. Rao, SUGGESTED DIAGNOSTIC REFERENCE LEVELS FOR MAMMOGRAPHY X-RAY EXAMINATION IN ETHIOPIA. Indian Journal of Medical Sciences, 2016. 68(1): p. 36-41.

2.6 DIAGNOSTIC REFERENCE LEVELS IN DIGITAL MAMMOGRAPHY: A SYSTEMATIC REVIEW

Moayyad E. Suleiman*, Patrick C. Brennan and Mark F. McEntee

Faculty of Health Sciences, The University of Sydney, M205, Cumberland Campus, 75 East St, Lidcombe, Sydney, NSW 2141, Australia

2.6.1 ABSTRACT

This study aims to review the literature on existing diagnostic reference levels (DRLs) in digital mammography and methodologies for establishing them. To this end, a systematic search through Medline, Cinahl, Web of Science, Scopus and Google scholar was conducted using search terms extracted from three terms: DRLs, digital mammography and breast screen. The search resulted in 1539 articles of which 22 were included after a screening process. Relevant data from the included studies were summarised and analysed. Differences were found in the methods utilised to establish DRLs including test subjects' types, protocols followed, conversion factors employed, breast compressed thicknesses and percentile values adopted. These differences complicate comparison of DRLs among countries; hence, an internationally accepted protocol would be valuable so that international comparisons can be made.

2.6.2 INTRODUCTION

Breast cancer causes almost half a million deaths in the world per year [(1)], but early detection has been demonstrated to reduce mortality by up to 30 %[(2)]. Mammography, radiographic imaging of the breast with X-rays, is the most important diagnostic tool for the early detection of breast cancer. There are two types of patients on whom mammograms are per- formed: symptomatic women in the clinic and asymptomatic women in breast screening programmes.

The Australian breast screening programme was established in 1991, targeting women aged 50 – 69y for 2-yearly screening mammograms with the aim of reducing deaths from breast cancer [(3)]. It has been estimated that since 1991 breast cancer mortality in Australia has been reduced by 21 – 28 % [(3)]; however, as with any other X-ray

examination, screening programmes can add to the risk of inducing cancer in healthy women by exposure to ionising radiation. Therefore, the dose to the patient must be kept as low as reasonably achievable [4]. The three pillars of radiation protection are justification, optimisation and dose limitation.

The International Commission of Radiation Protection (ICRP) introduced diagnostic reference levels (DRLs) in their 1996 publication 73 as a parameter to be used for quality control, comparison of dose levels, optimisation and limiting variations in dose among diagnostic imaging centres. DRLs were defined as follows:

"A form of investigation level, applied to an easily measured quantity, usually the absorbed dose in air, or tissue-equivalent material at the surface of a simple phantom or a representative patient" [4]

A year later, the European Council defined DRLs as:

"Dose levels in medical radiodiagnostic practices, for typical examinations for groups of standard- sized patients or standard phantoms for broadly defined types of equipment. These levels are expected not to be exceeded for standard procedures when good and normal practice regarding diagnostic and technical performance is applied" [5].

The methods through which the DRLs are established become important when trying to establish international comparisons as radiation dose measurements are required [3]. Historically, mammography was screen-film based [6–12], but now this technology is being phased out and replaced with digital mammography, which includes full-field digital mammography and computerised radiography systems; hence, only studies with digital mammography or a mix of digital mammography and screen-film mammography (SFM) are included. Measuring the radiation dose to the breast has been performed or represented using a variety of approaches including air kerma [13], entrance surface dose [14], mid-breast dose [15], total energy trans- mitted to the breast [16] and the average dose absorbed by the glandular tissue [17]. The latter was found to be the most effective way of measuring absorbed dose to the breast because the mammary glands are most sensitive to ionising radiation and have the highest risk of developing radiation-induced carcinogenesis [17]. Called mean glandular dose (MGD), this metric is now the recommended measure by many authorities such as the ICRP [18], the United States National Council on Radiation Protection and Measurements [19],

the British Institute of Physics and Engineering in Medicine (IPEM) [20], the European Council Protocol (EP) [21–23] and the International Atomic Energy Agency (IAEA) [24].

Dose to the glandular tissue of the breast cannot be directly measured during an X-ray examination but can be assessed with certain standard assumptions that depend on breast characteristics and X-ray spectra. MGD represents the effective dose absorbed by the breast and is calculated from conversion factors that have been established using Monte-Carlo techniques [25 – 28]. Such factors relate MGD to the entrance surface dose and allow for a wide and flexible range of X-ray spectra, breast thickness and breast glandularity [26, 29]. The estimation of this quantity can be done using either a standard phantom or a patient. Although phantoms are good indicators of machine quality and can be used as an inter-centre and inter-suite comparison tool, direct patient measurements can reveal much more information on technique and the relation between breast composition and absorbed dose [9, 30 – 32].

A number of countries around the world have established DRLs for mammography examination, but many others are yet to do so. The aim of this study is to review the literature on established DRLs and methodologies for establishing them in digital mammography.

2.6.3 **METHODS**

Search strategy

Using the Preferred Reporting Items for Systematic Reviews and Meta-Analyses methodology [33, 34], a systematic literature search of Medline, Cinahl, Web of Science, Scopus and Google scholar was conducted to identify studies that have established DRLs for digital mammography. The search terms shown in table 2.2 were applied; a search filter was used to limit results to specific criteria of population (female, human), age (adult .19), publication language (English) and publication year (1990 – 2014).

Selection criteria

An initial screening of identified abstracts and titles was conducted by two reviewers (M.S. and M.M.). Only abstracts that discussed MGDs in mammography were included in the full text review. Articles were independently considered for inclusion

in the review if they discussed DRLs in digital mammography and included data from phantoms or patients.

2.6.4 **RESULTS**

The combined search strategy identified 1539 citations: 494 were identified from MEDLINE, 626 from SCOPUS, 385 from Web of Science, 9 from Cinhal and 25 from Google Scholar and manual search. Of these, 270 were duplicates and 1058 citations were excluded after the initial screening based on titles and abstracts. Finally, 211 articles were considered eligible for full text review. On full text review of the remaining articles, 188 were excluded because they did not establish DRLs for digital mammography or had no clinical data (Figure 2.2). The final number of articles to be included in the systematic review was 22.

Table 2.2: The search terms used to find the relevant literature, separated in to the intervention, cohort and other, where the search formula was: (Intervention combined with "OR") AND (Cohort combined with "OR") AND (other combined with "OR")

Intervention	Cohort	Other
DRLs	Mammography	Breast screening
Diagnostic reference levels	Mammographic Examination	Mass screening
Dose reference levels	Mammogram	Population screening
Mean glandular dose	Digital mammography	
Average glandular dose		
Reference levels		
Dose survey		
Population dose		
Glandular dose		
Radiation dose		

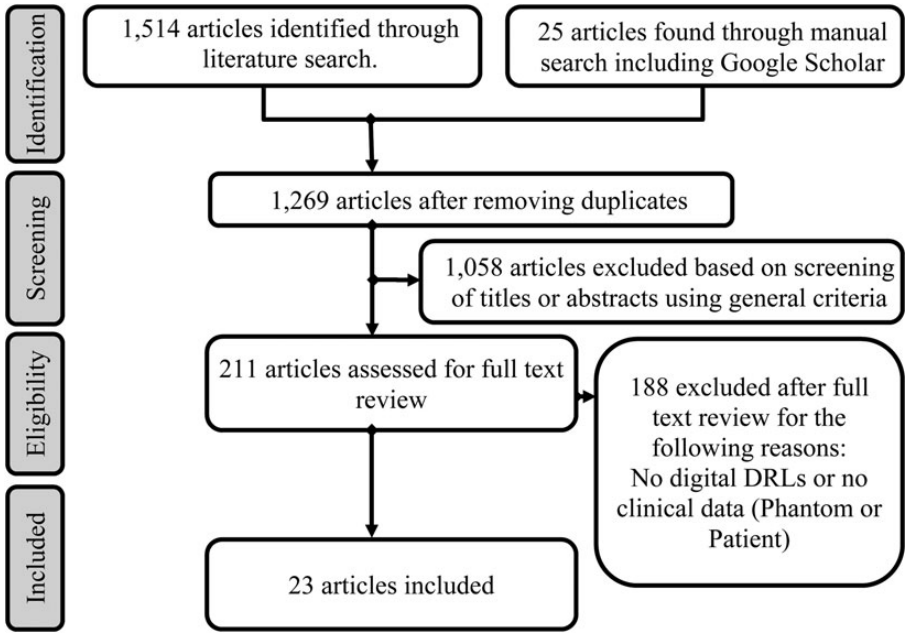

Figure 2.2: Flow diagram of included and excluded studies with specifics for DRLs in digital mammography.

Review

The included studies cover different regions in the world, with 13 from Europe [35 – 47], 5 from Asia and the Middle East [48–52], 1 worldwide study [53] and 1 each from Australia [54], the USA [55] and Nigeria [56]. The main characteristics of the studies are summarised in tables 2.3 and 2.4. Six of the 22 studies were based on phantom data, 13 on patient and 3 on both. For comparison purposes, studies with both phantom and patient data were included in both tables. The review demonstrated that four main quality control protocols were followed for estimating MGD and finding DRLs, those published by the American College of Radiology (ACR) [57], the European Council Protocol (EP) [21–23], the IAEA [24] and the British IPEM, formerly the Institute of Physical Sciences in Medicine (IPSM) [60].

Phantom studies: methods used

Phantom-based studies have the benefits of standard baseline, standard exposure protocols and quick inter- and intra-X-ray suites comparison. Therefore, it is not unexpected that 6 of the 22 studies investigating DRLs were performed using phantoms only (Tables 2.3) and 3 performed on patients and phantoms. Of the three studies that were performed on patients and phantoms, one reported DRLs for phantoms only, one reported for patients only and one reported for both patients and phantoms (Tables 2.3 and 2.4).

A total of eight studies reported DRLs for phantoms although the phantoms used were not of the same size and type; three used ACR polymethylmethacrylate (PMMA) phantoms [50,54,55], three used EP PMMA phantoms [35,45,47], one used a 45-mm RMI-156 phantom [51] and another used a 40-mm BR12 phantom [38].

The phantom types and the protocols used to collect measurements, the coefficients used for the conversion to MGD and the percentile used to report the DRL varied among the studies (Table 2.3). The ACR measurement protocol [57] and the Wu et al. MGD conversion factors [29,58] were followed by three of the seven PMMA studies [50,54,55], two followed European measurement protocol [21] and used the Dance et al. MGD conversion factors [45,47] and one followed the IAEA measurement protocol with the Dance et al. MGD conversion factors [35]. Thus, DRL values found in these studies

cannot be com- pared directly without conversion calculations; this complicates inter-study comparisons and detracts from the benefit of using a standard phantom.

Phantom studies: DRLs

The overall distribution of DRLs calculated from phantom studies are shown in figure 2.3. These are categorised by phantom types. However, other factors need to be discussed before these DRLs can be com- pared. The three ACR PMMA phantom studies reported overall 75th percentiles of 1.3 mGy [54], 1.75 mGy [50] and 2.0 mGy [55]. Although the same standard phantom and conversion factors were used to estimate the average MGDs, the results demonstrate a 0.7-mGy difference in the average MGDs between Australia (1.3 mGy) and the USA (2.0 mGy). The low DRL in the Australian study might be explained by the absence of film-screen mammography units in the study where the other two studies had a mix of digital and film-screen units. The RMI 156 phantom following the ACR protocol reported a 75th percentile of 1.44 [38]. The two EP PMMA phantom studies reported 75th percentile of 1.70 mGy [47] and 95th percentile of 2.08 mGy [45].

Table 2.3: Summary data from included phantom studies.

Country	Authors (year)	Data collection method	Dose protocol/ Conversion factors	Phantom type (Thickness /E-BCT/ G %)	Average MGD mGy (unless otherwise stated)	DRLs mGy		
						75%	95%	Recommended
Australia	Thiele et al. (2011) [54]	Measured ESAK	ACR[57]/Wu et al. [29,63]	ACR PMMA (45mm / 42mm / 50%)	All:1.16 DR:1.04 CR:1.28	All: 1.30 DR: 1.10 CR: 1.36		DR:1.10[A] CR:1.40 [A]
Taiwan	Hwang et al. (2009) [50]	Measured ESAK	ACR [57]/Wu et al. [29]	ACR PMMA (45mm / 42mm / 50%)	All: 1.48 DR: 1.47 SFM: 1.49	1.75		
USA[B]	Spelic et al. (2007) [55]	Measured ESAK	ACR [57]/Wu et al. [29]	ACR PMMA (45mm / 42mm /50%)	All: 1.78 DR:1.63 SFM:1.80	All: 2.0 DR:1.92 SFM: 2.04	All: 2.35 DR: 2.29 SFM: 2.39	
Slovenia	Zdesar (2008) [47]	Estimated ESAK	EP [21]/ Dance et al. [66]	PMMA (45mm / 53mm / 50%)	1.5	1.7		
Belgium	Smans et al. (2006) [C] [45]	Estimated ESAK	EP [21]/Dance et al. [64]	PMMA (45mm / 53mm / 50%)	*		2.08	
Bulgaria	Avramova & Vassileva (2011) [35]	Measured IAK	IAEA [24] /Dance et al. [66]	PMMA (45mm / 50mm/ 50%)	1.8	2.3		
Turkey	Bor et al. (2008) [38]	Measured ESAK	IPSM [58] / Dance et al. [D] [66]	BR12 (40 mm / 45mm / 50%)	1.46	2.0		
Malaysia	Jamal et al. (2003) [C] [51]	Measured ESAK	ACR [57]/Wu et al. [29]	RMI 156 [E] (45mm / 42mm / 50%)	1.23	1.44 4.61 (ESAK)		2.0 [A] (93.3 %)

ACR : American college of radiology.
EP : European Protocol.
IPSM : Institute of Physical Sciences in Medicine / now **IPEM** : Institute of Physical and Engineering in Medicine.
IAEA : International Atomic Energy Agency.
[A] : Recommended by the authors.
[B] : Data estimated from Figure 4 and 10 in Spelic et al. paper.
[C] : Study includes Phantom and Patient data.
[D] : Dance et al. not specifically mentioned.
[E] : RMI 156 is made from acrylic with wax inserts.

ESAK : Entrance surface air kerma.
IAK : Incident air kerma.
E-BCT : Equivalent Breast compressed thickness.
G % : Glandularity.
PMMA: Polymethyl-methacrylate.
DR : Digital radiography.
CR : Computed radiography.
SFM : Screen-film mammography**.**
*** :** No average MGD value mentioned in the study.

Table 2.4: Summary data from included patient studies

Country	Author(s) (year)	Number of patients	Data collection method	Dose protocol/ Conversion factors	Mean BCT mm	Average MGD mGy	DRLs mGy		
							75%	95%	Recommended
Japan	Asada et al. (2014) [48]	NA	Measured ESAK	EP [23]/Wu et al. [29]	42	1.58	1.91		
Iran	Bahreyni et al. (2013) [49]	100	Measured ESAK(TLDs)	EP [23]/Wu et al. [29]	CC: 47 MLO: 53 SMLO: 50-60	CC: 0.88 MLO: 1.11	SMLO: 1.33		
Nigeria	Ogundare et al. (2009) [56]	40	Measured ESAK (TLDs)	ACR [57]/Wu et al. [29]	All: 41.1 CC: 33.8 MLO: 48.5	All: 0.88 CC: 0.33 MLO: 1.43		2.5[A]	
Japan	Kawaguchi et al. (2014) [52]	300	Measured ESAK	EP [21, 73]/Dance et al. [66]	SMLO: 30-40 MLO: 37.6	SMLO: 1.88 MLO: 1.84	SMLO: 2.0		
Ireland	O'Leary (2013) [44]	1,010	Estimated ESAK	EP [23] /Dance et al. [27]	DR: 54.7 SFM: 52.3	DR: 1.33 SFM: 2.64	DR: 1.5 SFM: 3.17	DR: 2.26 SFM: 5.59	
					45-55	All:1.68 DR:1.13 SFM:2.16	All: 1.2 DR: 1.2 SFM: 2.55	All: 1.5 DR: 1.5 SFM: 3.85	
					55-65	All: 2.04 DR: 1.40 SFM: 2.88	All: 2.47 DR: 1.50 SFM: 3.41	All: 4.33 DR: 2.40 SFM: 5.84	
Malta	Borg et al. (2013) [C (39)]	759	Estimated ESAK	EP [21]/Dance et al. [66]	All: 57.5 CC: 53.8 MLO: 63.4	All: 1.07 CC: 1.06 MLO1.07	All: 1.11 CC: 1.11 MLO: 1.11	All: 1.68 CC: 1.65 MLO: 1.87	1.87[B]
Norway	Hauge et al. (2013) [41]	1,335	Estimated ESAK	EP [21]/Dance et al. [27, 66, 67]	SMLO: 55-65	SCC: 1.23 SMLO: 1.35 CC: 1.18 MLO: 1.31	SMLO: 1.44	SMLO: 1.98	2.0[B]
World wide	Geeraert et al. (2012) [53]	147,497	Estimated ESAK from DICOM data	N/A /Dance et al. [66]	Na	Europe: 1.48 N. America: 1.42 Asia-Pacific: 1.42	Europe: 1.6 N. America: 1.6 Asia-Pacific: 1.1	Europe: 2.4 N. America: 2.1 Asia-Pacific: 2.3	
Ireland	Baldelli et al. (2011) [36]	2910	Estimated ESAK from DICOM data	EP [21]/Dance et al. [27, 66, 67]	CC: 60.5 MLO: 63.0	CC: 1.27 MLO: 1.34		1.75	
Ireland	Baldelli et al. (2010) [37]	3016	Estimated ESAK from DICOM data	EP [21]/Dance et al. [67]	CC: 60 MLO: 62.5	CC: 1.27 MLO: 1.35		1.75	
Belgium	Michielsen (2008) [42]	NA	Estimated ESAK	EP [21]/Dance et al. [66]	SMLO: 48-58	All: 1.69		2.37	

Table 2.4, continued

Belgium	Smans et al. (2006) [C (45)]	10,093	Estimated ESAK	EP [(23)]/Dance et al. [(66)]	SMLO: 48-58	All: 1.67	2.44	
Spain	Moran et al. (2005) [(43)]	5034	Estimated ESAK from DICOM data	EP [(23)]/Dance et al. [(66)]	All: 52 CC: 49 MLO:54	All: 1.88 CC: 1.80 MLO: 1.95	All: 2.1 CC: 2.0 MLO:2.1	
UK	Young et al. (2005) [C (46)]	16505	Estimated ESAK	IPEM [(58)]/ Dance et al. [(27, 66)]	SMLO: 50-60 CC: 54.1 MLO: 56.8	SMLO: 2.03 CC: 1.96 MLO: 2.23		SMLO: 3.5 [D]
Spain	Chevalier et al. (2004) [(40)]	5034	Estimated ESAK from DICOM data	EP [(22)]/Dance et al. [(66)]	All: 52 CC: 49 MLO: 54	All: 1.88 CC: 1.80 MLO: 1.95	All: 2.1 CC: 2.0 MLO: 2.1	

ACR : American college of radiology.
EP : European protocol.
IPSM : Institute of physical sciences in medicine / now IPEM : Institute of physical and engineering in medicine.
ESAK: Entrance surface air kerma.
CC : Cranio-caudal.
MLO : Mediolateral oblique.
SMLO: Standard Mediolateral oblique (only standard breast thickness range included for DRLs calculations).
TLDs : Thermoluminescent dosemeters**.**

DR: Digital radiography.
CR: Computed radiography.
SFM : Screen-film mammography.
[A] : Reported 92.5 percentile.
[B] : Recommended by authors.
[C] : Study includes Phantom and Patient data.
[D] : Reported 96.5 percentile.

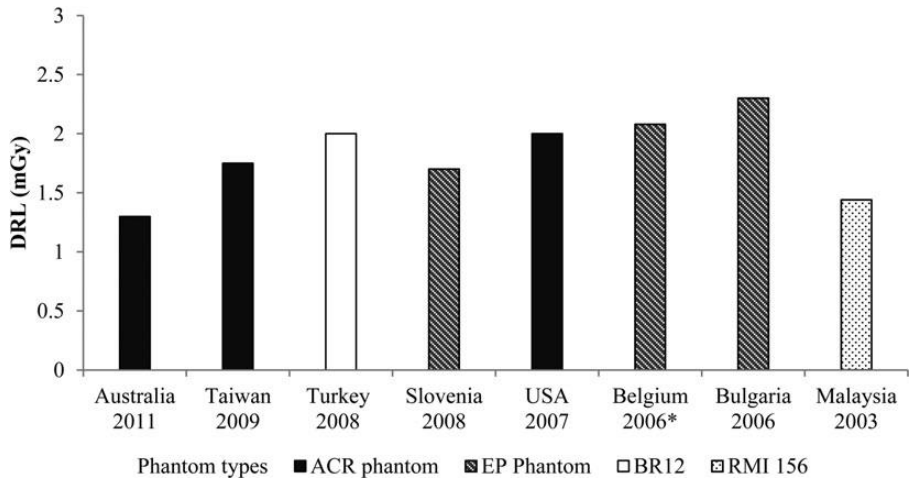

*Figure 2.3: DRLs for phantom studies categorised by phantom types (*95th percentile).*

Although the two studies used the same phantom and same conversion factors to report MGD DRLs, a comparison cannot be made because the percentiles used were different [45, 47]. A PMMA phantom study following the IAEA protocol reported an MGD 75th percentile of 2.30 mGy. The authors reported non-standardised techniques and lack of optimisation as possible causes for the higher dose [35]. A BR12 phantom following the IPSM protocol reported a 75th percentile of 2.0 mGy [38].

Patient studies: methods

Patient studies have an advantage over phantom studies that they offer a more realistic and comprehensive assessment of the doses delivered to patients with different breast sizes and compositions. A total of 15 patient studies investigating DRLs were reviewed (Table 2.4) and once again, methods of data collection varied. Two studies used thermoluminescence dosemeters (TLDs) to measure ESAK values [49, 56] and the rest estimated ESAK values from exposure parameters such as tube output and tube loading [36, 37, 39–46, 48, 52, 53]. Two different methods of calculating MGDs have been used: the Wu et al. MGD conversion factors were used to calculate MGDs in 3 of the 15 patient studies [48, 49, 56] and 12 used the Dance et al. conversion factors [36, 37, 39–46, 53]. A wide range of mean breast compressed thicknesses (BCTs) was reported. These diverse methodologies complicate direct comparison among results; hence, studies are categorised according to reported average BCT and plotted in figure 2.4 and 2.5.

Patient studies: DRLs

A range of DRLs have been reported with 75th percentiles ranging from 1.11 [39] to 2.47 mGy [44] and the 95th percentiles ranging from 1.5 [44] to 4.33 mGy [44], in the

average BCT range of 55–65 mm. The three Irish studies reported different 95th percentile values from each other, two breast screening mammography studies with only digital units reported a 1.75mGy [36,37] of DRL value and the third that included SFM units and symptomatic patients reported a 2.40mGy for digital units only (an overall digital and SFM value of 4.33 mGy), which is the highest among the three; this may be due to the inclusion of symptomatic patients [44]. A Norwegian study, which included only digital units in a breast screening programme, reported a 95th percentile of 1.98 mGy [41] and a Maltese study reported a lower value of 1.87 mGy [39]; both though are higher than the two breast screening Irish studies that used the same percentile value [36,37]. International differences may be due to variation in population breast composition and the use of certain type of units that contribute to higher patient dose. Many authors have discussed the differences in breast dose when using different makes and models of mammography units on similar size and composition breasts [36,41].

In the BCT range of 45–55 mm, international comparison can be made. Two Belgian studies reported similar 95th percentiles of 2.44 [45] and 2.37 mGy [42]. For the same average BCT range, two Spanish studies reported a 75th percentile of 2.1 mGy [40, 43], which is almost double the 1.2 mGy reported by an Irish study [44] and 1.33 mGy reported by an Iranian study [49]. Studies with equal BCT, measurement protocol, MGD conversion factors and percentile reported facilitate easier international comparison; however, they do show a worrying outcome of large variations in the dose received by women in different countries. The reasons for these potential differences are thoroughly discussed in the discussion section but include, technique, technology and population characteristics.

In the BCT range of, 45 mm, two Japanese studies reported 75th percentiles of 1.91 [48] and 2 mGy [52]. The authors followed two different protocols and methods to calculate the dose, which could explain the 0.09 (5 %) difference in their results, as a 9 – 21 % difference would be expected between Dance et al. and Wu et al. methods [63].

An all-digital worldwide study that collected dose information from different geographical areas (and did not report BCT) showed the 95th percentiles for Europe, North America and Asia-Pacific of 2.4, 2.1 and 2.3 mGy, respectively [53] and 75th percentiles of 1.6, 1.6 and 1.1 mGy, respectively.

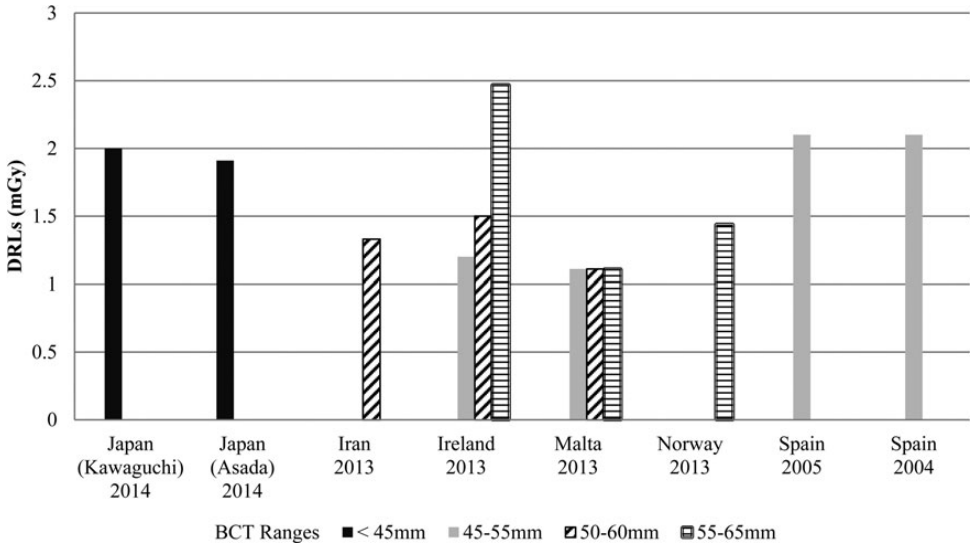

Figure 2.4:DRLs (75th percentile) for patient studies categorised by BCT.

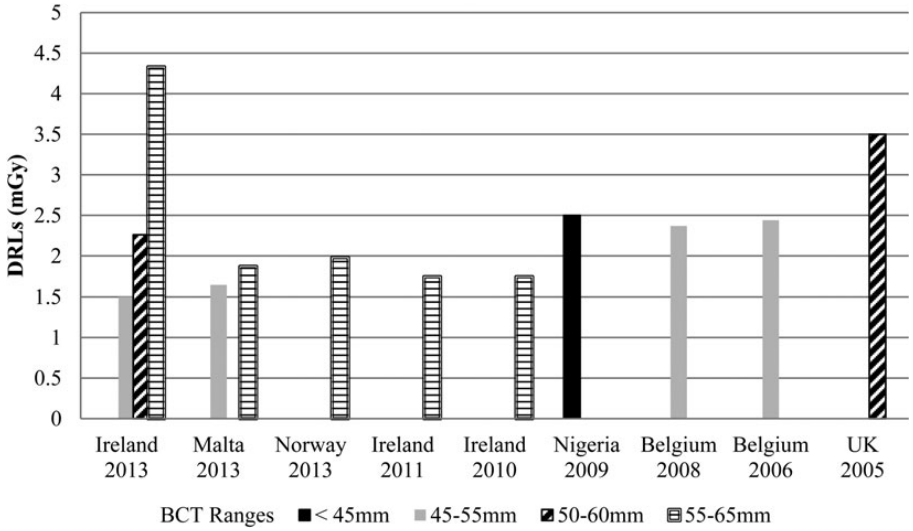

Figure 2.5:DRLs (95th percentile) for patient studies categorised by BCT

Table 2.5:Summary of quality control protocols followed by the included studies.

Protocol	Test subjects		Digital / SFM	Conversion factors	Reference level of MGD (mGy) to standard breast
	Phantom (Thickness /E-BCT/ G %)	**Patients number**			
IAEA 2011 [74]	Blocks of PMMA (20, 45, 70 mm/21, 53, 90 mm /50%)	N/A	Digital	Dance (2000)	< 1, 2.5, 6.5 respectively
IAEA 2009 [75]	Standard breast: PMMA (45mm/53mm/29%)	N/A	SFM	Dance (2000)	< 2.5
IAEA 2007 [24]	Standard breast: PMMA (45mm/50mm/50%)	10-50 patients BCT 50-60 mm	Both	Dance (2000)	N/A
EP 2006[2] [21]	Standard breast: PMMA (45mm/53mm/50%) Or blocks of PMMA (20-80 mm)	Minimum 10 patient BCT 40-60 mm	Both	Dance (2000)	< 2.5
IPEM 2005 [76]	Standard breast: PMMA (45mm/53mm/29%) Or blocks of PMMA (20-80 mm)	Minimum 10 patient BCT 50-60 mm	Both	Dance (2000)	< 3.5
ACR 1999 [57]	Standard breast: PMMA (40mm/42mm/50%) Blocks of PMMA (20-80 mm)	N/A	SFM	Wu (1991) Dance (1990) Sobol (1997)	≤ 3.0

E-BCT : Equivalent Breast compressed thickness
G % : Breast glandularity
SFM : Screen-film mammography
IAEA : International Atomic Energy Agency
EP : European Council protocol
IPEM : Institute of Physics and Engineering in Medicine
ACR : American College of Radiology
PMMA: Polymethyl-methacrylate
[1] Technical (Phantom) / Clinical (Patient)
[2] Different reference values available for different BCT

2.6.5 **DISCUSSION**

The studies reviewed followed two main groups of authors that reported conversion factors for the calculation of breast dose: Dance et al. [27, 59, 62, 64] and Wu et al. [29, 58], which are both used to compensate for the X-ray spectrum characteristics and breast composition (glandularity). Four phantom studies [50, 51, 54, 55] and 3 patient studies [48, 49, 56] used Wu et al. conversion factors whereas 4 phantoms [35, 38, 45, 47] and 12 patient studies [36, 37, 39 – 46, 52, 53] used Dance et al. conversion factors. It has been reported that MGD calculated from exposure measurements using Wu et al. conversion factors was 9–21% less compared with Dance et al. conversion factors [63]. Dance et al. acknowledged that a variation of up to 16 % exists between the two methods; this is due to differences in the breast model, X-ray spectra and photon interaction cross sections [59] (this will not be discussed as it is beyond the scope of this paper). Wu et al. conversion factors are still valid for newer technologies and can report accurate results [65]. Dance et al. conversion factors though have been updated to include new factors that compensate for different technologies, different types of target/ filter combinations and wider range of BCTs and breast glandularities (59, 62, 64).

Four different quality control protocols that have different approaches to exposure measurements (Table 2.5) were followed. The two most common are the EP [21 – 23] and the ACR [57]; both are well-established protocols. The EP was updated to include digital mammography [21], a supplement fourth edition of the European guidelines has been published [69], and according to the European Reference Organisation for Quality Assured Breast Screening and Diagnostic Services website, a further update is on the way [70]. An update of the ACR protocol to cover digital mammography is also known to be in progress [71]; information regarding calculation standards and conversion factors to be used has not been released yet. However, the authors would suggest the use of Dance et al. conversion factors as the latest published data are based on newer technologies.

Two main percentiles were used to establish DRLs, the 75th and 95th percentiles. The 75th percentile is more common and is used when there is a large range of MGDs. Its use encourages 25 % of the centres to reduce their dose. On the other hand, the 95th per- centile is used when there is a small range of MGDs and means that only 5 % of the centres require an intervention to reduce dose. Thus, the 95th percentile is more

suited to well-established screening environments whose variation in doses is likely to be small. Nonetheless, when establishing DRLs, any recommendations of lowering dose should be balanced with a measure of image quality as poor image quality degrades image interpretation accuracy [72 – 75]

A diverse range of standard BCTs has been reported depending on the protocol followed. Phantom studies that followed the EP used thicker equivalent BCT phantoms (53 mm) and hence reported higher average MGDs than ACR protocol studies that used thinner equivalent BCT phantoms (42 mm). In patient studies, the range of standard BCT varied even for the same protocol. In general, a thicker BCT requires higher exposure and is expected to receive higher dose in a similar X-ray examination environment. The most two common ranges of BCT used among the reviewed studies are 45 – 55 and 55 – 65 mm, which falls within the range followed by the EP for patient studies (40 – 60 mm). The standard EP phantom also has an equivalent BCT of 53 mm, which falls into that range.

Although establishing DRLs normally requires the use of standard BCT, any study that aims to establish DRLs for mammography could also include a range of BCTs, which would result in a more accurate measure of dose variations across the population. Plotting graphically BCT versus DRL would be a good quality control measure that radiographers could refer to in order to assure that useful data are available for the non-standard breast thickness. Although breast thickness is not the only factor to have an effect on MGD, it is the most consistently reported. Other factors that affect MGD are not consistently reported; for example, kVp is reported in 13 of the 22 papers included in this review, target filter combination in 13 of the 22, HVL in 5 of the 22, and mAs in 8 of the 22. Therefore, for the purpose of consistency, a detailed comparison of these factors was not feasible and is not included.

The lack of consistency and a worldwide standard methodology to establish DRLs complicates comparison of dose among countries. International comparisons have shown differences that are often discussed by authors; for example, the difference in the digital screening services of Ireland (1.75 mGy) [36] and Norway (1.98 mGy) [41]. Hauge et al. explained the lower DRL in the Irish study to be a result of including more of a certain mammography unit that was proven to contribute to lower dose values and hence lower DRLs within the Irish study [41]. Both studies found that MGDs varied depending on the model of mammography units; Hauge et al. reported that eliminating

one type of mammography units resulted in the reduction of the 95th percentile from 1.98 to 1.65 mGy bringing the results closer to Baldelli et al. 95th percentile (1.75 mGy) [41].

2.6.6 **CONCLUSION**

DRLs for mammography have been established across the world, and variable methods and techniques were used. The most common method used was patient studies following the EP combined with Dance et al. MGD conversion factors for BCT ranges of 45 – 55 and 55 – 65 mm. DRLs for these ranges varied with the 75th percentiles ranging from 1.11 to 2.47 mGy and the 95th percentiles from 1.5 to 3.5 mGy. However, an internationally accepted protocol that includes dose measurement method, conversion factor, BCT for patients or phantoms and DRL per- centile needs to be established before important, useful and accurate international comparison can be made.

2.6.7 REFERENCES

1. World Health Organisation. Cancer. [Accessed on 11 November 2013]; Available from: http://www.who.int/mediacentre/factsheets/fs297/en/.
2. Tabar, L., Vitak, B., Chen, T. H., Yen, A. M., Cohen, A., Tot, T., Chiu, S. Y., Chen, S. L., Fann, J. C., Rosell, J. et al. Swedish two-county trial: impact of mammographic screening on breast cancer mortality during 3 decades. Radiology. 260, 658-63 (2011).
3. Cancer series no 77 cat no CAN 74. BreastScreen Australia Monitoring Report 2010-2011. 77. (2013).
4. International Commission of Radiation Protection. Radiological protection and safety in medicine. Ann ICRP. ICRP Publication 73. Ann. ICRP 26 (2). 1-47 (1996).
5. CEC. Council Directive 97/43/Euratom of 30 June 1997 on health protection of individuals against the dangers of ionizing radiation in relation to medical exposure. (1997).
6. González, L., Vañó, E., Oliete, S., Manrique, J., Hernáez, J. M., Lahuerta, J. and Ruiz, J. Report of an image quality and dose audit according to directive 97/43/Euratom at Spanish private radiodiagnostics facilities. The British journal of radiology. 72, 186-192 (1999).
7. Nassivera, E. and Nardin, L. Quality control programme in mammography: second level quality controls. The British journal of radiology. 70, 612-618 (1997).
8. Heggie, J. C. Survey of doses in screening mammography. Australasian physical & engineering sciences in medicine / supported by the Australasian College of Physical Scientists in Medicine and the Australasian Association of Physical Sciences in Medicine. 19, 207-16 (1996).
9. Faulkner, K., Law, J. and Robson, K. J. Assessment of mean glandular dose in mammography. British Journal of Radiology. 68, 877-881 (1995).
10. Morán, P., Chevalier, M. and Vañó, E. Comparative study of dose values and image quality in mammography in the area of Madrid. The British journal of radiology. 67, 556-563 (1994).
11. Heggie, J. C. A survey of doses to patients in a large public hospital resulting from common plain film radiographic procedures. Australasian physical & engineering sciences in medicine / supported by the Australasian College of Physical Scientists in Medicine and the Australasian Association of Physical Sciences in Medicine. 13, 71-80 (1990).
12. Ciraj-Bjelac, O., Beciric, S., Arandjic, D., Kosutic, D. and Kovacevic, M. Mammography radiation dose: initial results from Serbia based on mean glandular dose assessment for phantoms and patients. Radiation Protection Dosimetry. 140, 75-80 (2010).
13. Jensen, J. E. and Butler, P. F. Breast exposure: nationwide trends; a mammographic quality assurance program--results to date. Radiologic technology. 50, 251-257 (1978).

14. Fitzgerald, M., White, D. R., White, E. and Young, J. Mammographic practice and dosimetry in Britain. British Journal of Radiology. 54, 212-220 (1981).

15. Breslow, L., Thomas, L. B. and Upton, A. C. Final reports of the National Cancer Institute ad hoc Working Groups on Mammography in Screening for Breast Cancer and a summary report of their joint findings and recommendations. Journal of the National Cancer Institute. 59, 467-541 (1977).

16. Boag, J. W., Stacey, A. J. and Davis, R. Radiation exposure to the patient in xeroradiography. British Journal of Radiology. 49, 253-261 (1976).

17. Karlsson, M., Nygren, K., Wickman, G. and Hettinger, G. Absorbed dose in mammary radiography. Acta radiologica: therapy, physics, biology. 15, 252-8 (1976).

18. International Commission of Radiation Protection and measurements. Protection of the Patient in Nuclear Medicine (and Statement from the 1987 Como Meeting of ICRP). ICRP Publication 52. Ann. ICRP 17(1987).

19. National Council on Radiation Protection. Report 85. Mammography - a user's guide. (1986).

20. Institute of Physics and Engineering in Medicine. Report 88. Guidance on the Establishment and Use of Diagnostic Reference Levels for Medical X-ray Examinations. (2004).

21. Perry, N., Broeders, M., De Wolf, C., Törnberg, S., Holland, R., Von Karsa, L. and Puthaar, E. European guidelines for quality assurance in breast cancer screening and diagnosis Fourth Edition. Luxembourg office for official publications of the European Communities (2006).

22. Perry, N. and Schouten, J. European guidelines for quality assurance in mammography screening. Office for official publications of the European communities) (2001) ISBN 9289411457.

23. Zoetelief, J., Fitzgerald, M., Leitz, W. and Säbel, M. European protocol on dosimetry in mammography. Office for Official Publications of the European Communities) (1996) ISBN 9282772896.

24. International Atomic Energy Agency. Dosimetry in diagnostic radiology: an international code of practice. (Vienna: International Atomic Energy Agency) (2007) ISBN 92-0-115406-2.

25. Kereiakes, J. G. and Rosenstein, M. Handbook of radiation doses in nuclear medicine and diagnostic X-ray. CRC Press Boca Raton, FL) (1980) ISBN 0849332451.

26. Dance, D. The Monte Carlo calculation of integral radiation dose in xeromammography. Physics in Medicine and Biology. 25, 25 (1980).

27. Dance, D. Monte-Carlo calculation of conversion factors for the estimation of mean glandular breast dose. Physics in medicine and biology. 35, 1211 (1990).

28. Rosenstein, M., Andersen, L. W. and Warner, G. G. Handbook of glandular tissue doses in mammography. US Department of Health and Human Services, Public Health Service, Food and Drug Administration, Center for Devices and Radiological Health) (1985).

29. Wu, X., Barnes, G. T. and Tucker, D. M. Spectral dependence of glandular tissue dose in screen-film mammography. Radiology. 179, 143-148 (1991).

30. Fabiszewska, E., Jankowska, K., Grabska, I. and Skrzynski, W. Individual doses for women undergoing screening mammography examinations in Poland in 2007. Journal of Radiological Protection. 31, 467-75 (2011).

31. Khoury, H. J., Barros, V. S. and Lopes, C. Evaluation of patient dose for mammography in Pernambuco, Brazil. Radiation Protection Dosimetry. 115, 337-339 (2005).

32. Seeram, E. and Brennan, P. C. Diagnostic reference levels in radiology. Radiologic Technology. 77, 373-384 (2006).

33. Liberati, A., Altman, D. G., Tetzlaff, J., Mulrow, C., Gøtzsche, P. C., Ioannidis, J. P. A., Clarke, M., Devereaux, P. J., Kleijnen, J. and Moher, D. The PRISMA statement for reporting systematic reviews and meta-analyses of studies that evaluate healthcare interventions: explanation and elaboration. BMJ. 339(2009).

34. Moher, D., Liberati, A., Tetzlaff, J. and Altman, D. G. Preferred reporting items for systematic reviews and meta-analyses: the PRISMA statement. British Medical Journal. 339(2009).

35. Avramova-Cholakova, S. and Vassileva, J. A survey of the state of mammography practice in Bulgaria. Radiation Protection Dosimetry. 147, 184-6 (2011).

36. Baldelli, P., McCullagh, J., Phelan, N. and Flanagan, F. Comprehensive dose survey of breast screening in Ireland. Radiation Protection Dosimetry. 145, 52-60 (2011).

37. Baldelli, P., McCullagh, J. B., Phelan, N. and Flanagan, F. Results of Comprehensive Dose Survey for Mammography. (Berlin: Springer-Verlag Berlin) (2010).

38. Bor, D., Akyol, O. and Olgar, T. Performance measurements of mammographic systems. Radiation Protection Dosimetry. 129, 165-169 (2008).

39. Borg, M., Badr, I. and Royle, G. J. Mammography equipment performance, image quality and mean glandular dose in Malta. Radiation Protection Dosimetry. 156, 168-83 (2013).

40. Chevalier, M., Moran, P., Ten, J. I., Soto, J. M. F., Cepeda, T. and Vano, E. Patient dose in digital mammography. Medical Physics. 31, 2471-2479 (2004).

41. Hauge, I. H. R., Bredholt, K. and Olerud, H. M. New diagnostic reference level for full-field digital mammography units. Radiation Protection Dosimetry. 157, 181-192 (2013).

42. Michielsen, K., Jacobs, J., Lemmens, K., Nens, J., Zoetelief, J., Faulkner, K. and Bosmans, H. Results of a European dose survey for mammography. Radiation Protection Dosimetry. 129, 199-203 (2008).

43. Moran, P., Chevalier, M., Ten, J. I., Sot, J. M. F. and Vano, E. A survey of patient dose and clinical factors in a full-field digital mammography system. Radiation Protection Dosimetry. 114, 375-379 (2005).

44. O'Leary, D. and Rainford, L. A comparison of mean glandular dose diagnostic reference levels within the all-digital Irish National Breast Screening

Programme and the Irish Symptomatic Breast Services. Radiation Protection Dosimetry. 153, 300-8 (2013).

45. Smans, K. Towards a proposition of a diagnostic (dose) reference level for mammographic acquisitions in breast screening measurements in Belgium. Radiation Protection Dosimetry. 117, 321-326 (2006).

46. Young, K. C., Burch, A. and Oduko, J. M. Radiation doses received in the UK Breast Screening Programme in 2001 and 2002. British Journal of Radiology. 78, 207-218 (2005).

47. Zdesar, U. Reference levels for image quality in mammography. Radiation Protection Dosimetry. 129, 170-2 (2008).

48. Asada, Y., Suzuki, S., Minami, K. and Shirakawa, S. Results of a 2011 national questionnaire for investigation of mean glandular dose from mammography in Japan. Journal of radiological protection : official journal of the Society for Radiological Protection. 34, 125-132 (2014).

49. Bahreyni Toossi, M. T., Zare, H., Bayani Roodi, S., Hashemi, M., Akbari, F. and Malekzadeh, M. Towards proposition of a diagnostic reference level for mammographic examination in the greater Khorasan Province, Iran. Radiation Protection Dosimetry. 155, 96-9 (2013).

50. Hwang, Y. S., Tsai, H. Y., Chen, C. C., Chia, S. H., Lin, J. H., Wan, Y. L., Hsu, G. C., Chen, C. P. and Liu, H. L. Survey of Radiation Dose, Image Quality and Equipment Performance of Mammography Units in Taiwan. (New York: Springer) (2009).

51. Jamal, N., Ng, K. H. and McLean, D. A study of mean glandular dose during diagnostic mammography in Malaysia and some of the factors affecting it. British Journal of Radiology. 76, 238-245 (2003).

52. Kawaguchi, A., Matsunaga, Y., Otsuka, T. and Suzuki, S. Patient investigation of average glandular dose and incident air kerma for digital mammography. Radiological Physics and Technology. 7, 102-108 (2014).

53. Geeraert, N., Klausza, R. and Mullera, S. Breast characteristics and dosimetric data in X-ray mammography A large sample worldwide survey. Bonn: IAEA conference. 2012.

54. Thiele, D. L., Irvine, M., Want, D. and Bernardo, M. Diagnostic reference levels for mammography in BreastScreen Queensland. Australasian physical & engineering sciences in medicine / supported by the Australasian College of Physical Scientists in Medicine and the Australasian Association of Physical Sciences in Medicine. 34, 415-8 (2011).

55. Spelic, D., Kaczmarek, R., Hilohi, M. and Belella, S. United States radiological health activities: inspection results of mammography facilities. Biomedical imaging and intervention journal. 3, 1-16 (2007).

56. Ogundare, F. O., Odita, A. N., Obed, R. I. and Balogun, F. A. Mean glandular doses for women undergoing mammographic breast screening in Oyo state, Nigeria. Radiography. 15, 327-332 (2009).

57. Hendrick, R., Bassett, L., Botsco, M., Deibel, D., Feig, S., Gray, J., Haus, A., Heinlein, R., Kitts, E. and McCrohan, J. Mammography quality control manual. Reston, Va: American College of Radiology(1999).

58. Law, J., Dance, D., Faulkner, K., Fitzgerald, M., Ramsdale, M., Robinson, A. and Hendee, W. The commissioning and routine testing of mammographic X-ray systems (IPSM Report 59/2). American Journal of Roentgenology. 164, 842-842 (1995).

59. Seradour, B., Heid, P. and Esteve, J. Comparison of direct digital mammography, computed radiography, and film-screen in the French national breast cancer screening program. AJR Am J Roentgenol. 202, 229-36 (2014).

60. Chiarelli, A. M., Edwards, S. A., Prummel, M. V., Muradali, D., Majpruz, V., Done, S. J., Brown, P., Shumak, R. S. and Yaffe, M. J. Digital compared with screen-film mammography: performance measures in concurrent cohorts within an organized breast screening program. Radiology. 268, 684-93 (2013).

61. Warren, L. M., Mackenzie, A., Cooke, J., Given-Wilson, R. M., Wallis, M. G., Chakraborty, D. P., Dance, D. R., Bosmans, H. and Young, K. C. Effect of image quality on calcification detection in digital mammography. Medical Physics. 39, 3202-13 (2012).

62. Ruschin, M., Timberg, P., Bath, M., Hemdal, B., Svahn, T., Saunders, R. S., Samei, E., Andersson, I., Mattsson, S., Chakrabort, D. P. et al. Dose dependence of mass and microcalcification detection in digital mammography: free response human observer studies. Medical Physics. 34, 400-7 (2007).

63. Wu, X., Gingold, E. L., Barnes, G. T. and Tucker, D. M. Normalized average glandular dose in molybdenum target-rhodium filter and rhodium target-rhodium filter mammography. Radiology. 193, 83-89 (1994).

64. Vassileva, J., Dimov, A., Slavchev, A. and Karadjov, A. Bulgarian experience in the establishment of reference dose levels and implementation of a quality control system in diagnostic radiology. Radiation Protection Dosimetry. 117, 131-134 (2006).

65. Tsai, H. Y., Chong, N. S., Ho, Y. J. and Tyan, Y. S. Evaluation of depth dose and glandular dose for digital mammography. Radiation Measurements. 45, 726-728 (2010).

66. Dance, D. R., Skinner, C. L., Young, K. C., Beckett, J. R. and Kotre, C. J. Additional factors for the estimation of mean glandular breast dose using the UK mammography dosimetry protocol. Physics in Medicine and Biology. 45, 3225-3240 (2000).

67. Dance, D. R., Young, K. C. and van Engen, R. E. Further factors for the estimation of mean glandular dose using the United Kingdom, European and IAEA breast dosimetry protocols. Physics in Medicine and Biology. 54, 4361-72 (2009).

68. Dance, D. R., Young, K. C. and van Engen, R. E. Estimation of mean glandular dose for breast tomosynthesis: factors for use with the UK, European and IAEA breast dosimetry protocols. Physics in Medicine and Biology. 56, 453-71 (2011).

69. Tomon, J. J., Johnson, T. E., Swenson, K. N. and Schauer, D. A. Applicability of ACR breast dosimetry methodology to a digital mammography system. Medical Physics. 33, 799-807 (2006).

70. Perry N, B. M., de Wolf C, Törnberg S, Holland R, von Karsa L Executive summary. In: European guidelines for quality assurance in breast cancer

screening and diagnosis. Fourth edition, Supplements. European Commission, Office for Official Publications of the European Union, Luxembourg, pp XIV–XX (2013).

71. European Reference Organisation for Quality Assured Breast Screening and Diagnostic Services. European guidelines (5th edition). 2013 [Accessed on 26 June 2014]; Available from: http://www.euref.org/european-guidelines/5th-edition.

72. Kanal, K., Krupinski, E., Berns, E., Geiser, W., Karellas, A., Mainiero, M., Martin, M., Patel, S., Rubin, D., Shepard, J. et al. ACR–AAPM–SIIM Practice Guideline for Determinants of Image Quality in Digital Mammography. Journal of Digital Imaging. 26, 10-25 (2013).

73. (Luxembourg: CEC) EUR 16263. European protocol on dosimetry in mammography. (1996).

74. International Atomic Energy Agency. Quality Assurance Programme for Digital Mammography. Human Health Series. No. 17. (Vienna: IAEA) (2011).

75. International Atomic Energy Agency. Quality Assurance Programme for Screen Film Mammography. Human Health Series. No. 2. (Vienna: IAEA) (2009).

76. Moore, A. The Commissioning and Routine Testing of Mammographic X-ray Systems: A Protocol Produced by a Working Party of the Diagnostic Breast Screening Quality Assurance Coordinating Group for Physics. Institute of Physics and Engineering in Medicine) (2005) ISBN 1903613213.

Chapter Three

Diagnostic Reference Levels for digital mammography in New South Wales

Section 3.2 of this chapter has been published as:

Suleiman, M. E., McEntee, M. F., Cartwright, L., Diffey, J., & Brennan, P. C. (2016). Diagnostic reference levels for digital mammography in New South Wales. ***Journal of Medical Imaging and Radiation Oncology*****, n/a-n/a. doi:10.1111/1754-9485.12540**

[Published copy is available in Appendix 7.3]

I had had substantial contribution to this work. I designed the study, collected and analysed the data, was the primary author, wrote and edited each draft of the manuscript.

3.1 Bridging section

The literature [1] shows that many countries have established DRLs for mammography, however, this is not the case for Australian mammography services. There was a single study published in 2011 however, [2] this was based on phantom data collected from Queensland hospitals. The new ICRP publication [3] recommends that a patient survey is critically important for establishing DRLs and should not be replaced by phantom surveys, it is stated in table 2.1 in the ICRP document that: "Patient survey to set DRL and phantom measurements as standard dose comparator" [3]. Furthermore, the ICRP recommends that DRLs should be updated every three to five years, so even with this previous work, an update is now required [3]. Consequently, the first of the three aims of this chapter was to recommend DRLs for digital mammography in Australia using patient data.

The definition of DRLs is based on the comparison between X-ray systems. In mammography, MGD is used to describe breast absorbed dose. It is well known that MGD depends on the compressed thickness of the irradiated breast, hence, when countries or screening services establish DRLs using different "standard patient" sizes, the comparability of DRLs becomes ineffective. Wide variations in the methods and compressed breast thicknesses used to establish DRLs have been shown in the literature as detailed in chapter 2 of this thesis. In other modalities, such as Radiography, Fluoroscopy, CT and Paediatric examinations, patients are categorised by weight or age range, therefore, the effectiveness of using one breast thickness to establish DRLs should be explored. The published journal article titled: Diagnostic reference levels for digital mammography in New South Wales [4], recommends Australian DRLs stratified by breast thickness ranges, such a method provides the necessary information to make national and international comparisons of DRLs more effective. The second aim of this chapter therefore, was to explore whether DRLs should be stratified by compressed breast thickness.

Furthermore, my published article [4] showed a wide variation in MGD delivered using different detector technologies. The importance of these results is around highlighting the need to stratify DRLs per detector technology as new mammography units, namely photon counting technology (PCT), deliver much lower doses to the patients. PCT delivers less than half the doses of flat panel detectors for CR and DR

technologies. When these three technologies exist in one screening programme, PCT should always be in the lower percentile and will therefore never be targeted for optimisation. Hence the last aim of this chapter was to explore the effect of different detector technologies on the effectiveness of DRLs and whether DRLs should be stratified by detector technology.

The journal article titled: "Diagnostic reference levels for digital mammography in New South Wales" has been published in the journal of Medical Imaging and Radiation Oncology in 2016 [4]. Results of this study were also presented at two conferences: The Engineering and Physical Sciences in Medicine 2016 in Sydney titled "Diagnostic reference levels in digital mammography: time for a new paradigm", and in the European council of radiology in Vienna 2017 titled "Radiation doses received by women attending BreastScreen NSW in 2014".

3.1.1 **Detailed methodology**

Due to word limit and figures restrictions in the publishing processes, detailed information on the methods have not been presented in the papers published. Namely, the equations utilised in the calculations of MGD. A Microsoft Excel workbook was developed to automate the calculation process for the complete set of mammograms. Two medical physicists then verified the workbook to ensure the accuracy of calculations. Table 3.1 shows the DICOM header information extracted from each mammogram, table 3.2 shows an example of medical physics report for a mammography unit. Figure 3.1 presents the calculation processes and equations utilised in the Excel workbook.

It is important to highlight the reason behind my choice of calculating MGD using Dance et al. method rather than extracting the Organ Dose from DICOM headers. Although the Organ Dose tag for digital mammography X-ray images (0040,0316) is equivalent to MGD, the data sample included was acquired from different mammography units, some of which were CR units. The CR units had no Organ Dose values in the DICOM headers. Hence, I decided to calculate MGD from first principles for all manufacturers in order to make use of the complete data set and to ensure consistency.

Table 3.1: Information extracted from the DICOM headers of digital mammograms, used in the calculation of MGD [4].

Information	DICOM tag
Patient age	0019,1052
Body Part thickness	0018,11A0
Implant present	0028,1300
Patient orientation	0020,0020
Image laterality	0020,0062
Tube voltage (kVp)	0018,0060
Exposure (mAs)	0018,1152
Anode target material	0018,1191
Filter material	0018,7050
Exposure control mode	0018,7060
Detector ID	0018,700A
Manufacturer's Model Name	0008,1090
Manufacturer	0008,0070

Table 3.2: Example of the medical physics report for a mammography unit.

	Site	Site 1
2 cm PMMA	Testing Date	01/01/00
	SID (source to image distance mm)	660
	Image to support distance (mm)	20
	kV	25
	T/F	Mo/Mo
	HVL (mm Al)	0.339
	Set mAs	22.5
	Measured Dose (mGy)	1.735
	Detector Position above support (mm)	7
ACR Phantom	kV	27
	T/F	Mo/Rh
	HVL (mm Al)	0.432
	Set mAs	45
	Measured Dose (mGy)	3.574
	Detector Position above support (mm)	7
6 cm PMMA	kV	31
	T/F	Rh/Rh
	HVL (mm Al)	0.475
	Set mAs	50
	Measured Dose (mGy)	5.475
	Detector Position above support (mm)	7
6 cm PMMA in mag mode	kV	32
	T/F	Rh/Rh
	HVL (mm Al)	0.488
	Set mAs	71
	Measured Dose (mGy)	21.62
	Detector Position above support (mm)	280.3333333
Additional HVL measurements	kV	
	T/F	
	HVL (mm Al)	
	Set mAs	
	Measured Dose (mGy)	
	Detector Position above support (mm)	

3.1.2 MGD calculation

MGD is calculated using Dance et al. method [5-7], which utilises the following equation:

MGD = gcs * K ---1

Where:

K is Incident air kerma at the surface of the breast without backscatter,

g is the conversion factor that accounts for a 50:50 breast model and is tabulated depending on HVL and CBT (Table 3.3), its value is calculated through interpolation.

c is a conversion factor to account for glandularities different from the 50:50 model and is tabulated depending on age, HVL and CBT (Tables 3.4 and 3.5), its value is also calculated through interpolation.

s is the conversion factor accounting for different X-ray spectra and is tabulated depending on Anode /filter combination (Table 3.6).

Two calculation procedures were followed for the MGD estimation, QA data and the conversion factors. Figure 3.1 shows the steps and equations followed, which are explained next.

Table 3.3: g-factors (mGy/mGy) for breast thicknesses of 2-11 cm and the HVL range 0.30-0.60 mm Al [5-7].

CBT	HVL (mm Al)						
	0.3	0.35	0.4	0.45	0.5	0.55	0.6
20	0.3900	0.4330	0.4730	0.5090	0.5430	0.5730	0.5870
30	0.2740	0.3090	0.3420	0.3740	0.4060	0.4370	0.4660
40	0.2070	0.2350	0.2610	0.2890	0.3180	0.3460	0.3740
45	0.1830	0.2080	0.2320	0.2580	0.2850	0.3110	0.3390
50	0.1640	0.1870	0.2090	0.2320	0.2580	0.2870	0.3100
60	0.1350	0.1540	0.1720	0.1920	0.2140	0.2360	0.2610
70	0.1140	0.1300	0.1450	0.1630	0.1770	0.2020	0.2240
80	0.0980	0.1120	0.1260	0.1400	0.1540	0.1750	0.1950
90	0.0859	0.0981	0.1106	0.1233	0.1357	0.1543	0.1723
100	0.0763	0.0873	0.0986	0.1096	0.1207	0.1375	0.1540
110	0.0687	0.0786	0.0887	0.0988	0.1088	0.1240	0.1385

Table 3.4: c-factors for average breasts for women in age group 40 to 49 [5-7].

CBT	HVL (mm Al)						
	0.30	0.35	0.40	0.45	0.50	0.55	0.60
20	0.885	0.891	0.900	0.905	0.910	0.914	0.919
30	0.894	0.898	0.903	0.906	0.911	0.915	0.918
40	0.940	0.943	0.945	0.947	0.948	0.952	0.955
50	1.005	1.005	1.005	1.004	1.004	1.004	1.004
60	1.080	1.078	1.074	1.074	1.071	1.068	1.066
70	1.152	1.147	1.141	1.138	1.135	1.130	1.127
80	1.220	1.213	1.206	1.205	1.199	1.190	1.183
90	1.270	1.264	1.254	1.248	1.244	1.235	1.225
100	1.295	1.287	1.279	1.275	1.272	1.262	1.251
110	1.294	1.290	1.283	1.281	1.273	1.264	1.256

Table 3.5: c-factors for average breasts for women in age group 50 to 64 [5-7].

CBT	HVL (mm Al)						
	0.3	0.35	0.4	0.45	0.5	0.55	0.6
20	0.885	0.891	0.900	0.905	0.910	0.914	0.919
30	0.925	0.929	0.931	0.933	0.937	0.940	0.941
40	1.000	1.000	1.000	1.000	1.000	1.000	1.000
50	1.086	1.082	1.081	1.078	1.075	1.071	1.069
60	1.164	1.160	1.151	1.150	1.144	1.139	1.134
70	1.232	1.225	1.214	1.208	1.204	1.196	1.188
80	1.275	1.265	1.257	1.254	1.247	1.237	1.227
90	1.299	1.292	1.282	1.275	1.270	1.260	1.249
100	1.307	1.298	1.290	1.286	1.283	1.272	1.261
110	1.306	1.301	1.294	1.291	1.283	1.274	1.266

Table 3.6: s-factors for clinically used spectra [5-7].

A/F	**S factor**
Mo/Mo	1.000
Mo/Rh	1.017
Rh/Rh	1.061
Rh/Al	1.044
W/Rh	1.042
W/Ag	1.042
W/Al	1.05

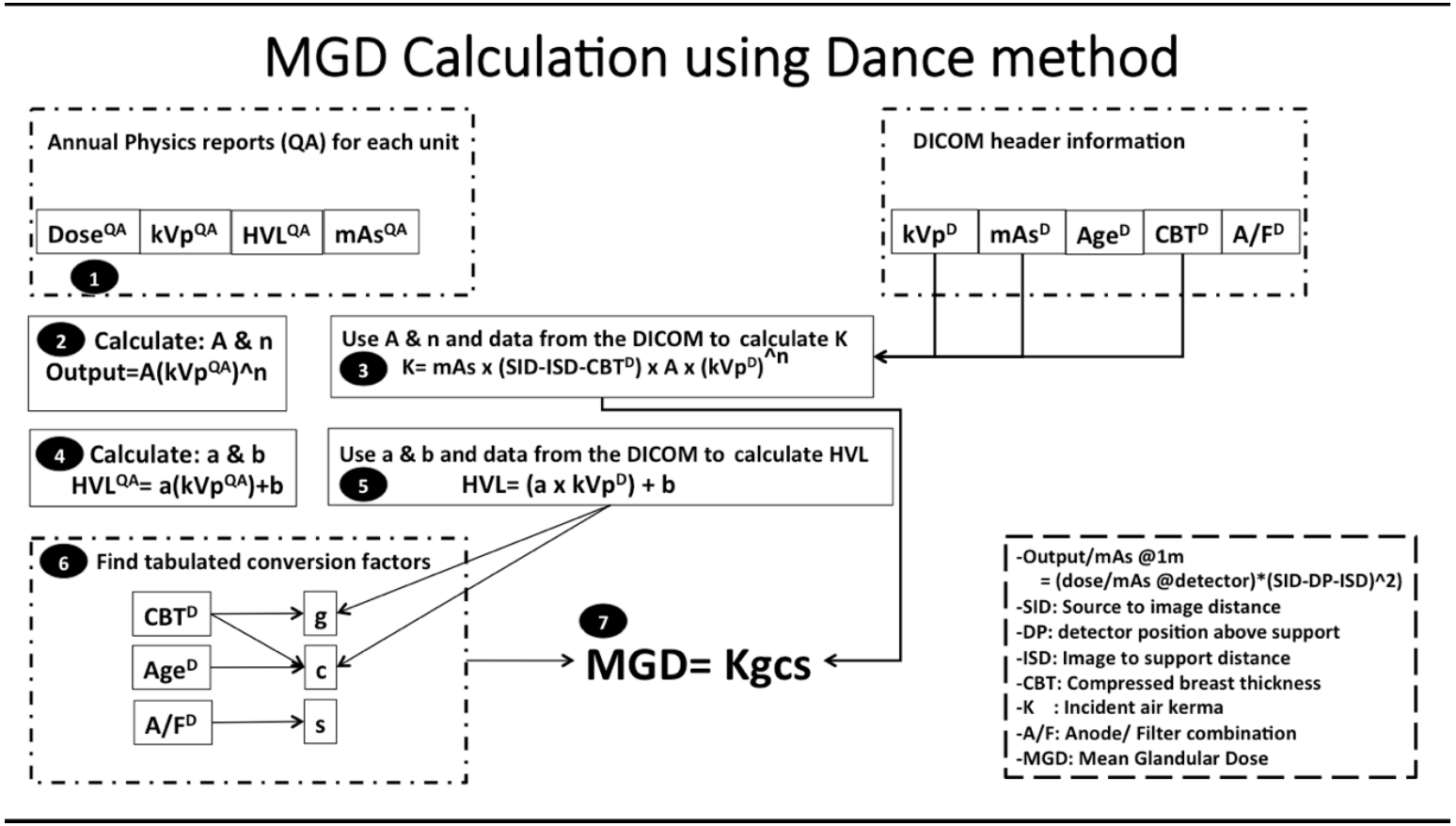

Figure 3.1: Dance calculation method: input information that needs to be available for the calculation of MGD, the steps taken to calculate MGD for a mammogram and the equations utilised for that process [8].

QA report data

The first step is to use the data from the QA report within equations 2, 3 and 4 to calculate the constants that will be used later to estimate HVL and K used for the image acquisition. For each anode/filter combination, the QA reports provide the following information:

$Dose^{QA}$: the dose to the phantom

mAs^{QA}: milliampere value

kVp^{QA}: kilovolt peak value

HVL^{QA}: half value layer measured at the detector

$HVL^{QA} = a \times kVp^{QA} + b$ --- 2

Where: 'a' and 'b' are the constants we need to calculate using the QA data, the calculation is a simple linear equation solved for the variables using a minimum two sets of data.

For i =1 to n-1 (n: number of test points)

$a = \text{Average } (HVL^{QA}_i - HVL^{QA}_{i+1})/(kVp^{QA}_i - kVp^{QA}_{i+1})$

$b = \text{Average } (HVL_i^{QA} - a*kVp_{i+1}^{QA})$

P^{QA} = (dose^{QA}/mAs^{QA} at detector) x (SID^{QA}-DP^{QA}-ISD^{QA})^2) --- 3

Where: P^{QA} is the output per mAs calculated at 1 m from the detector

SID^{QA} is the source to image distance

DP^{QA} is the detector position above support

ISD^{QA} is the Image to support distance

$P^{QA} = A \times (kVp^{QA})^n$ --- 4

Where: 'A' and 'n' are the constants we need to calculate using the QA data, the calculation is a simple exponential equation solved for the variables using a minimum two sets of data.

$n = \text{Average } [\text{Log}(P_i/P_{i+1})/\text{Log}(kVp^{QA}_i/kVp^{QA}_{i+1})]$

$A = \text{Average } [P_i/kV_i^n]$

Solving equations 1, 2 and three we will have the values for the constants a, b, A, and n, these will be used in the next step to calculate HVL and K

DICOM header data

DICOM header information (kVp^D, mAs^D, Age^D, CBT^D, and $Anode/filter^D$ combination) were extracted to a CSV format file using a third-party software [9]. Equations 5 and 6 are used to calculate HVL and K respectively.

To estimate HVL for each image we use equation 5

$$\mathbf{HVL^D = a \times kVp^D + b \quad --- 5}$$

Where: HVL^D is the HVL used for the image acquisition (which we will calculate). kVp^D is the kVp value used for the image acquisition. The constants a and b were calculated in earlier step.

$$\mathbf{K = mAs^D \times (SID^D - SDI^D - CBT^D) \times A \times (kVp^D)^{\wedge n} \quad --- 6}$$

Where: SID^D is the source to image distance during the image acquisition.

DP^D is the detector position above support during the image acquisition.

ISD^D is the Image to support distance during the image acquisition.

Conversion factors

g and c factors are calculated using linear interpolation, two sets of values for HVL and CBT were needed for equations 7-9, one lower and one higher than HVL^D and CBT^D.

$gc_{11.5} = gc_{11} - (gc_{11} - gc_{12}) / (CBT_2 - CBT_1) * (CBT - CBT_1)$ --- 7

$gc_{21.5} = gc_{21} - (g_{21} - gc_{22}) / (CBT_2 - CBT_1) * (CBT - CBT_1)$ ---8

$gc = gc_{11.5} + (gc_{21.5} - gc_{11.5}) / (HVL_2 - HVL_1) * (HVL - HVL_1)$ ---9

Where:

HVL_1 and CBT_1, are value, in tables 3.4, 3.5 and 3.6, that are lower than HVL^D and CBT^D for the mammogram.

HVL_2 and CBT_2, are the value in, tables 3.4, 3.5 and 3.6, that are higher than HVL^D and CBT^D for the mammogram.

gc_{11} is (g x c) extracted from tables 3.4, 3.5 and 3.6 using HVL_1 and CBT_1 and age^D.

gc_{12} is (g x c) extracted from tables 3.4, 3.5 and 3.6 using HVL_1 and CBT_2 and age^D.

gc_{21} is (g x c) extracted from tables 3.4, 3.5 and 3.6 using HVL_2 and CBT_1 and age^D.

gc_{22} is (g x c) extracted from tables 3.4, 3.5 and 3.6 using HVL_2 and CBT_2 and age^D.

$gc_{11.5}$ is (g x c) interpolated using equation 7 and gc_{11} and gc_{21}.

$g_{22.5}$ is (g x c) interpolated using equation 8 and gc_{12} and gc_{22}.

s factor is extracted from table 3.6 using the anode / $filter^D$ combination used for the image acquisition. Figure 3.2 shows an example of the calculations used.

1: Annual Physics reports (QA) for each unit (example)

Phantom size	20mm	42mm	60mm
SID (mm)	660	660	660
ISD (mm)	20	20	20
kV	26	32	35
A/F	W/Al	W/Al	W/Al
HVL (mm Al)	0.354	0.451	0.494
mAs	10	10	20
Measured dose (mGy)	1.037	1.710	4.097
DP (mm)	12	12	12

Output@1m = (dose/mAs @detector) x (SID-ISD-DP)$^{\wedge 2}$
Output@1m = A x (kVp)^n
A= 0.028995962, n= 2.24

HVL= (a x kV) +b
a= 0.015351852, b= - 0.042907407

2: Exposure factors extracted from each mammogram DICOM header

A/F	Age	CBT(mm)	kV	mAs
W/Al	53	61	32	15.28

HVL= (a x kV) + b
HVL= 0.45

Find tabulated conversion factors using interpolation (Dance et al 2009):
g: depends on HVL & CBT
c: depends on HVL, CBT, & Age
s: depends on A/F

K= mAs x (SID-ISD-CBT) x A x (kV)$^{\wedge n}$
K= 3.084 mGy

SID: Source to image distance
ISD: Image to support distance
DP: detector position above support
A/F: anode filter combination
K: Incident air Kerma

3: MGD= Kgcs
MGD= 0.705 mGy

Figure 3.2: Example for the calculation Mean Glandular Dose (MGD) using Dance et al formula.

Further estimations

Some QA reports had missing tests for certain anode / filter combinations, in the sense that in such centre, an anode / filter combination was tested for one phantom thickness only. In these cases, the method of Robson et al. [10] was used to estimate HVL and K, which method uses a phantom test values when kVp = 28 kV. Nonetheless, for other kVp values it seems to give a good estimation of HVL and K, Robson et al. method follows the following formulas:

$HVL = a(kVp)^2 + b\,(kVp) + c$ --- 10

$\log_{10}(K) = n \times \log_{10}(kVp) + \log_{10} \times A$ ---11

The constants a, b, and n are provided in table 3.7, however, the constants c and A are calculated using K and kVp values from the QA reports data for the associated anode / filter combinations.

Table 3.7: Calculated values of the constants n, a, and b for a range of anode / filter combinations [10].

Target/Filter	Filter thickness	n	a	b
Mo/30 μm Mo	36.1 μm	3.06	-0.000326	0.0273
Mo/25 μm Rh	29.9 μm	3.24	-0.000624	0.0445
Rh/25 μm Rh	29.9 μm	3.03	-0.000514	0.0425
W/50 μm Rh	58.9 μm	1.96	-0.000539	0.0403
Rh/1.0 mm Al	1.20 μm	4.39	-0.00113	0.0909
Mo/1.0 mm Al	1.20 mm	4.23	-0.000775	0.0593
W/Ag [11]	35.00 mm	3.1521	-0.0009	0.0733

3.1.3 **Results**

The published paper did not include some of the figures and data resulting from our calculations, hence these are presented here. Figures 3.3 to 3.11 shows the variations in median MGD between centres when MGD is stratified according to CBTs. Figures 3.3 to 3.11 also shows the variations in median MGD for different detector technologies; different colours mark different detector technologies. Such variations triggered the use of stratified DRLs according to CBT and detector technology as explained in the published paper.

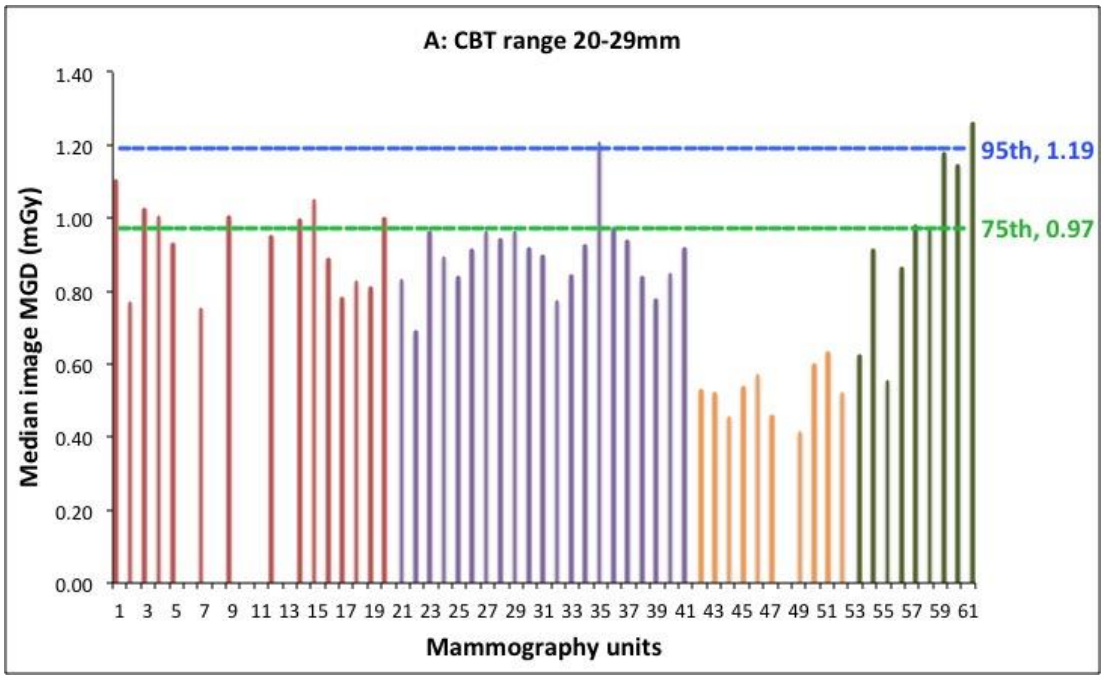

Figure 3.3: Median MGD, 75thand 95th percentiles for centre included in the study, for CBT range 20-29 mm, color coded for different mammography unit make (with detector technologies). Red: GE, Purple: Hologic, Orange: Phillips, Green: Fujifilm.

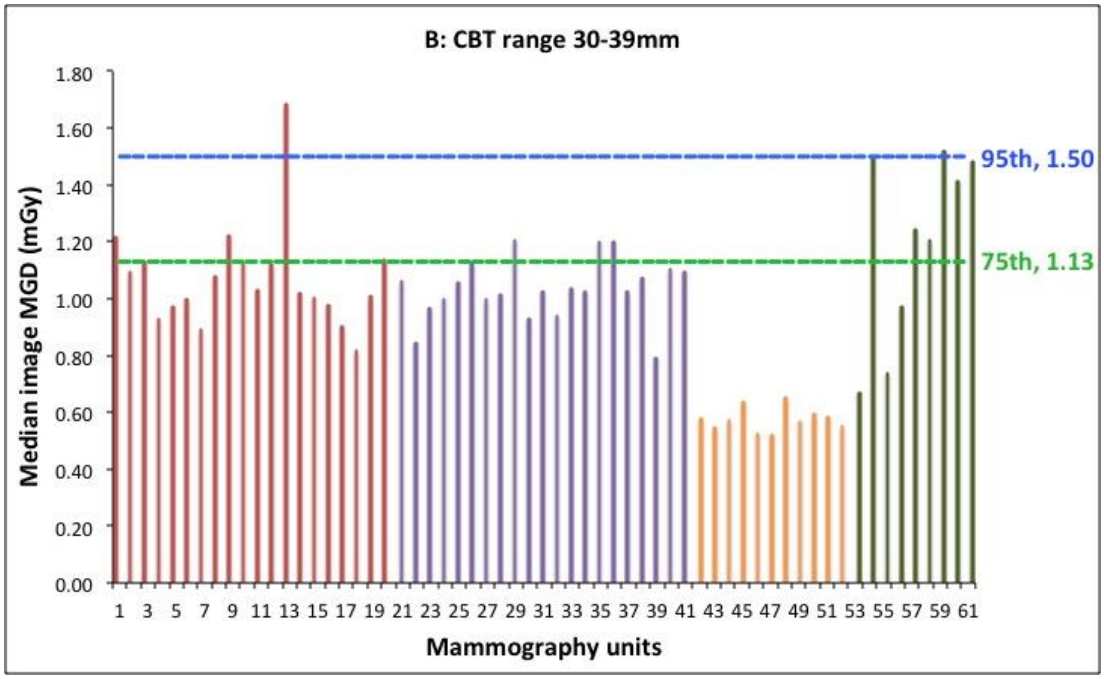

Figure 3.4: Median MGD, 75thand 95th percentiles for centre included in the study, for CBT range 30-39 mm, color coded for different mammography unit make (with detector technologies). Red: GE, Purple: Hologic, Orange: Phillips, Green: Fujifilm.

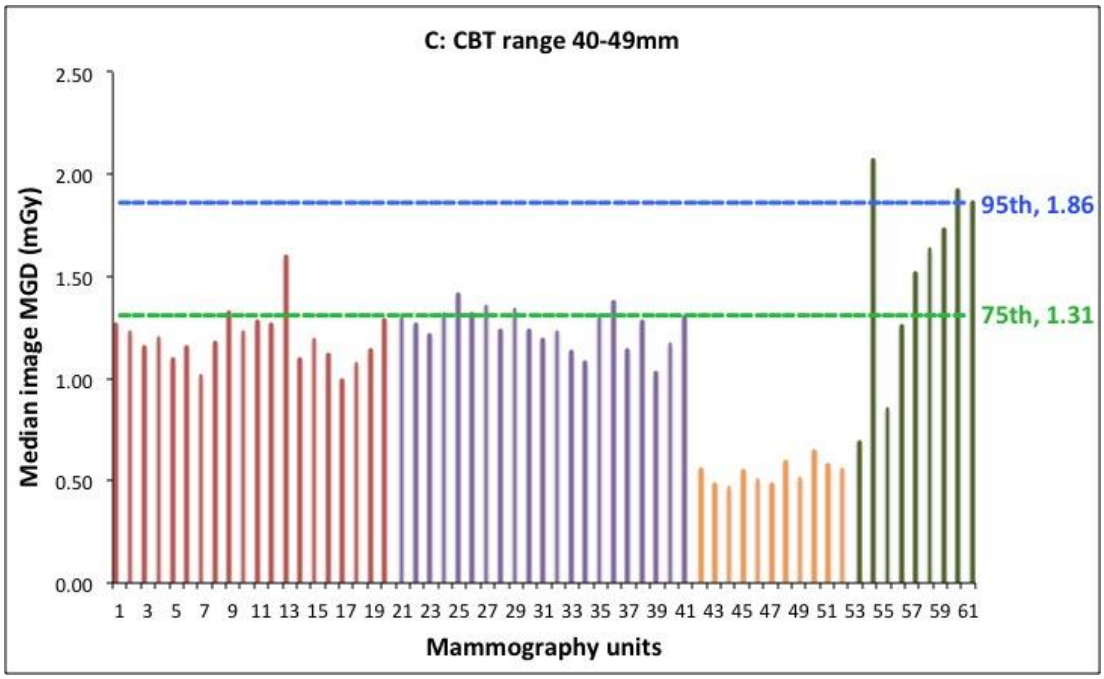

Figure 3.5: Median MGD, 75thand 95th percentiles for centre included in the study, for CBT range 40-49 mm, color coded for different mammography unit make (with detector technologies). Red: GE, Purple: Hologic, Orange: Phillips, Green: Fujifilm.

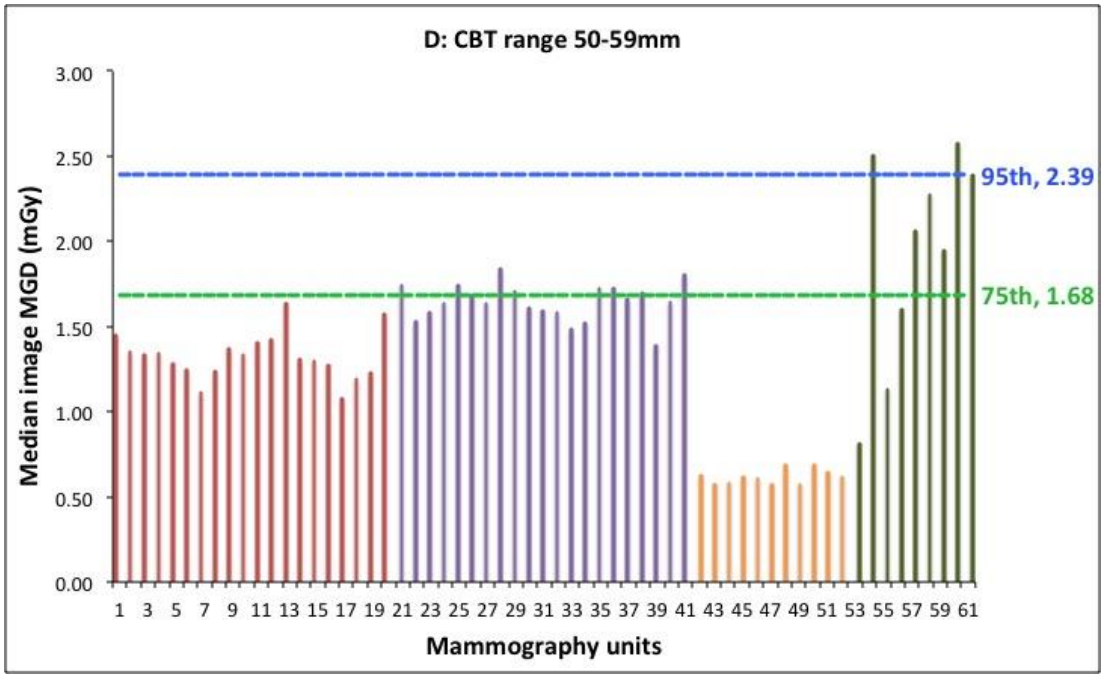

Figure 3.6: Median MGD, 75thand 95th percentiles for centre included in the study, for CBT range 50-59 mm, color coded for different mammography unit make (with detector technologies). Red: GE, Purple: Hologic, Orange: Phillips, Green: Fujifilm.

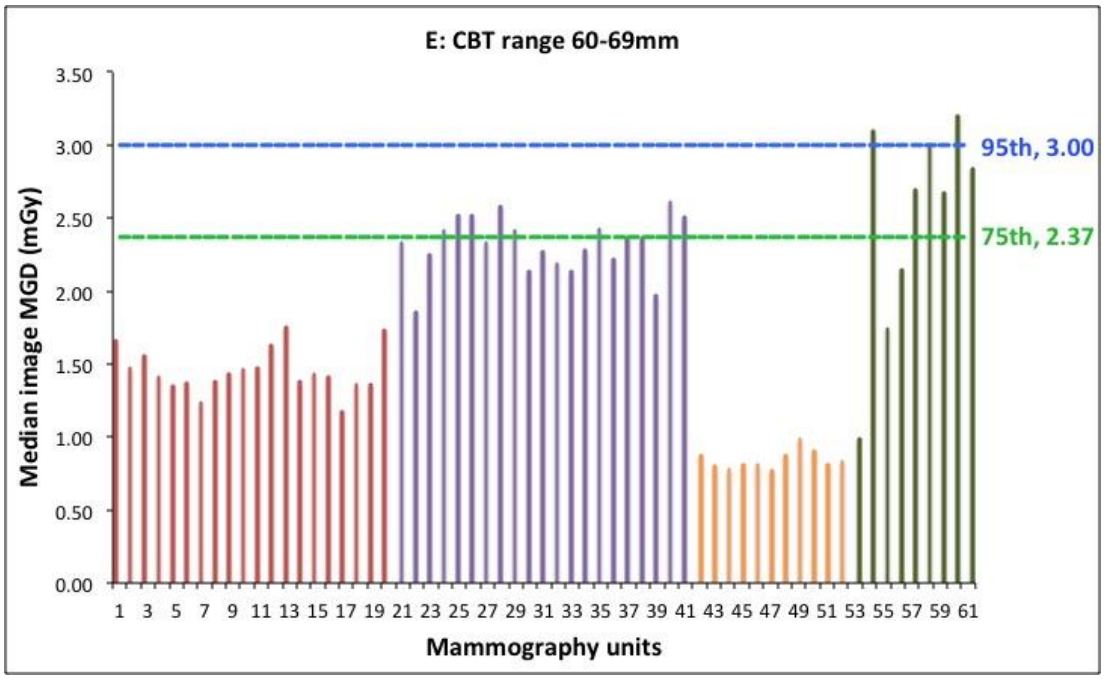

Figure 3.7: Median MGD, 75thand 95th percentiles for centre included in the study, for CBT range 60-69 mm, color coded for different mammography unit make (with detector technologies). Red: GE, Purple: Hologic, Orange: Phillips, Green: Fujifilm.

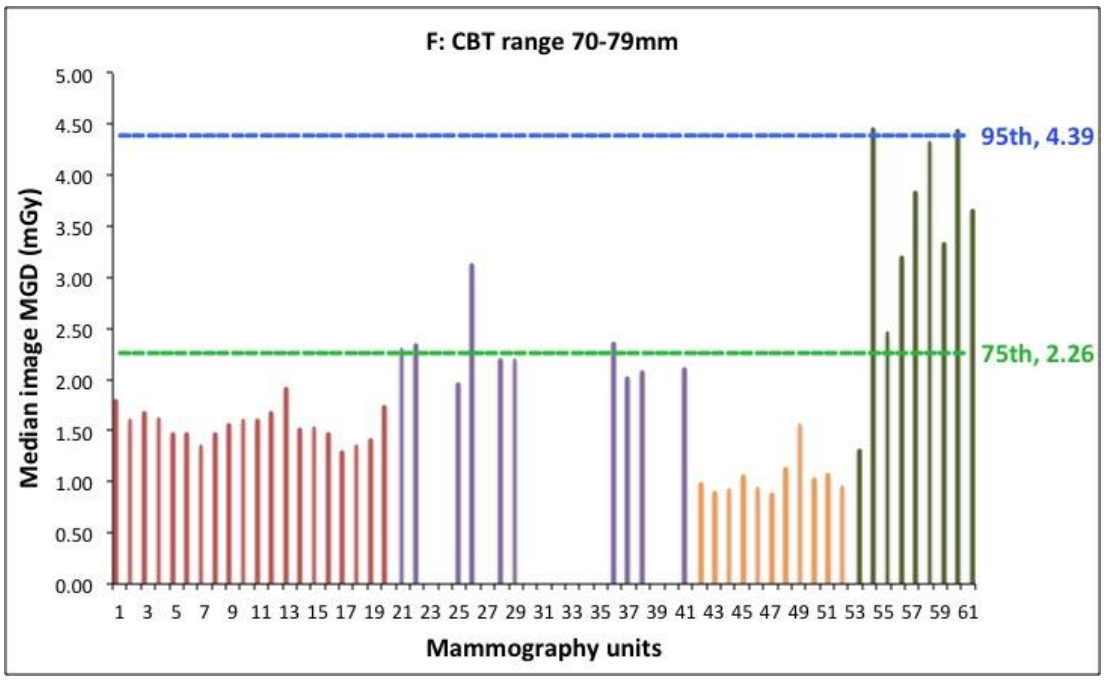

Figure 3.8: Median MGD, 75thand 95th percentiles for centre included in the study, for CBT range 70-79 mm, color coded for different mammography unit make (with detector technologies). Red: GE, Purple: Hologic, Orange: Phillips, Green: Fujifilm.

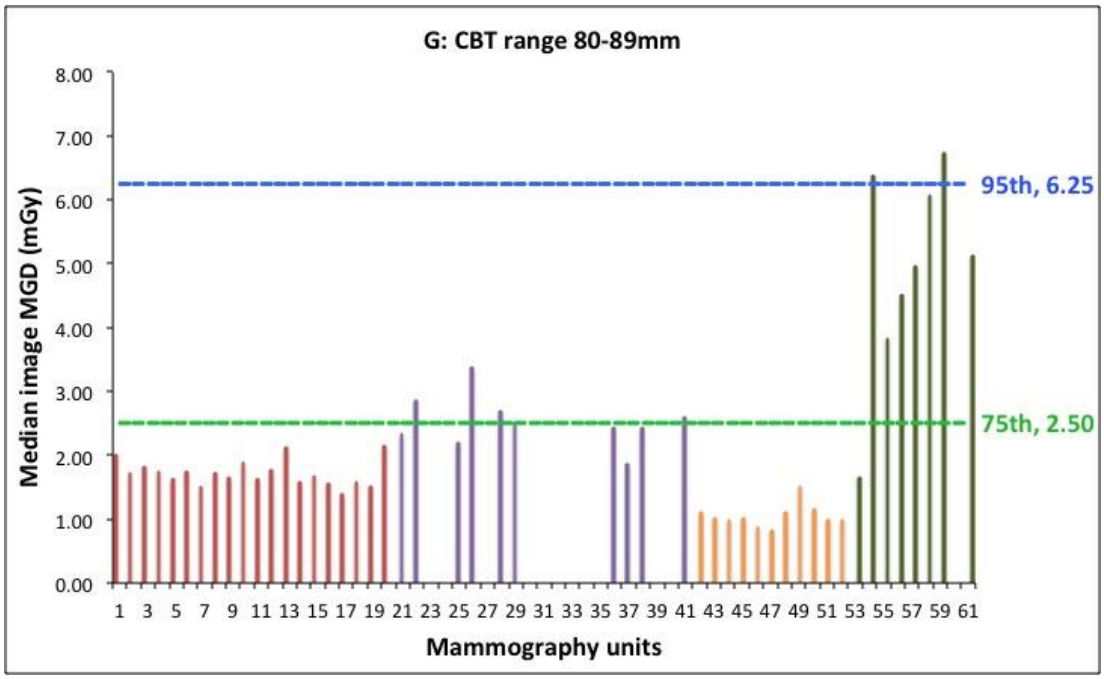

Figure 3.9: Median MGD, 75thand 95th percentiles for centre included in the study, for CBT range 80-89 mm, color coded for different mammography unit make (with detector technologies). Red: GE, Purple: Hologic, Orange: Phillips, Green: Fujifilm.

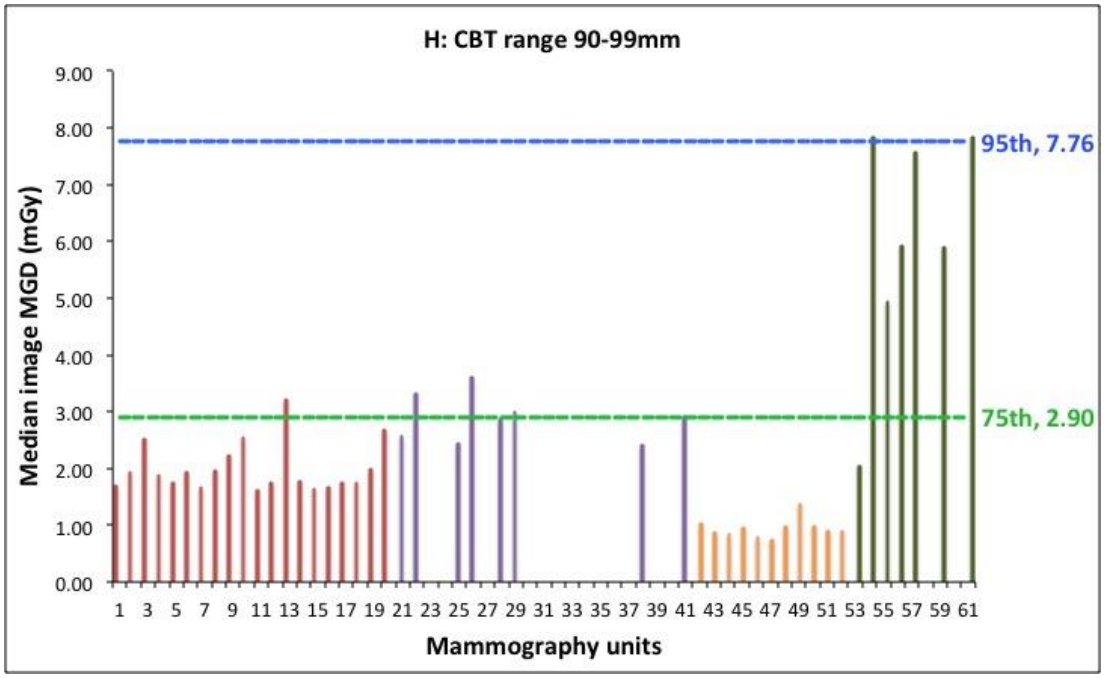

Figure 3.10: Median MGD, 75thand 95th percentiles for centre included in the study, for CBT range 90-99 mm, color coded for different mammography unit make (with detector technologies). Red: GE, Purple: Hologic, Orange: Phillips, Green: Fujifilm.

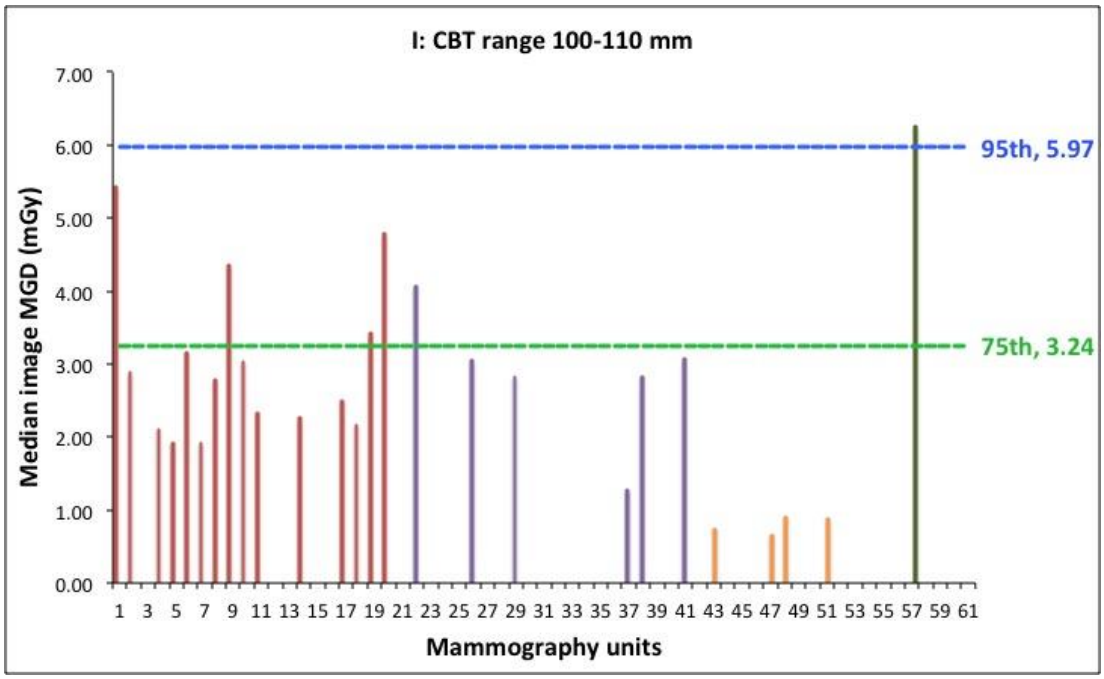

Figure 3.11: Median MGD, 75thand 95th percentiles for centre included in the study, for CBT range 100-109 mm, color coded for different mammography unit make (with detector technologies). Red: GE, Purple: Hologic, Orange: Phillips, Green: Fujifilm.

Parts of the results of this chapter were presented in the Engineering and Physical Sciences in Medicine (EPSM) conference in Sydney in 2016, the presentation was titled: "Diagnostic reference levels for digital mammography, time or a new paradigm". Some results were also presented in the European Council of Radiology (ECR) conference in Vienna, Austria in 2017, which was titled: "Radiation doses received by women attending BreastScreen NSW in 2014". The full results of this work were published the Journal of Medical Imaging and Radiation Oncology (JMIRO) in 2016 and is titled "Diagnostic reference levels for digital mammography in New South Wales" [4]. This article is presented in the next subsection.

Note: The published article contained an error in Table3.10, column 9 header, it reads "Mean image MGD/View" this should be "Median image MGD/View". A note has been sent to the editor.

3.1.4 References

1. Suleiman, M.E., P.C. Brennan, and M.F. McEntee, Diagnostic reference levels in digital mammography: a systematic review. Radiation Protection Dosimetry, 2015. 167(4): p. 608-619.
2. Thiele, D.L., et al., Diagnostic reference levels for mammography in BreastScreen Queensland. Australas Phys Eng Sci Med, 2011. 34(3): p. 415-8.
3. Vañó, E., et al., ICRP Publication 135: Diagnostic Reference Levels in Medical Imaging. Annals of the ICRP, 2017. 46(1): p. 1-144.
4. Suleiman, M.E., et al., Diagnostic reference levels for digital mammography in New South Wales. Journal of Medical Imaging and Radiation Oncology, 2016: p. n/a-n/a.
5. Dance, D., Monte-Carlo calculation of conversion factors for the estimation of mean glandular breast dose. Physics in medicine and biology, 1990. 35(9): p. 1211.
6. Dance, D.R., et al., Additional factors for the estimation of mean glandular breast dose using the UK mammography dosimetry protocol. Physics in Medicine and Biology, 2000. 45(11): p. 3225-3240.
7. Dance, D.R., K.C. Young, and R.E. van Engen, Further factors for the estimation of mean glandular dose using the United Kingdom, European and IAEA breast dosimetry protocols. Phys Med Biol, 2009. 54(14): p. 4361-72.
8. Suleiman, M.E., et al., Integrating mammographic breast density in glandular dose calculation. Br J Radiol, 2018: p. 20180032.
9. Yakami, M. YAKAMI DICOM Tools (Free DICOM Viewer/Converter/etc.). updated on 21 Jan 2014 [cited 2015 20 February]; Available from: http://www.kuhp.kyoto-u.ac.jp/~diag_rad/intro/tech/dicom_tools.html.
10. Robson, K.J., A parametric method for determining mammographic X-ray tube output and half value layer. Br J Radiol, 2001. 74(880): p. 335-40.
11. Borg, M., Badr, I., & Royle, G. J., A study to determine the differences between the displayed dose values for two full-field digital mammography units and values calculated using a range of Monte-Carlo-based techniques: a phantom study, 2013. Radiation Protection Dosimetry, 154(2), 217-228. doi:10.1093/rpd/ncs167.

3.2 Diagnostic reference levels for digital mammography in New South Wales

Moayyad E Suleiman,[1] Mark F McEntee,[1] Lucy Cartwright,[2] Jennifer Diffey[3] and Patrick C Brennan[1]

[1] Faculty of Health Sciences, The University of Sydney, Lidcombe, New South Wales, Australia

[2] Westmead Hospital, Westmead, New South Wales, Australia

[3] Hunter New England Imaging, John Hunter Hospital, New Lambton Heights, New South Wales, Australia

3.2.1 Abstract

Introduction: This work aims to explore radiation doses delivered in screening mammography in Australia, with a focus on whether compressed breast thickness should be used as a guide when determining patient derived diagnostic reference levels (DRLs).

Methods: Anonymized mammograms (52,405) were retrieved from a central database, and DICOM headers were extracted using third party software. Women with breast implants; breast thicknesses outside 20-110 mm; and images with incomplete exposure or quality assurance (QA) data were excluded. Exposure and QA information were utilized to calculate the mean glandular dose (MGD) for 45,054 mammograms from 61 units representing four manufacturers using previously well-established methods. The 75th and 95th percentiles were calculated across median image MGDs obtained for all included data and according to specific compressed breast thickness ranges.

Results: The overall median image MGD, minimum, maximum were: 1.39 mGy, 0.19 mGy and 10.00 mGy respectively, the 75th and 95th percentiles across all units' median image MGD for 60±5 mm compressed breast thickness were 2.06 mGy and 2.69 mGy respectively. Median MGDs, minimum, maximum, 75th and 95th percentiles were presented for nine compressed breast thickness ranges, DRLs for NSW are suggested for the compressed breast thickness range of 60±5 mm for the whole study and three detector technologies CR, DR, and photon counting to be 2.06, mGy, 2.22 mGy, 2.04 mGy, and 0.79 mGy respectively.

Conclusion: MGD is dependent upon compressed breast thickness and it is recommended that DRL values should be specific to compressed breast thickness and image detector technology.

Keywords: Breast, Dosimetry, Mean Glandular dose, Optimization, Screening.

3.2.2 **Introduction**

Mammography is an important tool for the early detection of breast cancer as early detection has been demonstrated to reduce mortality by up to 30% [1]. Aiming to reduce breast cancer deaths, the Australian breast-screening programme has targeted 50-69 year old Australian women since 1991 for biennial screening mammograms, recently increasing this upper age limit to 74 [2]. Exposing healthy women to ionizing radiation however is associated with a risk of inducing breast cancer, therefore the dose to the breast must be kept as low as reasonably achievable [3]. Diagnostic Reference Levels (DRLs) provide a measure of quality control and optimization of protection to help limit variations in dose delivered among and within imaging centres and these levels are expected not to be exceeded for a standard diagnostic procedure when good and normal practice is applied [3]. A DRL was defined in the International Commission of Radiation Protection (ICRP) publication 73 in 1996 as:

"A form of investigation level, applied to an easily measured quantity, usually the absorbed dose in air, or tissue-equivalent material at the surface of a simple phantom or a representative patient." [3]

DRL establishment requires the use of readily available or easily calculated dose metrics. Measurements of radiation dose to the breast have been performed using different approaches including total energy transmitted to the breast [4], mid-breast dose [5], air kerma [6], entrance surface dose [7] and mean dose absorbed by the glandular tissue (MGD) [8]. Due to the radio-sensitivity of the glandular tissue of the breast, MGD is now considered to be the most relevant quantity [8], is widely used and is recommended by the ICRP [9], the United States National Council on Radiation Protection and Measurements [10], the British Institute of Physics and Engineering in Medicine (IPEM) [11], the European Council Protocol (EP) [12-14] and the International Atomic Energy Agency (IAEA) [15]. Most studies implementing DRLs have therefore focussed on MGD values.

To establish a DRL, appropriate groupings of standard sized patients should be used. For adult DRLs in radiography, Fluoroscopy and CT a weight range for a group of patients of 70 ± 10 kg is used. In paediatric examinations, patients are categorized by weight or age range. In mammography, researchers have used a "standard" compressed breast thickness that varies from 35 cm – 65 cm depending on the DRL[16].

Choosing a single thickness to represent an entire population, although a simple approach, is arguably inappropriate as the population is not homogenous and the breast can vary in thickness from 1cm to 10cm. Furthermore, it is well known that dose differs for different breast thicknesses. A more complex, but representative approach might be to establish DRLs for groups of standard-sized breasts.

While DRLs have been established for mammography in many countries around the world [17-22]; the Australian breast screening programmes are into their third decade; to date no patient based DRLs are available, nonetheless, phantom based DRLs were established in 2011 for Queensland hospitals. [23] However, Phantom based DRLs may not reflect the clinical environment; hence, this study aims to propose patient based DRLs for screening mammography in New South Wales, and to explore whether compressed breast thickness should be taken into account when determining DRLs.

3.2.3 **Methods**

This study was performed retrospectively using a patient data sample from 50 BreastScreen NSW centres and mobile units, ethical approval was granted by the Cancer Institute Human Research Ethics Committee (No.2014/08/552). In total, data were obtained from 63 mammography units. Radiation dose and supplementary data were assembled from 12,034 patient cases (52,405 mammograms).

Data relating to the patient and required for dose calculations were extracted from the Digital Imaging and Communication in Medicine (DICOM) headers (Table 3.8) and exported to a CSV format file using third party software (YAKAMI DICOM Tools ver. 1.4.1.0, Kyoto University, Japan).

Table 3.8: Information extracted from the DICOM headers of digital images.

Information	DICOM tag
Patient age	0019,1052
Body Part thickness	0018,11A0
Implant present	0028,1300
Patient orientation	0020,0020
Image laterality	0020,0062
Tube voltage (kVp)	0018,0060
Exposure (mAs)	0018,1152
Anode target material	0018,1191
Filter material	0018,7050
Exposure control mode	0018,7060
Detector ID	0018,700A
Manufacturer's Model Name	0008,1090
Manufacturer	0008,0070

Dose calculation also required data from the annual medical physics quality assurance (QA) reports for each center; these data included tube output and HVL for all kVps and anode/filter combinations available for each mammography unit.

Based on the information gathered, exclusion criteria were applied thus removing from the study mammograms involving breast implants (1337 images), and incomplete or unavailable QA data (1662 images), as well as images with compressed breast thickness not within 20-110mm (82 images). Data were then imported into an excel sheet with macros developed in-house that calculates MGD for each acquired image using the methods described by Dance et al. [24-26].

For each image, MGDs were calculated using the following equation:

MGD = K*gcs*

Where K is the incident air kerma (IAK) at the upper surface of the breast without backscatter, calculated from mAs, kVp and the tube output corrected using the inverse square law. The g factor is the IAK to MGD conversion factor for breasts with 50% glandularity and an anode/filter combination of Mo/Mo. The c factor corrects for any

difference in breast glandularity from 50% for different thickness breasts and is available for two ranges of age, 40-49 and 50-64, women aged over 64 were included in the 50-64 range table, we have moderately assumed here that the breast density of women over the age of 64 will behave in a similar way that the density of women aged 50-64; this is an estimation that will be investigated in future studies. The s factor corrects for any difference in the types of anode/filter combination used other than Mo/Mo [24-26].

Note: Both g and c factors are tabulated as functions of breast thickness and half-value layer (HVL) of the x-ray beam. The HVL for each system was obtained from concurrent QA data.

Table 3.9: Manufacturer, model, technology, Anode/ filter combinations, and number of Mammography units included in the dose audit from BreastScreen centres in NSW/Australia.

Manufacturer	Model	Technology	Anode/Filter	Unit number
General Electric (GE)	Senographe Essential ADS_54.11	DR	Mo/Mo, Mo/Rh, Rh/Rh	1-14
	Senographe Essential ADS_54.10	DR	Mo/Mo, Rh/Rh	15
	Senographe Essential ADS_53.40	DR	Mo/Mo, Mo/Rh, Rh/Rh	16
	Senographe DS ADS_54.11	DR	Mo/Mo, Mo/Rh, Rh/Rh	17,18
	Senographe DS ADS_53.40	DR	Mo/Mo, Rh/Rh	19
	Senographe 2000D ADS_17.4.5	DR	Mo/Mo, Mo/Rh, Rh/Rh	20
Hologic	Selenia Dimensions	DR	W/Ag, W/Rh	21-41
Philips (Sectra)	L30	DR	W/AL	42-52
Fuji Film	Amulet	DR	W/Rh	53
		CR	Mo/Mo, Mo/Rh	54-61

DR: Digital radiography **Mo: Molybdenum** **W: Tungsten**
CR: Computed radiography **Rh: Rhodium** **Ag: Silver** **Al: Aluminum**

For each woman and mammographic unit, the MGD median was found per image and examination, the median examination MGD was found by summing image MGDs for each examination and dividing the result by two; this is to average for one breast.

To determine DRLs, the 75th and 95th percentiles were calculated across the median image MGDs per mammography unit. Then values for each mammography unit were categorized according to their compressed breast thickness to ranges of 10 mm thicknesses and median image MGDs per mammography unit were calculated for each thickness range, an ANOVA with a Tukey post-hoc test was used to analyse the

significance of the differences between the median image MGDs for each thickness range. The 75th and 95th percentiles were determined for each thickness range.

3.2.4 **Results**

Summary of data

The final data set included 11,029 women with a mean age of 60 years and a total of 45,054 images (DR: 40,033 images and CR: 5,021 images). Forty-eight BreastScreen centres (Sixty-one digital mammography units) were involved, (Two centres were disqualified due to missing QA data) consisting of 53 DR and 8 CR units as shown in table 3.9, it is worth highlighting here that Rhodium (Rh) anodes were unavailable or disabled in the CR units included for this study during the period in question. Image sets included in the analysis comprised of the standard 4 view examinations (MLO and CC for left and right breasts) and extra projections, the latter representing less than 6% of all examinations.

The histogram of compressed breast thicknesses for the study showed a normal distribution with a mean of 58 mm (Figure 3.12), while image MGDs showed a skewed distribution that ranged from 0.19 mGy to 10.00 mGy with a mean and a median of 1.51 mGy and 1.39 mGy respectively (Figure 3.13). An overall summary of the background data for each unit is shown in table 3.10.

Radiation doses and percentile values

Median image MGD across all patients for each MLO and CC image were 1.43 mGy and 1.36 mGy, respectively, with individual doses per image ranging from 0.32 mGy to 10.00 mGy for the MLO and 0.19 mGy to 7.45 mGy for the CC. Also, the lowest and highest median image MGD per mammography unit, respectively, were 0.67 mGy and 2.43 mGy for MLO, 0.66 mGy and 2.24 mGy for CC.

Median MGD per examination for all women was 2.84 mGy with the smallest and highest dose being delivered being 0.68 mGy and 21.9 mGy, respectively. Furthermore, the lowest and highest median examination MGD per mammography unit were 1.40 mGy and 4.42 mGy in units 51 and 54 respectively.

Median MGD per image, view (MLO, CC) and examination as well as mean patient age, compressed breast thickness, kVp, mAs for each mammography unit are displayed in table 3.10. The 75th and 95th percentiles across all units' median image MGD for 60 ± 5 mm compressed breast thicknesses were 2.06 mGy and 2.69 mGy respectively (Figure 3.14). Percentile values and proposed DRLs are also presented for each of the nine compressed breast thickness ranges and for the three different detector technologies (Table 3.11), Tukey's post-hoc test showed statistically significant differences between median image MGDs for each 10 mm compressed breast thickness range examined ($p < 0.05$).

3.2.5 **Discussion and conclusion**

DRLs have been shown to be an effective method for dose optimization of protection in medical exposure of patients for diagnostics and interventional procedures. DRLs work by minimizing the wide variations in dose demonstrated across centres for the same examination for groups of standard sized patients [(27)]. Centres delivering the highest doses are identified using the percentile method. A 75th percentile which is often used for general X-ray examinations, identifies the 25% of centres that are giving higher doses and encourages them to optimize exposures, thus making DRLs a dynamic and changing value. Often in mammography, however, a 95th percentile is used due to rigorous quality assurance procedures and tight dose variations [(28)]. However, in the current work the long tail exhibited in figure 3.13 would suggest that at this time a 75th percentile maybe more prudent across the state from which our measurements are obtained.

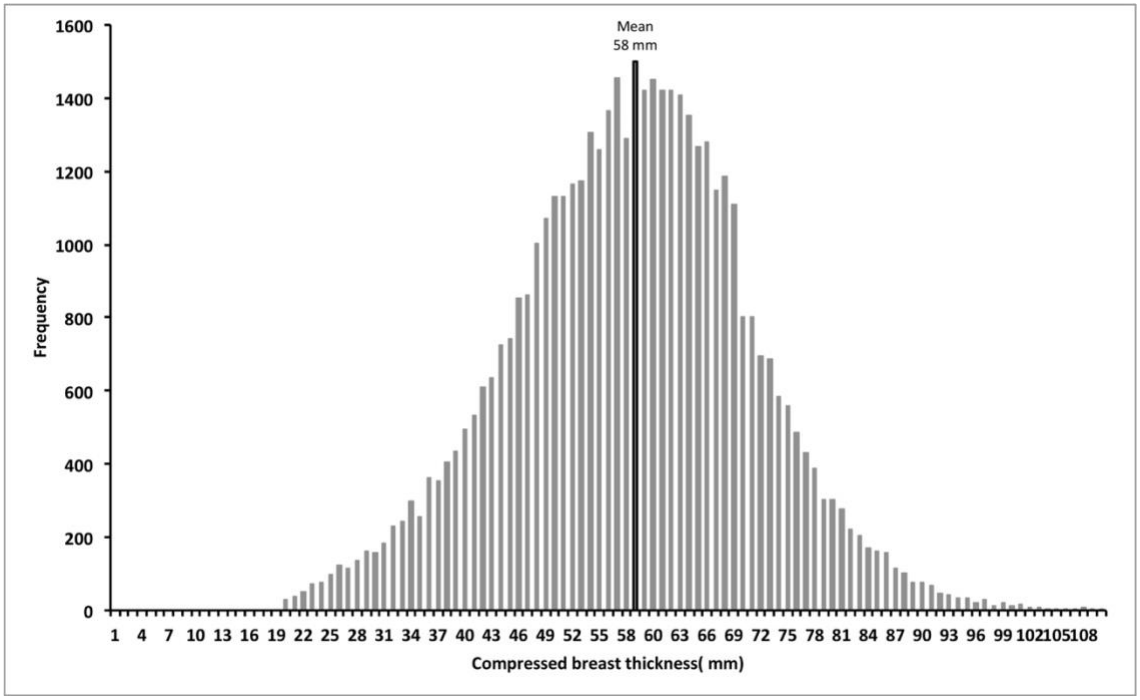

Figure 3.12: Distribution of compressed breast thickness for 45,054 mammography images.

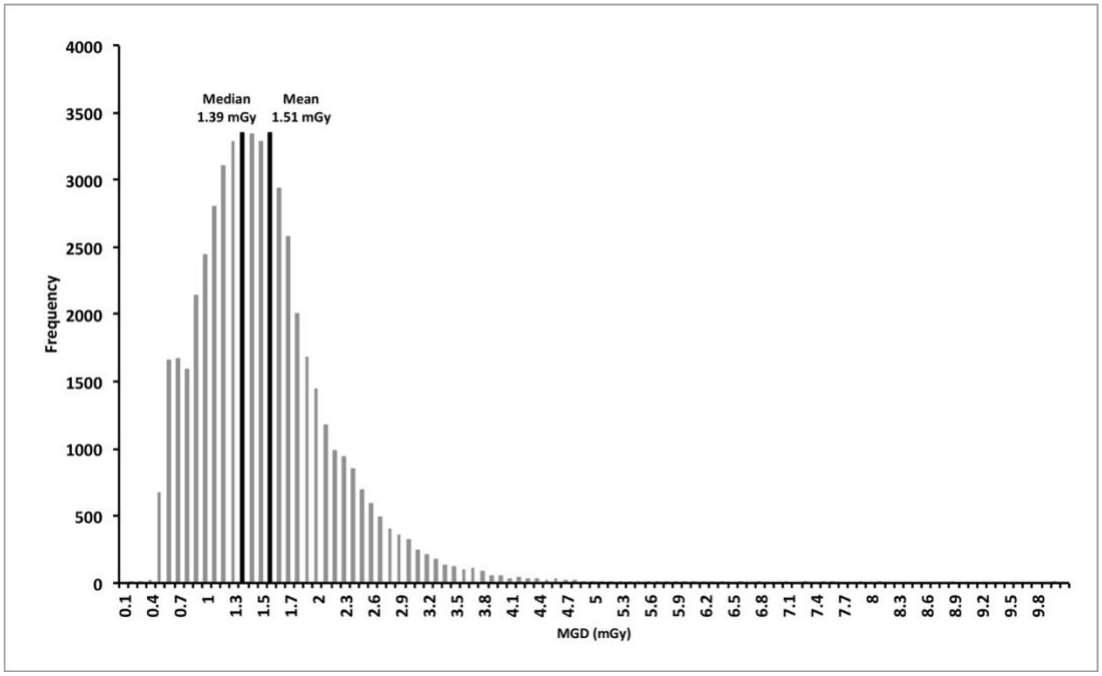

Figure 3.13: Distribution of image mean glandular dose (MGD) for 45,054 mammography images.

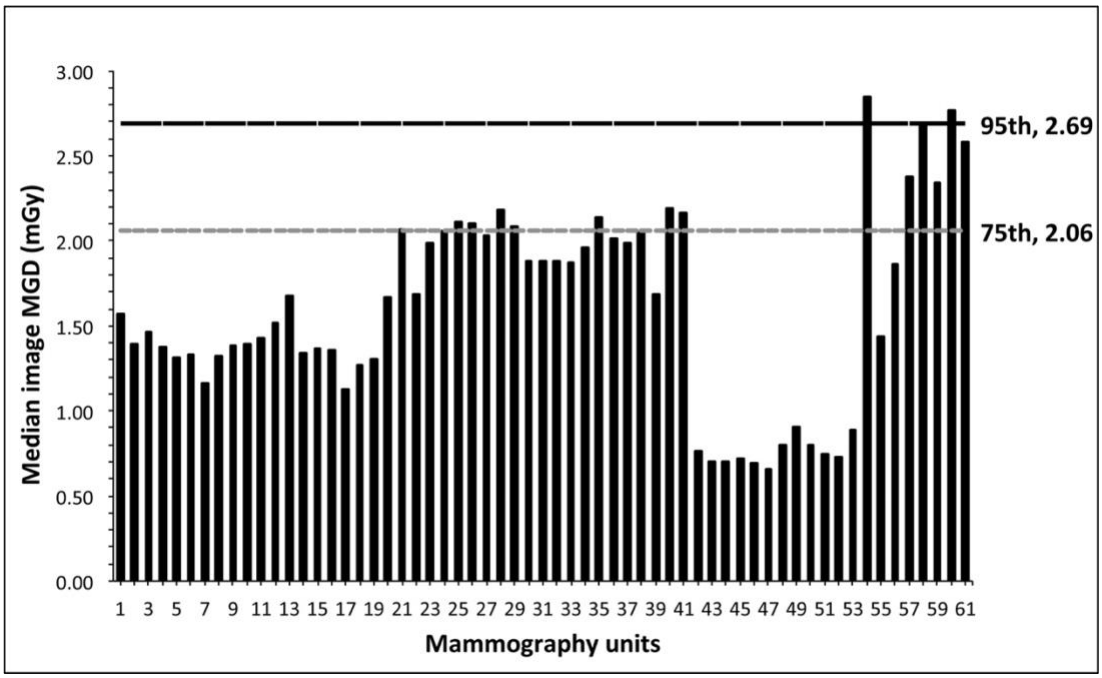

Figure 3.14: A histogram plot of the median image MGD for a compressed breast thickness of 60 _ 5 mm is indicated for each mammography unit, the 75th and 95th percentile values are indicated by the horizontal lines.

Table 3.10: Number of images/examinations per mammography unit, exposure parameters means, median Entrance surface air kerma and median mean glandular dose per view, image and case, for 45054 mammograms across 61 mammography units.

Unit	No. of images	No. of Cases	Mean Age (StDev)	Mean Thickness (StDev)	Mean kVp (StDev)	Mean mAs (StDev)	Median ESAK (IQR)	Mean image MGD/View						Median Image MGD (IQR)	Median Examination MGD (IQR)
								CC			MLO				
								R	L	All	R	L	All		
1	812	200	61.81 (7.88)	53.79 (12.10)	28.66 (1.27)	55.68 (13.54)	5.69 (2.53)	1.31	1.35	1.33	1.57	1.59	1.58	1.46 (0.45)	**2.98 (1.30)**
2	721	175	56.36 (7.67)	60.12 (12.62)	28.96 (0.83)	67.56 (16.74)	6.03 (2.32)	1.37	1.38	1.37	1.41	1.44	1.43	1.40 (0.34)	**2.85 (1.33)**
3	744	192	58.87 (7.17)	62.63 (10.89)	29.09 (0.71)	65.33 (14.64)	6.97 (2.56)	1.44	1.48	1.46	1.54	1.55	1.54	1.51 (0.39)	**2.98 (1.69)**
4	775	200	60.11 (7.72)	60.67 (10.26)	29.01 (0.64)	59.26 (14.56)	6.09 (2.18)	1.37	1.39	1.38	1.40	1.40	1.40	1.39 (0.35)	**2.77 (1.42)**
5	960	219	59.44 (7.82)	59.09 (12.67)	28.64 (0.96)	57.07 (12.87)	5.87 (2.39)	1.29	1.27	1.29	1.33	1.36	1.34	1.32 (0.35)	**2.75 (1.81)**
6	680	172	60.20 (8.04)	63.07 (11.11)	29.00 (0.66)	59.43 (15.91)	6.22 (2.23)	1.29	1.31	1.30	1.45	1.41	1.44	1.36 (0.35)	**2.74 (1.61)**
7	770	203	60.06 (7.50)	61.52 (11.86)	28.96 (0.78)	57.65 (12.48)	5.41 (2.09)	1.17	1.19	1.18	1.22	1.24	1.23	1.21 (0.32)	**2.43 (1.25)**
8	926	233	59.60 (6.53)	65.65 (11.10)	29.21 (0.69)	63.10 (15.16)	6.56 (2.18)	1.37	1.34	1.36	1.46	1.43	1.45	1.39 (0.37)	**2.83 (1.41)**
9	844	208	58.20 (6.85)	60.59 (15.52)	29.31 (1.10)	61.68 (22.66)	6.30 (2.63)	1.30	1.34	1.32	1.49	1.57	1.53	1.43 (0.35)	**2.91 (1.19)**
10	828	184	59.81 (6.70)	65.83 (10.93)	29.15 (0.56)	69.83 (19.05)	7.21 (2.62)	1.44	1.46	1.45	1.56	1.59	1.57	1.50 (0.38)	**3.25 (2.73)**
11	826	187	58.90 (6.79)	60.45 (11.74)	28.85 (0.82)	65.20 (13.77)	6.37 (2.49)	1.43	1.43	1.43	1.48	1.48	1.48	1.46 (0.32)	**3.05 (1.77)**
12	881	202	59.65 (8.13)	61.68 (13.43)	28.88 (0.91)	65.20 (13.57)	7.05 (2.99)	1.48	1.52	1.50	1.56	1.57	1.57	1.54 (0.37)	**3.21 (1.94)**
13	651	174	60.07 (7.69)	58.43 (12.05)	29.58 (0.73)	73.91 (19.50)	7.17 (2.44)	1.64	1.66	1.65	1.80	1.76	1.77	1.71 (0.35)	**3.44 (1.60)**
14	848	194	58.51 (7.34)	61.73 (13.21)	28.96 (0.88)	60.22 (13.57)	6.11 (2.36)	1.33	1.35	1.34	1.37	1.41	1.39	1.37 (0.33)	**2.80 (1.56)**
15	746	192	59.84 (8.26)	63.90 (11.67)	29.17 (0.84)	61.15 (14.06)	6.28 (2.39)	1.37	1.35	1.36	1.46	1.45	1.45	1.39 (0.38)	**2.81 (1.75)**
16	1057	242	59.55 (8.07)	58.61 (13.73)	28.76 (0.94)	55.75 (11.64)	5.70 (2.57)	1.32	1.32	1.32	1.31	1.37	1.34	1.33 (0.33)	**2.78 (1.60)**
17	915	195	62.15 (7.38)	57.89 (13.50)	28.86 (0.98)	46.44 (12.51)	4.84 (2.15)	1.08	1.07	1.08	1.12	1.14	1.14	1.10 (0.35)	**2.35 (1.66)**
18	574	137	59.65 (6.58)	59.13 (11.14)	29.11 (0.71)	50.77 (11.90)	5.17 (1.79)	1.24	1.20	1.21	1.27	1.28	1.27	1.25 (0.28)	**2.56 (1.82)**
19	721	166	61.02 (7.30)	61.80 (11.39)	29.02 (0.74)	58.86 (13.09)	6.02 (2.24)	1.29	1.30	1.30	1.36	1.34	1.34	1.33 (0.31)	**2.74 (1.89)**
20	589	116	62.67 (6.83)	56.83 (12.57)	28.87 (1.45)	67.75 (18.39)	6.76 (2.58)	1.51	1.47	1.50	1.62	1.62	1.62	1.56 (0.46)	**3.59 (2.92)**
21	787	188	60.07 (7.96)	59.37 (12.83)	29.96 (1.65)	139.43 (38.92)	7.09 (4.10)	1.90	1.83	1.85	2.16	2.13	2.14	2.00 (0.88)	**4.13 (3.29)**
22	734	178	58.26 (9.12)	65.00 (12.20)	28.54 (1.16)	199.27 (71.79)	7.63 (4.73)	1.72	1.71	1.72	2.22	2.08	2.14	1.94 (0.92)	**3.95 (3.75)**
23	587	167	63.81 (8.32)	54.73 (9.96)	29.68 (1.68)	137.04 (36.57)	6.04 (3.67)	1.70	1.71	1.70	1.83	1.85	1.84	1.75 (0.88)	**3.12 (3.24)**
24	636	181	59.45 (9.07)	54.83 (9.61)	29.71 (1.62)	133.45 (38.44)	6.04 (3.70)	1.73	1.77	1.76	1.83	1.92	1.84	1.80 (0.90)	**3.22 (3.56)**
25	812	192	60.27 (8.28)	59.25 (13.36)	29.91 (1.71)	171.09 (53.05)	6.81 (3.59)	1.97	1.97	1.97	1.98	1.89	1.94	1.95 (0.83)	**3.98 (3.68)**
26	845	202	59.61 (7.24)	54.46 (14.49)	29.36 (1.95)	175.42 (85.60)	5.41 (5.30)	1.80	1.77	1.78	1.63	1.70	1.68	1.72 (1.28)	**3.57 (5.40)**
27	575	163	60.52 (8.23)	54.03 (9.59)	29.57 (1.64)	131.55 (37.04)	5.74 (3.50)	1.82	1.72	1.76	1.71	1.80	1.73	1.75 (0.88)	**3.17 (2.90)**
28	815	189	58.60 (7.18)	55.00 (13.05)	29.42 (1.75)	159.72 (52.66)	6.29 (4.38)	1.81	1.76	1.80	1.91	1.92	1.91	1.86 (1.09)	**3.98 (4.58)**
29	909	206	58.60 (7.18)	60.22 (13.75)	30.02 (1.75)	156.72 (49.99)	7.03 (4.09)	1.86	1.93	1.89	2.13	2.02	2.08	1.98 (0.90)	**4.27 (3.97)**
30	578	170	60.43 (8.76)	55.39 (10.04)	29.85 (1.73)	115.45 (34.23)	5.95 (3.45)	1.65	1.68	1.66	1.79	1.85	1.84	1.71 (0.82)	**3.05 (3.11)**
31	344	99	60.48 (9.28)	55.75 (9.73)	29.92 (1.61)	126.10 (40.56)	6.03 (3.42)	1.72	1.75	1.73	1.83	1.79	1.82	1.76 (0.85)	**3.12 (3.56)**
32	530	157	61.57 (9.28)	56.87 (8.83)	30.06 (1.55)	123.59 (35.75)	6.18 (3.36)	1.72	1.73	1.72	1.86	1.84	1.84	1.76 (0.82)	**3.00 (3.76)**

Table 3.10 Continued

Unit	No. of images	No. of Cases	Mean Age (StDev)	Mean Thickness (StDev)	Mean kVp (StDev)	Mean mAs (StDev)	Median ESAK (IQR)	Mean image MGD/View						Median Image MGD (IQR)	**Median Examination MGD (IQR)**
								CC			**MLO**				
								R	**L**	**All**	**R**	**L**	**All**		
33	536	156	60.26 (10.43)	55.57 (10.37)	29.87 (1.73)	121.67 (35.45)	5.75 (3.73)	1.67	1.71	1.70	1.68	1.68	1.68	1.69 (0.91)	**2.88 (3.37)**
34	509	143	59.56 (8.05)	56.02 (9.28)	29.91 (1.60)	129.63 (41.12)	5.85 (3.90)	1.72	1.75	1.74	1.72	1.66	1.69	1.72 (0.94)	**3.10 (3.77)**
35	577	162	61.65 (7.96)	53.37 (10.84)	29.49 (1.78)	116.21 (34.92)	6.25 (4.37)	1.81	1.84	1.84	1.85	1.72	1.77	1.81 (0.97)	**3.26 (3.25)**
36	844	203	59.89 (7.67)	51.65 (11.94)	29.07 (1.71)	138.38 (42.00)	5.20 (3.57)	1.70	1.72	1.71	1.69	1.46	1.63	1.67 (0.87)	**3.37 (3.47)**
37	846	205	60.63 (8.09)	55.13 (13.92)	29.46 (1.86)	137.89 (45.41)	5.82 (4.25)	1.68	1.70	1.69	1.67	1.74	1.71	1.70 (0.99)	**3.56 (3.97)**
38	830	185	58.77 (6.63)	57.20 (14.10)	29.68 (1.85)	151.77 (52.47)	6.22 (4.18)	1.76	1.79	1.77	1.85	1.90	1.87	1.83 (0.96)	**4.09 (4.57)**
39	310	98	63.05 (7.39)	56.18 (9.12)	29.95 (1.60)	108.82 (28.41)	5.49 (3.32)	1.54	1.58	1.55	1.59	1.54	1.55	1.55 (0.81)	**2.44 (2.80)**
40	634	195	61.08 (9.18)	56.94 (9.53)	30.10 (1.66)	128.68 (40.11)	7.13 (5.35)	2.00	1.97	1.98	1.98	2.06	2.01	2.00 (1.29)	**3.14 (4.03)**
41	826	201	60.54 (8.10)	56.77 (13.50)	29.70 (1.81)	137.95 (39.37)	6.55 (4.07)	1.81	1.78	1.80	2.01	2.05	2.03	1.91 (0.93)	**3.93 (3.42)**
42	876	188	59.23 (7.52)	59.02 (13.11)	33.31 (2.04)	14.52 (3.41)	3.18 (1.85)	0.69	0.71	0.70	0.81	0.84	0.82	0.77 (0.34)	**1.72 (1.61)**
43	1320	299	58.78 (7.23)	62.89 (14.36)	34.03 (2.18)	14.47 (3.27)	3.22 (1.89)	0.73	0.72	0.73	0.81	0.81	0.81	0.77 (0.33)	**1.65 (1.37)**
44	346	79	58.10 (6.91)	59.65 (13.36)	34.02 (2.17)	14.37 (2.96)	2.86 (1.51)	0.69	0.67	0.68	0.76	0.78	0.78	0.73 (0.27)	**1.53 (1.31)**
45	949	203	60.49 (7.98)	58.97 (12.67)	33.68 (2.33)	14.61 (2.96)	2.93 (1.66)	0.71	0.69	0.69	0.75	0.75	0.75	0.72 (0.29)	**1.55 (1.47)**
46	559	132	59.89 (7.65)	59.29 (13.34)	33.07 (1.73)	14.41 (3.52)	2.96 (1.87)	0.70	0.69	0.70	0.70	0.73	0.72	0.71 (0.32)	**1.45 (1.16)**
47	774	180	62.02 (6.21)	62.97 (13.48)	33.20 (1.73)	14.42 (3.23)	3.26 (1.72)	0.66	0.65	0.66	0.79	0.81	0.80	0.74 (0.27)	**1.50 (1.21)**
48	825	198	60.46 (9.50)	63.16 (12.53)	34.89 (2.33)	15.38 (3.36)	3.43 (1.89)	0.82	0.79	0.81	0.96	0.94	0.95	0.87 (0.39)	**1.83 (1.38)**
49	952	240	60.34 (9.47)	62.40 (13.34)	34.85 (2.41)	15.36 (3.08)	3.99 (3.78)	0.92	0.94	0.93	1.02	1.03	1.03	0.97 (0.84)	**2.07 (2.85)**
50	921	197	59.38 (7.42)	60.89 (13.26)	33.57 (1.95)	15.18 (3.42)	3.61 (1.95)	0.84	0.84	0.84	0.88	0.86	0.88	0.86 (0.34)	**1.82 (2.01)**
51	556	136	61.69 (7.08)	55.45 (13.88)	33.42 (2.23)	13.88 (2.92)	2.69 (1.45)	0.68	0.69	0.69	0.71	0.70	0.71	0.70 (0.25)	**1.40 (0.96)**
52	786	186	58.94 (7.75)	55.32 (13.99)	33.07 (2.15)	14.76 (3.48)	2.61 (1.84)	0.70	0.70	0.70	0.65	0.69	0.67	0.69 (0.32)	**1.41 (1.38)**
53	1237	280	58.42 (8.09)	55.64 (13.47)	29.20 (1.46)	77.24 (29.96)	2.84 (1.94)	0.83	0.82	0.82	0.96	0.99	0.96	0.89 (0.45)	**1.92 (2.21)**
54	723	192	61.54 (6.58)	48.92 (10.39)	27.28 (0.82)	110.62 (45.98)	9.70 (5.27)	2.15	2.07	2.09	2.42	2.46	2.43	2.26 (1.01)	**4.41 (5.62)**
55	638	162	63.74 (7.68)	56.63 (11.96)	27.09 (0.29)	86.00 (55.34)	5.82 (5.30)	1.16	1.22	1.18	1.43	1.40	1.40	1.26 (0.88)	**2.53 (3.26)**
56	527	145	61.93 (8.69)	55.66 (12.06)	27.32 (0.66)	88.34 (47.40)	8.06 (6.15)	1.62	1.66	1.64	1.84	1.85	1.85	1.72 (0.94)	**3.20 (4.18)**
57	863	204	61.72 (7.68)	51.45 (12.31)	28.24 (0.65)	80.92 (43.81)	9.43 (6.56)	1.81	1.84	1.82	1.96	2.13	2.05	1.91 (0.98)	**3.95 (4.13)**
58	590	145	62.01 (6.79)	48.38 (11.92)	27.94 (0.76)	88.96 (43.58)	9.08 (7.46)	1.85	1.80	1.84	1.96	2.00	1.98	1.90 (1.17)	**3.85 (4.86)**
59	731	192	56.70 (7.58)	45.63 (11.63)	27.41 (0.83)	80.11 (36.53)	7.56 (4.07)	1.77	1.80	1.79	1.77	1.70	1.74	1.77 (0.74)	**3.37 (3.18)**
60	169	44	61.51 (6.83)	46.75 (10.79)	27.91 (0.65)	79.60 (39.38)	9.95 (7.22)	2.08	2.28	2.24	1.91	1.98	1.97	2.09 (1.23)	**4.21 (5.30)**
61	780	197	60.05 (6.92)	46.82 (11.93)	28.22 (1.01)	79.14 (37.04)	8.88 (5.71)	1.96	1.89	1.94	1.98	2.06	2.02	1.97 (0.90)	**3.51 (4.38)**
Overall	**45054**	**11030**	**60.03 (7.88)**	**58.01 (13.19)**	**30.00 (2.49)**	**80.97 (58.77)**	**5.62 (3.75)**	**1.36**	**1.37**	**1.36**	**1.43**	**1.43**	**1.43**	**1.39 (0.78)**	**2.84 (3.29)**

StDev: Standard deviation.
Thickness: compressed breast thickness.
kVp: X-ray tube potential.
mAs: X-ray tube current time product.
IQR: Interquartile range
MGD: Mean glandular dose.
ESAK: Entrance surface air kerma
CC: Craniocaudal view.
MLO: Mediolateral Oblique view.
R: Right breast
L: Left breast

Table 3.11: 75th and 95th percentiles for different compressed breast thickness ranges and three different detector technologies, representing 45,054 mammograms from 61 BreastScreen units (Proposed DRLs for 60±5 mm breast thickness are in **bold**).

Breast thickness range ()	All Units		CR		DR		Photon counting	
	75th % (mGy)	95th % (mGy)	75th % (mGy)	95th % (mGy)	75th % (mGy)	95th % (mGy)	75th % (mGy)	95th % (mGy)
20-29	0.97	1.19	1.17	1.26	0.97	1.11	0.58	0.63
30-39	1.13	1.50	1.50	1.52	1.12	1.22	0.60	0.65
40-49	1.31	1.86	1.92	2.08	1.30	1.41	0.58	0.65
50-59	1.67	2.38	2.48	2.58	1.65	1.80	0.65	0.69
60-69	2.37	3.00	3.08	3.21	2.35	2.57	0.88	0.99
70-79	2.23	4.38	4.41	4.46	2.08	2.67	1.08	1.56
80-89	2.48	6.24	6.39	6.74	2.34	3.07	1.12	1.52
90-99	2.89	7.75	7.84	7.85	2.63	3.48	0.99	1.39
100-110	3.24	5.97	6.26	6.26	3.31	5.38	0.91	0.92
DRLs 60±5	**2.06**		**2.22**		**2.04**		**0.79**	

CR, Computed Radiography; **DR,** Digital Radiography

Examination of the data in table 3.10 demonstrates minimal differences in dose between left and right breasts and between the CC and MLO projections compared with the inter-centre differences, hence and in alignment with previous authors, the *median image MGD* will be used throughout this discussion [17, 29, 30]. Examination of the median image MGD, demonstrated that the lowest values belong to the Philips L30 (Sectra) units (units 51 and 52), with all of the Philips units reporting median MGDs below the 20th percentile. The low dose associated with these units is in line with other studies in the literature [19, 31], and is likely linked to the effective utilization of tightly collimated scanning slot beam of x-rays and a detector technology that employs photon counting with energy discrimination, so scattered photons are rejected from the image. This means that a grid is not required and consequently, doses are lower. The highest median image MGD and case MGD were delivered in CR units (Fujifilm Corporation) in a mobile setting with five of the eight CR units reporting an overall median image MGD that was over the 75th percentile for all compressed breast thickness ranges. It is interesting to note that all Hologic units reported median image MGDs higher than the 50th percentile while 11 out of the 20 GE units reported median image MGDs less than or equal to the 50th percentile. These data emphasise the impact of technology on reported dose variations. It should be stressed however that drawing conclusions

regarding technology, based on dose values alone without a full consideration of diagnostic efficacy must be treated with caution.

While it is important to acknowledge the variations shown in figure 3.14 and to focus on existing units/centres that are responsible for the higher doses, it is important to put these inter-unit or inter-centre dose variations into context. The variations in dose values represented in the long-tailed distribution in figure 3.13 are similar to the distribution reported in an earlier large UK study [32]. In addition, the level of difference between the highest and the lowest dose units/centres reported here are not dissimilar from that expressed in other countries with other work demonstrating marginally less [20, 28, 33], comparable [18, 19] or higher variations [34]. It should be acknowledged that the higher doses in this study as discussed above, mainly relate to CR units, which at the time of writing have generally now been replaced and the next round of DRL surveys should reflect this. Overall, when taking into consideration the reported compressed breast thicknesses by other international studies, it was found that our reported dose medians and percentiles were less than most of patient studies reviewed by Suleiman et al in 2014 [16].

The median MGD and 75th percentile for compressed breast thicknesses of 60±5 mm were 1.62 and 2.06 mGy respectively (Mean compressed breast thickness for the study is 58 mm), while, for comparison reasons, the median MGD and 75th percentile for compressed breast thicknesses of 50 ± 5 mm were 1.35 and 1.50 mGy respectively. These values are lower than the 1.88 and 2.1 mGy reported in a Spanish study in 2005, which used similar methods to estimate the dose, albeit with a lower overall mean compressed breast thickness of 52 mm [35]. The higher doses reported in the Spanish work are most likely due to possibly different technology and the study's focus on diagnostic mammography (symptomatic women). With regard to this last point, O'Leary et al. suggested that the higher mean dose received by symptomatic women could be explained by the inclusion of younger women with denser breasts and the less strict mammographic educational requirements for radiographers compared with those involved in the breast screening services [28]. More recent studies in Ireland and Malta reporting a closer overall mean compressed breast thicknesses (57.5 and 54.7 mm respectively) to our findings indicated lower mean MGDs (1.07 and 1.33 mGy respectively) and 75th percentiles (1.11 and 1.5 mGy respectively) than those reported here. [28, 36] While differences in technology and subtle differences in compressed

breast thickness may contribute to the higher doses reported here, the results suggest some potential for optimization of the units or practices included in this study.

It is important to revisit the interpretation of DRL definitions, particularly since these have been available and employed for 20 years. In particular, the term "*representative patient*" has often been translated in mammography to mean average compressed breast thickness of the study sample. However, some authors have calculated DRLs for groups of standard compressed breast thickness in order to facilitate national and international comparisons [28]. Differences in compressed breast thicknesses are clearly responsible for at least some of the statistically significant MGD variations displayed in our work. If we use a standard sized group of patients with compressed breast thickness 60 ±5 mm to represent the overall population, the 75th percentile at this value is more than double and almost half that of the lowest and highest compressed breast thickness categories respectively. These results alongside the compressed breast thickness dependent dose variations demonstrated elsewhere highlight the importance of clearly identifying standard sized groups of compressed breast thicknesses when specifying DRLs [16]. Although to date this is not often seen, such stratification would extend the translation of a "*representative patient*" from average compressed breast thickness to ranges of compressed breast thicknesses that are more representative of the population of women. In addition, such a compressed breast thickness specific approach if used universally would facilitate useful and accurate national and international comparisons.

Finally, it is important to acknowledge that this paper is limited to radiation dose values. It should be stressed that similar to almost all previous DRL work, comparing dose data does not factor in image quality variations, therefore the potential for highest dose locations offering best diagnostic efficacy cannot be out-ruled. Equally however, currently there is no evidence here or elsewhere that those centres or units with the lowest dose are offering less accurate diagnoses than elsewhere. This is an area of research that requires much more attention.

In conclusion, patient-based DRL values for different compressed breast thickness ranges and different image detector technology have been proposed for the first time in Australia, providing valuable insights into the radiation dose status of screening mammography in NSW. DRL values in mammography should be specific to breast

thickness and image detector technology, as large variations between compressed breast thickness ranges and different image detector technologies were shown.

3.2.6 References

1. Tabar L, Vitak B, Chen TH, et al. Swedish two-county trial: impact of mammographic screening on breast cancer mortality during 3 decades. Radiology. 2011;260(3):658-63. doi: 10.1148/radiol.11110469
2. AIHW. BreastScreen Australia Monitoring Report 2010-2011. Canberra: AIHW, 2013 2013. Report No.: 77.
3. ICRP. Radiological protection and safety in medicine. ICRP Publication 73. 1996;ICRP Publication 73. Ann. ICRP 26 (2).(2):1-47.
4. Boag JW, Stacey AJ, Davis R. Radiation exposure to the patient in xeroradiography. Br J Radiol. 1976;49(579):253-61.
5. Breslow L, Thomas LB, Upton AC. Final reports of the National Cancer Institute ad hoc Working Groups on Mammography in Screening for Breast Cancer and a summary report of their joint findings and recommendations. J Natl Cancer Inst. 1977;59(2):467-541.
6. Jensen JE, Butler PF. Breast exposure: nationwide trends; a mammographic quality assurance program--results to date. Radiol Technol. 1978;50(3):251-7.
7. Fitzgerald M, White DR, White E, Young J. Mammographic practice and dosimetry in Britain. Br J Radiol. 1981;54(639):212-20. doi: 10.1259/0007-1285-54-639-212
8. Karlsson M, Nygren K, Wickman G, Hettinger G. Absorbed dose in mammary radiography. Acta Radiol Ther Phys Biol. 1976;15(3):252-8.
9. ICRP. Protection of the Patient in Nuclear Medicine (and Statement from the 1987 Como Meeting of ICRP). ICRP Publication 52. 1987;Ann. ICRP 17(4).
10. NCRP. Mammography - a user's guide. Bethesda: National Council on Radiation Protection and Measurements, 1986.
11. IPEM. Guidance on the Establishment and Use of Diagnostic Reference Levels for Medical X-ray Examinations. Institute of Physics and Engineering in Medicine, 2004.
12. Perry N, Broeders M, De Wolf C, et al. European guidelines for quality assurance in breast cancer screening and diagnosis Fourth Edition. Luxembourg office for official publications of the European Communities. 2006.
13. Perry N, Schouten J. European guidelines for quality assurance in mammography screening: Office for official publications of the European communities; 2001.
14. Zoetelief J, Fitzgerald M, Leitz W, Säbel M. European protocol on dosimetry in mammography. European Protocol on Dosimetry in Mammography. 1996. doi:
15. IAEA. Dosimetry in diagnostic radiology: an international code of practice. Vienna: International Atomic Energy Agency; 2007. Available from URL: http://www-pub.iaea.org/MTCD/publications/PDF/TRS457_web.pdf.
16. Suleiman ME, Brennan PC, McEntee MF. Diagnostic reference levels in digital mammography: A systematic review. Radiat Prot Dosimetry. 2015; 167: 608–19.

17. Asada Y, Suzuki S, Minami K, Shirakawa S. Results of a 2011 national questionnaire for investigation of mean glandular dose from mammography in Japan. J radiol prot 2014;34(1):125-32. doi: 10.1088/0952-4746/34/1/125

18. Baldelli P, McCullagh J, Phelan N, Flanagan F. Comprehensive dose survey of breast screening in Ireland. Radiat Prot Dosimetry. 2011;145(1):52-60. doi: 10.1093/rpd/ncq375

19. Hauge IHR, Bredholt K, Olerud HM. New diagnostic reference level for full-field digital mammography units. Radiation Protection Dosimetry. 2013;157(2):181-92. doi: 10.1093/rpd/nct136

20. Smans K. Towards a proposition of a diagnostic (dose) reference level for mammographic acquisitions in breast screening measurements in Belgium. Radiation Protection Dosimetry. 2006;117(1-3):321-6.

21. Vassileva J, Dimov A, Slavchev A, Karadjov A. Bulgarian experience in the establishment of reference dose levels and implementation of a quality control system in diagnostic radiology. Radiation Protection Dosimetry. 2006;117(1-3):131-4. doi: 10.1093/rpd/nci720

22. Zdesar U. Reference levels for image quality in mammography. Radiat Prot Dosimetry. 2008;129(1-3):170-2. doi: 10.1093/rpd/ncn080

23. Thiele DL, Irvine M, Want D, Bernardo M (2011) Diagnostic reference levels for mammography in BreastScreen Queensland. Australas Phys Eng Sci Med 34 (3):415-418. doi:10.1007/s13246-011-0078-0

24. Dance D. Monte-Carlo calculation of conversion factors for the estimation of mean glandular breast dose. Phys Med Biol. 1990;35(9):1211.

25. Dance DR, Skinner CL, Young KC, Beckett JR, Kotre CJ. Additional factors for the estimation of mean glandular breast dose using the UK mammography dosimetry protocol. Phys Med Biol. 2000;45(11):3225-40.

26. Dance DR, Young KC, van Engen RE. Further factors for the estimation of mean glandular dose using the United Kingdom, European and IAEA breast dosimetry protocols. Phys Med Biol. 2009;54(14):4361-72. doi: 10.1088/0031-9155/54/14/002

27. Seeram E, Brennan PC. Diagnostic reference levels in radiology. Radiol Technol. 2006;77(5):373-84.

28. O'Leary D, Rainford L. A comparison of mean glandular dose diagnostic reference levels within the all-digital Irish National Breast Screening Programme and the Irish Symptomatic Breast Services. Radiat Prot Dosimetry. 2013;153(3):300-8. doi: 10.1093/rpd/ncs112

29. Geeraert N, Klausza R, Mullera S, editors. Breast characteristics and dosimetric data in X-ray mammography A large sample worldwide survey. Bonn: IAEA conference; 2012.

30. Michielsen K, Jacobs J, Lemmens K, et al. Results of a European dose survey for mammography. Radiation Protection Dosimetry. 2008;129(1-3):199-203. doi: 10.1093/rpd/ncn152

31. Hemdal B, Herrnsdorf L, Andersson I, Bengtsson G, Heddson B, Olsson M. Average glandular dose in routine mammography screening using a Sectra

MicroDose Mammography unit. Radiation Protection Dosimetry. 2005;114(1-3):436-43. doi: 10.1093/rpd/nch556

32. Young KC, Burch A, Oduko JM. Radiation doses received in the UK Breast Screening Programme in 2001 and 2002. Br J Radiol. 2005;78(927):207-18. doi: 10.1259/bjr/41095952

33. Chevalier M, Moran P, Ten JI, Soto JMF, Cepeda T, Vano E. Patient dose in digital mammography. Med Phys. 2004;31(9):2471-9. doi: 10.1118/1.1784591

34. Bor D, Akyol O, Olgar T. Performance measurements of mammographic systems. Radiation Protection Dosimetry. 2008;129(1-3):165-9. doi: 10.1093/rpd/ncn141

35. Moran P, Chevalier M, Ten JI, Sot JMF, Vano E. A survey of patient dose and clinical factors in a full-field digital mammography system. Radiation Protection Dosimetry. 2005;114(1-3):375-9. doi: 10.1093/rpd/nch514

36. Borg M, Badr I, Royle GJ. Mammography equipment performance, image quality and mean glandular dose in Malta. Radiat Prot Dosimetry. 2013;156(2):168-83. doi: 10.1093/rpd/nct051

Chapter Four

Mean Glandular Dose in digital mammography, a dose calculation method comparison.

Section 4.3 of this chapter has been published as:

Suleiman, M. E., Brennan, P. C., & McEntee, M. F. (2017). Mean glandular dose in digital mammography: a dose calculation method comparison. *Journal of Medical Imaging, 4*(1), 013502-013502. doi:10.1117/1.JMI.4.1.013502

[Published copy is available in Appendix 7.5]

I had had substantial contribution to this work. I designed the study, collected and analysed the data, was the primary author, wrote and edited each draft of the manuscript.

4.1 Bridging section

The definition of a DRL as established by the ICRP has been explained in chapter one. It requires "an easily measured quantity", that describes the absorbed dose to the patient [1]. For mammography, MGD is the absorbed dose descriptor, this quantity is a sophisticated measure that has evolved over time. The ICRP however, recommends the use of MGD for the calculation of DRLs. Nonetheless, as chapter three demonstrated, MGD has some weaknesses, mainly the complicated calculations for a large data set; such complexity could become an obstacle for authorized bodies entrusted with establishing local and national DRLs. Nonetheless, MGD is not only used for the optimisation process and establishing DRLs, results from dose audits are also utilised for the estimation of risk of radiation exposure to the patient, hence, it is important to maintain a balance between complexity and accuracy.

The high degree of digitisation in mammography has the potential to ease the fulfilment of the ICRP goal of keeping dose to the breast optimized and thereby reducing radiation risk to the patients. "Organ Dose", a readily available estimation of MGD within the DICOM header of digital mammograms, provides a simpler measure of dose to the breast than MGD. It is an automated estimation of MGD that requires less human involvement than the manual calculations of MGD. Therefore, it could facilitate making MGD estimation easier. This automated measurement of MGD has the potential to reduce the work load involved in establishing DRLs and provide a more efficient dose measure to be used for the optimisation of mammography investigations. Nonetheless, such automation should be consistent across all mammography vendors to produce consistent, comparable data.

This chapter explores consistency of the Organ Dose across the four mammography vendors utilised within BreastScreen NSW centers, namely, GE medical systems, Phillips (Sectra), Fujifilm systems and Hologic systems. The findings of this work have been published as "Mean glandular dose in digital mammography: a dose calculation method comparison" [2]. That publication compared Organ Dose and MGD calculated using three Monte-Carlo techniques: Dance et al. [3-5], Sobol and Wu [6], and Boone et al. [7-9]. The aforementioned calculation methods are utilised by the four mammography unit vendors; GE medical systems utilise Wu et al. method,

Phillips (Sectra) and Fujifilm systems utilise Dance et al. method, while Hologic systems utilise a method by Boone et al.

The results of this work show a statistically significant bias between the Organ Dose and our calculated MGD for all systems, with different bias levels for each vendor. Phillips systems had the lowest bias, meaning they overestimated MGD by an average of 0.03 ($p < 0.001$) mGy while GE resulted in the highest bias underestimating MGD by 0.20 mGy ($p < 0.001$), with inconsistency also being seen across different GE models (Table 4.1).

Through the process of investigating Organ Doses, it was found in the study that GE systems use an estimation of glandularity that feeds into the calculations of Organ Dose. At the time, GE's glandularity estimation method was unclear. However, communication with a GE representative revealed that the systems utilise a computation method described by Desponds et al. at RSNA 1994 [10]. The peak density is computed as a function of CBT using Desponds et al. method within the automatic exposure control (AEC) process [11]. Furthermore, The Senographe Essential uses a flexible paddle with higher uncertainty on compressed breast thickness. The use of the flexible paddle overrides the AEC system applying a standard 50% density value to the Organ Dose estimation, this is regardless of the actual density. Inconsistency in the use of density for the estimation of Organ Dose could explain the differences found between GE's Organ Dose and the calculated MGD (Table 4.1) as a 50% glandularity was used to calculate MGD for the mammograms produced by GE units in my work. As for the inconsistency between different models, GE's representative explained that Organ Dose estimation methods do not vary across GE models utilised within BreastScreen NSW, making the variation in results unclear.

Table 4.1: Bland-Altman bias and 95% limits of agreement (LOA) to study the agreement between Organ Dose (displayed by the digital mammography unit) and dose calculated using three Monte-Carlo methods (Dance et al, Wu et al, and Boone et al) for different mammography unit models from 27,869 digital mammography images (Table from Suleiman et al. [2]).

Make	Model	Systems	Images	Organ Vs. Dance			Organ Vs. Wu			Organ Vs. Boone		
				Bias (mGy)	LOAs (mGy)	p value	Bias (mGy)	LOAs (mGy)	p value	Bias (mGy)	LOAs (mGy)	p value
Philips (Sectra)	L30	11	6210	0.03	-0.15, 0.21	<0.001	N/A	N/A	<0.001	-0.09	-0.33, 0.15	<0.001
GE MEDICAL SYSTEMS	Senographe Essential ADS_54.11	14	8282	-0.03	-0.29, 0.35	<0.001	0.21	-0.13, 0.54	<0.001	-0.20	-0.68, 0.28	<0.001
	Senographe Essential ADS_54.10	1	488	0.03	-0.27, 0.22	<0.001	0.26	0.00, 0.53	<0.001	-0.14	-0.54, 0.26	<0.001
	Senographe Essential ADS_53.40	1	727	-0.08	-0.13, 0.29	<0.001	0.13	-0.13, 0.38	<0.001	-0.22	-0.54, 0.10	<0.001
	Senograph DS ADS_54.11	2	982	-0.07	-0.17, 0.30	<0.001	0.12	-0.17, 0.42	<0.001	-0.14	-0.50, 0.23	<0.001
	Senograph DS ADS_53.40	1	454	0.13	-0.16, 0.43	<0.001	0.36	0.01, 0.71	<0.001	-0.04	-0.44, 0.37	<0.001
	Senograph 2000D ADS_17.4.5	1	316	-0.10	-0.37, 0.17	<0.001	0.17	-0.47, 0.126	<0.001	-0.04	-0.43, 0.35	<0.001
	GE Systems	20	11249	-0.03	-0.34, 0.28	<0.001	0.20	-0.14, 0.54	<0.001	-0.18	-0.64, 0.28	<0.001
	GE Systems with glandularity	20	11249	-0.03	-0.34, 0.28	<0.001	0.03	-0.14, 0.21	<0.001	-0.18	-0.64, 0.28	<0.001
HOLOGIC	Selenia Dimensions	21	9504	-0.24	-0.74, 0.27	<0.001	N/A	N/A	<0.001	-0.07	-0.67, 0.53	<0.001
Fujifilm	Amulet	1	906	-0.09	-0.35, 0.18	<0.001	N/A	N/A	<0.001	0.01	-0.28, 0.30	<0.001
Overall		53	27869	-0.09	-0.52, 0.34	<0.001	N/A	N/A	<0.001	-0.12	-0.60, 0.37	<0.001

4.1.1 **Extended methods**

The published article did not detail the methods used for MGD estimations, hence a detailed methodology of the work is presented below. Dance et al. method was explained comprehensively in chapter three, thus the following explains the methods of Sobol and Wu [6], and Boone et al. [7-9].

Sobol and Wu method was based on the work of Wu et al. [12, 13], which was explained in chapter two. The authors aimed to computerize the manual calculations of MGD by providing a set of functions that estimate the normalized average glandular dose (D_{gN}) taking into consideration the input parameters of CBT, glandularity, kVp and HVL. The functions were provided for three anode/filter combinations (Mo/Mo, Mo/Rh and Rh/Rh) and 100%, 50% and 0% glandular compositions, allowing for arbitrary composition. Figure 4.1 shows one of the functions.

```
Function MoRh(kVp, HVL, d, G)
'Moly Target - Rhodium Filter
'kVp range: 25 - 35 kVp
'HVL range: 0.3 - 0.54 mm
'Breast thickness d range: 3 - 8 cm
'Glandular tissue fraction range: 0 - 1
    'y1 = dose for 100% adipose breast (G=0)
        a = -167.925 + 12.6919 * kVp - 0.21961 * kVp ^ 2
        b = 2.47933 + 0.169961 * kVp - 0.00192616 * kVp ^ 2
        c = 1.27486 - 0.049889 * kVp + 0.000798223 * kVp ^ 2
        u = -291.171 + 39.4749 * kVp - 0.911079 * kVp ^ 2
        v = 10.3131 - 0.220194 * kVp + 0.00335665 * kVp ^ 2
        w = 0.455175 - 0.00925076 * kVp - 0.0000200714 * kVp ^ 2
        y1 = a + Exp(b - c * d) + (u + Exp(v - w * d)) * HVL
    'y2 = dose for 50% adipose breast (G=0.5)
        a = -151.97 + 11.4944 * kVp - 0.203044 * kVp ^ 2
        b = 2.06904 + 0.174721 * kVp - 0.00173687 * kVp ^ 2
        c = 1.48633 - 0.0631283 * kVp + 0.00110439 * kVp ^ 2
        u = 269.633 - 6.76953 * kVp + 0.0538371 * kVp ^ 2
        v = 9.14712 - 0.129615 * kVp + 0.00164991 * kVp ^ 2
        w = 0.468064 - 0.00538406 * kVp - 0.0000708036 * kVp ^ 2
        y2 = a + Exp(b - c * d) + (u + Exp(v - w * d)) * HVL
    'y3 = dose for 100% glandular breast (G=1)
        a = -138.774 + 10.4925 * kVp - 0.187584 * kVp ^ 2
        b = 2.07901 + 0.14281 * kVp - 0.000838839 * kVp ^ 2
        c = 1.81787 - 0.0888723 * kVp + 0.00167435 * kVp ^ 2
        u = 292.202 - 11.1746 * kVp + 0.173223 * kVp ^ 2
        v = 8.69168 - 0.0984208 * kVp + 0.00114853 * kVp ^ 2
        w = 0.456586 - 0.000851682 * kVp - 0.000139299 * kVp ^ 2
        y3 = a + Exp(b - c * d) + (u + Exp(v - w * d)) * HVL
   'Interpolating polynomial for arbitrary breast composition
   MoRh = y1 - (3 * y1 - 4 * y2 + y3) * G + 2 * (y1 - 2 * y2 + y3) * G ^ 2
```

Figure 4.1:An example of Sobol and Wu functions to parameterize the normalised average glandular dose (D_{gN}). Half Value Layer (HVL), peak kilovoltage value (kVp), breast thickness (d) and glandularity (G) are the values utilised for image acquisition. y1, y2, or y3 are the calculated MGDs for 0%, 50%, and 100% glandularities. a, b, c, u, v and w are parameters calculated by the authors to be used in the equations set to estimate MGD. [6].

Boone et al. method provides algorithms implemented in a Microsoft Excel work book that generates DgN values. Figure 4.2 provides an example of the fit equations used to write these algorithms.

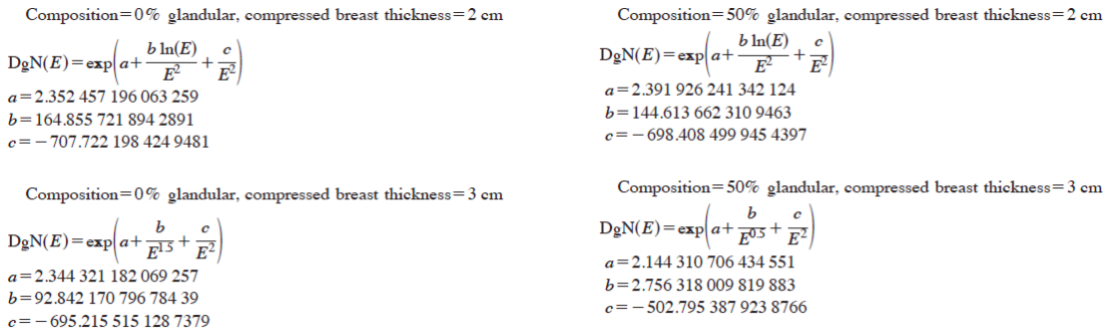

Figure 4.2: example of the fit equations from the work of Boone et al., used for the estimation of normalised average glandular dose (D_{GN}). E is the X-ray energy measured in keV which is known as kVp used for the image acquisition. a, b and c are parameters estimated by the authors to be used for the calculation of D_{gN}[8].

The preliminary results of this chapter were presented in the International society for optics and photonics (SPIE) conference in San Diego, USA in 2016, which led to a conference proceeding paper entitled "DICOM Organ Dose does not accurately represent calculated dose in mammography" [14]. The complete results were published in the Journal of Medical Imaging and are entitled "Mean glandular dose in digital mammography: a dose calculation method comparison" [2]. This article is presented in the next subsection.

4.2 References

1. Vañó, E., et al., ICRP Publication 135: Diagnostic Reference Levels in Medical Imaging. Annals of the ICRP, 2017. 46(1): p. 1-144.
2. Suleiman, M.E., P.C. Brennan, and M.F. McEntee, Mean glandular dose in digital mammography: a dose calculation method comparison. Journal of Medical Imaging, 2017. 4(1): p. 013502-013502.
3. Dance, D., Monte-Carlo calculation of conversion factors for the estimation of mean glandular breast dose. Physics in medicine and biology, 1990. 35(9): p. 1211.
4. Dance, D.R., et al., Additional factors for the estimation of mean glandular breast dose using the UK mammography dosimetry protocol. Physics in Medicine and Biology, 2000. 45(11): p. 3225-3240.
5. Dance, D.R., K.C. Young, and R.E. van Engen, Further factors for the estimation of mean glandular dose using the United Kingdom, European and IAEA breast dosimetry protocols. Phys Med Biol, 2009. 54(14): p. 4361-72.
6. Sobol, W.T. and X. Wu, Parametre of mammography normalized average glandular dose tables. Med Phys, 1997. 24(4): p. 547-54.
7. Boone, J.M., Glandular breast dose for monoenergetic and high-energy X-ray beams: Monte Carlo assessment. Radiology, 1999. 213(1): p. 23-37.
8. Boone, J.M., Normalized glandular dose (DgN) coefficients for arbitrary X-ray spectra in mammography: computer-fit values of Monte Carlo derived data. Med Phys, 2002. 29(5): p. 869-75.
9. Boone, J.M., T.R. Fewell, and R.J. Jennings, Molybdenum, rhodium, and tungsten anode spectral models using interpolating polynomials with application to mammography. Med Phys, 1997. 24(12): p. 1863-74.
10. Desponds, L. and R. Klausz, Automatic estimation of breast composition with mammographic X-ray systems. Radiology, 1994. 193: p. 200.
11. Geeraert, N., R. Klausza, and S. Mullera. Breast characteristics and dosimetric data in X-ray mammography A large sample worldwide survey. in Bonn: IAEA conference. 2012. Citeseer.
12. Wu, X., G.T. Barnes, and D.M. Tucker, Spectral dependence of glandular tissue dose in screen-film mammography. Radiology, 1991. 179(1): p. 143-148.
13. Wu, X., et al., Normalized average glandular dose in molybdenum target-rhodium filter and rhodium target-rhodium filter mammography. Radiology, 1994. 193(1): p. 83-89.
14. Suleiman, M.E., P.C. Brennan, and M.F. McEntee. DICOM organ dose does not accurately represent calculated dose in mammography. 2016. Proc. SPIE 9783, Medical Imaging 2016: Physics of Medical Imaging, 97832L (22 March 2016); doi:10.1117/12.2216698

4.3 Mean glandular dose in digital mammography: A dose calculation method comparison

Moayyad E. Suleiman, * Patrick C. Brennan, and Mark F. McEntee
The University of Sydney, Faculty of Health Sciences, M205, Cumberland Campus, 75 East Street, Lidcombe, New South Wales 2141, Australia

Abstract. Our objective was to analyze the agreement between Organ Dose estimated by different digital mammography units and calculated dose for clinical data. Digital Imaging and Communication in Medicine header information was extracted from 52,405 anonymized mammograms. Data were filtered to include images with no breast implants, breast thicknesses 20 to 110 mm, and complete exposure and quality assurance data. Mean glandular dose was calculated using methods by Dance et al., Wu et al., and Boone et al. Bland–Altman analysis and regression were used to study the agreement and correlation between organ and calculated doses. Bland– Altman showed statistically significant bias between organ and calculated doses. The bias differed for different unit makes and models; Philips had the lowest bias, overestimating Dance method by 0.03 mGy, while general electric had the highest bias, overestimating Wu method by 0.20 mGy, the Hologic Organ Dose underestimated Boone method by 0.07 mGy, and the Fujifilm Organ Dose underestimated Dance method by 0.09 mGy. Organ Dose was found to disagree with our calculated dose, yet Organ Dose is potentially beneficial for rapid dose audits. Conclusions drawn based on the Organ Dose alone come with a risk of over or underestimating the calculated dose to the patient and this error should be considered in any reported results. [DOI: 10.1117/1.JMI.4.1.013502]

Keywords: dosimetry; screening mammography; radiation; organ dose.

Paper 16146PRR received Jul. 17, 2016; accepted for publication Dec. 27, 2016; published online Jan. 24, 2017.

4.3.1 Introduction

Screening mammography invites healthy women for an x-ray examination of the breast, with the aim of early detection of breast cancer. The benefits of screening mammography have been scientifically examined and it has been shown, on the basis of randomized controlled trials, that screening mammography reduces breast cancer mortality by up to 25%. [1-4] This evidence was revisited in 2015 to find out if it is still valid today, the International Agency for Research on Cancer conducted a review of all published peer-reviewed literature through which they concluded that mammography screening is still effective in reducing breast cancer mortality [5].

Mammography efficacy in detecting breast cancer in early stages comes with a small but nonnegligible risk of radiation-induced cancer to the fibroglandular tissues of the breast [6], and possibly other exposed organs [7]. Monitoring the breast-absorbed dose is thus vital to ensure unnecessarily high doses do not occur; therefore, many quality assurance (QA) protocols have included breast dose assessments to govern the diagnostic adequacy of the imaging techniques in mammography [8-11].

Mean glandular dose (MGD) is the main descriptor of absorbed dose to the breast. MGD is calculated using conversion factors established by Monte-Carlo simulations. Dance et al [12-14], Sobol and Wu [15], Wu et al [16] and Boone et al [17-19] have established conversion factors that are widely used to estimate MGD. The three models differ slightly in the simulation method but all reported conversion factors dependent on breast thickness, glandularity, x-ray spectra, and beam quality. The conditions underlying Monte-Carlo simulation employed by different authors can impact the estimated dose by up to 19% [20].

The estimation of MGD is dependent on the values of half value layer (HVL) and output, while these values are also dependent on the measurement methods and can change substantially depending on the dosimeters and how they are used [21]. Furthermore, MGD is estimated using Monte-Carlo simulations which that utilize a computer model of the breast to simulate photon absorption in the glandular tissue of the breast, hence making MGD a dose to a breast model rather than a dose to the breast. This makes the estimation of MGD prone to errors regardless of the method used, hence, it is important to highlight that MGD is and will always be an estimation as it is not possible to measure the dose absorbed by the glandular tissue directly as well as

the differences in density distribution of the glandular tissue that also depend on the thickness of the breast and age of women.

Modern technology and the introduction of digital mammography provide valuable utility to easily collect data required to facilitate dose audits. The readily available estimation of MGD displayed by the digital systems provides a digital indication of the breast dose named organ dose, as well as information on radiographic technique and the performance of the imaging system. However, this estimated Organ Dose needs to be validated against other calculation methods before it can be used for dose audits or as an alternative approach to establish diagnostic reference levels (DRLs). Borg et al studied two mammography units [General Electric (GE) essential and Hologic Selenia] to establish the correlation between Organ Dose and the dose calculated for different thickness phantoms using the three Monte-Carlo estimations mentioned earlier, the authors concluded that Organ Dose compares well with the Monte-Carlo estimations within small to medium phantom thicknesses and differs slightly with thicker phantoms [22].

This study aims to analyze the agreement and correlation between Organ Dose displayed by four types of digital mammography units and calculated dose values for clinical data with a wide range of breast thicknesses using methods published by Dance et al [12-14], Wu et al [15, 16] and Boone et al [17-19].

4.3.2 Materials and methods

Data collection

Ethical approval was granted by the Human Research Ethics Committee (HREC) of the Cancer Institute of NSW (No.2014/08/552). The dose assessment included 61 mammography units from 50 BreastScreen centers and mobile vans throughout the state of NSW Australia. 52,405 (12,034 women) anonymized mammograms were downloaded from the Picture Archiving and Communication System located at the Cancer institute of NSW.

The following information was extracted from the Digital Imaging and Communication in Medicine (DICOM) headers using a third-party software

(YAKAMI DICOM Tools ver. 1.4.1.0, Kyoto University, Japan), namely: age, study date, compressed breast thickness (CBT), presence of implants, view, laterality, tube voltage (kVp), tube current exposure time product (mAs), target material, filter material, exposure control mode, organ dose, detector ID, and mammographic unit model. Further quality assurance (QA) data required for the calculation of mean glandular dose (MGD) were collected from the annual QA medical physics reports of participating centers through the Cancer Institute of NSW, these reports consisted of dose measurements on 20 mm, 42 mm American College of Radiology (ACR) mammography accreditation phantom, and 60 mm phantom thicknesses for different anode/filter combinations. It should be noted here that as QA reports vary in detail given, some estimation is necessitated to calculate the output and HVL. The normal QA practice for mammography units is made on three different phantoms, hence, different sets of data (HVL, output, and mAs) were provided for different anode/filter combinations. Extrapolation was used to estimate the HVL for mammograms taken by anode/filter combinations that had one set of QA data using the method published by Robson et al. and expanded by Borg et al. [22, 23]. Also, different dosimeters utilized to measure the output may have slight differences some of which are stated in the calibration certificates provided from the manufacturers and could carry up to 5% error in calibration [24, 25].

Data preparation

Only mammograms for women with no breast implants, aged 40 to 64 and a compressed breast thickness (CBT) 20 to 110 mm were included. Any exposure information with manual exposure settings, no Organ Dose in DICOM header, or missing QA data were excluded due to the lack of exposure information to calculate MGD. The final data set included 27,869 mammograms from 40 BreastScreen centers and mobile vans (53 digital mammography units).

Mean Glandular Dose estimation

Mammography system vendors utilize different methods for the estimation of Organ Dose displayed by the imaging systems. Philips (Sectra) and Fujifilm utilize Dance method, while Hologic utilize Boone method and GE utilize Wu method [26] (it is important to stress here that the calculation methods are not clear) (Table 4.2). Hence,

for each mammogram, MGD was calculated using an in-house developed excel workbook utilizing the three methods published by Dance et al [12-14], Sobol and Wu [15] and Boone et al [17-19].

Table 4.2: Calculation methods and glandularities known to be used by each system included in this study for the estimation of displayed Organ Dose (vendor Method).

Manufacturer	**Displayed organ dose**	
	Calculation method	Glandularity
Philips (Sectra)	Dance	Unknown
GE Medical systems	Wu	Proprietary measure
Hologic	Boone	Unknown
Fujifilm	Dance	Unknown

Dance's method

Dance et al method utilizes the following equation to calculate MGD:

MGD = Kgcs

where: **K** is the incident air kerma (IAK) at the upper surface of the breast. **g** converts IAK to MGD for a breast with 50% glandularity. This method incorporates an estimation of glandularity provided as the **c** factor which corrects for differences in glandularity other than the 50% and is given for two age groups 40 to 49 and 50 to 64 years. g and c are dependent on HVL and CBT. **s** is spectra dependent, it corrects for different types of spectra where s = 1 for Mo/Mo anode/filter combination and changes for other combinations.

Wu's method

Wu's method utilizes the following formula:

MGD = K x DgN

Where K is the IAK at the upper surface of the breast and DgN is the normalized glandular dose per unit IAK. This method was applied using the paper published by Sobol and Wu [15] which provides parameter equations to calculate DgN for different anode/ filter combinations and different glandularities. The parameter equations were implemented into our excel workbook using 50% glandularity. Wu's method is limited

to three spectra namely Mo/Mo, Mo/Rh and Rh/Rh hence it could only be applied on the GE units.

Boone et al method

Boone's method [17-19] utilizes Wu's equation to calculate the MGD with data tables having an extended utility to include more anode/filter combinations (W/Rh and W/Ag) and thicker breasts. Boone data tables are provided for 0%, 50% and 100% glandularities and those tables were used to calculate the MGD with the assumption of 50% glandularity.

Table 4.3: Average mean glandular dose (MGD) for system displayed dose, three dose calculation methods and their standard deviation (SD) for 27,869 digital mammography images from four different mammography unit makes.

Make	**Model**	**Images**	**Average MGD (mGy), SD**			
			System	Dance	Wu	Boone
Philips (Sectra)	L30	6210	0.86, 0.25	0.83, 0.26	N/A	0.95, 0.27
GE Medical systems	All	11249	1.42, 0.31	1.45, 0.34	1.22, 0.26	1.60, 0.41
Hologic	Selenia Dimensions	9504	1.73, 0.66	1.97, 0.74	N/A	1.80, 0.68
Fujifilm	Amulet	906	0.93, 0.32	1.01, 0.42	N/A	0.91, 0.41

Data analysis

Bland-Altman analysis was used to study the agreement between Organ Dose and each of the three other calculation methods. Multiple regression analysis was performed to study the correlation between Organ Dose and each calculation method (SPSS v22, Excel 2011).

4.3.3 **Results**

Table 4.3 shows the average MGD values and standard deviation (SD) for the Organ Dose and the three calculation methods. The Bland-Altman analysis revealed statistically significant bias between Organ Dose and the three calculation methods with bias values, 95% limits of agreements (LOA), and p values shown in table 4.4. Linear regression models for each mammography unit make are shown in figures. 4.3(a), 4.4(a), 4.5 and 4.6.

Table 4.4: Bland-Altman bias and 95% limits of agreement (LOA) to study the agreement between Organ Dose (displayed by the digital mammography unit) and dose calculated using three Monte-Carlo methods (Dance et al, Wu et al, and Boone et al) for different mammography unit models from 27,869 digital mammography images.

Make	Model	Systems	Images	Organ Vs. Dance			Organ Vs. Wu			Organ Vs. Boone		
				Bias (mGy)	LOAs (mGy)	p value	Bias (mGy)	LOAs (mGy)	p value	Bias (mGy)	LOAs (mGy)	p value
Philips (Sectra)	L30	11	6210	0.03	-0.15, 0.21	<0.001	N/A	N/A	<0.001	-0.09	-0.33, 0.15	<0.001
GE MEDICAL SYSTEMS	Senographe Essential ADS_54.11	14	8282	-0.03	-0.29, 0.35	<0.001	0.21	-0.13, 0.54	<0.001	-0.20	-0.68, 0.28	<0.001
	Senographe Essential ADS_54.10	1	488	0.03	-0.27, 0.22	<0.001	0.26	0.00, 0.53	<0.001	-0.14	-0.54, 0.26	<0.001
	Senographe Essential ADS_53.40	1	727	-0.08	-0.13, 0.29	<0.001	0.13	-0.13, 0.38	<0.001	-0.22	-0.54, 0.10	<0.001
	Senograph DS ADS_54.11	2	982	-0.07	-0.17, 0.30	<0.001	0.12	-0.17, 0.42	<0.001	-0.14	-0.50, 0.23	<0.001
	Senograph DS ADS_53.40	1	454	0.13	-0.16, 0.43	<0.001	0.36	0.01, 0.71	<0.001	-0.04	-0.44, 0.37	<0.001
	Senograph 2000D ADS_17.4.5	1	316	-0.10	-0.37, 0.17	<0.001	0.17	-0.47, 0.126	<0.001	-0.04	-0.43, 0.35	<0.001
	GE Systems	20	11249	-0.03	-0.34, 0.28	<0.001	0.20	-0.14, 0.54	<0.001	-0.18	-0.64, 0.28	<0.001
	GE Systems with glandularity	20	11249	-0.03	-0.34, 0.28	<0.001	0.03	-0.14, 0.21	<0.001	-0.18	-0.64, 0.28	<0.001
HOLOGIC	Selenia Dimensions	21	9504	-0.24	-0.74, 0.27	<0.001	N/A	N/A	<0.001	-0.07	-0.67, 0.53	<0.001
Fujifilm	Amulet	1	906	-0.09	-0.35, 0.18	<0.001	N/A	N/A	<0.001	0.01	-0.28, 0.30	<0.001
Overall		53	27869	-0.09	-0.52, 0.34	<0.001	N/A	N/A	<0.001	-0.12	-0.60, 0.37	<0.001

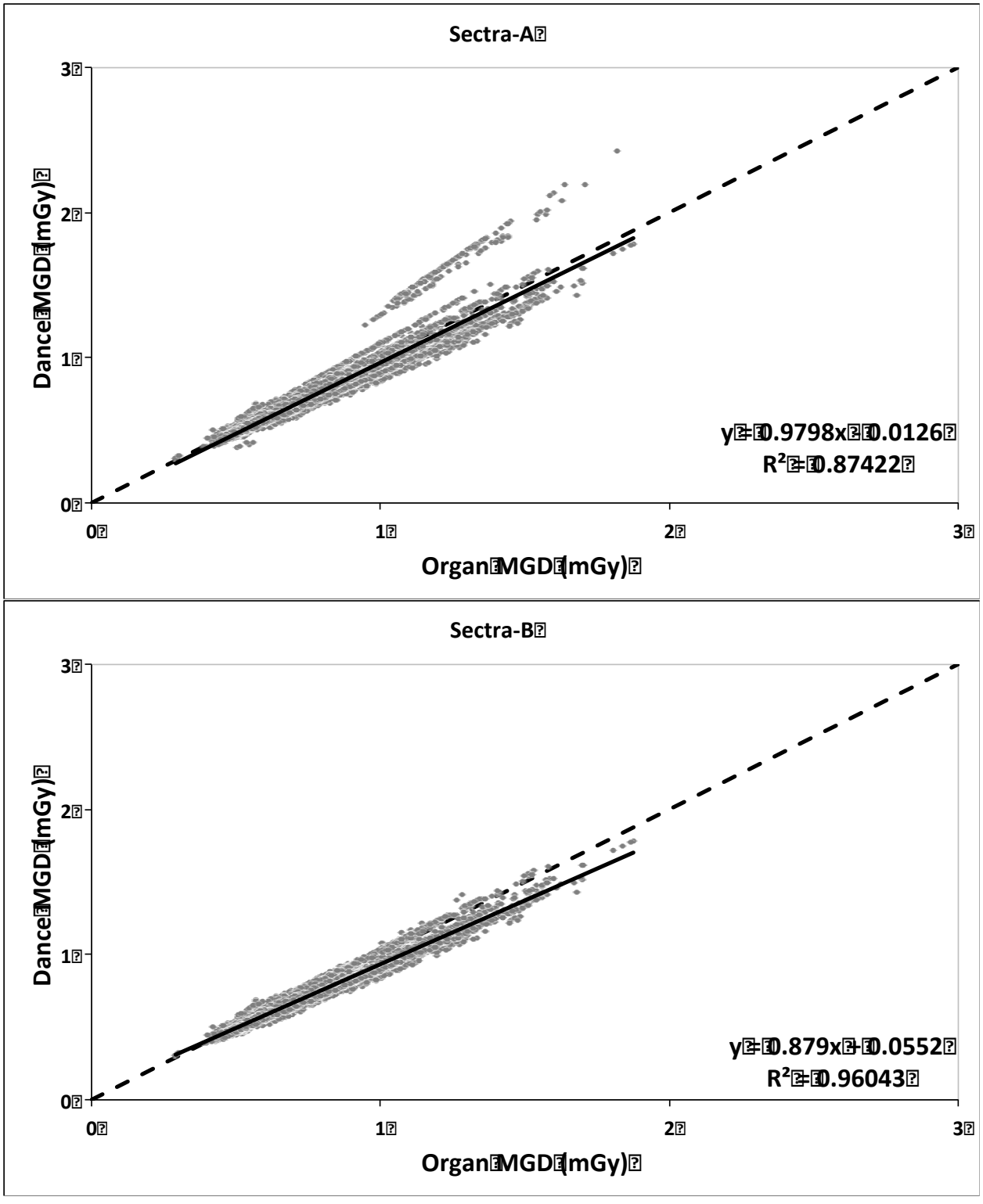

Figure 4.3:Linear regression scatter plots showing the line of best-fit between MGD calculated using Dance method and Organ Dose dis- played by Philips (Sectra) units for 6210 digital mammograms: (a) full data and (b) data after removing a problematic unit. (Philips systems utilize Dance method for the estimation of organ dose).

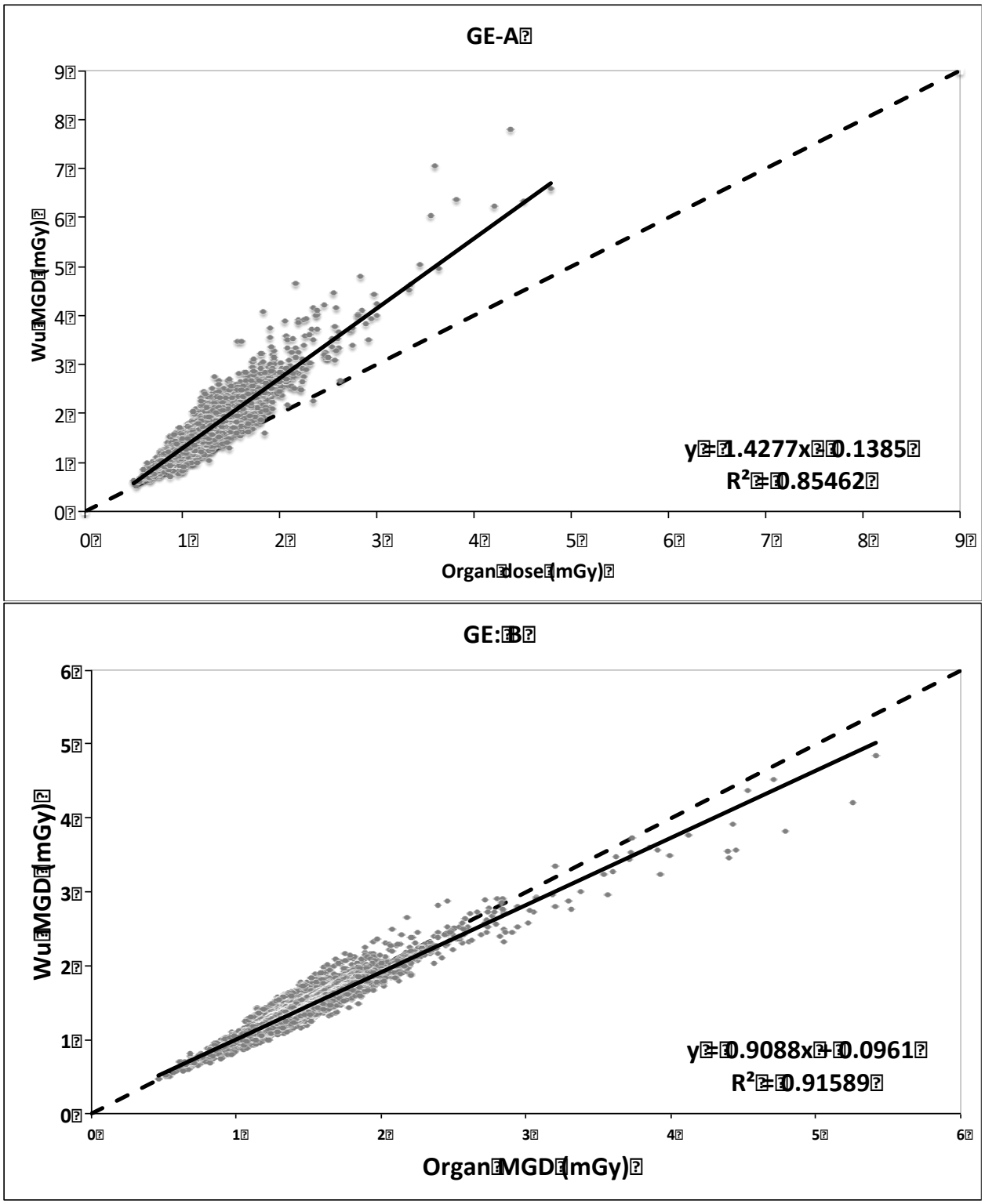

Figure 4.4: Linear regression scatter plots showing the line of best-fit between (a) MGD calculated using Wu method assuming 50% glandularity and Organ Dose displayed by GE units and (b) MGD calculated using Wu method and using the DICOM glandularity (0040,0310 comments on radiation dose) and Organ Dose displayed by GE units for 11,249 digital mammograms. (GE systems utilize Wu method for the estimation of organ dose).

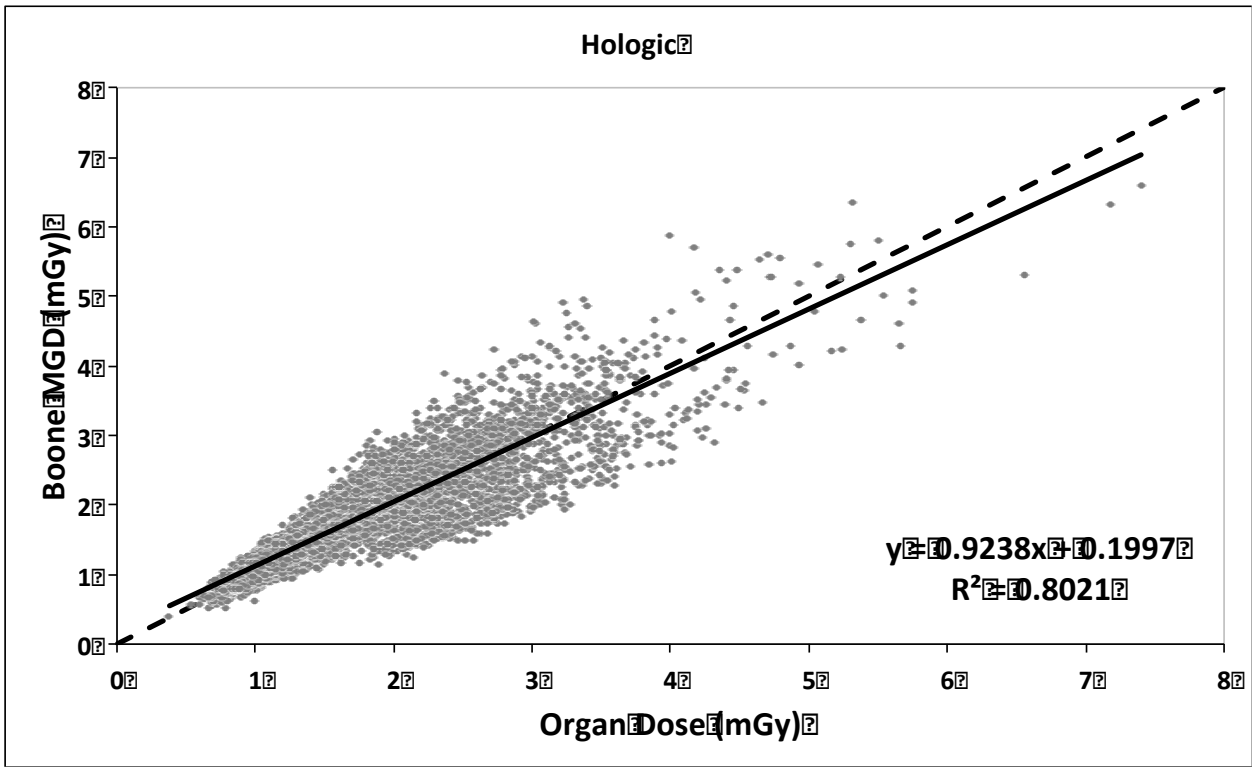

Figure 4.5:Linear regression scatter plot that shows the line of best-fit between MGD calculated using Boone method and Organ Dose dis- played by Hologic units for 9504 digital mammograms. (Hologic systems utilize Boone method for the estimation of organ dose).

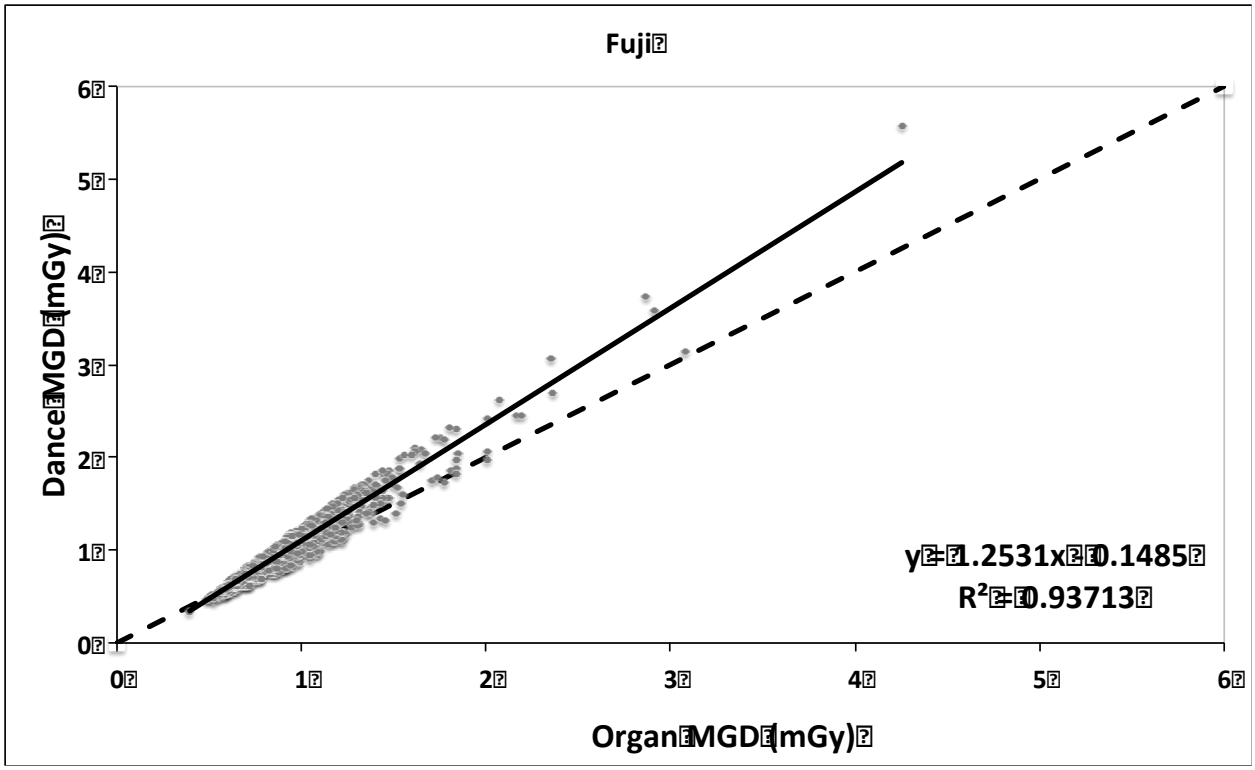

Figure 4.6:Linear regression scatter plot that shows the line of best-fit between MGD calculated using Dance method and Organ Dose dis- played by Fujifilm units for 906 digital mammograms. (Fujifilm systems utilize Dance method for the estimation of organ dose).

4.3.4 **Discussion**

The variation in methods used to estimate MGD makes international comparisons. The same issue exists for the Organ Dose displayed by the imaging system, where different vendors are using different methods to estimate the organ dose, although it is important to emphasize here that the calculation methods employed by different vendors are not clear. Organ Dose displayed by the system could be used as a robust method to evaluate the dose for a wide range of breast thicknesses and systems, as well as facilitating larger sample sizes. However, the use of Organ Dose needs to be validated against other dose calculation methods before it can be implemented. This study examined the agreement and correlation between MGDs calculated using three Monte-Carlo methods and the Organ Dose displayed by the mammography systems.

Philips systems showed a statistically significant bias indicating the displayed Organ Dose is overestimating Dance MGD by an average of 0.03 mGy, while Boone MGD under estimated the Organ Dose by a higher bias (Table 4.4). This is expected as the Philips (Sectra) systems employ Dance conversion factors for the Organ Dose estimation. On the other hand, the scatter plot for the Philips systems revealed a group of dose points that have a higher difference between the organ and Dance MGD [Figure 4.3(a)]. These belonged to one system and are due to an error in the QA data collection for that system or an error in the system calibration. A scatter plot with those dose points removed shows a higher correlation increasing from R2 = 0.87 to R2 = 0.96. [Figure 4.3(b)]. Removing that system from the analysis increased the bias from 0.03 to 0.047 mGy. Therefore, as the bias is small in comparison to the clinical dose of 2.0 mGy, and there is a narrow upper and lower 95% LOA (Table 4.4), we can conclude that the calculated dose and Organ Dose are in agreement.

GE systems varied in performance depending on the model and version; in total though, they showed an average bias overestimated the Organ Dose by a 0.20 mGy, a few units had higher or lower bias, one of which overestimated the calculated dose by an average of 0.36 mGy. Figure 4.4(a) shows the correlation between calculated dose (Wu method) and the Organ Dose with R^2 =0.85. Due to the higher bias further investigation was carried out and it was discovered that GE systems utilize a proprietary measure of glandularity and they enter this into the DICOM header at tag

0040,0310 “Comments on radiation dose”. It was also found that the glandularity estimation was set to 50% in some centres and many mammograms had 0% or 100% estimations, regardless of the breast thickness. Neither the glandularity estimation method nor its accuracy is described in the literature. Nonetheless, once the calculations were adjusted to account for the proprietary glandularity estimation the bias was substantially reduced (Table 4.4) and showed a much better correlation with an $R^2 = 0.92$ [Figure 4.4(B)]. Although the GE Organ Dose had a higher level of agreement with the Wu method after the inclusion of the proprietary glandularity estimation, these 0% glandularity estimations in many of the GE systems mean that these organ doses cannot reflect the calculated MGD correctly as they do not account for any glandularity.

Hologic system’s Organ Dose reported a small bias (Table 4.4) underestimating the Boone calculated MGD, nonetheless, it shows a difference of up to 0.67 mGy, which represents the complete absorbed dose for small breast thicknesses. The correlation between calculated dose (Boone method) and Organ Dose show an $R^2 = 0.8$, which although good, is the lowest correlation out of the four vendors. We can conclude that in our study the Hologic system Organ Dose did not accurately reflect our calculated dose.

Fujifilm constitutes less than 4% of the total sample. Only one Fujifilm amulet unit was included in this survey hence, no intrasystem comparison was possible. Other Fujifilm units were computed radiography (CR) systems and did not recorded organ dose. The Fujifilm amulet unit showed average results underestimating Dance MGD with a small positive bias of 0.09 mGy. Linear regression showed an excellent correlation with $R^2 = 0.94$ (Figure 4.6).

Organ Dose from the four systems showed a statistically significant bias when compared to the calculated dose. It has been reported that the statistical significance of the bias in the Bland-Altman method should not be the only value considered; however, the clinical significance of that value and the LOA should be considered as well. In this study, the bias reported for Philips (Sectra) Hologic, and Fujifilm are considered clinically insignificant, being much smaller than the clinical dose, nonetheless, when considering how wide the LOA are, it can be concluded that a disagreement between organ and calculated doses was found. Furthermore, it should be stressed that vendors using different methods of estimating the Organ Dose make

reporting the dose across systems unreliable, as the dose reported by the three methods differ by up to 19%. Nonetheless, with vendors using various algorithms, some of which are not particularly well defined, there is a need for further work to establish a benchmark and allow comparison of doses between systems.

MGD calculation methods are all estimates; they are prone to systematic errors throughout measurement and calculation. Earlier methods of measuring the entrance dose using TLDs, although difficult, time consuming and having smaller sample sizes, offered more accurate measurements. The bias reported here for some systems was 0.36 mGy which is 18% of the acceptable dose level of 2.00 mGy reported by the European commission for a 45 mm breast thickness [11]. This is still within the error value that is reported for the dose calculation methods. However, choosing to use Organ Dose may risk underestimating the dose by up to an overall average of 0.09 mGy with a range from -0.52 to 0.34 mGy, this range of bias could result in a clinically important discrepancy between calculated and Organ Dose of up to 0.52 mGy. Considering that the European protocol DRL for a 45 mm breast thickness is 2.0 mGy [11], this could have important implications for reporting doses locally and nationally. Further work might examine actual air kerma using TLDs on select phantoms such as the ACR phantom and phantoms with different thicknesses.

4.3.5 **Conclusion**

Organ Dose was found to disagree with calculated dose, with a bias ranging from -0.24 to 0.36 mGy. However, Organ Dose is potentially beneficial for rapid dose audits in centres using mammography units of the same make. Conclusions drawn based on the Organ Dose alone, whether to establish DRLs or for dose audits, come with a risk of over or underestimating the calculated dose to the patient by up to 18% for a standard breast and this error should be considered in any reported results.

4.3.6 **Disclosures**

The authors have nothing to disclose.

4.3.7 References

1. Vainio, H. and F. Bianchini, Breast cancer screening, IARC handbooks of cancer prevention. IARC, Lyon, 2002: p. 157-170.
2. Chu, K.C., C.R. Smart, and R.E. Tarone, Analysis of Breast Cancer Mortality and Stage Distribution by Age for the Health Insurance Plan Clinical Trial. Journal of the National Cancer Institute, 1988. 80(14): p. 1125-1132.
3. Miller, A.B., et al., Canadian National Breast Screening Study: 2. Breast cancer detection and death rates among women aged 50 to 59 years. CMAJ: Canadian Medical Association Journal, 1992. 147(10): p. 1477-1488.
4. Nyström, L., et al., Breast cancer screening with mammography: overview of Swedish randomised trials. The Lancet, 1993. 341(8851): p. 973-978.
5. Lauby-Secretan, B., et al., Breast-cancer screening—viewpoint of the IARC Working Group. New England Journal of Medicine, 2015. 372(24): p. 2353-2358.
6. Yaffe, M.J. and J.G. Mainprize, Risk of Radiation-induced Breast Cancer from Mammographic Screening. Radiology, 2011. 258(1): p. 98-105.
7. M. Ali, R., et al., A method for calculating effective lifetime risk of radiation-induced cancer from screening mammography. Radiography, 2015. 21(4): p. 298-303.
8. Hendrick, R., et al., Mammography quality control manual. Reston, Va: American College of Radiology, 1999.
9. IAEA, Quality Assurance Programme for Digital Mammography. Human Health Series. No. 17. 2011, Vienna: IAEA. 177.
10. Moore, A., The Commissioning and Routine Testing of Mammographic X-ray Systems: A Protocol Produced by a Working Party of the Diagnostic Breast Screening Quality Assurance Coordinating Group for Physics. 2005: Institute of Physics and Engineering in Medicine.
11. Perry, N., et al., European guidelines for quality assurance in breast cancer screening and diagnosis Fourth Edition. Luxembourg office for official publications of the European Communities, 2006.
12. Dance, D., Monte-Carlo calculation of conversion factors for the estimation of mean glandular breast dose. Physics in medicine and biology, 1990. 35(9): p. 1211.
13. Dance, D.R., et al., Additional factors for the estimation of mean glandular breast dose using the UK mammography dosimetry protocol. Physics in Medicine and Biology, 2000. 45(11): p. 3225-3240.
14. Dance, D.R., K.C. Young, and R.E. van Engen, Further factors for the estimation of mean glandular dose using the United Kingdom, European and IAEA breast dosimetry protocols. Phys Med Biol, 2009. 54(14): p. 4361-72.
15. Sobol, W.T. and X. Wu, Parametrization of mammography normalized average glandular dose tables. Med Phys, 1997. 24(4): p. 547-54.

16. Wu, X., et al., Normalized average glandular dose in molybdenum target-rhodium filter and rhodium target-rhodium filter mammography. Radiology, 1994. 193(1): p. 83-89.

17. Boone, J.M., Glandular breast dose for monoenergetic and high-energy X-ray beams: Monte Carlo assessment. Radiology, 1999. 213(1): p. 23-37.

18. Boone, J.M., Normalized glandular dose (DgN) coefficients for arbitrary X-ray spectra in mammography: computer-fit values of Monte Carlo derived data. Med Phys, 2002. 29(5): p. 869-75.

19. Boone, J.M., T.R. Fewell, and R.J. Jennings, Molybdenum, rhodium, and tungsten anode spectral models using interpolating polynomials with application to mammography. Med Phys, 1997. 24(12): p. 1863-74.

20. Zoetelief, J. and J.T.M. Jansen, Calculation of Air Kerma to Average Glandular Tissue Dose Conversion Factors for Mammography. Radiation Protection Dosimetry, 1995. 57(1-4): p. 397-400.

21. Avramova-Cholakova, S., et al., An estimate of the influence of the measurement procedure on patient and phantom doses in breast imaging. Radiation Protection Dosimetry, 2008. 129(1-3): p. 150-154.

22. Borg, M., I. Badr, and G.J. Royle, A study to determine the differences between the displayed dose values for two full-field digital mammography units and values calculated using a range of Monte-Carlo-based techniques: a phantom study. Radiat Prot Dosimetry, 2012. 154(2): p. 217-28.

23. Robson, K.J., A parametric method for determining mammographic X-ray tube output and half value layer. Br J Radiol, 2001. 74(880): p. 335-40.

24. RaySafe, "RaySafe Xi classic specifications," 2015, http://mediabank.raysafe.com/A/RaySafe+Media+Bank/1599?encoding=UTF-8 (10 October 2016).

25. RTIgroup, "Piranha specification," 2016, http://rtigroup.com/content/downloads/brochures/Specifications_Piranha.pdf (10 October 2016).

26. McCullagh, J.B., P. Baldelli, and N. Phelan, Clinical dose performance of full field digital mammography in a breast screening programme. Br J Radiol, 2011. 84(1007): p. 1027-33.

Chapter Five

Integrating mammographic breast density in glandular dose calculation

Section 5.2 of this chapter has been published as:

Suleiman, M. E., Brennan, P. C., Ekpo, E., Kench, P., & McEntee, M. F. (2018). Integrating mammographic breast density in glandular dose calculation. *British Journal of Radiology*, 20180032. doi:10.1259/bjr.20180032

[Published copy is available in Appendix 7.6]

I had had substantial contribution to this work. I designed the study, collected and analysed the data, was the primary author, wrote and edited each draft of the manuscript.

5.1 Bridging section

Radiation exposure to the population has doubled since the 1980s [1], and it has been established that radiologic examinations can cause biological changes in humans [1]. In mammography, the fibroglandular tissue of the breast is considered most radiosensitive, and low radiation doses could have different effects on cell damage, repair, and apoptosis depending on the gene mutations that an individual may have [2, 3]. Gene mutations involving damage to the repair pathway may reduce an individual's ability to successfully repair any damage, including that caused by radiation [2].

Repair of radiation-induced cellular damage has a complex pathway. Briefly, it involves several crucial genes including Histone variant H2AX, Phosophoprotein p53, serine/threonine protein kinase (ATM), and BReast CAncer susceptibility genes (BRCA1 and BRCA2). These are known as tumour suppression genes and produce proteins that help in the repair of the damaged DNA organic molecules. Mutation in any of these genes will prevent or disrupt the production of repair proteins thereby preventing DNA damage to be successfully repaired. Failure to repair may result in cell death or progenitor cells with mutated DNA [3]; this mutated cell develops different social behavioural pathways to its neighbouring cells, and operates out of the system, allowing it to divide and escape suicide, consuming resources and growing outside of the planned structure of the body, it is a new growth, a neoplasm. This is carcinogenesis. Furthermore, blood within the breast is exposed to radiation during mammography. Although the amount of blood within the breast during mammography is small due to compression which expresses it out of the breast, blood samples drawn from women attending mammography have shown signs of DNA damage [4]. Other body tissues are also affected by radiation during mammography. Ali et al. studied the effective radiation risk during mammography on other major body parts and found that some organs received radiation dose ranging from 0.006 to 26.6 μGy [5]. Hence, the risk of developing cancer from mammography screening is noticeable, and the need to accurately quantify this risk is evident [6].

Radiation risk to the breast is quantified using the Mean Glandular Dose (MGD). Thus, to appropriately estimate cancer risk from mammography, a measure of the fibroglandular tissue of the breast should be included in the calculations of MGD. However, MGD calculation methods mentioned in chapter two are all based on a

simple breast model and estimates of breast composition. They assume a homogeneous breast composition with 50% glandularity; except for Dance et al. who refined the estimation of MGD by adjusting for different glandularities depending on age and CBT. Furthermore, Dance et al. investigated the effect of a heterogeneous breast composition on MGD, using a high-resolution voxel phantom. Dance et al. found up to 48% error in their conversion factors [7], and up to 30% overestimation of MGD when the heterogeneity in glandular tissue distribution within the breast was accounted for (compared to a homogeneous breast with Dance et al. model estimated glandularities) [8]. Also, the assumption of a homogeneous distribution of glandular tissue within the breast overestimates the glandular tissue near the entrance surface of the breast where radiation deposition is exponentially higher [8]. Hence, the risk of mammography is overestimated when using a simple breast model to estimate MGD.

Previously mentioned MGD calculation methods acknowledge the need for a more accurate estimate of glandularity to be included within the calculations of MGD [9-12]. Accurate measures of glandularity will lead to better individualised MGD and risk estimations. Further to the limitations detailed above, this chapter proposed the Actual Glandular Dose (AGD), a new method that integrates MBD in the calculations of MGD. A brief explanation of breast biology and composition, and the methods used to estimate breast composition is presented in the next subsections. This explanation aims to provide a rationale to supports the integration of breast composition within the calculations of AGD.

5.1.1 **Glandularity of the breast**

The female breast overlies the anterior aspect of pectoral muscle; it is generally composed of glandular and adipose tissues. The glandular tissue continuously develops starting at puberty until maturity [13] after which it is replaced gradually by adipose tissue [14]. The glandular tissue is made up of concealed lobes, which have varying numbers of lobules and ducts and are surrounded by adipose tissue (Figure 5.1). The ducts are made up of epithelial cells and surrounded by myoepithelial cells. The higher density of fibroglandular tissue is associated with high levels of epithelial cells, stroma and collagen. Epithelial cells are precursors of stromal cells and collagen. Altered interaction between breast epithelium, stroma and collagen makes the breast

more tensile and activate mechanisms through the lipoproteins lumican and decorin that increase breast density and cancer. Therefore, if the dense area absorbs more radiation and contain all the cells that support carcinogenesis, as epithelial cells are considered highly radiosensitive and 90% of cancers develop from epithelial cells [15], an accurate measure of fibroglandular tissue presence in the breast should be included in dose and risk assessment from mammography.

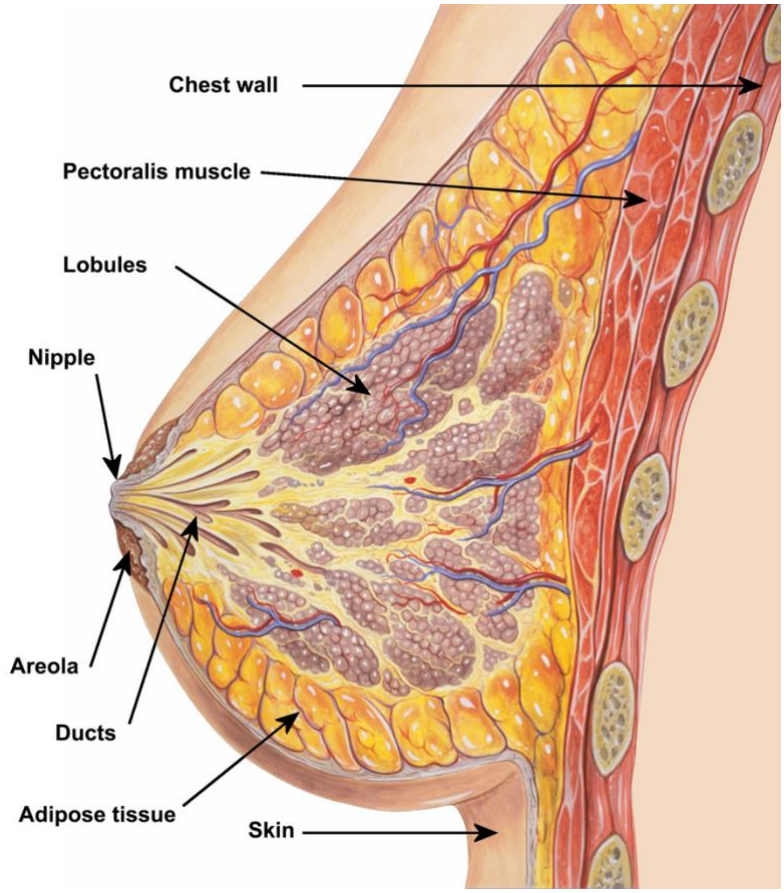

Figure 5.1: Breast composition

(Original author: Patrick J. Lynch. Reworked by Morgoth666 to add numbered legend arrows. (https://commons.wikimedia.org/wiki/File:Breast_anatomy_normal_scheme.png), „Breast anatomy normal scheme“, https://creativecommons.org/licenses/by/3.0/legalcode)

Breast composition is a major determinant of breast cancer risk as high density of fibroglandular tissue is associated with increased risk of cancer and dose in mammography. Hence, breast composition investigations rely on the use of the parenchymal patterns as it appears on a mammogram. Mammographic breast density studies consider breast composition as a simple model with two elements; radiopaque and radiolucent areas. Fibroglandular tissues are radiopaque, hence appearing as white areas on a mammogram. Fatty tissues on the other hand, are more radiolucent,

allowing X-rays to pass through more freely. The proportion of radiopaque breast tissue in a mammogram is referred to as the percentage mammographic density, which we refer to here as mammographic breast density (MBD). MBD is important for several reasons:

1. Radiation is absorbed more by dense than by fatty tissue;
2. The dense tissue reduces the visibility of other breast tissue, often referred to as masking effect; although recent studies on radiologists' performance showed that a high MBD digital mammogram may change the radiologists' attention behaviour and enhance cancer detection [16, 17].
3. A woman's risk of breast cancer is linked to her breast density [18]. However, previous studies on MBD have only focused on risk of cancer and masking.

5.1.2 **Mammographic breast density (MBD) measurements**

MBD has been studied extensively since it was associated with breast cancer risk [19, 20]. Women with the highest MBDs have shown a four-fold to six-fold increased risk of cancer compared to those with the lowest MBDs [21]. MBD has been measured qualitatively or quantitatively (Figure 5.2). Qualitative approaches depend on subjective visual assessment and observer opinion, while quantitative approaches rely on objective measurements of MBD. These approaches have been developed to quantify MBD for predicting risk of cancer and masking and are detailed below.

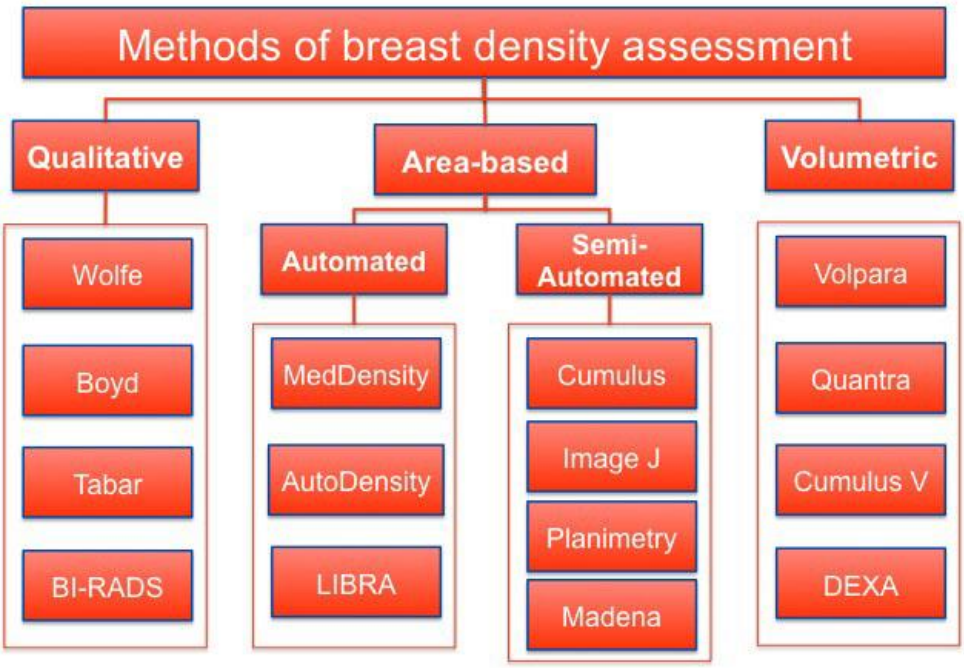

Figure 5.2: Commonly used approaches for mammographic breast density (MBD) assessment. BI-RADS®: Breast Imaging Reporting and Data System; LIBRA: Laboratory for Breast Radiodensity Assessment; DEXA: Dual-energy X-ray Absorptiometry. (Reproduced with permission [22])

5.1.3 **Qualitative measurements**

Wolfe's method: This method was proposed in 1976 by John Wolfe, and include four categories of MBD [19]:

- *N1-lowest risk: Parenchyma composed primarily of fat with at most small amounts of "dysplasia." No ducts visible.*
- *P1, low risk: Parenchyma chiefly fat with prominent ducts in anterior portion up to one-fourth of volume of breast. Also, may be a thin band of ducts extending into a quadrant.*
- *P2, high risk: Severe involvement with prominent duct pattern occupying more than one-fourth of volume of breast.*
- *DY, highest risk: Severe involvement with "dysplasia." Often obscures an underlying prominent duct pattern.*

Boyd's method: In 1980, Boyd classified MBD into six categories according to the proportion of the breast that appears dense on a mammogram [23-25], mammograms

were categorised as: 0%, 0-10%, 10-25%, 25-50%, 50-75% and >75%. Tabar's classifying method categorised the mammographic patterns of the breast into five patterns according to risk [26].

I. Evenly distributed tissue densities with slightly prominent fibrous tissue presence.
II. Almost entirely fatty with 1mm distributed fibrous tissue.
III. Fibrous tissue presence in retro areolar area.
IV. Extensive fibrous tissue with nodular masses larger than normal lobules.
V. Structure-less homogeneous apparel with predominant fibrous tissue.

BI-RADS®: In 2000, the ACR introduced the Breast Imaging-Reporting and Data System (BI-RADS) to standardise mammographic densities reporting. The latest edition of BI-RADS (5th edition) classifies breast density into four categories according to the amount and distribution of the dense area [27]:

A. The breasts are almost entirely fatty.
B. There are scattered areas of fibroglandular density.
C. The breasts are heterogeneously dense, which may obscure small masses.
D. The breasts are extremely dense, which lowers the sensitivity of mammography.

The use of qualitative approaches to measure MBD carries limitation that relate to the radiologist experience and subjectivity. Intra- and inter-reader disagreement and the inconsistency of MBD measurements across readers can be overcome by training the readers to reduce such disagreements [28-30]. Another limitation is the categorisation scale and distinguishing small differences in MBD. A simple answer to this limitation is to increase the number of categories, however, this may increase reader's disagreements. The use of qualitative methods to estimate MBD and the lack of reproducibility needed for the consistency in reading mammograms may limit MBD's effectiveness as a tool to predict cancer risk in women. Hence, quantitative methods were developed to estimate MBD.

5.1.4 Quantitative measurements

Computer assisted planimetry is an area-based technique that was developed in 1987 [31] to eliminate errors from the readers subjectivity and create reproducible results in

MBD measurements. Dense areas on the mammogram were marked manually by placing overlay acetate on the mammogram and using a wax pencil to mark dense areas.

Interactive thresholding was developed to replace hand drawing of the dense areas, this semi-automated method utilised manual segmentation of digitised mammograms using pixel brightness threshold value to distinguish dense from fatty tissue [32]. Cumulus (University of Toronto, Canada) and Madena (University of Southern California, US), are semi-automated methods that utilise interactive thresholding. Cumulus, published in 1994 [33], has been considered as the gold standard in breast density measurements [34]. The reader using Cumulus sets two thresholds: firstly, the reader identifies the breast tissue from the background; secondly, the reader sets the threshold of dense and non-dense tissue. The computer software then calculates the area of the breast, the area of dense and non-dense tissue, then calculates the percentage of dense tissue in the breast. Similarly, Madena software, coded in 1998 [35], utilises manual thresholding. The reader would tint (in yellow) dense regions of the breast, excluding the pectoral muscle, and the software then calculates the percentage of the yellow areas from the breast area. Limitations to the semi-automated methods in MBD measurements such as human intervention, high workload of thresholding and segmentation, and the influence of the reading environment have led to increasing interest in automated methods.

The advances in computing and technology have facilitated the automation of segmentation and thresholding. Several automated programs have been developed to measure MBD from mammograms; MedDensity, Image J, Autodensity and Laboratory for Individualised Breast Radiodensity Assessment (LIBRA) are examples of automated software that utilise thresholding to measure MBD.

MedDensity utilises automatic segmentation of the beast, differentiating dense from fatty tissue based on maximum entropy and spatial information. Pixel values are then used to estimate dense tissue and the breast area, the breast density is then calculated as the ratio of dense area to the area of the breast [36].

Image J [37], an established Java-based image analysis software was utilised by Li et al. in 2012 [38] to automate breast density measurements. Li et al. separated the breast region from the background by superimposing a mask using greyscale filters then

implementing automated thresholding to separate dense tissue from other areas of the breast.

AutoDensity, automatically identifies the breast area using segmentation, and classifies white areas in the breast as dense similar to Cumulus. AutoDensity, however, does not use a standard threshold across images; rather it finds an optimal distinct threshold level for each image in a data set independently from other images [39]. LIBRA [40, 41], is freely available software developed at the University of Pennsylvania Section for Biomedical Image Analysis (SBIA) in 2011.

LIBRA utilises a thresholding technique to identify the breast region and the pectoral muscle on a mammogram. An "adaptive multi-class fuzzy c-means" algorithm then partitions the mammographic breast tissue into clusters of similar intensity that are then aggregated to a dense tissue area. The software then assesses breast area, dense tissue area, and calculates MBD by dividing the dense area by the total breast area [40, 41].

The previously mentioned quantitative methods utilise two-dimensional mammograms to estimate MBD, which does not account for the volumetric presence of dense tissue, such as large volumes of dense tissue stacked up and projected down to an area representation on the mammogram. Furthermore, differences in positioning and exposure parameters resulting in quantum and anatomical noise may affect the appearance of MBD hence producing inconsistent result, which have led to a rational need for volumetric measurements of MBD.

Volumetric measurements of MBD, such as Volpara and Quantra, utilise X-ray attenuation information and CBT to calculate volumetric MBD [42]. Volumetric techniques have shown reliable [43] and reproducible [44] results. However, commercial volumetric MBD measurement methods carry limitations related to the cost for initial setup. The software is networked and tailored to the mammography unit make, this software needs to be supported by the mammography unit vendors before it can be implemented. Another limitation is the use of raw data to estimate MBD, which restricts its use to prospective data only. Such limitations will render current volumetric MBD estimations unreachable to centres with constrained budget and no demand for the measurement.

The limitations of automated volumetric methods emphasise the need for cost-effective and convenient methods that can measure MBD from both raw and processed images and have the ability to patch-process large volumes of images. LIBRA is a freely available, cost-effective, automated, and reliable and reproducible tool for MBD assessment. It also allows retrospective analyses of large volumes of raw and processed images and is capable of calibration. These abilities and advantages of LIBRA make it suitable for both clinical and experimental studies, including mammography dosimetry explored in this thesis. This chapter 5 used the MBD estimates of LIBRA from retrospective data to propose a new method for individualised MGD calculation. This work titled: "Integrating mammographic breast density in glandular dose calculation" [45], and published in the British journal of radiology, adapted Dance et al. method to calculate AGD. This was done by replacing Dance et al. estimations of MBD with the individual MBDs estimated using LIBRA software package. The results show that MGD underestimates the dose absorbed by the breast by up to 10%, having a bigger effect on small breasts and almost no effect on larger breasts. Some figures were not included in the journal article, which are presented here. Figure 5.3 shows a skewed distribution of MBDs estimated using LIBRA software, with a median and mean of 8% and 13% respectively.

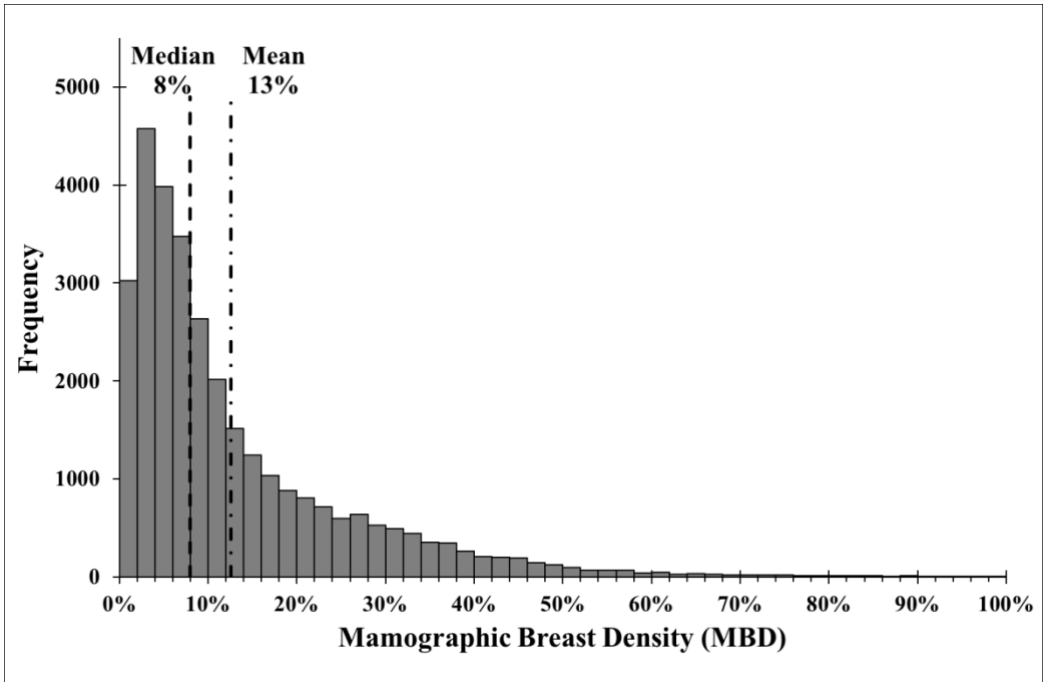

Figure 5.3: Distribution of glandularity for 31,097 mammography images.

Figure 5.4 shows MBD changes with age, MBD increased until the age of 42 then started to steadily decrease to the age of 60, then smaller decreases after. A peak was

noted at 89 years old, which seems to be an outlier as it had a very high error (seen by the wide confidence intervals). Figure 5.5 presents the linear regression line between MGD and AGD, showing a high correlation between the two methods (R^2 = 0.987), which is reasonable given that the base calculation method is similar, however, this does not mean there is an agreement as that is measured by the Bland-Altman analysis presented in the paper. The complete published journal article is presented in the next section.

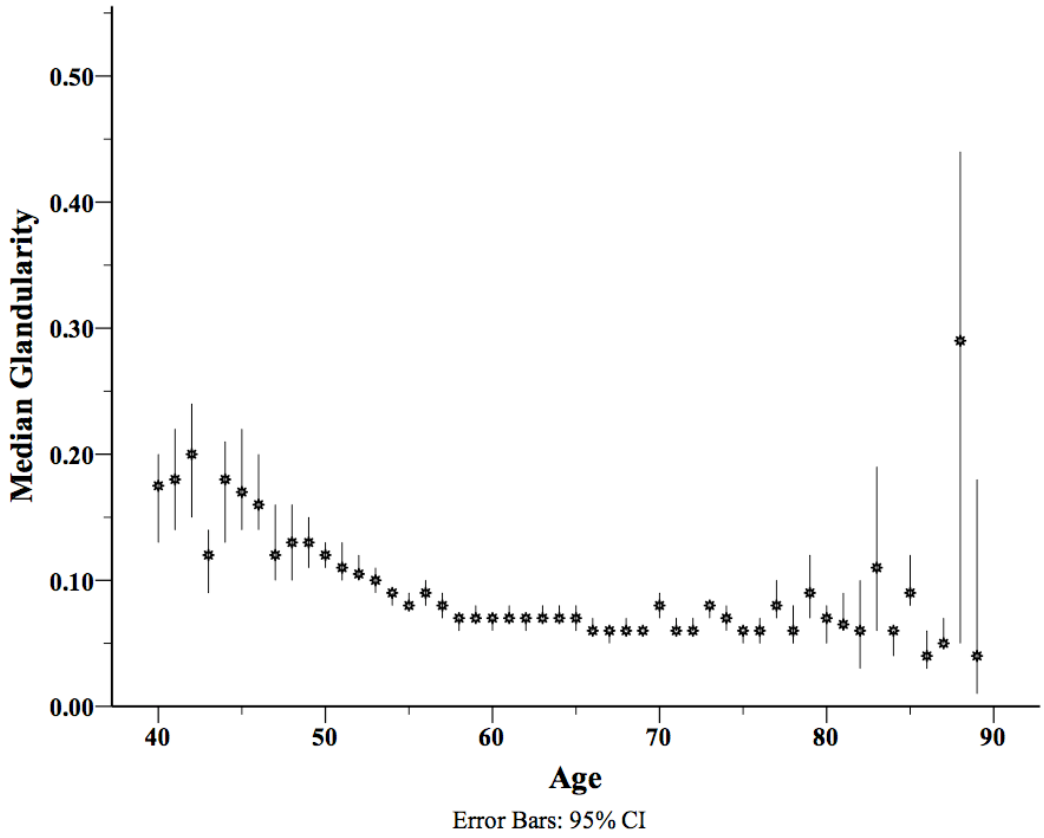

Figure 5.4: Median MBD behaviour with age, error bars represent the 95% confidence intervals (CI).

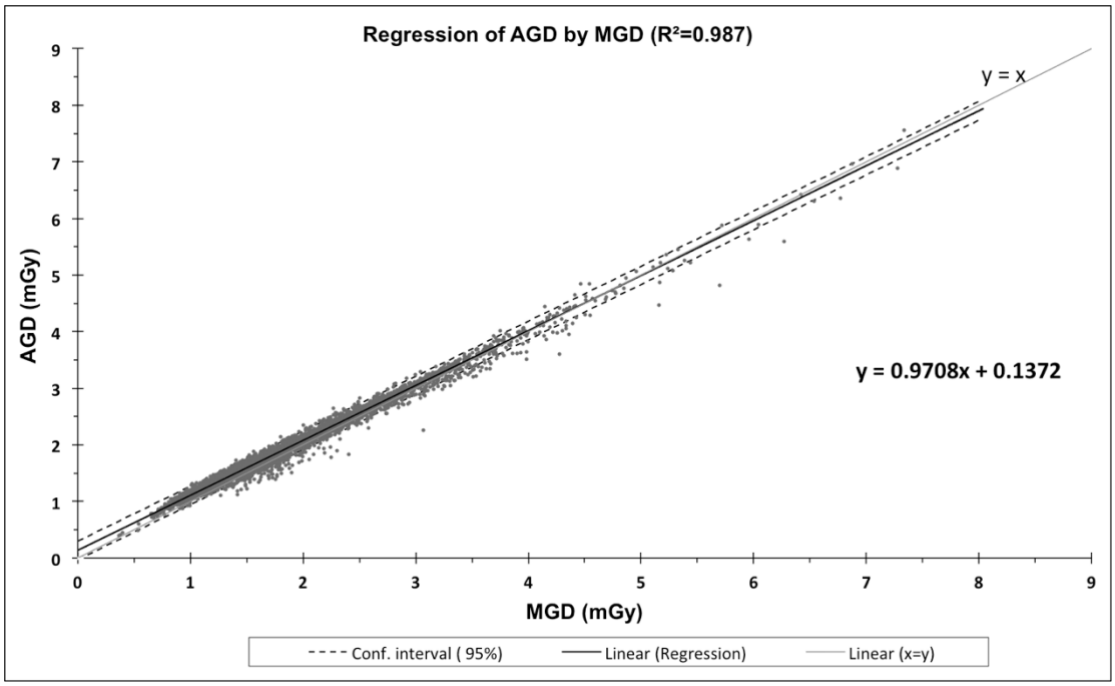

Figure 5.5: Linear regression scatter plots showing the line of best-fit between Actual glandular dose (AGD) and Mean glandular dose (MGD) for 31,097 mammograms.

5.1.5 References

1. Linet, M.S., et al., Cancer Risks Associated with External Radiation from Diagnostic Imaging Procedures. CA: a cancer journal for clinicians, 2012. 62(2): p. 75-100.

2. Heyes, G.J., A.J. Mill, and M.W. Charles, Mammography - Oncogenecity at low doses. Journal of Radiological Protection, 2009. 29(2): p. A123-A132.

3. Nguyen, P.K., et al., Assessment of the Radiation Effects of Cardiac CT Angiography Using Protein and Genetic Biomarkers. JACC: Cardiovascular Imaging, 2015. 8(8): p. 873-884.

4. Schwab, S.A., et al., X-ray induced formation of γ-H2AX foci after full-field digital mammography and digital breast-tomosynthesis. PloS one, 2013. 8(7): p. e70660.

5. M. Ali, R., et al., A method for calculating effective lifetime risk of radiation-induced cancer from screening mammography. Radiography, 2015. 21(4): p. 298-303.

6. Yaffe, M.J. and J.G. Mainprize, Risk of radiation-induced breast cancer from mammographic screening. Radiology, 2011. 258(1): p. 98-105.

7. Dance, D.R., et al., Breast dosimetry using high-resolution voxel phantoms. Radiation Protection Dosimetry, 2005. 114(1-3): p. 359-363.

8. Hernandez, A.M., J.A. Seibert, and J.M. Boone, Breast dose in mammography is about 30% lower when realistic heterogeneous glandular distributions are considered. Med Phys, 2015. 42(11): p. 6337-48.

9. Dance, D., Monte-Carlo calculation of conversion factors for the estimation of mean glandular breast dose. Physics in medicine and biology, 1990. 35(9): p. 1211.

10. Dance, D.R., et al., Additional factors for the estimation of mean glandular breast dose using the UK mammography dosimetry protocol. Physics in Medicine and Biology, 2000. 45(11): p. 3225-3240.

11. Dance, D.R., K.C. Young, and R.E. van Engen, Further factors for the estimation of mean glandular dose using the United Kingdom, European and IAEA breast dosimetry protocols. Phys Med Biol, 2009. 54(14): p. 4361-72.

12. Hammerstein, G.R., et al., Absorbed radiation dose in mammography. Radiology, 1979. 130(2): p. 485-91.

13. Macias, H. and L. Hinck, Mammary Gland Development. Wiley interdisciplinary reviews. Developmental biology, 2012. 1(4): p. 533-557.

14. Boyd, N., et al., A longitudinal study of the effects of menopause on mammographic features. Cancer Epidemiol Biomarkers Prev, 2002. 11(10 Pt 1): p. 1048-53.

15. GM., C., The Cell: A Molecular Approach. 2nd edition ed. 2000: Sunderland (MA): Sinauer Associates.

16. Al Mousa, D.S., et al., How mammographic breast density affects radiologists' visual search patterns. Acad Radiol, 2014. 21(11): p. 1386-93.

17. Al Mousa, D.S., et al., Mammographic density and cancer detection: does digital imaging challenge our current understanding? Acad Radiol, 2014. 21(11): p. 1377-85.

18. Boyd, N.F., et al., Mammographic density and breast cancer risk: current understanding and future prospects. Breast Cancer Research, 2011. 13(6): p. 223.

19. Wolfe, J.N., Breast patterns as an index of risk for developing breast cancer. AJR Am J Roentgenol, 1976. 126(6): p. 1130-7.

20. Wolfe, J.N., Risk for breast cancer development determined by mammographic parenchymal pattern. Cancer, 1976. 37(5): p. 2486-92.

21. Boyd , N.F., et al., Mammographic Density and the Risk and Detection of Breast Cancer. New England Journal of Medicine, 2007. 356(3): p. 227-236.

22. Ekpo, E.U., Measurement of Breast Density with Digital Mammography and Tomosynthesis, in Faculty of Health Sciences Discipline of Medical Radiation Sciences. 2016, University of Sydney.

23. Boyd, N.F., et al., Bias and the association of mammographic parenchymal patterns with breast cancer. Br J Cancer, 1982. 45(2): p. 179-84.

24. Boyd, N.F., et al., Mammographic patterns and breast cancer risk: methodologic standards and contradictory results. J Natl Cancer Inst, 1984. 72(6): p. 1253-9.

25. Boyd, N.F., et al., Quantitative Classification of Mammographic Densities and Breast Cancer Risk: Results from the Canadian National Breast Screening Study. JNCI: Journal of the National Cancer Institute, 1995. 87(9): p. 670-675.

26. Gram, I.T., E. Funkhouser, and L. Tabár, The Tabár classification of mammographic parenchymal patterns. European Journal of Radiology, 1997. 24(2): p. 131-136.

27. Sickles, E.A., et al., Acr bi-rads® mammography. ACR BI-RADS® atlas, breast imaging reporting and data system, 2013. 5.

28. Bernardi, D., et al., Interobserver agreement in breast radiological density attribution according to BI-RADS quantitative classification. Radiol Med, 2012. 117(4): p. 519-28.

29. Ciatto, S., et al., Categorizing breast mammographic density: intra- and interobserver reproducibility of BI-RADS density categories. Breast, 2005. 14(4): p. 269-75.

30. Ekpo, E.U. and M.F. McEntee, Measurement of breast density with digital breast tomosynthesis--a systematic review. Br J Radiol, 2014. 87(1043): p. 20140460.

31. Wolfe, J.N., A.F. Saftlas, and M. Salane, Mammographic parenchymal patterns and quantitative evaluation of mammographic densities: a case-control study. AJR Am J Roentgenol, 1987. 148(6): p. 1087-92.

32. Byng, J.W., et al., Analysis of mammographic density and breast cancer risk from digitized mammograms. Radiographics, 1998. 18(6): p. 1587-98.

33. Byng, J.W., et al., The quantitative analysis of mammographic densities. Phys Med Biol, 1994. 39(10): p. 1629-38.

34. Destounis, S., et al., Qualitative Versus Quantitative Mammographic Breast Density Assessment: Applications for the US and Abroad. Diagnostics, 2017. 7(2): p. 30.

35. Ursin, G., et al., The detection of changes in mammographic densities. Cancer Epidemiology Biomarkers & Prevention, 1998. 7(1): p. 43-47.

36. Tagliafico, A., et al., Mammographic density estimation: Comparison among BI-RADS categories, a semi-automated software and a fully automated one. The Breast, 2009. 18(1): p. 35-40.

37. ImageJ, U.S. [cited 2018 1 Mar]; Available from: https://imagej.nih.gov/ij/.

38. Li, J., et al., High-throughput mammographic-density measurement: a tool for risk prediction of breast cancer. Breast Cancer Research, 2012. 14(4): p. R114.

39. Nickson, C., et al., AutoDensity: an automated method to measure mammographic breast density that predicts breast cancer risk and screening outcomes. Breast Cancer Res, 2013. 15(5): p. R80.

40. Keller, B., et al., Adaptive multi-cluster fuzzy C-means segmentation of breast parenchymal tissue in digital mammography. Med Image Comput Comput Assist Interv, 2011. 14.

41. Keller, B.M., et al., Estimation of breast percent density in raw and processed full field digital mammography images via adaptive fuzzy c-means clustering and support vector machine segmentation. Med Phys, 2012. 39(8): p. 4903-17.

42. Highnam, R., et al. Breast Composition Measurements Using Retrospective Standard Mammogram Form (SMF). 2006. Berlin, Heidelberg: Springer Berlin Heidelberg.

43. Alonzo-Proulx, O., et al., Reliability of Automated Breast Density Measurements. Radiology, 2015. 275(2): p. 366-376.

44. Engelken, F., et al., Volumetric breast composition analysis: reproducibility of breast percent density and fibroglandular tissue volume measurements in serial mammograms. Acta Radiol, 2014. 55(1): p. 32-8.

45. Suleiman, M.E., et al., Integrating mammographic breast density in glandular dose calculation. Br J Radiol, 2018: p. 20180032.

5.2 Integrating mammographic breast density in glandular dose calculation

Moayyad E Suleiman, MSc, Patrick C Brennan, PhD, Ernest Ekpo, PhD, Peter Kench, PhD and Mark F McEntee, BSc (Hons), PhD
Medical Radiation Sciences, The University of Sydney, Faculty of Health Sciences, Cumberland Campus, Lidcombe, NSW, Australia
Address correspondence to: Mr Moayyad E Suleiman

E-mail: msul1801@ uni. sydney. edu. au

5.2.1 Abstract

Objectives: This work proposes the use of mammographic breast density (MBD) to estimate actual glandular dose (AGD), and assesses how AGD compares to mean glandular dose (MGD) estimated using Dance et al. method.

Methods: A retrospective sample of anonymised mammograms (52,405) was retrieved from a central database. Technical parameters and patient characteristics were exported from the Digital Imaging and Communication in Medicine (DICOM) header using third party software. LIBRA (Laboratory for Individualized Breast Radiodensity Assessment) software package was used to estimate MBDs for each mammogram included in the dataset. MGD was estimated using Dance et al. method, whilst AGD was calculated by replacing Dance et al.'s standard glandularities with LIBRA estimated MBDs. A linear regression analysis was used to assess the association between MGD and AGD, and a Bland-Altman analysis was performed to assess their mean difference.

Results: The final data set included 31,097 mammograms from 7,728 women. MGD, AGD, and MBD medians were 1.53 mGy, 1.62 mGy and 8% respectively. When stratified per breast thickness ranges, median MBDs were lower than Dance's standard glandularities. There was a strong positive correlation ($R^2 = 0.987$, $p<0.0001$) between MGD and AGD although the Bland-Altman analysis revealed a small statistically significant bias of 0.087 mGy between MGD and AGD ($p < 0.001$).

Conclusion: AGD estimated from MBD is highly correlated to MGD from Dance method, albeit the Dance method underestimates dose at smaller CBTs

Advances in knowledge: Our work should provide a stepping-stone towards an individualised dose estimation using automated clinical measures of MBD.

5.2.2 **Introduction**

Screening mammography is an effective tool for the early detection of breast cancer, and has been shown to reduce cancer mortality by 25 - 40% [1-3]. Since screening mammography was first instigated at a national level in Sweden in 1977, there has been continuous debate about the extent of benefits and the nature of the risk [4]. The risks arising from screening mammography are two-fold: risk from radiologist's errors such as false positives, false negatives and over diagnosis [5]; radiation-induced cancer risk arising from the high radiosensitivity of rapidly dividing epithelial cells in the fibroglandular tissues [6]. Therefore, it is increasingly important to appropriately account for the effect of radiation when assessing the risk vs benefit of screening mammography [5]. The relative risk of radiation-induced cancer from mammography is quantified by the mean glandular dose (MGD).

MGD is an estimate of the energy deposited per unit mass of glandular tissue averaged over all glandular tissue in the breast [7]. MGD is estimated using conversion factors derived from Monte-Carlo simulations [8-10]. All estimates use assumptions and the available MGD estimation methods operate on the assumption that the breast is 50% glandular and 50% fatty (50:50 model) [11] or that glandularity is proportional to compressed breast thickness [12, 13]. The 50:50 model proposed by Hammerstein et al. [11] was based on a phantom with homogeneous distribution of glandular tissue and the authors suggested that the 50:50 model can be used for comparing mammography doses delivered using different techniques and equipment. MGD calculation models such as Wu et al. [10, 14] and Boone et al. [8, 15, 16] are based on the 50:50 model. However, it is well known that the breast composition is not homogeneous [17]. Additionally, it has been shown, in a volumetric breast density study, that about 80% of females have breasts with less than 27% fibroglandular tissue [18]. Thus, the assumptions made in the 50:50 model are clearly not true for all breasts, and do not represent the glandularity of the population. To address these limitations, another model was established by Dance et al. [12, 13]. To account for the increased cancer risk in glandular tissue, this model incorporates estimates of breast glandularity taking into consideration patient age and compressed breast thickness (CBT).

Although the incorporation of glandularity and CBT in the Dance et al. model is logical, this approach to estimation of glandularity has some limitations. First, the

Dance et al. method estimates changes in glandularity using CBT and age. However, breast composition differs across females within age groups and CBTs. Second breasts with similar CBT can have different glandular compositions. Third, females of the same age and CBT can have different amount of glandular tissues. Thus, it is increasingly relevant to explore alternative models that account for a female's actual breast composition when estimating glandularity. Also, breast density, which is the amount of fibroglandular tissue in the breast, is a determinant of X-ray attenuation and risk of cancer [19]. The fibroglandular tissue contains high concentrations of primitive epithelial cells, the most susceptible to radiation damage, and from which 80% of cancers arise [20]. As the proportion of dense breast influences susceptibility to cancer, it is important that we should be exploring mammographic breast density (MBD) data when estimating radiation-induced risk from mammography. This makes individualized MBD a promising alternative to the 50:50 and Dance models for estimating glandularity and patient-specific dose estimates.

MBD is a representation of the fibroglandular tissue of the breast as seen by the X-ray attenuation patterns on a mammogram. MBD can be assessed qualitatively (visual grading) and quantitatively (area-based (2D) or volumetric (3D) methods) [21, 22]. However, qualitative visual methods are prone to intra-and inter-reader variability [23], suggesting a need to automate MBD measurement for dose calculation. The automated use of MBD for dose assessment has been developed [24] and a white paper by Highnam et al. [24] was the first to report MGD using MBD. This approach has now been incorporated into Volpara™ software to propose Volpara Dose for patient-specific MGD estimation from mammography unit firmware [24]. Although Volpara Dose is robust, and automated it has a hardware and software cost, it requires networked systems and needs to be supported by the mammography equipment vendors. Furthermore, Volpara Dose only works on the "Raw Projection" data. These challenges limit its applicability for low-resource facilities and countries, and highlight the need for less costly, accessible and versatile automated alternative. Automated area-based methods utilise computer assisted interactive thresholding techniques to measure the percentage area covered by the dense tissue on a radiograph and uses this as a proxy for fibroglandular tissue. The Laboratory for Individualized Breast Radiodensity Assessment (LIBRA) software for MBD estimation uses post-processed images, can do batch processing, is freely available and is therefore a possible low

cost, low man-power alternative. LIBRA is freely available, fully automated software for the estimation of MBD. It estimates MBD on both "raw projection" data and "post processed" images, and has been validated for GE and Hologic digital mammography systems [25].

The current work proposes the use of a demale's automatically generated actual MBD to estimate the actual glandular dose (AGD) to the breast. This work explores the use of MBD measured by LIBRA to estimate AGD. It also assesses whether the AGD estimated using MBD compares to MGD estimates from Dance et al. method.

5.2.3 **Materials and methods**

The work involved a retrospective sample of screening mammograms. A total of 52,405 mammograms from 12,034 women were used. Mammograms were acquired on 63 mammography units across 50 Breast Screen centres in New South Wales, Australia between September and October 2014. The data were retrieved from the Cancer Institute of New South Wales Picture Archiving and Communication System, following ethics approval (HREC2014/08/552) from the Cancer Institute Human Research Ethics Committee.

Patient related information such as mammographic projections, age and breast thickness, exposure parameters, and mammography unit information (make, model) were exported from the Digital Imaging and Communication in Medicine (DICOM) image header to MS Excel using a third party software (YAKAMI DICOM Tools ver. 1.4.1.0, Kyoto University, Japan) [26]. Medical physics annual reports were also obtained from participating centres, as the calculation of MGD requires these data.

MBD was estimated for the data set using LIBRA software [27]. LIBRA uses a thresholding technique to detect the boundaries of the breast and the pectoral muscle on the mammogram. An "adaptive multi-class fuzzy c-means" algorithm is then applied to partition the mammographic breast tissue into clusters of similar intensity These clusters are then aggregated to a dense tissue area. The software package then generates quantitative estimates of breast area, dense tissue area, and calculates MBD by dividing the dense area by the total breast area [27, 28].

LIBRA has only been validated for GE and Hologic mammography units [25]. Therefore, mammograms obtained using Philips and Fujifilm units (14,065

mammograms) were excluded in the current work. Further exclusion criteria related to the calculation method were applied on the data. These included mammograms reported to have 0% glandularity by LIBRA (180 mammograms) which were considered as an indicative of measurement error, mammograms with breast implants (1337 mammograms), mammograms not within 20-110 mm CBT (39 mammograms), incomplete calculation data (1971 mammograms). The final data set was imported to an excel workbook developed in-house which calculated MGD and our proposed AGD.

The calculation of MGD in our study followed the methods described by Dance et al. [9, 12, 13]. This method calculates MGD using entrance air kerma and three conversion factors that depend on age, CBT, half value layer (HVL), and anode/filter combination. A full explanation of the methodology has been previously described [29] (Figure 5.6). AGD in our work was calculated by replacing the original *c* factor values (box 6 in figure 5.6) with a look-up table of interpolated *c* values for MBDs ranging from 1% to 100%.

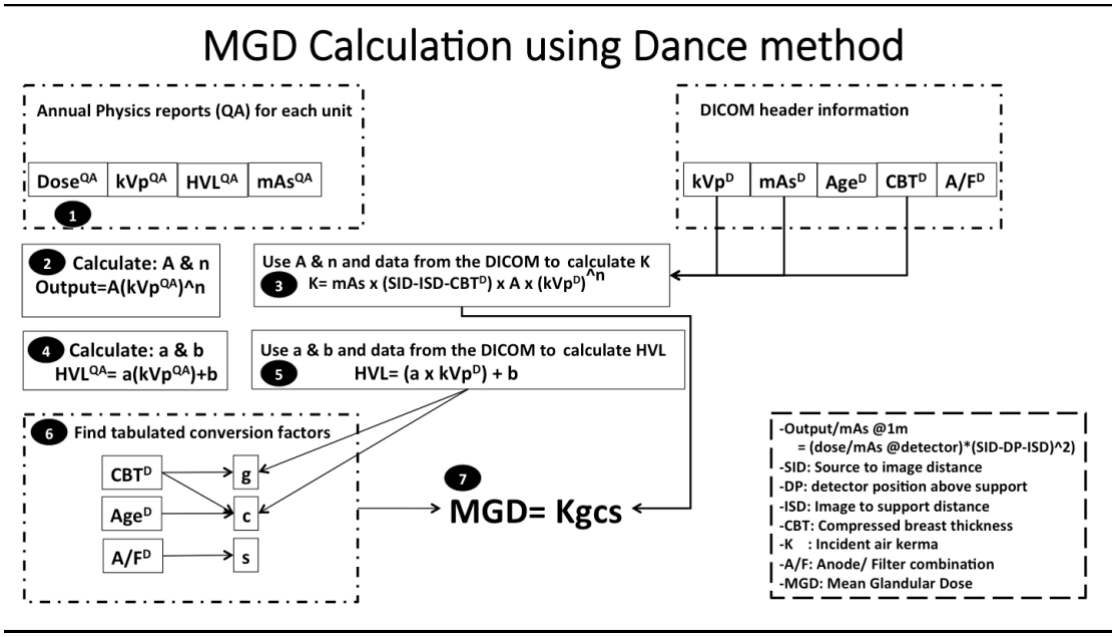

Figure 5.6: Dance calculation method: input information that needs to be available for the calculation of MGD, the steps taken to calculate MGD for a mammogram and the equations utilized for that process

The data were stratified by age (40-49 and 50-64) and CBT (20mm – 110mm in 10mm increments). For each age group, our estimated median MBD was compared to

Dance's glandularity for each CBT (Figure 5.7). The distribution of the data was assessed using a D'Agostino & Pearson normality test, and a non-parametric Spearman's correlation was used to assess the relationship between median MBD and age.

MGD and AGD medians were calculated per mammogram. The median MGD and AGD were compared across different breast thicknesses (Figure 5.8). Bland-Altman analysis was performed to show the mean difference between the two dose estimation methods. Bland-Altman analysis also provided a measure of the bias and 95% limits of agreement (LOA) between MGD and AGD [30]. A linear regression analysis was performed to assess the linear correlation between MGD and AGD. AGDs and MGDs were stratified by CBT, and the median differences between AGD and MGD as well as their 95% confidence intervals were calculated for each range of CBTs.

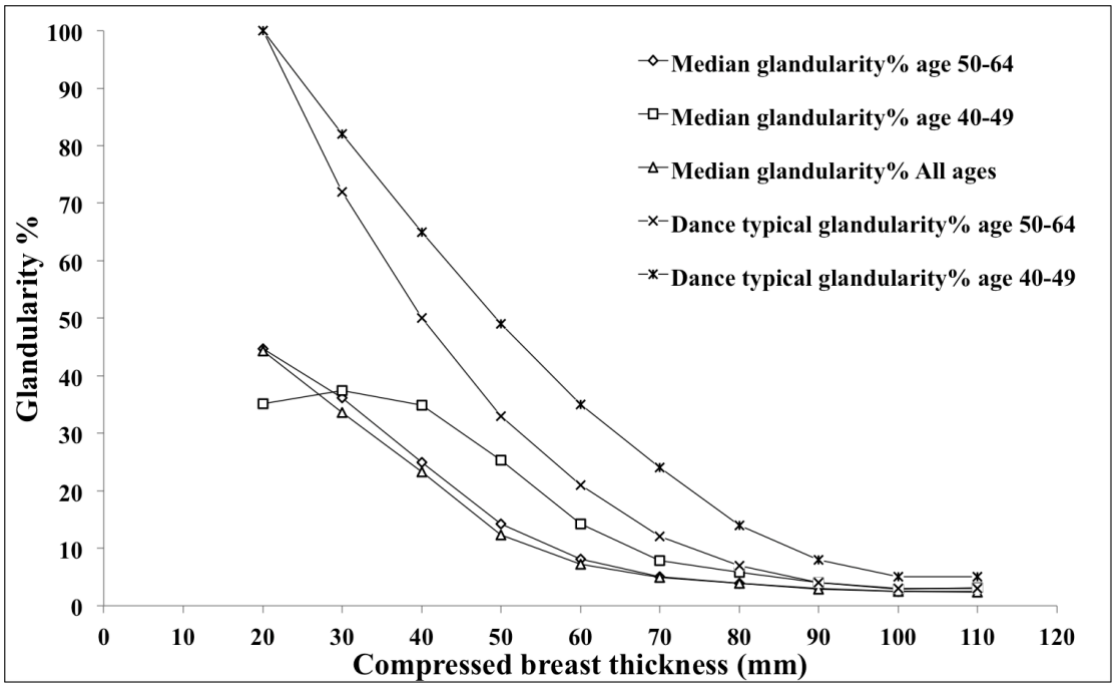

Figure 5.7:Average glandularity vs. breast thickness for 31,097 mammograms, glandularity estimated using LIBRA, and compared to Dance method typical glandularity for two age groups (40-49, 50-64).

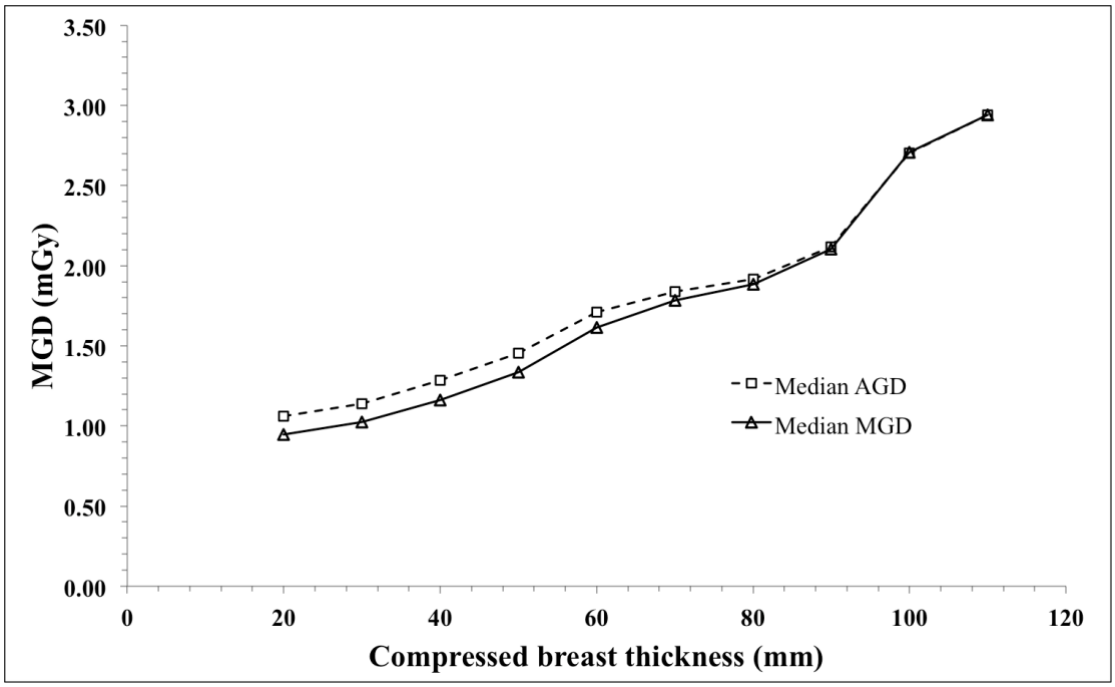

Figure 5.8: Mean glandular dose (MGD) and Actual glandular dose (AGD) variation with different compressed breast thicknesses (CBT). The difference between median AGD and MGD for different CBT ranges becomes insignificant at CBTs greater than 80mm.

5.2.4 **Results**

A further 3,716 mammograms failed LIBRA analysis, and the final data set comprised of 31,097 mammograms (7728 women) from 48 Breast screen centres. Table 5.1 provides a descriptive summary of the data set, including the minimum, maximum, 1st and 3rd quartiles, median, mean, variance, and standard deviation for age, CBT, compression, MBD, MGD, and AGD. Both MGD and AGD showed skewed distributions with medians of 1.53 mGy and 1.62 mGy respectively. MBD showed a skewed distribution with a median and a mean of 8% and 13% respectively.

Table 5.1: Statistical description of the included dataset (31,097 mammograms)

Statistic	Age	CBT	MBD	MGD	AGD
Minimum	40	20	0.01	0.37	0.40
Maximum	89	110	0.99	14.53	13.93
1st Quartile	54	50	0.04	1.27	1.37
Median	60	59	0.08	1.53	1.62
Mean	60	59	0.13	1.71	1.80
3rd Quartile	66	68	0.17	1.96	2.03
Variance (n-1)	63	175	0.02	0.58	0.55
SD (n-1)	8	13	0.13	0.76	0.74

AGD, Actual glandular dose; CBT, Compressed breast thickness; MBD, Mammographic breast density; MGD, Mean glandular dose; SD, Standard deviation.

Findings show that the median MBD decreased at higher CBTs but were lower than the Dance method at corresponding phantom CBTs for all age groups (Figure 5.7). There was a direct relationship between dose and compressed breast thickness. The AGD calculated using MBD followed a similar trend as the MGD estimated using Dance Method. However, the Dance method MGD underestimated dose at lower CBTs (below 80 mm) compared to AGD (Figure 5.8). Further analysis showed that the 95% confidence interval of the difference between median AGD and MGD for different CBT ranges becomes insignificant at CBTs greater than 80 mm (Figure 5.9).

Bland-Altman analysis revealed a small yet statistically significant bias of 0.087 mGy between MGD and AGD (Figure 5.10), with 95% confidence intervals and p value of -0.08 - 0.26 and < 0.0001 respectively. Linear regression analysis demonstrated a strong positive correlation ($R^2 = 0.987$, $p<0.001$) between MGD and AGD.

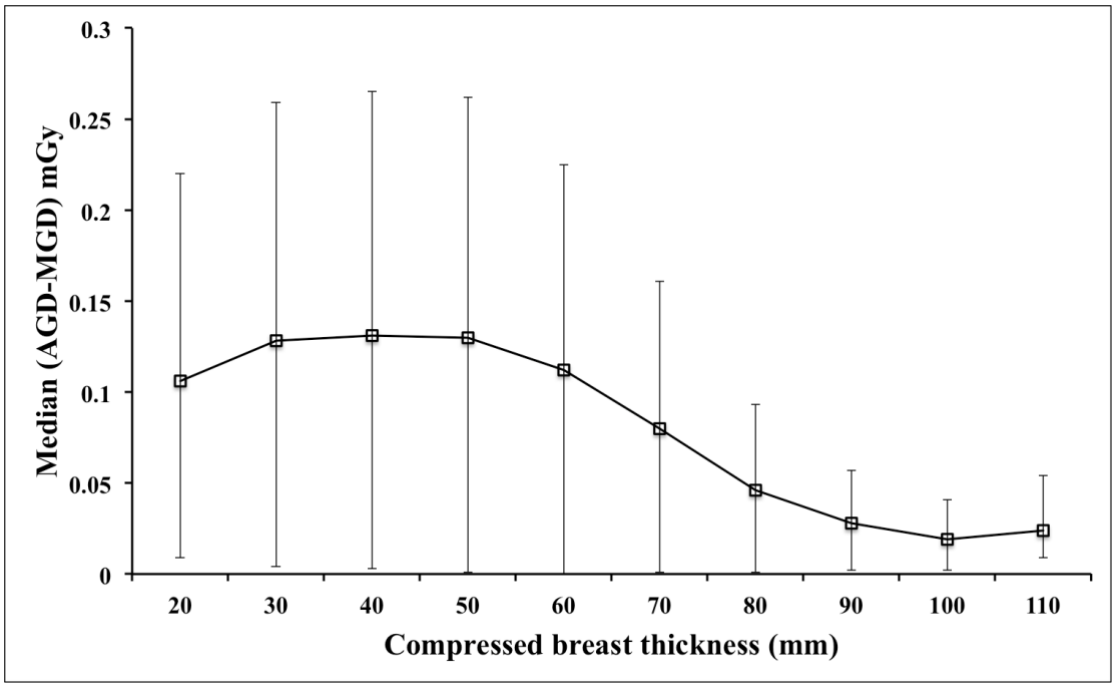

Figure 5.9: Median difference between Actual glandular dose (AGD) and Mean Glandular Dose (MGD) at different Compressed Breast Thicknesses (CBTs) and the 95% confidence intervals (shown in bars).

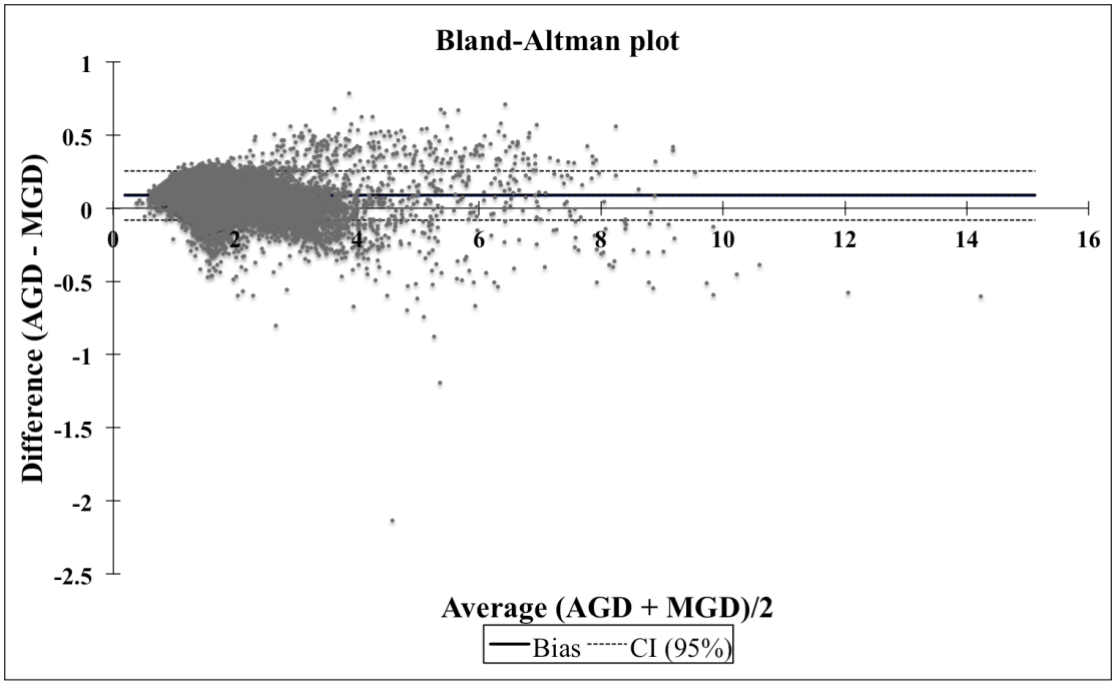

Figure 5.10: Bland-Altman plot for mean glandular dose (MGD) and Actual glandular dose (AGD) showing a Bias of 0.087 and 95% LOA of -0.08, 0.26 for 31,097 digital mammography images.

5.2.5 **Discussion**

Previous studies estimating radiation risk from mammography made assumptions that are not necessarily true for all breast compositions. Given that the breast is infrequently 50% glandular, and that breasts with the same CBT and age vary in glandularity, the current work argues the importance of integrating actual measures of glandularity in dose calculation. The current work proposes the use of MBD to quantify individual's glandularity for the purpose of patient-specific dose estimation during mammography. Our work demonstrates that MBD is inversely related to CBT, with our median MBDs being lower than the glandularity estimated by Dance et al. [12, 13] at corresponding CBTs for all age groups. Findings also demonstrated a direct association between CBT and AGD as well as MGD. MGD was lower than AGD at smaller CBTs, with the difference becoming insignificant at higher CBTs (>80 mm). Bland-Altman analysis showed a small yet statistically significant bias between MGD and AGD.

The median breast glandular tissue content in our data set was 8%, with a mean of 13%, similar to that previously reported (17.4% -27%) elsewhere [18, 31] and for Australian females (8.1%) [32]. These values are substantially lower than the 50% glandularity used in the standard breast composition model for mammography dose optimisation. These findings suggest that the 50:50 model overestimates glandularity and that there is in reality the same dose going to less glandular tissue. Therefore, the mean glandular dose is actually higher than estimated by the 50:50 model. This same finding is explained by Dance et al [12] in a different way, they indicate that "The increase of the c-factor with decreasing glandularity is due to the increased percentage depth dose for fattier breasts". In other words, fattier breasts allow more photon penetration. Therefore, underestimating the dose absorbed per 1 gm of fibroglandular tissue, lead to an underestimation of radiation risk from mammography. Similarly, in comparison to the current work, the Dance et al. method, which accounted for variation in breast composition using CBT, overestimated glandularity at smaller CBTs for all ages. We found that the glandularity estimated using the Dance method was almost double the actual glandularity at smaller CBTs, suggesting an overestimation of glandularity in small breasts. Such overestimation may result in underestimation of dose and risk to patients undergoing mammography procedures, limiting the applicability of Dance model for patient-specific dose estimation, particularly for small breasts.

Further analysis demonstrated a linear increase in AGD and MGD with CBT. MGD was consistently significantly lower (6% difference; $p<0.001$) than AGD at CBTs <80 mm. However, Bland-Altman analysis, revealed a small but significant positive bias towards AGD and a narrow LOA. Although the bias was statistically significant, it represents less than 5% of the average dose to the standard breast described by the European protocol [33]. Nonetheless, when females were stratified into different CBTs, the differences in MBD for smaller CBTs resulted in a higher difference (10%) between MGD and AGD, while larger CBTs (over 80 mm) demonstrated under a 2% difference, with narrower 95% confidence intervals (Figure 5.9). Smaller breast may have lesser fibroglandular content than larger ones but demonstrate higher percentage glandularity. This is perhaps the reason why AGD was higher in smaller breast when individuals' MBDs were accounted for. This finding implies that Dance et al., model may not be suitable for dose calculation in smaller breasts. The high correlation between AGD and MGD reported in the current work may be due to the use of a similar methodology for estimating both parameters.

The 2%–10% difference in AGD and MGD at different CBTs has implications for risk and lifetime effective risk, as MGD contributes to 98% of effective lifetime risk, while the other body parts (irradiated during mammography) such as contralateral breast, thyroid and lungs contribute to only 2% [34]. Furthermore, according to the Linear Non-Threshold (LNT) model, which is often used for radiation-induced risk assessment, cancer risk from radiation exposure increases linearly with dose. This suggests that underestimation of dose using MGD will result in an underestimation of risk. Although the LNT model is still being debated due to the lack of drop-off effect from death at higher doses and the paucity of data at lower doses, it is still used to quantify risk. There are contentions about the effects of radiation at low doses. Whilst one theory suggests that the processes by which our cells repair damage (hormesis) and destroy unrepairable cells (apoptosis) occur at low doses [35] another asserts that cells are hypersensitive to low level doses [36]. Importantly, it has been shown that radiation-induced genetic effects vary between individuals [37]. These individual differences in risk emphasise the need to personalise glandularity and dose measurements in order to provide patient-specific estimates of radiation-induced risk.

The overestimation of glandularity at lower CBTs and underestimation of dose by Dance et al. model highlights the limitations in the current mammography dosimetry

approaches. The current work provides a more objective clinical approach to patient-specific mammography dose estimate. Although the difference between AGD and MGD was small (2–10%), it constitutes a significant difference in terms of risk according to the LNT model, and should be considered when estimating radiation-induced risk from mammography.

Another factor supporting individualized dose and risk estimation is the fact that risk from radiation and DNA repair differ between individuals even at similar dose levels [36]. For example, females with BRCA1&2 mutations as well as those with single nucleotide polymorphisms (SNPs) are less likely to successfully repair and more likely to develop breast cancer [38, 39]. Unfortunately, because 45-65% of women with BRCA mutations will develop breast cancer by the age of 70 [40], they are targeted for more regular screening. Cancer risk will also vary between individuals due to difference glandular content. Therefore, it is important to take into consideration these differences when estimating risk from mammography.

Although doses from medical procedures are relatively small, the effect of medical exposure to radiation is well established. A longitudinal study has reported an overall 24% increase in cancer incidence in individuals exposed to low doses compared to unexposed individuals [41]. Evidence also shows that oncogenecity in younger females may be higher at low mammography doses compared to higher doses [36] . A significant relationship has also been established between low doses and cell repair [42]. Therefore, one cannot definitely say that low doses are beneficial, harmful or have no effect, as radiation effects may vary between individuals.

The uncertainty of radiation effects at all doses suggests a conservative risk strategy should be adopted, and that actual measures of the radiosensitive fibroglandular tissues be included in dose calculation models for individualised dose estimation. Thus, AGD may be a better dosimetric parameter, as it accounts for the actual glandular content at risk. Importantly, advances in technology and automation of MBD measurement should facilitate easier estimation of breast glandular tissue content and AGD. This will provide actual measures of dose received by each patient and the potential risk from screening mammography.

The current work is limited in that only images retrieved from two mammography vendors were used. LIBRA is currently being tested on mammography units from different vendors, and may become more versatile in the future. Future work will

explore AGD with LIBRA MBD measures from Philips (Sectra), Fuji, and Siemens systems. The strengths of our work include the use of clinical images rather than phantoms for dose calculation as well as a large sample. Furthermore, the use of an automated MBD measurement software package (LIBRA) eliminates the variability associated with subjective human assessment. It does not however, deal with heterogeneous glandular tissue distribution in the breast. Using a voxel phantom Dance et al. [43] found that accounting for different glandular distributions in the breast could give up to 48% error in the conversion factors estimated using simple homogenous phantoms. He concluded, "For accurate breast dosimetry, it is therefore very important to take the distribution of glandular tissues into account". Therefore, the MBD proposed in the current work although not yet accounting for heterogeneity, is a reasonable alternative. Our work should provide a stepping-stone towards an individualised dose estimation using automated clinical measures of MBD.

5.2.6 **Conclusion**

The use of MGD underestimates dose from screening mammography compared to AGD. There are inconsistent differences between AGD and MGD at different CBTs, with larger differences seen in smaller breasts. This inconsistency may result in the underestimation of radiation risk during mammography for women with smaller CBTs.

5.2.7 References

1. Glasziou P, Houssami N. The evidence base for breast cancer screening. Prev Med. 2011;53(3):100-2.

2. Lauby-Secretan B, Scoccianti C, Loomis D, Benbrahim-Tallaa L, Bouvard V, Bianchini F, et al. Breast-cancer screening—viewpoint of the IARC Working Group. N Engl J Med. 2015;372(24):2353-58.

3. Njor S, Nystrom L, Moss S, Paci E, Broeders M, Segnan N, et al. Breast cancer mortality in mammographic screening in Europe: a review of incidence-based mortality studies. J Med Screen. 2012;19 Suppl 1:33-41.

4. Beckett JR, Kotre CJ, Michaelson JS. Analysis of benefit: Risk ratio and mortality reduction for the UK Breast Screening Programme. Br J Radiol. 2003;76(905):309-20.

5. Jin J. Breast cancer screening: Benefits and harms. JAMA. 2014;312(23):2585-85.

6. Yaffe MJ, Mainprize JG. Risk of Radiation-induced Breast Cancer from Mammographic Screening. Radiology. 2011;258(1):98-105.

7. Hendrick R, Bassett L, Botsco M, Deibel D, Feig S, Gray J, et al. Mammography quality control manual. Reston, Va: American College of Radiology. 1999.

8. Boone JM, Fewell TR, Jennings RJ. Molybdenum, rhodium, and tungsten anode spectral models using interpolating polynomials with application to mammography. Med Phys. 1997;24(12):1863-74.

9. Dance D. Monte-Carlo calculation of conversion factors for the estimation of mean glandular breast dose. Phys Med Biol. 1990;35(9):1211.

10. Wu X, Gingold EL, Barnes GT, Tucker DM. Normalized average glandular dose in molybdenum target-rhodium filter and rhodium target-rhodium filter mammography. Radiology. 1994;193(1):83-89.

11. Hammerstein GR, Miller DW, White DR, Masterson ME, Woodard HQ, Laughlin JS. Absorbed radiation dose in mammography. Radiology. 1979;130(2):485-91.

12. Dance DR, Skinner CL, Young KC, Beckett JR, Kotre CJ. Additional factors for the estimation of mean glandular breast dose using the UK mammography dosimetry protocol. Phys Med Biol. 2000;45(11):3225-40.

13. Dance DR, Young KC, van Engen RE. Further factors for the estimation of mean glandular dose using the United Kingdom, European and IAEA breast dosimetry protocols. Phys Med Biol. 2009;54(14):4361-72.

14. Sobol WT, Wu X. Parametrization of mammography normalized average glandular dose tables. Med Phys. 1997;24(4):547-54.

15. Boone JM. Glandular breast dose for monoenergetic and high-energy X-ray beams: Monte Carlo assessment. Radiology. 1999;213(1):23-37.

16. Boone JM. Normalized glandular dose (DgN) coefficients for arbitrary X-ray spectra in mammography: computer-fit values of Monte Carlo derived data. Med Phys. 2002;29(5):869-75.

17. McCormack VA, dos Santos Silva I. Breast density and parenchymal patterns as markers of breast cancer risk: a meta-analysis. Cancer Epidemiol Biomarkers Prev. 2006;15(6):1159-69.

18. Yaffe MJ, Boone JM, Packard N, Alonzo-Proulx O, Huang SY, Peressotti CL, et al. The myth of the 50-50 breast. Med Phys. 2009;36(12):5437-43.

19. Yaffe MJ. Mammographic density. Measurement of mammographic density. Breast Cancer Res. 2008;10(3):209.

20. Dimri G, Band H, Band V. Mammary epithelial cell transformation: insights from cell culture and mouse models. Breast Cancer Res. 2005;7(4):171.

21. Ekpo EU, Hogg P, Highnam R, McEntee MF. Breast composition: Measurement and clinical use. Radiography. 2015;21(4):324-33.

22. Ekpo EU, McEntee MF. Measurement of breast density with digital breast tomosynthesis--a systematic review. The British journal of radiology. 2014;87(1043):20140460.

23. Ekpo EU, Ujong UP, Mello-Thoms C, McEntee MF. Assessment of Interradiologist Agreement Regarding Mammographic Breast Density Classification Using the Fifth Edition of the BI-RADS Atlas. AJR American journal of roentgenology. 2016;206(5):1119-23.

24. Highnam R, Solutions V. Patient-Specific Radiation Dose Estimation in Breast Cancer Screening.

25. CBIG. LIBRA. University of Pennsylvania: Section for Biomedical Image Analysis (SBIA) | Perelman School of Medicine at the University of Pennsylvania; 2017 [cited 2017 27 October]; Available from: http://www.med.upenn.edu/sbia/libra.html.

26. Yakami M. YAKAMI DICOM Tools (Free DICOM Viewer/Converter/etc.). Japan: Department of Diagnostic Imaging and Nuclear Medicine, Kyoto University; [updated updated on 21 Jan 2014; cited 2015 20 February]; Available from: http://www.kuhp.kyoto-u.ac.jp/~diag_rad/intro/tech/dicom_tools.html.

27. Keller BM, Nathan DL, Wang Y, Zheng Y, Gee JC, Conant EF, et al. Estimation of breast percent density in raw and processed full field digital

mammography images via adaptive fuzzy c-means clustering and support vector machine segmentation. Med Phys. 2012;39(8):4903-17.

28. Keller B, Nathan D, Wang Y, Zheng Y, Gee J, Conant E, et al. Adaptive multi-cluster fuzzy C-means segmentation of breast parenchymal tissue in digital mammography. Med Image Comput Comput Assist Interv. 2011;14.

29. Suleiman ME, McEntee MF, Cartwright L, Diffey J, Brennan PC. Diagnostic reference levels for digital mammography in New South Wales. J Med Imaging Radiat Oncol. 2016:n/a-n/a.

30. Myles PS, Cui J. Using the Bland-Altman method to measure agreement with repeated measures. Br J Anaesth. 2007;99(3):309-11.

31. Olgar T, Kahn T, Gosch D. Average glandular dose in digital mammography and breast tomosynthesis. Rofo. 2012;184(10):911-8.

32. Hill M, editor. Large variation in mammography compression internationally2016: European Congress of Radiology 2017.

33. Perry N, Broeders M, De Wolf C, Törnberg S, Holland R, Von Karsa L, et al. European guidelines for quality assurance in breast cancer screening and diagnosis Fourth Edition. Luxembourg office for official publications of the European Communities. 2006.

34. M.Ali RMK, England A, Mercer C, Tootell A, Walton L, Schaake W, et al. Mathematical modelling of radiation-induced cancer risk from breast screening by mammography. Eur J Radiol. 96:98-103.

35. Baldwin J, Grantham V. Radiation Hormesis: Historical and Current Perspectives. J Nucl Med Technol. 2015;43(4):242-46.

36. Heyes GJ, Mill AJ, Charles MW. Mammography - Oncogenecity at low doses. J Radiol Prot. 2009;29(2):A123-A32.

37. Nguyen PK, Lee WH, Li YF, Hong WX, Hu S, Chan C, et al. Assessment of the Radiation Effects of Cardiac CT Angiography Using Protein and Genetic Biomarkers. JACC Cardiovasc Imaging. 2015;8(8):873-84.

38. Yue W, Yager JD, Wang J-P, Jupe ER, Santen RJ. Estrogen receptor-dependent and independent mechanisms of breast cancer carcinogenesis. Steroids. 2013;78(2):161-70.

39. Pijpe A, Andrieu N, Easton DF, Kesminiene A, Cardis E, Noguès C, et al. Exposure to diagnostic radiation and risk of breast cancer among carriers of BRCA1/2 mutations: retrospective cohort study (GENE-RAD-RISK). BMJ : British Medical Journal. 2012;345.

40. Antoniou A, Pharoah PD, Narod S, Risch HA, Eyfjord JE, Hopper JL, et al. Average risks of breast and ovarian cancer associated with BRCA1 or BRCA2 mutations detected in case Series unselected for family history: a combined analysis of 22 studies. Am J Hum Genet. 2003;72(5):1117-30.

41. Mathews JD, Forsythe AV, Brady Z, Butler MW, Goergen SK, Byrnes GB, et al. Cancer risk in 680 000 people exposed to computed tomography scans in childhood or adolescence: data linkage study of 11 million Australians. BMJ : British Medical Journal. 2013;346.

42. Jeggo P. The Role of the DNA Damage Response Mechanisms after Low-Dose Radiation Exposure and a Consideration of Potentially Sensitive Individuals. Radiat Res. 2010;174(6b):825-32.

43. Dance DR, Hunt RA, Bakic PR, Maidment ADA, Sandborg M, Ullman G, et al. Breast dosimetry using high-resolution voxel phantoms. Radiation Protection Dosimetry. 2005;114(1-3):359-63.

Chapter six

Discussion

The current work proposes Diagnostic Reference Levels for digital mammography in NSW. While the initial aim of providing a DRL value for all women was achieved, the results revealed high degree of variability in MGD for different ranges of CBTs, this led to the proposal of stratified DRLs for nine CBT ranges. Furthermore, the results revealed variability in MGD delivered using different detector technologies, which also suggested that DRLs should be stratified according to detector technology. Hence, the proposed DRLs can be interpreted by the conventional definition of a DRL and can also be used in a stratified way for specific CBTs and detector technology.

The results of our investigation of dose in mammography not only reveals the technical issues affecting dose, it also reveals the need for greater urgency in the collection and communication of medical imaging dose data. Most of the focus in mammography is rightly on diagnosis, whilst dose appears unimportant comparatively. Radiation dose research in mammography would benefit from a 21st century mindset, where the digital image is not seen as a replacement for film. A digital image is data and has associated metadata that could be useful for more than detecting abnormalities [1].

In other domains, the digital image is being converted to 'high-dimensional' mineable data, a process called radiomics, where information from multiple sources can be analysed to better support decision making. In medical imaging this could provide a potential improvement in quality control, diagnosis, prognosis and predictive accuracy of image interpretation and disease detection.

Recent studies have shown the potential benefits of radiomics in the diagnosis of cancer, an example is the use of mathematical analysis of extracted data from prostate MRI to distinguish cancerous from benign tissue in prostate [2]. Another example is extracting quantitative lesion characteristics such as texture intensity, tumour shape, and tumour texture from CT lung images. The analysis of such information with the help of bio-markers improves the prognosis of lung cancer by predicting clinically relevant factors such as distant metastasis [3]. Furthermore, in multi-contrast brain MRI images, contrast enhanced regions were used to extract certain features to predict the overall survival of glioblastoma multiforme (GBM) patients, showing the advantages of tissue texture analysis to predict the prognosis of GBM patients [4].

In mammography, machine learning (ML) and artificial intelligence (AI) could be used for the diagnosis of cancer, and analysing tissue texture to predict the potential risk of malignant legions. Furthermore, the raw data may have a role in the use of ML

and AI, however, most of it is not visible or cannot be displayed with sufficient contrast for the human eye, therefore removed. A 16-bit image is reduced to a 10-bit image so that it can be displayed on a 10-bit monochrome monitor. The amount of data lost is underestimated as it may be used in the colorisation of mammograms, diagnosis and prognosis of cancer. The under-utilised raw image has potential to be a driver for innovation. Raw images are mostly discarded after being processed to a "for presentation" image. If there were raw images, even in this project, VOLPARA and QUANTRA usage to estimate breast density become possible. Storing raw data is now cheaper than ever before.

Deleting data to save storage space is again the mindset of the 20th century, where the limitations of hardware in the 1980 and 90's pushed vendors to look at and store only the necessary information. The 21st century has seen exponential advancements in computational power, data storage, transfer and analysis, supported by the low-cost hardware, and the abundant number of programming professionals who can write highly sophisticated algorithms to mine such expansive amounts of information.

The answer to shifting from a 20th to a 21st century paradigm rests in the hands of responsible authorities, researchers and vendors. Collaboration between these groups could see a consistent, compatible and shareable output from medical imaging technologies. Sadly, developing *proprietary* technology is still the major driver of profit and therefore innovations are not shared or made open sources. This is understandable, as each vendor is a competitor in the market, with profit as one of its major drivers. However, this may mean that strategic opportunities for research and optimisation that could help patients are lost.

The American College of Radiology (ACR) and the National Electrical Manufacturers Association (NEMA) standard "DICOM" and the "Integrating health enterprise" (IHE) are in place to connect vendors and improve cross-communications. "The DICOM standard aims to facilitate interoperability of devices claiming conformance, this is realised by:

- Addressing the semantics of Commands and associated data. For devices to interact, there must be standards on how devices are expected to react to Commands and associated data, not just the information that is to be moved between devices.

- Addressing the semantics of file services, file formats and information directories necessary for off-line communication.
- Is explicit in defining the conformance requirements of implementations of the Standard. In particular, a conformance statement must specify enough information to determine the functions for which interoperability can be expected with another device claiming conformance.
- Facilitating operation in a networked environment.
- Is structured to accommodate the introduction of new services, thus facilitating support for future medical imaging applications.
- Making use of existing international standards wherever applicable, and itself conforms to established documentation guidelines for international standards [5]."

The key point in this to our "Organ Dose" research is "Addressing the semantics of file services, file formats and information directories…" Despite these standards, there are considerable variations between manufacturers. There are 4,115 tags in a DICOM header, some of which are used in different ways by different manufacturers. For example, the "Organ Dose" is used by all vendors, however, the information each manufacturer stores under that tag is derived from different calculations. The calculations used for "Organ Dose" by the four manufacturers studied in this work are discussed in detail in chapter four.

The problems that can arise with data being stored inconsistently by different manufacturers is exemplified in chapter four. Through the process of examining DRLs for NSWs, the complexity of calculating MGD for multiple systems and multiple centres triggered a search for a more efficient measure; a measure that could facilitate regular and convenient evaluation of DRLs. The benefits of "big data" come when algorithms can be applied to large consistent data sets. Big data is often defined as "extremely large data sets that may be analysed computationally to reveal patterns, trends, and associations, especially relating to human behaviour and interactions." When all fields are present and consistent, then we can maximise the potential of the analysis. Missing values in the database or inconsistent values (sometimes called noise) mean that a record cannot be used or is of limited use. In chapter three for example, we lost 1662 data sets due to missing QA data.

Hence, chapter four explored the "Organ Dose", which is DICOM header tag number 0040,0316. Organ Dose is an MGD estimate available within the DICOM header of a mammogram. Chapter four examined whether MGD has the potential to be used in DRLs. The findings showed that the Organ Dose varied across different vendors due to differences in the methods utilised for dose estimation. Clearly, there has been a lack of collaboration between vendors, or perhaps limited discussion between them, resulting in an inconsistent approach to Organ Dose calculation. A consistent approach would have been for the ultimate good of the patient, and certainly would ease the process of generating DRLs in countries that have networked imaging centres. Nonetheless, Organ Dose was found to have potential for dose audits limited to similar mammography unit types. Organ Dose therefore, could be used to compare local DRLs between NSW mammography centres with similar mammography units. Using Organ Dose for DRLs would reduce the administrative burden and the time spent on dose audits and the establishment DRL. This is a major advantage for developed countries, where resources are networked, and cost is a major consideration. The frequency of QA tests is of great importance, as more frequent QA tests can make screening programs more expensive, while less frequent test will affect the reliability of screening units [6]. Cost savings could be possible because the dose audit process has many manual steps. However, the use of readily available reliable dose data, embedded within the image, could reduce the cost of performing QA tests.

Previous works assumed predetermined percentages of glandularity, a 50% glandularity [7-13] or a CBT and age related glandularities [14, 15], and that risk from exposure is proportional to CBT. However, recent evidence shows that 95% of women have less than 50% of fibroglandular tissue [16], and that the epithelial cells and the connective tissue within the fibroglandular component of the breast are most radiosensitive due to the mitotic phases. Furthermore, in chapter four variations were found when MGD was calculated using different factors within the estimation methodologies, particularly, the use of breast fibroglandular content estimations. To address these limitations, this thesis proposed the use of mammographic breast density (MBD) for dose and radiation risk assessment, since it was the best descriptor of the amount of fibroglandular tissue. MBD also provides opportunities to calculate individualised dose estimates rather than extrapolations based on assumption set by earlier studies. This led to a new measure known as Actual Glandular Dose (AGD)

being proposed in chapter five to more appropriately account for the dose absorbed by the fibroglandular tissue. The proposed method enables patient-specific dose assessment and is derived from the widely used Dance et al. method for MGD calculation.

In summary, this thesis has advanced the knowledge base pertaining to DRLs for mammography in NSW, and dose optimisation for digital mammography breast screening services. The study in chapter three proposed DRLs for mammography screening services in NSW, providing a benchmark for dose optimisation strategies for women undergoing screening investigations. The use of stratified DRLs according to breast thickness explored in this work should facilitate the optimisation of screening practices across all CBTs, hence, protecting all women from unnecessarily radiation doses that do not contribute to the clinical benefits of a mammogram. Furthermore, the stratification of DRLs according to detector technology in the work also provided a more robust QA process, which when adopted should improve the efficiency of a mammography units with regards to the delivery of radiation doses to the patients. The study in chapter four examined the consistency in Organ Dose across vendors; the results however showed that the use of Organ Dose for optimisation practices should only be limited to similar vendors, as variations were found between Organ Dose estimated across different vendors. These results will provide guidance on the suitable use of Organ Dose and its limitations as a tool for QA practices. The study in chapter five proposed an Individualised dose estimation method, which provides the basis of Individualised risk assessment. Dose assessment using this method will lead to more accurate radiation risk estimation for each patient undergoing mammography examination. Furthermore, the consistent integration of MBD in clinical decision-making will inform patient-specific screening methods to improve early detection and minimise risks from screening. The results provided should facilitate strategies to reduce dose and dose variations across mammography screening services. The findings of this thesis should also contribute to an improvement in the optimisation of dose in digital mammography, and the estimation of risk from radiation delivered during screening mammography practices.

6.1 Major findings of the thesis and clinical implications

The next subsections discuss how the aims of this thesis were realised and their clinical implications. Finally, I present the limitations of this thesis, future directions, and end with suggestions to the industry backed by the results presented for each aim.

6.1.1 To establish DRLs for digital mammography in NSW Australia

DRLs in mammography are mainly used to identify mammography centres delivering higher median dose to women undergoing screening and aims to trigger an investigation into the reasons. Centres with a median dose above the mammography DRL can trigger optimisation strategies such as modified protocols or new equipment, to help achieve doses below the DRL level while maintaining an acceptable image quality.

Arising from my studies I see that, aside from implementing photon counting technology, dose optimisation in mammography can be achieved at the table side. Which is done through the optimisation of exposure parameters such as AEC (which controls Anode/Filter combinations), mAs, and kVp, which determine the amount of radiation delivered to the breast. The optimisation of automatic exposure control (AEC) is achieved through the proper choice of AEC mode, available in some mammography units such as GE systems, which offer three AEC modes, contrast (CNT), standard (STD), and dose (DOSE). These modes vary the balance between low dose and image quality. It has been shown that the dose may be lowered by up to 50% when using the DOSE mode with acceptable image quality [17].

Radiographers training on optimisation strategies can play a major role in dose reduction [18]. The proper use of compression, image plate, exposure parameters, and positioning are all factors that may affect the dose delivered to the patient. Also, training radiographers to understand the application of DRLs and how to interpret the dose displayed by a mammography unit will allow the radiographer to assess risk There may be a gap in radiographer knowledge due to the complexity of dosimetry of the breast. for example, MGD and Organ Dose are measured in mGy and reflects the absorbed dose. ESAK is measured in mGy and reflects the amount of radiation at the surface of the breast. Effective dose is measured in mSv and reflects the risk to the

breast as it includes the tissue weighing factor. Navigating this and understanding how to apply this knowledge will assist with dose reduction and can reduced variation in doses. Knowledge of these factors should be an accreditation requirement for radiographers.

In Australia ARPANSA is responsible for "promoting uniformity of radiation protection and nuclear safety policy and practices across all jurisdictions". However, there is a disconnect. The practise of radiography is regulated by Australian Health Practitioner Regulating Agency (AHPRA) and the Medical Radiation Practice Board of Australia (MRPBA). They set the accreditation standards for universities and professionals. They do not require this specific knowledge of DRLs. Radiation use has a complex web of regulatory bodies. Nonetheless, one part of ARPANSA's responsibilities is the establishment of DRLs for different modalities in medical imaging. Currently, there is no established DRLs for mammography in Australia, however, mammography DRL is listed in ARPANSA's corporate plan for 2016-2020, as 2016-2017 activity [19]. Nonetheless, the data published in chapter three was obtained in 2014; and published in 2016 since then mammography DRLs have not been established. DRLs should be reviewed every three/five year, so by 2019 the proposed DRLs will be ready for review. The DRLs proposed for NSW in this thesis, which have been presented to ARPANSA in the form of a peer-review published scientific paper [20], could be adopted by ARPANSA as the DRL for mammography dose surveillance across Australia.

The methods proposed in chapter three are also recommended by the ICRP, and the results presented in this chapter, and shared with ARPANSA, should provide a baseline for mammography dose optimisation in NSW if not Australia. My work proposes a single DRL as well as stratified DRLs according to CBT and detector technology. If the DRLs proposed in this thesis are adopted and strategies for implementation put in place, we could significantly lower doses from mammography and reduce dose variations.

> **Recommendation**: A process and quality control mechanisms for moving a DRL proposed by an academic institution into national DRLs should be put in place.
>
> **Recommendation**: ARPANSA should consider adopting the DRLs proposed in our study as the Australian national DRL for digital mammography.

While the results were established using patient data, an earlier study that proposed DRLs for Queensland hospitals has utilised phantom data [21]; in our work the study presented in chapter three resulted in higher DRLs than those proposed by Thiele et al. for similar average CBT, 1.92 and 1.30 mGy compared to 1.4 and 1.1 mGy for CR and DR, respectively. Although the comparison is not accurate as the method differed, it confirms that using phantom data can under or overestimate the dose to the breast and that there is no easy way to convert between patient breast composition and phantom thicknesses [22]. Another explanation for the higher DRLs in the current study is that the phantom used by Thiele et al. was equivalent to a 42 mm CBT which was compared to an average CBT of 45 mm, although this is a small difference in CBT, it will have an effect on the dose as larger CBTs attract higher doses [11].

A comparison with international studies that established DRLs have revealed differences in the results with the DRLs proposed for NSW Australia in chapter three. Figures 6.1 and 6.2 show a comparison of the DRLs for NSW screening services and DRLs internationally when the 75th and 95th percentiles are used, respectively. Differences in results are mainly explained by the different technologies utilised within the international studies. The work in chapter three included CR units, which have since been upgraded to DR units. Nonetheless, comparisons with international studies suggest potential need for the optimisation of mammography units surveyed in NSW so that the DRLs comparable to international standards.

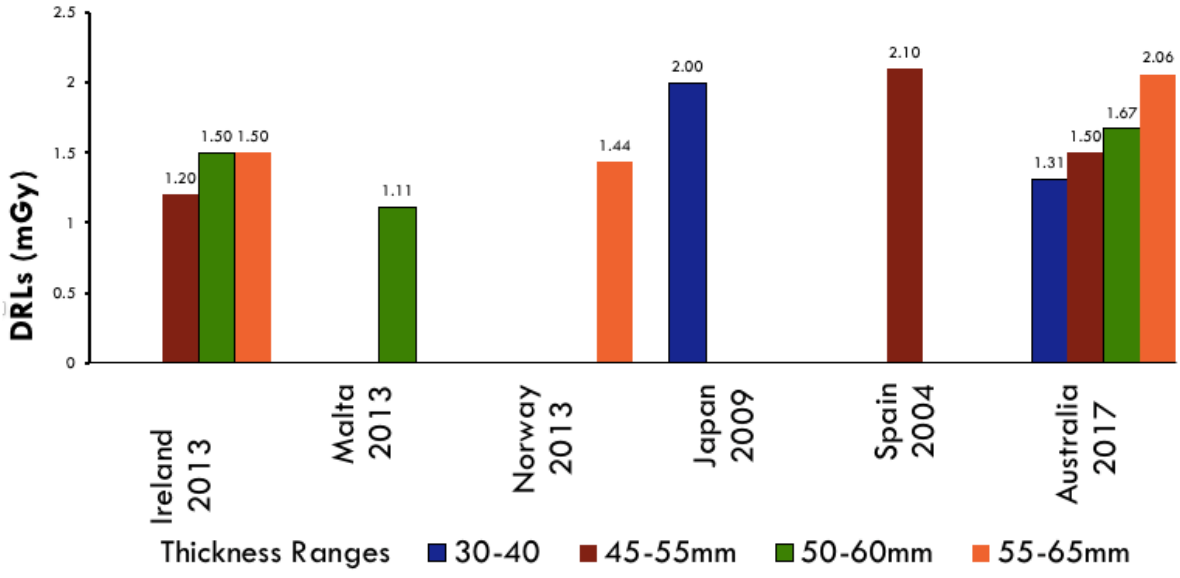

Figure 6.1: DRLs (75th percentile) for patient studies categorised by Compressed Breast Thickness.

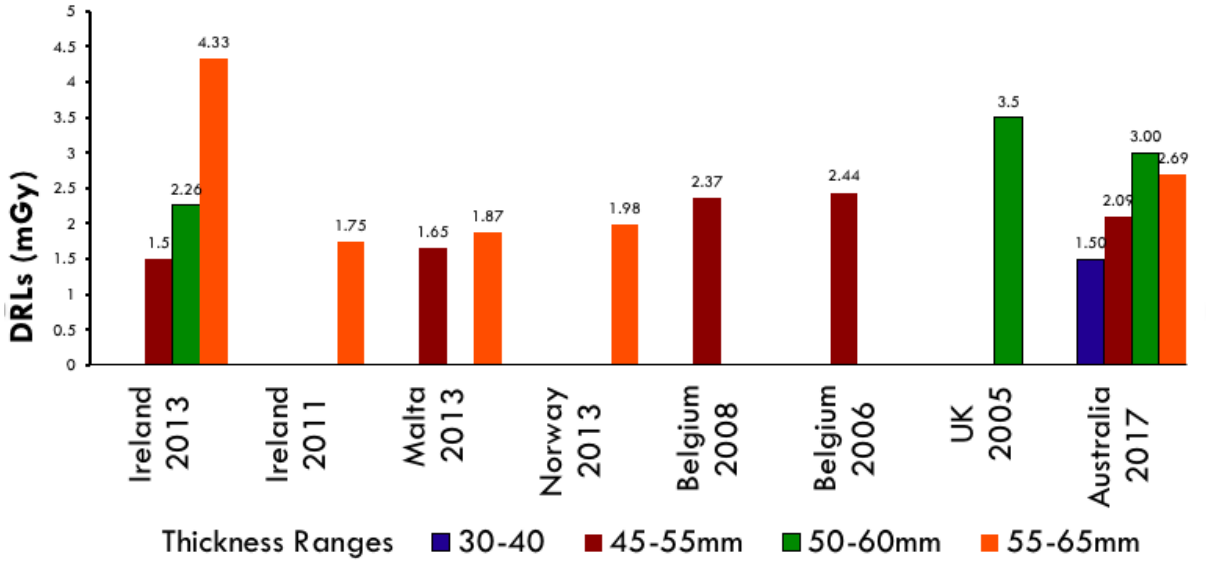

Figure 6.2: DRLs (95th percentile) for patient studies categorised by Compressed Breast Thickness.

The reader might ask "why has this study used patient data and Dance et al. method?" when ACPSEM, the authority entrusted with dose monitoring and QA policies in Australia, have had a different recommended MGD calculation method at the time this study was designed. If phantom data was used to estimate MGD, with Wu et al. or Boone et al. methods, the results would have lacked utility for international comparison. Furthermore, since this study was published, ACPSEM have changed the recommendation to reflect the international move towards Patient dose audits and Dance et al. MGD calculation method [23], hence, confirming the validity of my methodology.

The method used to establish the DRLs in this thesis has some initial weaknesses: it required computing power to process the collected data and new macros needed to be written to automate the calculation of MGD for the large sample of women. With technological advances such as high-powered computers that allow for fast and robust processing of high volumes of data, these limitations have been overcome. Further weaknesses are related to the data collection method, where a high volume of data requires a centralised source of images, and full QA data on the included mammography units. However, this is now mostly available as international medical imaging authorities are moving toward digital technologies and reducing the number of film screen x-ray systems. The study in chapter three did not account for cofounding

factors for dose variation including, the degree of compression, and breast density. These factors affect the amount of radiation delivered to the patient, with dense breasts and lower compression requiring higher X-ray energy, thereby increasing the radiation dose. A better understanding and integration of these confounders into dose calculation could improve the accuracy of dose audit and quality control processes.

The strengths of this thesis however, include the large sample size which allows for a more extensive statistical analysis, examination of causal factors such as CBT and technology type and higher statistical power. Therefore, allowing for a higher chance of finding significant differences when they exist to support recommendations. Finally, a semi-automated method of MGD calculation may potentially pave the way for a fully automated data analysis with artificial intelligence (AI) warning systems for dose. An algorithm would utilise the PACS data to calculate the MGD and add it to the national DRLS Data, machine learning algorithms or simpler algorithms could be developed to identify anomalies in the data.

6.1.2 To explore whether DRLs should be stratified by compressed breast thickness.

Although the use of CBT to stratify doses adds to the complexity of establishing DRLs, it has been established that a single standard CBT proposed by previous studies does not account for the wide variability in the CBT of the population. One study [23] however, suggested three different DRLs depending on different average CBTs, with one being the average CBT and the other two to allow for comparisons with the European [24] and Irish [25, 26] guidelines for CBT ranges of 45 – 55 mm and 55 – 65 mm, respectively. Nonetheless, the limited presentation of DRLs to a single CBT in other studies reduces the power DRLs for assessing the dose of a population with varying CBTs. As shown in figures 6.1 and 6.2, the stratification of DRLs allow for international comparisons even where methodologies differ. This is important in comparing how the national DRLs compare to international norms. Although this is not of direct benefit to the patient, regulating authorities and screening centres could have the benefit of identifying dose anomalies within a given certain CBT range. A larger breast requires higher dose, and centre screening women with larger breast may consistently demonstrate doses higher than the recommended DRLs. Therefore, such higher doses are not necessarily due to errors arising from the screening method or

equipment in use and emphasise the need to account for larger CBTs when establishing DRLs.

It can be argued that the use of single standard CBT to establish DRLs is sufficient for QA practices as DRLs are used to compare mammography units' performance. However, the impact of differences in anthropometric factors on dose variations has been identified by the ICRP with regards to paediatric imaging. Thus, stratification is used in paediatric imaging, where the new ICRP recommendations for DRLs states that: "Establishing DRL values for children is more challenging than for adults, due to the broad range of sizes of Paediatric patients. Weight in children can vary by a factor of more than 100 from a premature infant to an obese adolescent. A single 'standard' patient should not be used to define DRL values for paediatric imaging" [27]. Given that CBT depends on breast size and composition, which can vary by a factor of more than 10, it is reasonable to stratify mammography dosimetry according to CBT to account for population differences in breast size and composition. Furthermore, Abdomen imaging utilises different methods, modalities and protocols depending on the clinical indications for the examination, each of which delivers a different dose value to the patient, as a result, different DRLs have been recommended for each method, modality, or protocol. It is clear that the new ICRP recommendation document recognises the need for further stratifications of the DRLs as needed [28]. However, DRLs stratification has not been recommended for mammography in the ICRP guidelines. With current understanding of causal factors for mammography dose variation and the big data in the digital era, it is logical to stratify DRLs according to patient characteristics and technology. Such stratification should account for differences in technologies average CBTs across centres and states. On the other hand, ARPANSA could also adopt the DRL for the average study population CBT, which should reflect the national average CBT as Australian states and territories have diverse ethnic representation of women that would make the national average CBT close to our sample's average CBT.

> **Recommendation:** The ICRP should introduce the stratification for DRLs in mammography to account for different compressed breast thicknesses.

6.1.3 To explore the effect of different detector technologies on the effectiveness of DRLs and whether DRLs should be stratified by detector technology.

The effect of detector technology on the dose delivered to women during mammography has been shown in many studies [27,29-31] and in figures 6.1 and 6.2 where comparisons are made between international DRLs, with differences in dose between detector technologies being as high as three-folds. Such variations in dose cannot be overlooked as it could have an effect on the efficiency of DRLs as an optimisation trigger tool. Further to the effect of detector technology on dose variation, this thesis explored the idea of stratifying DRLs per detector technology. The study in chapter three found that in a screening service where different technologies are utilised, a low dose technology, such as photon counting detectors, will always have a significantly lower median dose than other digital detectors, and therefore, will not be included in the optimisation practices.

The dose-saving performance of photon counting technology (PCT) compared to the conventional digital mammography systems was explored in an Irish study. This work found that PCT using a mean 40% lower dose compared to the digital mammography system was not inferior [32]. However, a German study, analysing the efficacy of PCT in screening mammography, concluded that PCT systems "enable detection of small invasive cancers and DCIS above the desirable level of the European guidelines", however, PCT recall rates were higher than those of other detector technology systems [33]. The natural question that should be asked is: if PCT has the lowest dose and provides high image quality, why shouldn't all mammography screening migrate to this technology? To answer this question, further research will have to explore the benefit of higher detection rates versus the harms of higher recall rate, this topic is still an open discussion. Nonetheless, an earlier study which surveyed 1570 women of which 1548 responded, found that 97% of women preferred the inconvenience and anxiety of recall, given the possibility of detecting cancer at earlier stages [34]. The overall cost of a PCT system to a screening service is comparable to other mammography units with different detector technologies therefore, PCT should be the first choice for new screening mammography systems [35]. The selling point of a PCT should then be the lower dose to patients. An informed patient may weigh the benefits of screening against the harms. The lower radiation may attract certain patients to a PCT systems. This lower dose was one of the selling points for the transition from

screen film mammography to digital mammography, and it should be for a transition to PCT too. Although this recommendation may be a driver for equipment replacement, replacement would be to the benefit of the patient but at a cost the exchequer. Perhaps a rolling replacement would mitigate that cost. Increasing the prioritisation of dose to the patient in tender selection criteria would support this recommendation.

> **Recommendation:** The ICRP should consider introducing the stratification of DRLs according to detector technology, because CR, DR and PCT are sufficiently different that they need a separate DRL.

6.1.4 To verify the consistency of Organ Dose provided by different mammography vendors.

An important practice during mammography screening is to monitor doses received by women to minimise harms of radiation to healthy women. The Organ Dose, which is available in the DICOM header for the radiographer to check during examination was explored for the purpose of establishing DRLs. However, it was found that this value is inconsistent across different mammography units, which has also been confirmed by other studies [36, 37]. Nonetheless, there is potential benefits to Organ Dose for monitoring dose to the patient and establishing DRLs given that mammography units vendors agree on a single estimation method which will eliminate the inconsistency in results.

Furthermore, a consistent Organ Dose estimate within the DICOM header of a digital image across all mammography vendors could potentially be beneficial for the development of automated systems that will help with the optimisation of imaging practices. An early warning system may support DRLs and QA processes, as it will act in a robust way to warn of increased doses and maintain image quality.

> **Recommendation**: Manufacturers should agree on one Organ Dose measurement methodology, just like they agreed on the structure of the DICOM header. This work should be led by the DICOM Standard Committee.

6.1.5 To propose the use of Mammographic Breast Density (MBD) for the calculation of Actual Glandular Dose (AGD)

Risk reduction from the exposure to harmful radiations during medical imaging is the single most important aim of all dose optimisation practices. Therefore, it is imperative that the dose to the patient be estimated with the highest accuracy possible. This thesis explored a method to produce more accurate estimation for the dose absorbed during mammography. The general acceptance of the 50:50 breast model for the purposes of QA practices in mammography is unreasonable and the need to change that practice is unequivocal. Although it is easier to use the 50:50 model, the results produced are not only used for the purposes of QA. Most dose audit results are used for the estimation of risk from mammography, making it increasingly important to produce accurate dose estimations.

The new method explored in the chapter five work incorporates MBD in the estimation of absorbed dose resulting in the Actual glandular dose (AGD). Although not 100% accurate, AGD provides an idealised estimation of dose, as an individualised risk estimator from radiation. It is illogical that a single inaccurate model of a woman's glandularity or CBT should be used to estimate the risk from radiation, as women's breasts differ in composition.

In chapter five, our results showed significant differences between MGD and AGD, with MGD underestimating the absorbed dose by up to 10% for smaller breasts, this is because MBD was found to be significantly less, up to 50% of Dance et al. model glandularities for smaller breasts. The underestimation of absorbed dose may be translated to an underestimation of risk when using the LNT model, as LNT model suggests a linear relation between cancer risk from radiation and absorbed dose.

Furthermore, it is reasonable to suggest that our MBD estimation method using 2D mammograms may carry errors as seen in figure 6.3, which shows the type of errors in estimating MBD in 2D mammograms versus volumetric estimation. Nonetheless, the average MBD presented in chapter five is almost identical to a volumetric study that explored Australian women's breast density [38].

> **Recommendation:** Further work should be carried out to assess the utility and differences in AGD calculated using area-based measures and volumetric measures of MBD.

6.2 Further remarks

The absorption of X-ray in biological tissues can either cause direct damage to DNA leading to mutation or indirect damage to the tissue through the hydrolysis of water within the tissue. Hydrolysis of water within the tissue results in free radical formation and biological changes which could lead to cancer. The effect of radiation transfer to the tissue can be predicted where the tissue is exposed to high energy radiation, and this type of effect is called a deterministic or non-stochastic effect. Low doses of radiation on the other hand, lead to random biological damage or stochastic effects, whose probability increases with energy absorbed.

Two risk models attempt to explain the effects of radiation exposure on healthy tissues. The Linear No Threshold model (LNT), which proposes a linear effect of radiation on tissues and oncogeneity. The other model suggests that there is a radiation energy threshold below which exposure is safe. Nonetheless, these are still under scrutiny each by the opposing communities [39]. Regardless of the correct model, it seems logical however, to take all measures available to ensure that exposure to medical is as low as reasonably achievable.

In this thesis, new methods were suggested to reduce the probability of oncogeneity due to mammography screening, whether by finetuning the dose optimisation process using stratified DRLs, or by introducing AGD for the estimation of individualised dose and risk. However, authorities carry the responsibility to inform women that there is a possibility, even if small, that screening may cause cancer. This small probability compared to other causes of death could be seen as negligible, however, stating this probability in numbers may change our view on radiation risk. For example, we all know smoking is bad for your health, and there have been many anti-smoking campaigns. In Australia in a 2014, Cancer Australia estimated the mortality from lung cancer to be 23 in 100,000, of which 77% are caused by smoking [40]. Now compare that to 11 deaths in 100,000 for women caused by radiation induced cancer due to screening from the age of 40 to 74 years [41], this is almost half the number of deaths caused by road accidents or smoking yet, it is not considered negligible. There are of course a lot of caveats to this type of comparison and certainly risk models are based on the multiplication of an estimated risk over many years. So clearly also multiplies the error of estimation.

To reduce the risk of radiation induced cancer and other harms of screening mammography, such as false negatives, other non-ionising modalities are used in conjunction with mammography. Using non-ionising imaging modalities reduces the use of extra mammography and DBT examinations, thus reducing the amount of radiation women are subjected to. MRI is used as an adjunctive screening tool for high risk women. This technique has shown higher sensitivity to digital mammography, 92 % compared to 30%, albeit with lower specificity 85% compared to 97% [42]. Combining digital mammography with MRI has proven beneficial as the combined use yields higher specificity and sensitivity, reducing recall rates [43]. Nonetheless, MRI carries higher costs, and should be used for women with dense breasts where tumours are hidden within the dense tissue and are hard to identify with digital mammography. MRI can also be beneficial for women with higher risk of developing breast cancer due to family history and the existence of the higher risk genes such as BRCA1 and BRCA2. Imaging modalities such as ultrasound is better in detecting small-sized lesions and cystic masses when utilised as an adjunct to mammography. Adjunctive ultrasound enhances the radiologist's ability to detect cancer and assess disease extent. Nonetheless, breast screening with ultrasound may increase recall rates [44, 45], increasing false positives and it is operator dependant [46].

6.3 Thesis limitations

The work presented here reflects results from digital mammography only, however our systematic review only included digital mammography studies, Furthermore, NSW screening service uses only digital mammography, consequently, our results reflect the present technologies available in NSW. Furthermore, Digital Breast Tomosynthesis (DBT) has not been included here as this technology has not been utilised for screening, hence there is no available data for DBT. Future studies should explore DRLs for DBT in diagnostic mammography.

Furthermore, results here did not reflect diagnostic mammography in NSW. DRLs should be explored in future studies and compared to screening DRLs, it is expected that diagnostic DRLs may be higher than screening DRLs as diagnostic services include younger women with denser breasts [23].

Although MGD calculations are accepted to be the descriptor of dose absorbed in mammography, it represents an estimation that has inherent errors relating to the composition of a woman's breast. Dance et al. found that the radiation absorption in a heterogeneous breast phantom gives rise to 48% variation in the ESAK to MGD conversion factors [47], and up to 30% error in MGD values [48]. Nonetheless, in patient studies the heterogeneity varies, and no method is available to quantify the heterogeneity of breast composition. Perhaps future work will fill this gap. Hence, our method still represents an acceptable estimation of MGD, and is the current best practice. Furthermore, certain estimations of HVL and ESAK were used to replace missing QA data. The methods applied for estimating this missing data have been previously published and are widely cited [49].

Finally, the estimation of MBD using 2D mammograms carries errors relating to the volumetric nature of breast density. Figure 6.3, is an example of how density estimation can vary between volumetric versus area-base breast density estimation methods.

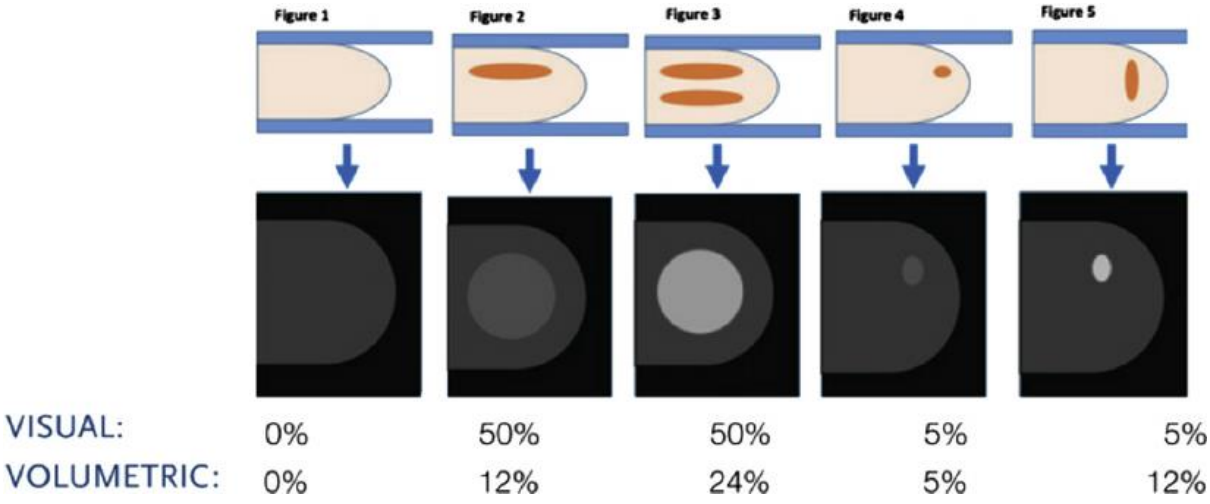

Figure 6.3:Illustrates the possibility of under- or over-estimating MBD by visual or area-based methods. "figures 2 and 3", show how stacked dense tissue could affect the result of area-based estimation of MBD compared to volumetric estimations (Reproduced with permission) [50].

nonetheless, the only way to estimate MBD retrospectively was to use 2D mammograms as volumetric density is not available for our data. Finally, the estimation of MBD using LIBRA software is limited to two vendors, as LIBRA has been tested only for GE and Hologic systems.

6.4 Future directions

- DRLs for DBT was not explored here, however the optimisation of this technology using DRLs should be explored, as DBT is utilised in the diagnostic services.
- Australia's northern territory (NT) has a unique population that is different from the rest of Australian population; indigenous individuals comprise almost 50% of the population of NT. Therefore, MBDs in the NT may be different, and DRLs for this population should be explored separately.
- Symptomatic mammography has not been explored in this thesis. MGD values may be different as the symptomatic population includes younger women with higher breast density. Hence DRLs may be different and needs to be explored in future studies and also compare symptomatic and asymptomatic DRLs.
- The effect of compression levels used within the included centres has not been quantified. Future work may assess such effect and recommend optimisation practices depending on the results of such study.
- Artificial Intelligence (AI) and Machine Learning (ML) are now at the forefront of research, and may be utilised to integrate automated MBD estimation into dose assessment modules. This can help streamline the use of MBD in the calculations of individualised dose and risk assessment.
- Further exploration of AGD is required for the purpose of estimating individualised patient dose and risk. Therefore, future studies may explore other mammography units, such as Philips, Fujifilm, and Siemens, to facilitate the use of LIBRA across all systems used in Australia to incorporate more estimates of breast density.

6.5 Summary of key results and recommendation from the thesis.

6.5.1 DRLs were proposed for Australian digital mammography screening services.

Recommendation 1: A process and quality control mechanisms for moving a DRL proposed by an academic institution into national DRLs should be put in place.

Recommendation 2: ARPANSA should consider adopting the DRLs proposed in our study as the Australian national DRL for digital mammography.

6.5.2 DRLs were presented in stratified format according to different CBTs and detector technologies.

Recommendation 3: The ICRP should consider introducing the stratification for DRLs in mammography to account for different CBTs.

Recommendation 4: The ICRP should consider introducing the stratification of DRLs according to detector technology, because CR, DR and PCT are sufficiently different that they need a separate DRL

6.5.3 Organ Dose was found to be inconsistent across different vendors, and an unreliable estimation of MGD for the purposes of establishing DRLs.

Recommendation 5: Manufacturers should agree on one Organ Dose measurement methodology, just like the agreed on the structure of the DICOM header. This work should be led by the ACR NEMA.

6.5.4 AGD was proposed as a more accurate method of estimating the dose absorbed by the breast during mammography.

Recommendation 6: Further work should be carried out to assess the utility and differences in AGD calculated using area-based measures and volumetric measures of MBD.

6.6 Conclusion

This thesis has established DRLs for mammography in Australia and shows that MGD is dependent upon compressed breast thickness and detector technology. The work also shows wide variation in Organ Dose and dose calculation methodologies across mammography vendors, and that organ doses reported by vendors vary from that calculated using established methodologies. Data produced also show that the use of MGD calculated using 50% glandularity and certain breast thicknesses to represent dose from screening mammography underestimates radiation risk, and proposed AGD, which considers differences in breast composition for individualised radiation-induced risk assessment.

6.7 References

1. Gillies, R.J., P.E. Kinahan, and H. Hricak, Radiomics: Images Are More than Pictures, They Are Data. Radiology, 2016. 278(2): p. 563-77.

2. Wibmer, A., et al., Haralick texture analysis of prostate MRI: utility for differentiating non-cancerous prostate from prostate cancer and differentiating prostate cancers with different Gleason scores. European Radiology, 2015. 25(10): p. 2840-2850.

3. Coroller, T.P., et al., CT-based radiomic signature predicts distant metastasis in lung adenocarcinoma. Radiotherapy and Oncology, 2015. 114(3): p. 345-350.

4. Chaddad, A., C. Desrosiers, and M. Toews. Radiomic analysis of multi-contrast brain MRI for the prediction of survival in patients with glioblastoma multiforme. in 2016 38th Annual International Conference of the IEEE Engineering in Medicine and Biology Society (EMBC). 2016.

5. NEMA. 5 Goals of The DICOM Standard. 2013; Available from: http://dicom.nema.org/DICOM/2013/output/chtml/part01/chapter_5.html

6. Hendrick, R.E., et al., Technical quality control practices in mammography screening programs in 22 countries. International Journal for Quality in Health Care, 2002. 14(3): p. 219-226.

7. Boone, J.M., Glandular breast dose for monoenergetic and high-energy X-ray beams: Monte Carlo assessment. Radiology, 1999. 213(1): p. 23-37.

8. Boone, J.M., Normalized glandular dose (DgN) coefficients for arbitrary X-ray spectra in mammography: computer-fit values of Monte Carlo derived data. Med Phys, 2002. 29(5): p. 869-75.

9. Boone, J.M., T.R. Fewell, and R.J. Jennings, Molybdenum, rhodium, and tungsten anode spectral models using interpolating polynomials with application to mammography. Med Phys, 1997. 24(12): p. 1863-74.

10. Hammerstein, G.R., et al., Absorbed radiation dose in mammography. Radiology, 1979. 130(2): p. 485-91.

11. Sobol, W.T. and X. Wu, Parametrization of mammography normalized average glandular dose tables. Med Phys, 1997. 24(4): p. 547-54.

12. Wu, X., G.T. Barnes, and D.M. Tucker, Spectral dependence of glandular tissue dose in screen-film mammography. Radiology, 1991. 179(1): p. 143-148.

13. Wu, X., et al., Normalized average glandular dose in molybdenum target-rhodium filter and rhodium target-rhodium filter mammography. Radiology, 1994. 193(1): p. 83-89.

14. Dance, D.R., et al., Additional factors for the estimation of mean glandular breast dose using the UK mammography dosimetry protocol. Physics in Medicine and Biology, 2000. 45(11): p. 3225-3240.

15. Dance, D.R., K.C. Young, and R.E. van Engen, Further factors for the estimation of mean glandular dose using the United Kingdom, European and IAEA breast dosimetry protocols. Phys Med Biol, 2009. 54(14): p. 4361-72.

16. Yaffe, M.J., et al., The myth of the 50-50 breast. Medical Physics, 2009. 36(12): p. 5437-5443.

17. Ko, M.-S., et al., Dose Reduction in Automatic Optimization Parameter of Full Field Digital Mammography: Breast Phantom Study. Journal of Breast Cancer, 2013. 16(1): p. 90-96.

18. O'Leary, D. and L. Rainford, Can radiation dose in mammography be further reduced by increasing the image quality? Breast Cancer Research, 2011. 13(1): p. P21.

19. ARPANSA. (2018). Corporate Plan 2016–20. [online] Available at: https://www.arpansa.gov.au/about-us/corporate-publications/corporate-plan/corporate-plan-2016-20 [Accessed 4 Oct. 2018].

20. Suleiman, M.E., et al., Diagnostic reference levels for digital mammography in New South Wales. Journal of Medical Imaging and Radiation Oncology, 2016: p. n/a-n/a.

21. Thiele, D.L., et al., Diagnostic reference levels for mammography in BreastScreen Queensland. Australas Phys Eng Sci Med, 2011. 34(3): p. 415-8.

22. Kelaranta, A., et al., Conformance of mean glandular dose from phantom and patient data in mammography. Radiat Prot Dosimetry, 2015. 164(3): p. 342-53.

23. Heggie, J.C.P., et al., *Position paper: recommendations for a digital mammography quality assurance program V4.0.* Australasian Physical & Engineering Sciences in Medicine, 2017. **40**(3): p. 491-543.

24. O'Leary, D. and L. Rainford, *A comparison of mean glandular dose diagnostic reference levels within the all-digital Irish National Breast Screening Programme and the Irish Symptomatic Breast Services.* Radiat Prot Dosimetry, 2013. **153**(3): p. 300-8.

25. Perry, N., et al., *European guidelines for quality assurance in breast cancer screening and diagnosis Fourth Edition.* Luxembourg office for official publications of the European Communities, 2006.

26. Baldelli, P., et al., *Comprehensive dose survey of breast screening in Ireland.* Radiat Prot Dosimetry, 2011. **145**(1): p. 52-60.

27. Vañó, E., et al., *ICRP Publication 135: Diagnostic Reference Levels in Medical Imaging.* Annals of the ICRP, 2017. **46**(1): p. 1-144.

28. McCullagh, J.B., P. Baldelli, and N. Phelan, *Clinical dose performance of full field digital mammography in a breast screening programme.* Br J Radiol, 2011. **84**(1007): p. 1027-33.

29. Diffey, J.L., *A comparison of digital mammography detectors and emerging technology.* Radiography, 2015. **21**(4): p. 315-323.

30. Baldelli, P., et al., *Comprehensive dose survey of breast screening in Ireland.* Radiation Protection Dosimetry, 2011. **145**(1): p. 52-60.

31. Oduko, J.M., K.C. Young, and A. Burch. *A Survey of Patient Doses from Digital Mammography Systems in the UK in 2007 to 2009*. 2010. Berlin, Heidelberg: Springer Berlin Heidelberg.

32. Hauge, I.H.R., et al., *Patient doses from screen-film and full-field digital mammography in a population-based screening programme.* Radiation Protection Dosimetry, 2012. **148**(1): p. 65-73.

33. Cole, E.B., et al., *Comparison of Radiologist Performance with Photon-Counting Full-Field Digital Mammography to Conventional Full-Field Digital Mammography.* Academic Radiology, 2012. **19**(8): p. 916-922.

34. Weigel, S., et al., *Digital Mammography Screening with Photon-counting Technique: Can a High Diagnostic Performance Be Realized at Low Mean Glandular Dose?* Radiology, 2014. **271**(2): p. 345-355.

35. Ganott, M.A., et al., *Screening mammography: do women prefer a higher recall rate given the possibility of earlier detection of cancer?* Radiology, 2006. **238**(3): p. 793-800.

36. Tu, R., R. Charafeddine, and T. Williams, *Transformation from film-screen to MicroDose digital mammography: Selection challenges, opportunity, and value.* Applied Radiology, 2012. **41**: p. 12.

37. McCullagh, J.B., P. Baldelli, and N. Phelan, *Measured Dose versus Organ Dose Performance in Digital Mammography Systems*, in *Digital Mammography*, J. Marti, et al., Editors. 2010, Springer-Verlag Berlin: Berlin. p. 86-91.

38. Pasicz, K., et al., *Mean glandular doses in mammography: a comparison of values displayed by a mammography unit with in-house values, both using the method proposed by Dance.* J Radiol Prot, 2016. **36**(3): p. 709-715.

39. Hill, M. *Large variation in mammography compression internationally*. 2016. European Congress of Radiology 2017. http://dx.doi.org/10.1594/ecr2017/C-2133.

40. Nguyen, P.K., et al., *Assessment of the Radiation Effects of Cardiac CT Angiography Using Protein and Genetic Biomarkers.* JACC: Cardiovascular Imaging, 2015. **8**(8): p. 873-884.

41. CancerAustralia. *Lung cancer statistics*. 2018 [cited 2018 19 June]; Available from: https://lung-cancer.canceraustralia.gov.au/statistics.

42. Yaffe, M.J. and J.G. Mainprize, *Risk of radiation-induced breast cancer from mammographic screening.* Radiology, 2011. **258**(1): p. 98-105.

43. Raikhlin, A., et al., *Breast MRI as an Adjunct to Mammography for Breast Cancer Screening in High-Risk Patients: Retrospective Review.* American Journal of Roentgenology, 2015. **204**(4): p. 889-897.

44. Kriege, M., et al., *Efficacy of MRI and mammography for breast-cancer screening in women with a familial or genetic predisposition.* N Engl J Med, 2004. **351**(5): p. 427-37.

45. Berg, W.A., et al., *Combined screening with ultrasound and mammography vs mammography alone in women at elevated risk of breast cancer.* JAMA, 2008. **299**(18): p. 2151-2163.

46. Corsetti, V., et al., *Breast screening with ultrasound in women with mammography-negative dense breasts: Evidence on incremental cancer detection and false positives, and associated cost.* European Journal of Cancer, 2008. **44**(4): p. 539-544.

47. Geisel, J., M. Raghu, and R. Hooley, *The Role of Ultrasound in Breast Cancer Screening: The Case for and Against Ultrasound.* Seminars in Ultrasound, CT and MRI, 2018. **39**(1): p. 25-34.

48. Dance, D.R., et al., *Breast dosimetry using high-resolution voxel phantoms.* Radiation Protection Dosimetry, 2005. **114**(1-3): p. 359-363.

49. Hernandez, A.M., J.A. Seibert, and J.M. Boone, *Breast dose in mammography is about 30% lower when realistic heterogeneous glandular distributions are considered.* Med Phys, 2015. **42**(11): p. 6337-48.

50. Robson, K.J., *A parametric method for determining mammographic X-ray tube output and half value layer.* Br J Radiol, 2001. **74**(880): p. 335-40.

51. Ekpo, E.U., et al., Breast composition: Measurement and clinical use. Radiography, 2015. 21(4): p. 324-333.

Appendices

Radiation Protection Dosimetry Advance Access published December 27, 2014

Radiation Protection Dosimetry (2014), pp. 1–12 doi:10.1093/rpd/ncu365

DIAGNOSTIC REFERENCE LEVELS IN DIGITAL MAMMOGRAPHY: A SYSTEMATIC REVIEW

Moayyad E. Suleiman*, Patrick C. Brennan and Mark F. McEntee
Faculty of Health Sciences, The University of Sydney, M205, Cumberland Campus, 75 East St, Lidcombe, Sydney, NSW 2141, Australia

*Corresponding author: msul1801@uni.sydney.edu.au

Received 7 October 2014; revised 24 November 2014; accepted 3 December 2014

This study aims to review the literature on existing diagnostic reference levels (DRLs) in digital mammography and methodologies for establishing them. To this end, a systematic search through Medline, Cinahl, Web of Science, Scopus and Google scholar was conducted using search terms extracted from three terms: DRLs, digital mammography and breast screen. The search resulted in 1539 articles of which 22 were included after a screening process. Relevant data from the included studies were summarised and analysed. Differences were found in the methods utilised to establish DRLs including test subjects types, protocols followed, conversion factors employed, breast compressed thicknesses and percentile values adopted. These differences complicate comparison of DRLs among countries; hence, an internationally accepted protocol would be valuable so that international comparisons can be made.

INTRODUCTION

Breast cancer causes almost half a million deaths in the world per year[1], but early detection has been demonstrated to reduce mortality by up to 30 %[2]. Mammography, radiographic imaging of the breast with X rays, is the most important diagnostic tool for the early detection of breast cancer. There are two types of patients on whom mammograms are performed: symptomatic women in the clinic and asymptomatic women in breast screening programmes.

The Australian breast screening programme was established in 1991, targeting women aged 50–69 y for 2-yearly screening mammograms with the aim of reducing deaths from breast cancer[3]. It has been estimated that since 1991 breast cancer mortality in Australia has been reduced by 21–28 %[3]; however, as with any other X-ray examination, screening programmes can add to the risk of inducing cancer in healthy women by exposure to ionising radiation. Therefore, the dose to the patient must be kept as low as reasonably achievable[4]. The three pillars of radiation protection are justification, optimisation and dose limitation.

The International Commission of Radiation Protection (ICRP) introduced diagnostic reference levels (DRLs) in their 1996 publication 73 as a parameter to be used for quality control, comparison of dose levels, optimisation and limiting variations in dose among diagnostic imaging centres. DRLs were defined as follows:

> A form of investigation level, applied to an easily measured quantity, usually the absorbed dose in air, or tissue-equivalent material at the surface of a simple phantom or a representative patient[4].

A year later, the European Council defined DRLs as:

> Dose levels in medical radiodiagnostic practices, for typical examinations for groups of standard-sized patients or standard phantoms for broadly defined types of equipment. These levels are expected not to be exceeded for standard procedures when good and normal practice regarding diagnostic and technical performance is applied[5].

The methods through which the DRLs are established become important when trying to establish international comparisons as radiation dose measurements are required[3]. Historically, mammography was screen-film based[6–12], but now this technology is being phased out and replaced with digital mammography, which includes full-field digital mammography and computerised radiography systems; hence, only studies with digital mammography or a mix of digital mammography and screen-film mammography (SFM) are included. Measuring the radiation dose to the breast has been performed or represented using a variety of approaches including air kerma[13], entrance surface dose[14], mid-breast dose[15], total energy transmitted to the breast[16] and the average dose absorbed by the glandular tissue[17]. The latter was found to be the most effective way of measuring absorbed dose to the breast because the mammary glands are most sensitive to ionising radiation and have the highest risk of developing radiation-induced carcinogenesis[17]. Called mean glandular dose (MGD), this metric is now the recommended measure by many authorities such as the ICRP[18], the United States National Council on Radiation Protection and Measurements[19], the British Institute of Physics and Engineering in Medicine

(IPEM)[20], the European Council Protocol (EP)[21–23] and the International Atomic Energy Agency (IAEA)[24].

Dose to the glandular tissue of the breast cannot be directly measured during an X-ray examination but can be assessed with certain standard assumptions that depend on breast characteristics and X-ray spectra. MGD represents the effective dose absorbed by the breast and is calculated from conversion factors that have been established using Monte-Carlo techniques[25–28]. Such factors relate MGD to the entrance surface dose and allow for a wide and flexible range of X-ray spectra, breast thickness and breast glandularity[26, 29]. The estimation of this quantity can be done using either a standard phantom or a patient. Although phantoms are good indicators of machine quality and can be used as an inter-centre and inter-suite comparison tool, direct patient measurements can reveal much more information on technique and the relation between breast composition and absorbed dose[9, 30–32].

A number of countries around the world have established DRLs for mammography examination, but many others are yet to do so. The aim of this study is to review the literature on established DRLs and methodologies for establishing them in digital mammography.

METHODS

Search strategy

Using the Preferred Reporting Items for Systematic Reviews and Meta-Analyses methodology[33, 34], a systematic literature search of Medline, Cinahl, Web of Science, Scopus and Google scholar was conducted to identify studies that have established DRLs for digital mammography. The search terms shown in Table 1 were applied; a search filter was used to limit results to specific criteria of population (female, human), age (adult >19), publication language (English) and publication year (1990–2014).

Selection criteria

An initial screening of identified abstracts and titles was conducted by two reviewers (M.S. and M.M.). Only abstracts that discussed MGDs in mammography were included in the full text review. Articles were independently considered for inclusion in the review if they discussed DRLs in digital mammography and included data from phantoms or patients.

RESULTS

The combined search strategy identified 1539 citations: 494 were identified from MEDLINE, 626 from SCOPUS, 385 from Web of Science, 9 from Cinhal and 25 from Google Scholar and manual search. Of these, 270 were duplicates and 1058 citations were excluded after the initial screening based on titles and abstracts. Finally, 211 articles were considered eligible for full text review. On full text review of the remaining articles, 188 were excluded because they did not establish DRLs for digital mammography or had no clinical data (Figure 1). The final number of articles to be included in the systematic review was 22.

Review

The included studies cover different regions in the world, with 13 from Europe[35–47], 5 from Asia and the Middle East[48–52], 1 worldwide study[53] and 1 each from Australia[54], the USA[55] and Nigeria[56]. The main characteristics of the studies are summarised in Tables 2 and 3. Six of the 22 studies were based on phantom data, 13 on patient and 3 on both. For comparison purposes, studies with both phantom and patient data were included in both tables. The review demonstrated that four main quality control

Table 1. The search terms used to find the relevant literature, separated into the intervention, cohort and other, where the search formula was (Intervention combined with 'OR') AND (Cohort combined with 'OR') AND (other combined with 'OR').

Intervention	Cohort	Other
DRLs	Mammography	Breast screening
DRLs	Mammographic Examination	Mass screening
Dose reference levels	Mammogram	Population screening
MGD	Digital mammography	
Average glandular dose		
Reference levels		
Dose survey		
Population dose		
Glandular dose		
Radiation dose		

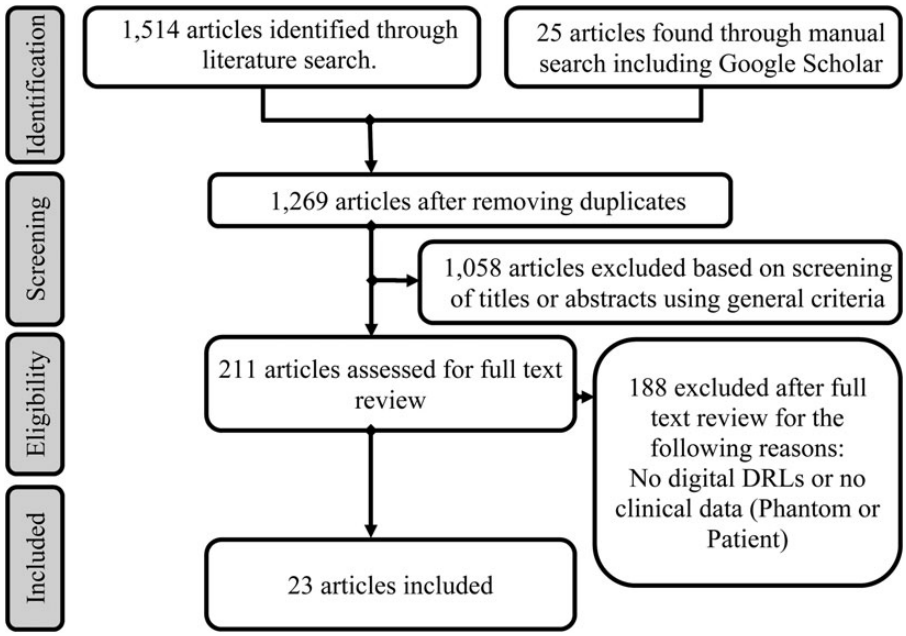

Figure 1. Flow diagram of included and excluded studies with specifics for DRLs in digital mammography.

protocols were followed for estimating MGD and finding DRLs, those published by the American College of Radiology (ACR)[57], the European Council Protocol (EP)[21–23], the IAEA[24] and the British IPEM, formerly the Institute of Physical Sciences in Medicine (IPSM)[60].

Phantom studies: methods used

Phantom-based studies have the benefits of standard baseline, standard exposure protocols and quick inter- and intra-X-ray suites comparison. Therefore, it is not unexpected that 6 of the 22 studies investigating DRLs were performed using phantoms only (Table 2) and 3 performed on patients and phantoms. Of the three studies that were performed on patients and phantoms, one reported DRLs for phantoms only, one reported for patients only and one reported for both patients and phantoms (Tables 2 and 3). A total of eight studies reported DRLs for phantoms although the phantoms used were not of the same size and type; three used ACR polymethylmethacrylate (PMMA) phantoms[50, 54, 55], three used EP PMMA phantoms[35, 45, 47], one used a 45-mm RMI-156 phantom[51] and another used a 40-mm BR12 phantom[38].

The phantom types and the protocols used to collect measurements, the coefficients used for the conversion to MGD and the percentile used to report the DRL varied among the studies (Table 2). The ACR measurement protocol[57] and the Wu *et al.* MGD conversion factors[29, 58] were followed by three of the seven PMMA studies[50, 54, 55], two followed European measurement protocol[21] and used the Dance *et al.* MGD conversion factors[45, 47] and one followed the IAEA measurement protocol with the Dance *et al.* MGD conversion factors[35]. Thus, DRL values found in these studies cannot be compared directly without conversion calculations; this complicates inter-study comparisons and detracts from the benefit of using a standard phantom.

Phantom studies: DRLs

The overall distribution of DRLs calculated from phantom studies are shown in Figure 2. These are categorised by phantom types. However, other factors need to be discussed before these DRLs can be compared. The three ACR PMMA phantom studies reported overall 75th percentiles of 1.3 mGy[54], 1.75 mGy[50] and 2.0 mGy[55]. Although the same standard phantom and conversion factors were used to estimate the average MGDs, the results demonstrate a 0.7-mGy difference in the average MGDs between Australia (1.3 mGy) and the USA (2.0 mGy). The low DRL in the Australian study might be explained by the absence of film-screen mammography units in the study where the other two studies had a mix of digital and film-screen units. The RMI 156 phantom following the ACR protocol reported a 75th percentile of 1.44[38].

The two EP PMMA phantom studies reported 75th percentile of 1.70 mGy[47] and 95th percentile of

Table 2. Summary data from included phantom studies.

Country	Authors (year)	Data collection method	Dose protocol/ conversion factors	Phantom type (thickness/ E-BCT/G %)	Average MGD mGy (unless otherwise stated)	DRLs mGy		
						75 %	95 %	Recommended
Australia	Thiele *et al.* (2011)[54]	Measured ESAK	ACR[57]/Wu *et al.*[29, 58]	ACR PMMA (45 mm/ 42 mm/50 %)	All: 1.16 DR: 1.04 CR: 1.28	All: 1.30 DR: 1.10 CR: 1.36		DR: 1.10[a] CR: 1.40[a]
Taiwan	Hwang *et al.* (2009)[50]	Measured ESAK	ACR[57]/Wu *et al.*[29]	ACR PMMA (45 mm/ 42 mm/50 %)	All: 1.48 DR: 1.47 SFM: 1.49	1.75		
USA[b]	Spelic *et al.* (2007)[55]	Measured ESAK	ACR[57]/Wu *et al.*[29]	ACR PMMA (45 mm/ 42 mm/50 %)	All: 1.78 DR: 1.63 SFM: 1.80	All: 2.0 DR: 1.92 SFM: 2.04	All: 2.35 DR: 2.29 SFM: 2.39	
Slovenia	Zdesar (2008)[47]	Estimated ESAK	EP[21]/ Dance *et al.*[59]	PMMA (45 mm/ 53 mm/50 %)	1.5	1.7		
Belgium	Smans *et al.* (2006)[c][45]	Estimated ESAK	EP[21]/Dance *et al.*[59]	PMMA (45 mm/ 53 mm/50 %)	[d]		2.08	
Bulgaria	Avramova and Vassileva (2011)[35]	Measured IAK	IAEA[24] /Dance *et al.*[59]	PMMA (45 mm/ 50 mm/50 %)	1.8	2.3		
Turkey	Bor *et al.* (2008)[38]	Measured ESAK	IPSM[60]/Dance *et al.*[e][59]	BR12 (40 mm/ 45 mm/50 %)	1.46	2.0		
Malaysia	Jamal *et al.* (2003)[c][51]	Measured ESAK	ACR[57]/Wu *et al.*[29]	RMI 156[f] (45 mm/ 42 mm/50 %)	1.23	1.44 4.61 (ESAK)		2.0 (93.3 %)[a]

ACR, American College of Radiology; EP, European protocol; IPSM, Institute of Physical Sciences in Medicine/now; IPEM, Institute of Physical and Engineering in Medicine; IAEA, International Atomic Energy Agency; ESAK, entrance surface air kerma; IAK, incident air kerma; E-BCT, equivalent breast compressed thickness; G %, glandularity; PMMA, polymethyl-methacrylate; DR, digital radiography; CR, computed radiography; SFM, screen-film mammography.
[a]Recommended by the authors.
[b]Data estimated from Figures 4 and 10 of Spelic *et al.*[55].
[c]Studies include phantom and patient data.
[d]No average MGD value mentioned in the study.
[e]Dance *et al.* not specifically mentioned.
[f]RMI 156 is made from acrylic with wax inserts.

Table 3. Summary data from included patient studies.

Country	Author(s) (year)	Number of patients	Data collection method	Dose protocol/ conversion factors	Mean BCT mm	Average MGD mGy	DRLs mGy		
							75 %	95 %	Recommended
Japan	Asada *et al.* (2014)[48]	NA	Measured ESAK	EP[23]/Wu *et al.*[29]	42	1.58	1.91		
Iran	Bahreyni *et al.* (2013)[49]	100	Measured ESAK (TLDs)	EP[23]/Wu *et al.*[29]	CC: 47 MLO: 53 SMLO: 50–60	CC: 0.88 MLO: 1.11	SMLO: 1.33		
Nigeria	Ogundare *et al.* (2009)[56]	40	Measured ESAK (TLDs)	ACR[57]/Wu *et al.*[29]	All: 41.1 CC: 33.8 MLO: 48.5	All: 0.88 CC: 0.33 MLO: 1.43		2.5[a]	
Japan	Kawaguchi *et al.* (2014)[52]	300	Measured ESAK	EP[21, 61]/Dance *et al.*[59]	SMLO: 30–40 MLO: 37.6	SMLO: 1.88 MLO: 1.84	SMLO: 2.0		
Ireland	O'Leary (2013)[44]	1010	Estimated ESAK	EP[23] /Dance *et al.*[27]	DR: 54.7 SFM: 52.3	DR: 1.33 SFM: 2.64	DR: 1.5 SFM: 3.17	DR: 2.26 SFM: 5.59	
					45–55	All: 1.68 DR: 1.13 SFM: 2.16	All: 1.2 DR: 1.2 SFM: 2.55	All: 1.5 DR: 1.5 SFM: 3.85	
					55–65	All: 2.04 DR: 1.40 SFM: 2.88	All: 2.47 DR: 1.50 SFM: 3.41	All: 4.33 DR: 2.40 SFM: 5.84	
Malta	Borg *et al.* (2013)[b][39]	759	Estimated ESAK	EP[21]/Dance *et al.*[59]	All: 57.5 CC: 53.8 MLO: 63.4	All: 1.07 CC: 1.06 MLO1.07	All: 1.11 CC: 1.11 MLO: 1.11	All: 1.68 CC: 1.65 MLO: 1.87	1.87[c]
Norway	Hauge *et al.* (2013)[41]	1335	Estimated ESAK	EP[21]/Dance *et al.*[27, 59, 62]	SMLO: 55–65	SCC: 1.23 SMLO: 1.35 CC: 1.18 MLO: 1.31	SMLO : 1.44	SMLO : 1.98	2.0[c]
Worldwide	Geeraert *et al.* (2012)[53]	14 7497	Estimated ESAK from DICOM data	N/A /Dance *et al.*[59]	Na	Europe: 1.48 North America: 1.42 Asia-Pacific: 1.42	Europe: 1.6 North America: 1.6 Asia-Pacific: 1.1	Europe: 2.4 North America: 2.1 Asia-Pacific: 2.3	

Continued

Table 3. *Continued*

Country	Author(s) (year)	Number of patients	Data collection method	Dose protocol/ conversion factors	Mean BCT mm	Average MGD mGy	DRLs mGy		
							75 %	95 %	Recommended
Ireland	Baldelli *et al.* (2011)[36]	2910	Estimated ESAK from DICOM data	EP[21]/Dance *et al.*[27, 59, 62]	CC: 60.5 MLO: 63.0	CC: 1.27 MLO: 1.34		1.75	
Ireland	Baldelli *et al.* (2010)[37]	3016	Estimated ESAK from DICOM data	EP[21]/Dance *et al.*[62]	CC: 60 MLO: 62.5	CC: 1.27 MLO: 1.35		1.75	
Belgium	Michielsen (2008)[42]	NA	Estimated ESAK	EP[21]/Dance *et al.*[59]	SMLO: 48–58	All: 1.69		2.37	
Belgium	Smans *et al.* (2006)[b][45]	10 093	Estimated ESAK	EP[23]/Dance *et al.*[59]	SMLO: 48–58	All: 1.67		2.44	
Spain	Moran *et al.* (2005)[43]	5034	Estimated ESAK from DICOM data	EP[23]/Dance *et al.*[59]	All: 52 CC: 49 MLO: 54	All: 1.88 CC: 1.80 MLO: 1.95	All: 2.1 CC: 2.0 MLO: 2.1		
UK	Young *et al.* (2005)[b][46]	16 505	Estimated ESAK	IPEM[60]/ Dance *et al.*[27, 59]	SMLO: 50–60 CC: 54.1 MLO: 56.8	SMLO: 2.03 CC: 1.96 MLO: 2.23			SMLO: 3.5[d]
Spain	Chevalier *et al.* (2004)[40]	5034	Estimated ESAK from DICOM data	EP[22]/Dance *et al.*[59]	All: 52 CC: 49 MLO: 54	All: 1.88 CC: 1.80 MLO: 1.95	All: 2.1 CC: 2.0 MLO: 2.1		

ACR, American College of Radiology; EP, European protocol; IPSM, Institute of Physical Sciences in Medicine/now; IPEM, Institute of Physical and Engineering in Medicine; ESAK, entrance surface air kerma; CC, cranio-caudal; MLO, mediolateral oblique; SMLO, standard mediolateral oblique (only standard breast thickness range included for DRLs calculations); TLDs, thermoluminescence dosemeters; DR, digital radiography; CR, computed radiography; SFM, screen-film mammography.
[a]Reported 92.5 percentile.
[b]Studies include phantom and patient data.
[c]Recommended by authors.
[d]Reported 96.5 percentile.

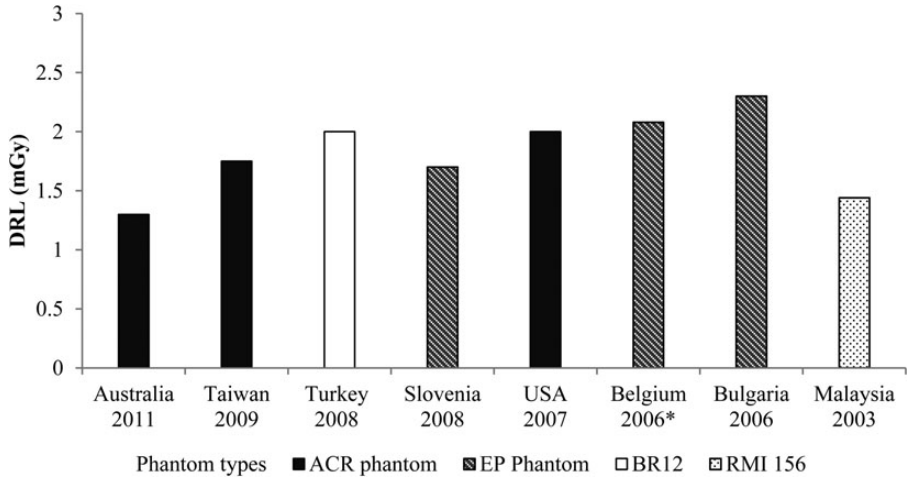

Figure 2. DRLs for phantom studies categorised by phantom types (*95th percentile).

2.08 mGy[45]. Although the two studies used the same phantom and same conversion factors to report MGD DRLs, a comparison cannot be made because the percentiles used were different[45, 47]. A PMMA phantom study following the IAEA protocol reported an MGD 75th percentile of 2.30 mGy. The authors reported non-standardised techniques and lack of optimisation as possible causes for the higher dose[35]. A BR12 phantom following the IPSM protocol reported a 75th percentile of 2.0 mGy[38].

Patient studies: methods

Patient studies have an advantage over phantom studies that they offer a more realistic and comprehensive assessment of the doses delivered to patients with different breast sizes and compositions. A total of 15 patient studies investigating DRLs were reviewed (Table 3) and once again, methods of data collection varied. Two studies used thermoluminescence dosemeters (TLDs) to measure ESAK values[49, 56] and the rest estimated ESAK values from exposure parameters such as tube output and tube loading[36, 37, 39–46, 48, 52, 53]. Two different methods of calculating MGDs have been used: the Wu *et al.* MGD conversion factors were used to calculate MGDs in 3 of the 15 patient studies[48, 49, 56] and 12 used the Dance *et al.* conversion factors[36, 37, 39–46, 53]. A wide range of mean breast compressed thicknesses (BCTs) was reported. These diverse methodologies complicate direct comparison among results; hence, studies are categorised according to reported average BCT and plotted in Figures 3 and 4.

Patient studies: DRLs

A range of DRLs have been reported with 75th percentiles ranging from 1.11[39] to 2.47 mGy[44] and the 95th percentiles ranging from 1.5[44] to 4.33 mGy[44], in the average BCT range of 55–65 mm. The three Irish studies reported different 95th percentile values from each other, two breast screening mammography studies with only digital units reported a 1.75 mGy[36, 37] of DRL value and the third that included SFM units and symptomatic patients reported a 2.40 mGy for digital units only (an overall digital and SFM value of 4.33 mGy), which is the highest among the three; this may be due to the inclusion of symptomatic patients[44]. A Norwegian study, which included only digital units in a breast screening programme, reported a 95th percentile of 1.98 mGy[41] and a Maltese study reported a lower value of 1.87 mGy[39]; both though are higher than the two breast screening Irish studies that used the same percentile value[36, 37]. International differences may be due to variation in population breast composition and the use of certain type of units that contribute to higher patient dose. Many authors have discussed the differences in breast dose when using different makes and models of mammography units on similar size and composition breasts[36, 41].

In the BCT range of 45–55 mm, international comparisons can be made. Two Belgian studies reported similar 95th percentiles of 2.44[45] and 2.37 mGy[42]. For the same average BCT range, two Spanish studies reported a 75th percentile of 2.1 mGy[40, 43], which is almost double the 1.2 mGy reported by an Irish study[44] and 1.33 mGy reported by an Iranian study[49]. Studies with equal BCT, measurement protocol, MGD conversion factors and percentile reported facilitate easier international comparison; however, they do show a worrying outcome of large variations in the dose received by women in different countries. The reasons for these potential differences are thoroughly

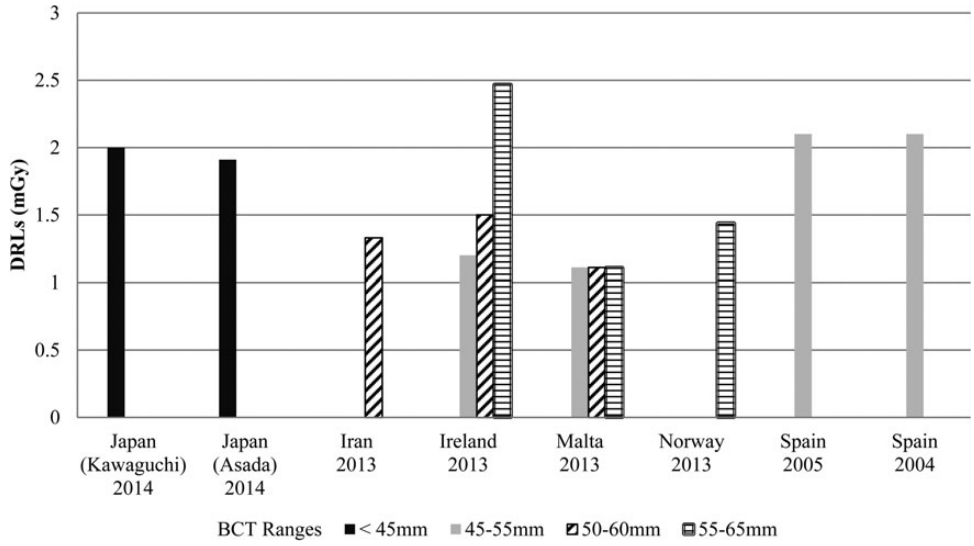

Figure 3. DRLs (75th percentile) for patient studies categorised by BCT.

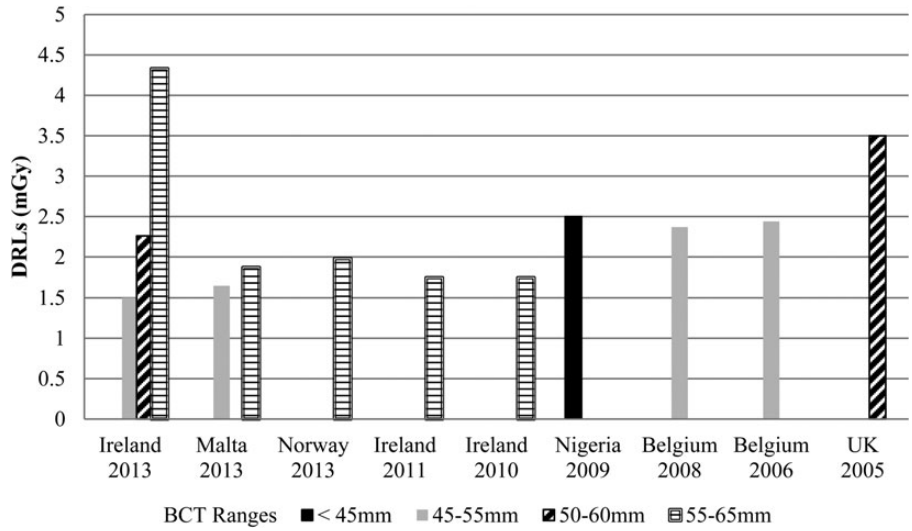

Figure 4. DRLs (95th percentile) for patient studies categorised by BCT.

discussed in the discussion section but include, technique, technology and population characteristics.

In the BCT range of <45 mm, two Japanese studies reported 75th percentiles of 1.91[48] and 2 mGy[52]. The authors followed two different protocols and methods to calculate the dose, which could explain the 0.09 (5 %) difference in their results, as a 9–21 % difference would be expected between Dance *et al.* and Wu *et al.* methods[63].

An all-digital worldwide study that collected dose information from different geographical areas (and did not report BCT) showed the 95th percentiles for Europe, North America and Asia-Pacific of 2.4, 2.1 and 2.3 mGy, respectively[53] and 75th percentiles of 1.6, 1.6 and 1.1 mGy, respectively.

DISCUSSION

The studies reviewed followed two main groups of authors that reported conversion factors for the calculation of breast dose: Dance *et al.*[27, 59, 62, 64] and Wu *et al.*[29, 58], which are both used to compensate for the

X-ray spectrum characteristics and breast composition (glandularity). Four phantom studies[50, 51, 54, 55] and 3 patient studies[48, 49, 56] used Wu *et al.* conversion factors whereas 4 phantom[35, 38, 45, 47] and 12 patient studies[36, 37, 39–46, 52, 53] used Dance *et al.* conversion factors. It has been reported that MGD calculated from exposure measurements using Wu *et al.* conversion factors was 9–21 % less compared with Dance *et al.* conversion factors[63]. Dance *et al.* acknowledged that a variation of up to 16 % exists between the two methods; this is due to differences in the breast model, X-ray spectra and photon interaction cross sections[59] (this will not be discussed as it is beyond the scope of this paper). Wu *et al.* conversion factors are still valid for newer technologies and can report accurate results[65]. Dance *et al.* conversion factors though have been updated to include new factors that compensate for different technologies, different types of target/filter combinations and wider range of BCTs and breast glandularities[59, 62, 64].

Four different quality control protocols that have different approaches to exposure measurements (Table 4) were followed. The two most common are the EP[21–23] and the ACR[57]; both are well-established protocols. The EP was updated to include digital mammography[21], a supplement fourth edition of the European guidelines has been published[69], and according to the European Reference Organisation for Quality Assured Breast Screening and Diagnostic Services website, a further update is on the way[70]. An update of the ACR protocol to cover digital mammography is also known to be in progress[71]; information regarding calculation standards and conversion factors to be used has not been released yet. However, the authors would suggest the use of Dance *et al.* conversion factors as the latest published data are based on newer technologies.

Two main percentiles were used to establish DRLs, the 75th and 95th percentiles. The 75th percentile is more common and is used when there is a large range of MGDs. Its use encourages 25 % of the centres to reduce their dose. On the other hand, the 95th percentile is used when there is a small range of MGDs and means that only 5 % of the centres require an intervention to reduce dose. Thus, the 95th percentile is more suited to well-established screening environments whose variation in doses is likely to be small. Nonetheless, when establishing DRLs, any recommendations of lowering dose should be balanced with a measure of image quality as poor image quality degrades image interpretation accuracy[72–75].

A diverse range of standard BCTs has been reported depending on the protocol followed. Phantom studies that followed the EP used thicker equivalent BCT phantoms (53 mm) and hence reported higher average MGDs than ACR protocol studies that used thinner equivalent BCT phantoms (42 mm). In patient studies, the range of standard BCT varied even for the same

Table 4. Summary of quality control protocols followed by the included studies.

Protocol	Test subjects		Digital/SFM	Conversion factors	Reference level of MGD (mGy) to standard breast
	Phantom (thickness /E-BCT/G %)	Patients number			
IAEA 2011[66]	Blocks of PMMA (20, 45, 70 mm/21, 53, 90 mm/50 %)	N/A	Digital	Dance (2000)	<1, 2.5, 6.5, respectively
IAEA 2009[67]	Standard breast: PMMA (45/53 mm/29 %)	N/A	SFM	Dance (2000)	<2.5
IAEA 2007[24]	Standard breast: PMMA (45/50 mm/50 %)	10–50 patients BCT 50–60 mm	Both	Dance (2000)	N/A
EP 2006[a][21]	Standard breast: PMMA (45/53 mm/50 %)	Minimum 10 patient	Both	Dance (2000)	<2.5
	Or blocks of PMMA (20–80 mm)	BCT 40–60 mm			
IPEM 2005[68]	Standard breast: PMMA (45/53 mm/29%)	Minimum 10 patient	Both	Dance (2000)	<3.5
	Or blocks of PMMA (20–80 mm)	BCT 50–60 mm			
ACR 1999[57]	Standard breast: PMMA (40/42 mm/50 %)	N/A	SFM	Wu (1991)	≤3.0
	Blocks of PMMA (20–80 mm)			Dance (1990)	
				Sobol (1997)	

E-BCT, equivalent breast compressed thickness; G %, breast glandularity; SFM, screen-film mammography; IAEA, International Atomic Energy Agency; EP, European Council protocol; IPEM, Institute of Physical and Engineering in Medicine; ACR, American College of Radiology; PMMA, polymethyl-methacrylate.
[a]Different reference values available for different BCT.
[b]Technical (phantom)/clinical (patient).

protocol. In general, a thicker BCT requires higher exposure and is expected to receive higher dose in a similar X-ray examination environment. The most two common ranges of BCT used among the reviewed studies are 45–55 and 55–65 mm, which falls within the range followed by the EP for patient studies (40–60 mm). The standard EP phantom also has an equivalent BCT of 53 mm, which falls into that range. Although establishing DRLs normally requires the use of standard BCT, any study that aims to establish DRLs for mammography could also include a range of BCTs, which would result in a more accurate measure of dose variations across the population. Plotting graphically BCT versus DRL would be a good quality control measure that radiographers could refer to in order to assure that useful data are available for the non-standard breast thickness.

Although breast thickness is not the only factor to have an effect on MGD, it is the most consistently reported. Other factors that effect MGD are not consistently reported; for example, kVp is reported in 13 of the 22 papers included in this review, target filter combination in 13 of the 22, HVL in 5 of the 22, and mAs in 8 of the 22. Therefore, for the purpose of consistency, a detailed comparison of these factors was not feasible and is not included.

The lack of consistency and a worldwide standard methodology to establish DRLs complicates comparison of dose among countries. International comparisons have shown differences that are often discussed by authors; for example, the difference in the digital screening services of Ireland (1.75 mGy)[36] and Norway (1.98 mGy)[41]. Hauge *et al.* explained the lower DRL in the Irish study to be a result of including more of a certain mammography unit that was proven to contribute to lower dose values and hence lower DRLs within the Irish study[41]. Both studies found that MGDs varied depending on the model of mammography units; Hauge *et al.* reported that eliminating one type of mammography units resulted in the reduction of the 95th percentile from 1.98 to 1.65 mGy bringing the results closer to Baldelli *et al.* 95th percentile (1.75 mGy)[41].

CONCLUSION

DRLs for mammography have been established across the world, and variable methods and techniques were used. The most common method used was patient studies following the EP combined with Dance *et al.* MGD conversion factors for BCT ranges of 45–55 and 55–65 mm. DRLs for these ranges varied with the 75th percentiles ranging from 1.11 to 2.47 mGy and the 95th percentiles from 1.5 to 3.5 mGy. However, an internationally accepted protocol that includes dose measurement method, conversion factor, BCT for patients or phantoms and DRL percentile needs to be established before important, useful and accurate international comparison can be made.

REFERENCES

1. World Health Organisation. *Cancer*. Available on http://www.who.int/mediacentre/factsheets/fs297/en/ (11 November 2013, date last accessed).
2. Tabar, L. *et al*. *Swedish two-county trial: impact of mammographic screening on breast cancer mortality during 3 decades*. Radiology. **260**, 658–663 (2011).
3. AIHW. *BreastScreen Australia monitoring report 2010-2011*. Cancer series 77. Cat. no. CAN 74. (Canberra: AIHW) (2013).
4. International Commission of Radiation Protection. *Radiological protection and safety in medicine*. Ann ICRP. ICRP Publication 73. Ann. ICRP 26(2), 1–47 (1996).
5. CEC. *Council Directive 97/43 EURATOM (1997) on health protection of individuals against the dangers of ionising radiation in relation to medical exposures*. Official J. Eur. Commun., Medical Exposure Directive of June 30, 1997, No. L 180/22.
6. González, L., Vañó, E., Oliete, S., Manrique, J., Hernáez, J. M., Lahuerta, J. and Ruiz, J. *Report of an image quality and dose audit according to directive 97/43/Euratom at Spanish private radiodiagnostics facilities*. Br. J. Radiol. **72**, 186–192 (1999).
7. Nassivera, E. and Nardin, L. *Quality control programme in mammography: second level quality controls*. Br. J. Radiol. **70**, 612–618 (1997).
8. Heggie, J. C. *Survey of doses in screening mammography*. Australas. Phys. Eng. Sci. Med. **19**, 207–216 (1996).
9. Faulkner, K., Law, J. and Robson, K. J. *Assessment of mean glandular dose in mammography*. Br. J. Radiol. **68**, 877–881 (1995).
10. Morán, P., Chevalier, M. and Vañó, E. *Comparative study of dose values and image quality in mammography in the area of Madrid*. Br. J. Radiol. **67**, 556–563 (1994).
11. Heggie, J. C. *A survey of doses to patients in a large public hospital resulting from common plain film radiographic procedures*. Australas. Phys. Eng. Sci. Med. **13**, 71–80 (1990).
12. Ciraj-Bjelac, O., Beciric, S., Arandjic, D., Kosutic, D. and Kovacevic, M. *Mammography radiation dose: initial results from Serbia based on mean glandular dose assessment for phantoms and patients*. Radiat. Prot. Dosim. **140**, 75–80 (2010).
13. Jensen, J. E. and Butler, P. F. *Breast exposure: nationwide trends; a mammographic quality assurance program—results to date*. Radiol. Technol. **50**, 251–257 (1978).
14. Fitzgerald, M., White, D. R., White, E. and Young, J. *Mammographic practice and dosimetry in Britain*. Br. J. Radiol. **54**, 212–220 (1981).
15. Breslow, L., Thomas, L. B. and Upton, A. C. *Final reports of the National Cancer Institute ad hoc Working Groups on Mammography in Screening for Breast Cancer and a summary report of their joint findings and recommendations*. J. Natl. Cancer Inst. **59**, 467–541 (1977).
16. Boag, J. W., Stacey, A. J. and Davis, R. *Radiation exposure to the patient in xeroradiography*. Br. J. Radiol. **49**, 253–261 (1976).

17. Karlsson, M., Nygren, K., Wickman, G. and Hettinger, G. *Absorbed dose in mammary radiography*. Acta. Radiol. Ther. Phys. Biol. **15**, 252–258 (1976).
18. International Commission of Radiation Protection and measurements. *Protection of the patient in nuclear medicine (and Statement from the 1987 Como Meeting of ICRP)*. ICRP Publication 52. Ann. ICRP 17 (1987).
19. Rothenberg, L. N. *Mammography: A User's Guide. NCRP Report No. 85* (Bethesda, MD: National Council on Radiation Protection and Measurement) (1986).
20. IPEM. *Guidance on the establishment and use of diagnostic reference levels for medical X-ray examinations*. IPEM Report 88 (Institute of Physics and Engineering in Medicine) 2004.
21. Perry, N., Broeders, M., De Wolf, C., Törnberg, S., Holland, R., Von Karsa, L. and Puthaar, E. *European Guidelines for Quality Assurance in Breast Cancer Screening and Diagnosis*, 4th edn. Luxembourg office for official publications of the European Communities (2006).
22. Perry, N. and Schouten, J. *European Guidelines for Quality Assurance in Mammography Screening*. Office for official publications of the European communities (2001).
23. Zoetelief, J., Fitzgerald, M., Leitz, W. and Säbel, M. *European Protocol on Dosimetry in Mammography*. Office for Official Publications of the European Communities (1996).
24. International Atomic Energy Agency. *Dosimetry in Diagnostic Radiology: An International Code of Practice*. International Atomic Energy Agency (2007).
25. Kereiakes, J. G. and Rosenstein, M. *Handbook of Radiation Doses in Nuclear Medicine and Diagnostic X-ray*. CRC Press Boca Raton (1980).
26. Dance, D. *The Monte Carlo calculation of integral radiation dose in xeromammography*. Phys. Med. Biol. **25**, 25 (1980).
27. Dance, D. *Monte-Carlo calculation of conversion factors for the estimation of mean glandular breast dose*. Phys. Med. Biol. **35**, 1211 (1990).
28. Rosenstein, M., Andersen, L. W. and Warner, G. G. *Handbook of Glandular Tissue Doses in Mammography*. US Department of Health and Human Services, Public Health Service, Food and Drug Administration, Center for Devices and Radiological Health (1985).
29. Wu, X., Barnes, G. T. and Tucker, D. M. *Spectral dependence of glandular tissue dose in screen-film mammography*. Radiology **179**, 143–148 (1991).
30. Fabiszewska, E., Jankowska, K., Grabska, I. and Skrzynski, W. *Individual doses for women undergoing screening mammography examinations in Poland in 2007*. J. Radiol. Prot. **31**, 467–475 (2011).
31. Khoury, H. J., Barros, V. S. and Lopes, C. *Evaluation of patient dose for mammography in Pernambuco, Brazil*. Radiat. Prot. Dosim. **115**, 337–339 (2005).
32. Seeram, E. and Brennan, P. C. *Diagnostic reference levels in radiology*. Radiol. Technol. **77**, 373–384 (2006).
33. Liberati, A., Altman, D. G., Tetzlaff, J., Mulrow, C., Gøtzsche, P. C., Ioannidis, J. P. A., Clarke, M., Devereaux, P. J., Kleijnen, J. and Moher, D. *The PRISMA statement for reporting systematic reviews and meta-analyses of studies that evaluate healthcare interventions: explanation and elaboration*. BMJ 339:b2700 (2009).
34. Moher, D., Liberati, A., Tetzlaff, J. and Altman, D. G. *Preferred reporting items for systematic reviews and meta-analyses: the PRISMA statement*. Br. Med. J. **339**, 332–336 (2009).
35. Avramova-Cholakova, S. and Vassileva, J. *A survey of the state of mammography practice in Bulgaria*. Radiat. Prot. Dosim. **147**, 184 (2011).
36. Baldelli, P., McCullagh, J., Phelan, N. and Flanagan, F. *Comprehensive dose survey of breast screening in Ireland*. Radiat. Prot. Dosim. **145**, 52–60 (2011).
37. Baldelli, P., McCullagh, J. B., Phelan, N. and Flanagan, F. *Results of Comprehensive Dose Survey for Mammography*. Springer-Verlag Berlin (2010).
38. Bor, D., Akyol, O. and Olgar, T. *Performance measurements of mammographic systems*. Radiat. Prot. Dosim. **129**, 165–169 (2008).
39. Borg, M., Badr, I. and Royle, G. J. *Mammography equipment performance, image quality and mean glandular dose in Malta*. Radiat. Prot. Dosim. **156**, 168–183 (2013).
40. Chevalier, M., Moran, P., Ten, J. I., Soto, J. M. F., Cepeda, T. and Vano, E. *Patient dose in digital mammography*. Med. Phys. **31**, 2471–2479 (2004).
41. Hauge, I. H. R., Bredholt, K. and Olerud, H. M. *New diagnostic reference level for full-field digital mammography units*. Radiat. Prot. Dosim. **157**, 181–192 (2013).
42. Michielsen, K., Jacobs, J., Lemmens, K., Nens, J., Zoetelief, J., Faulkner, K. and Bosmans, H. *Results of a European dose survey for mammography*. Radiat. Prot. Dosim. **129**, 199–203 (2008).
43. Moran, P., Chevalier, M., Ten, J. I., Sot, J. M. F. and Vano, E. *A survey of patient dose and clinical factors in a full-field digital mammography system*. Radiat. Prot. Dosim. **114**, 375–379 (2005).
44. O'Leary, D. and Rainford, L. *A comparison of mean glandular dose diagnostic reference levels within the all-digital Irish National Breast Screening Programme and the Irish Symptomatic Breast Services*. Radiat. Prot. Dosim. **153**, 300–308 (2013).
45. Smans, K. *Towards a proposition of a diagnostic (dose) reference level for mammographic acquisitions in breast screening measurements in Belgium*. Radiat. Prot. Dosim. **117**, 321–326 (2006).
46. Young, K. C., Burch, A. and Oduko, J. M. *Radiation doses received in the UK Breast Screening Programme in 2001 and 2002*. Br. J. Radiol. **78**, 207–218 (2005).
47. Zdesar, U. *Reference levels for image quality in mammography*. Radiat. Prot. Dosim. **129**, 170–172 (2008).
48. Asada, Y., Suzuki, S., Minami, K. and Shirakawa, S. *Results of a 2011 national questionnaire for investigation of mean glandular dose from mammography in Japan*. J. Radiol. Prot. **34**, 125–132 (2014).
49. Bahreyni Toossi, M. T., Zare, H., Bayani Roodi, S., Hashemi, M., Akbari, F. and Malekzadeh, M. *Towards proposition of a diagnostic reference level for mammographic examination in the greater Khorasan Province, Iran*. Radiat. Prot. Dosim. **155**, 96–99 (2013).
50. Hwang, Y. S., Tsai, H. Y., Chen, C. C., Chia, S. H., Lin, J. H., Wan, Y. L., Hsu, G. C., Chen, C. P. and Liu, H. L. *Survey of Radiation Dose, Image Quality and Equipment Performance of Mammography Units in Taiwan*. Springer (2009).
51. Jamal, N., Ng, K. H. and McLean, D. *A study of mean glandular dose during diagnostic mammography in*

Malaysia and some of the factors affecting it. Br. J. Radiol. **76**, 238–245 (2003).
52. Kawaguchi, A., Matsunaga, Y., Otsuka, T. and Suzuki, S. *Patient investigation of average glandular dose and incident air kerma for digital mammography*. Radiol. Phys. Technol. **7**, 102–108 (2014).
53. Geeraert, N., Klausza, R. and Mullera, S. *Breast characteristics and dosimetric data in X-ray mammography A large sample worldwide survey*. IAEA (conference) (2012).
54. Thiele, D. L., Irvine, M., Want, D. and Bernardo, M. *Diagnostic reference levels for mammography in BreastScreen Queensland*. Australas. Phys. Eng. Sci. Med. **34**, 415–418 (2011).
55. Spelic, D., Kaczmarek, R., Hilohi, M. and Belella, S. *United States radiological health activities: inspection results of mammography facilities*. Biomed. Imag. Interv. J. **3**, 1–16 (2007).
56. Ogundare, F. O., Odita, A. N., Obed, R. I. and Balogun, F. A. *Mean glandular doses for women undergoing mammographic breast screening in Oyo state, Nigeria*. Radiography. **15**, 327–332 (2009).
57. Hendrick, R., Bassett, L., Botsco, M., Deibel, D., Feig, S., Gray, J., Haus, A., Heinlein, R., Kitts, E. and McCrohan, J. *Mammography Quality Control Manual*. American College of Radiology (1999).
58. Wu, X., Gingold, E. L., Barnes, G. T. and Tucker, D. M. *Normalized average glandular dose in molybdenum target-rhodium filter and rhodium target-rhodium filter mammography*. Radiology. **193**, 83–89 (1994).
59. Dance, D. R., Skinner, C. L., Young, K. C., Beckett, J. R. and Kotre, C. J. *Additional factors for the estimation of mean glandular breast dose using the UK mammography dosimetry protocol*. Phys. Med. Biol. **45**, 3225–3240 (2000).
60. Law, J., Dance, D., Faulkner, K., Fitzgerald, M., Ramsdale, M., Robinson, A. and Hendee, W. *The commissioning and routine testing of mammographic X-ray systems (IPSM Report 59/2)*. Am. J. Roentgenol. **164**, 842 (1995).
61. EUR 16263. *European Protocol on Dosimetry in Mammography*. CEC (1996).
62. Dance, D. R., Young, K. C. and van Engen, R. E. *Further factors for the estimation of mean glandular dose using the United Kingdom, European and IAEA breast dosimetry protocols*. Phys. Med. Biol. **54**, 4361–4372 (2009).
63. Tsai, H. Y., Chong, N. S., Ho, Y. J. and Tyan, Y. S. *Evaluation of depth dose and glandular dose for digital mammography*. Radiat. Meas. **45**, 726–728 (2010).
64. Dance, D. R., Young, K. C. and van Engen, R. E. *Estimation of mean glandular dose for breast tomosynthesis: factors for use with the UK, European and IAEA breast dosimetry protocols*. Phys. Med. Biol. **56**, 453–471 (2011).
65. Tomon, J. J., Johnson, T. E., Swenson, K. N. and Schauer, D. A. *Applicability of ACR breast dosimetry methodology to a digital mammography system*. Med. Phys. **33**, 799–807 (2006).
66. International Atomic Energy Agency. *Quality Assurance Programme for Digital Mammography*. Human Health Series. No. 17. IAEA (2011).
67. International Atomic Energy Agency. *Quality Assurance Programme for Screen Film Mammography*. Human Health Series. No. 2. IAEA (2009).
68. Moore, A. *The Commissioning and Routine Testing of Mammographic X-ray Systems: A Protocol Produced by a Working Party of the Diagnostic Breast Screening Quality Assurance Coordinating Group for Physics*. Institute of Physics and Engineering in Medicine (2005).
69. Perry, N., Broeders, M., de Wolf, C., Törnberg, S., Holland, R. and von Karsa, L. *Executive summary*. In: European guidelines for quality assurance in breast cancer screening and diagnosis, 4th edn, Supplements. European Commission, Office for Official Publications of the European Union, pp. XIV–XXX (2013).
70. European Reference Organisation for Quality Assured Breast Screening and Diagnostic Services.: *European Guidelines*, 5th edn. (2013) Available on http://www.euref.org/european-guidelines/5th-edition (26 June 2014, date last accessed).
71. Kanal, K. *et al. ACR–AAPM–SIIM practice guideline for determinants of image quality in digital mammography*. J. Digital Imag. **26**, 10–25 (2013).
72. Seradour, B., Heid, P. and Esteve, J. *Comparison of direct digital mammography, computed radiography, and film-screen in the French national breast cancer screening program*. AJR **202**, 229–236 (2014).
73. Chiarelli, A. M., Edwards, S. A., Prummel, M. V., Muradali, D., Majpruz, V., Done, S. J., Brown, P., Shumak, R. S. and Yaffe, M. J. *Digital compared with screen-film mammography: performance measures in concurrent cohorts within an organized breast screening program*. Radiology. **268**, 684–693 (2013).
74. Warren, L. M., Mackenzie, A., Cooke, J., Given-Wilson, R. M., Wallis, M. G., Chakraborty, D. P., Dance, D. R., Bosmans, H. and Young, K. C. *Effect of image quality on calcification detection in digital mammography*. Med. Phys. **39**, 3202–3213 (2012).
75. Ruschin, M. *et al. Dose dependence of mass and microcalcification detection in digital mammography: free response human observer studies*. Med. Phys. **34**, 400–407 (2007).

5 November 2014

Dr Mark McEntee
C43M – M Block
Cumberland Campus
University of Sydney
Lidcombe NSW 2141

Dear Dr McEntee,

NSW Population & Health Services Research Ethics Committee

AU RED Reference: HREC/14/CIPHS/55

Cancer Institute NSW reference number: 2014/08/552

Project Title: Establishing Diagnostic Reference Levels (DRLs) for Digital Mammography in Australia

Thank you for your correspondence dated 28 October 2014 responding to a second request for further information/clarification of the above referenced study, submitted to the NSW Population & Health Services Research Ethics Committee. The Committee has reviewed your response and I am pleased to advise you that full ethical approval has been granted.

The documents reviewed and approved include:

- Submission Checklist
- NSW National Ethics Application Form, v2.2, submission code AU/1/49F9111, signed 26 September 2014
- Protocol, version 4.0 – tracked, dated 27 October 2014
- NSW Health Privacy Form
- Data Custodian Sign Off Form, Picture Archiving and communication System (PACS), dated 18 August 2014
- BreastScreen NSW Screening Consent Form, dated 11, 2013
- Mark McEntee, Curriculum Vitae
- Response to request for further information, dated 26 September 2014
- Response to second request for further information, dated 28 October 2014

Approval is now valid for the following sites:

- Cancer Institute NSW, Sydney
- Calvary Mater Hospital, NSW
- The University of Sydney, Lidcombe

Cancer Institute NSW
ABN 48 538 442 594
Level 9, 8 Central Avenue, Australian Technology Park, Eveleigh NSW 2015
PO Box 41, Alexandria, NSW 1435
t +61 (0)2 8374 5600 **f** +61 (0)2 8374 3600 **e** information@cancerinstitute.org.au
www.cancerinstitute.org.au

The NSW Population & Health Services Research Ethics Committee has been accredited by the NSW Ministry of Health to provide single ethical and scientific review of research proposals conducted within the NSW public health system.

The Committee is a joint initiative of the Cancer Institute NSW and NSW Ministry of Health. The Committee has been constituted and operates in accordance with the National Health and Medical Research Council's *National Statement on Ethical Conduct in Human Research (2007)* and relevant legislation and guidelines.

Please note that ethical approval is valid for **5 years**, conditional on the following:

- Principal investigators will immediately report anything which might warrant a review of ethical approval of the research, including unforeseen events that might affect continued ethical acceptability.
- Proposed amendments to the research proposal or conduct of the research which may affect the ethical acceptability of the research are to be provided to the NSW Population & Health Services Research Ethics Committee for review.
- The NSW Population & Health Services Research Ethics Committee will be notified giving reasons, if the research is discontinued before the expected date of completion.
- The Principal Investigator will provide a progress report to the NSW Population & Health Services Research Ethics Committee annually and at the completion of the study.

Your first progress report will be due on 05/11/2015 and the duration of approval is until 05/11/2019, after which time a new submission to the Ethics Committee will be required.

You are reminded that this letter constitutes *'ethical approval'* only. This research project must not commence at a site until separate authorisation from the Chief Executive or delegate of that site has been obtained. It is your responsibility to forward a copy of this letter together with any approved documents as enumerated above, to all site investigators for submission to the site's Research Governance Officer. Where relevant, copies will also need to be provided to the CHeReL and the data custodian.

For further information about the NSW Population & Health Services Research Ethics Committee, please refer to our website www.cancerinstitute.org.au/research.

Should you have any queries about the ethical review of your research proposal, please contact me on 02 8374 3562 or email ethics@cancerinstitute.org.au.

Yours sincerely,

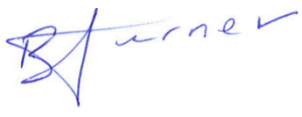

Dr Brie Turner
Ethics and Research Governance Manager
Cancer Institute NSW

Working together to lessen the impact of cancer

22 November 2016

Dr Mark McEntee
C43M – M Block
Cumberland Campus
University of Sydney
Lidcombe NSW 2141

Dear Dr McEntee,

NSW Population & Health Services Research Ethics Committee

AU RED Reference: HREC/14/CIPHS/55

Cancer Institute NSW reference number: 2014/08/552

Project Title: Establishing Diagnostic Reference Levels (DRLs) for Digital Mammography in Australia

Thank you for submitting an annual report for the above study. The NSW Population & Health Services Research Ethics Committee reviewed and noted your annual report at its meeting held on 16 November 2016 and I am pleased to advise that ongoing ethical approval has been granted. **Your next progress report will be due on 05/11/2017.**

The Committee reviewed and approved the following:

- Cancer Institute NSW Annual Report form, dated 28 September 2016

The NSW Population & Health Services Research Ethics Committee has been accredited by the NSW Ministry of Health to provide single ethical and scientific review of research proposals conducted within the NSW public health system.

The Committee is a joint initiative of the Cancer Institute NSW and NSW Ministry of Health. The Committee has been constituted and operates in accordance with the National Health and Medical Research Council's *National Statement on Ethical Conduct in Human Research (2007)* and relevant legislation and guidelines.

For further information about the NSW Population & Health Services Research Ethics Committee, please refer to our website www.cancerinstitute.org.au/research.

Should you have any queries about the ethical review of your research proposal, please contact ethics at ethics@cancerinstitute.org.au.

Yours sincerely,

Prof Sallie-Anne Pearson
Chairperson
NSW Population & Health Services Research Ethics Committee

RADIATION ONCOLOGY—ORIGINAL ARTICLE

Journal of Medical Imaging and Radiation Oncology

Diagnostic reference levels for digital mammography in New South Wales

Moayyad E Suleiman,[1] Mark F McEntee,[1] Lucy Cartwright,[2] Jennifer Diffey[3] and Patrick C Brennan[1]

1 Faculty of Health Sciences, The University of Sydney, Lidcombe, New South Wales, Australia
2 Westmead Hospital, Westmead, New South Wales, Australia
3 Hunter New England Imaging, John Hunter Hospital, New Lambton Heights, New South Wales, Australia

ME Suleiman Msc; **MF McEntee** PhD; **L Cartwright** MMedPhys; **J Diffey** PhD; **PC Brennan** PhD.

Correspondence
Dr Moayyad E Suleiman, Faculty of Health Sciences, The University of Sydney, M205, Cumberland Campus, 75 East St, Lidcombe, NSW 2141, Australia.
Email: msul1801@uni.sydney.edu.au

Conflict of interest: None declared.

Submitted 20 April 2016; accepted 31 August 2016.

doi:10.1111/1754-9485.12540

Abstract

Introduction: This work aims to explore radiation doses delivered in screening mammography in Australia, with a focus on whether compressed breast thickness should be used as a guide when determining patient derived diagnostic reference levels (DRLs).
Methods: Anonymized mammograms (52,405) were retrieved from a central database, and DICOM headers were extracted using third party software. Women with breast implants, breast thicknesses outside 20–110 mm and images with incomplete exposure or quality assurance (QA) data were excluded. Exposure and QA information were utilized to calculate the mean glandular dose (MGD) for 45,054 mammograms from 61 units representing four manufacturers using previously well-established methods. The 75th and 95th percentiles were calculated across median image MGDs obtained for all included data and according to specific compressed breast thickness ranges.
Results: The overall median image MGD, minimum, maximum were: 1.39, 0.19 and 10.00 mGy, respectively, the 75th and 95th percentiles across all units' median image MGD for 60 $\pm$ 5 mm compressed breast thickness were 2.06 and 2.69 mGy respectively. Median MGDs, minimum, maximum, 75th and 95th percentiles were presented for nine compressed breast thickness ranges, DRLs for NSW are suggested for the compressed breast thickness range of 60 $\pm$ 5 mm for the whole study and three detector technologies CR, DR, and photon counting to be 2.06, 2.22, 2.04 and 0.79 mGy respectively.
Conclusion: MGD is dependent upon compressed breast thickness and it is recommended that DRL values should be specific to compressed breast thickness and image detector technology.

Key words: breast; dosimetry; mean glandular dose; optimization; screening.

Introduction

Mammography is an important tool for the early detection of breast cancer as early detection has been demonstrated to reduce mortality by up to 30%.[1] Aiming to reduce breast cancer deaths, the Australian breast-screening programme has targeted 50–69 year old Australian women since 1991 for biennial screening mammograms, recently increasing this upper age limit to 74.[2] Exposing healthy women to ionizing radiation, however, is associated with a risk of inducing breast cancer, therefore the dose to the breast must be kept as low as reasonably achievable.[3] Diagnostic Reference Levels (DRLs) provide a measure of quality control and optimization of protection to help limit variations in dose delivered among and within imaging centres and these levels are expected not to be exceeded for a standard diagnostic procedure when good and normal practice is applied.[3] A DRL was defined in the International Commission of Radiation Protection (ICRP) publication 73 in 1996 as:

'A form of investigation level, applied to an easily measured quantity, usually the absorbed dose in air, or tissue-equivalent material at the surface of a simple phantom or a representative patient.'[3]

DRL establishment requires the use of readily available or easily calculated dose metrics. Measurements of radiation dose to the breast have been performed using

different approaches including total energy transmitted to the breast,[4] mid-breast dose,[5] air kerma,[6] entrance surface dose[7] and mean dose absorbed by the glandular tissue (MGD).[8] Due to the radiosensitivity of the glandular tissue of the breast, MGD is now considered to be the most relevant quantity,[8] is widely used and is recommended by the ICRP,[9] the United States National Council on Radiation Protection and Measurements,[10] the British Institute of Physics and Engineering in Medicine (IPEM),[11] the European Council Protocol (EP)[12–14] and the International Atomic Energy Agency (IAEA).[15] Most studies implementing DRLs have therefore focussed on MGD values.

To establish a DRL, appropriate groupings of standard-sized patients should be used. For adult DRLs in radiography, fluoroscopy and CT a weight range for a group of patients of 70 ± 10 kg is used. In paediatric examinations, patients are categorized by weight or age range. In mammography, researchers have used a 'standard' compressed breast thickness that varies from 35 to 65 cm depending on the DRL.[16] Choosing a single thickness to represent an entire population, although a simple approach, is arguably inappropriate as the population is not homogenous and the breast can vary in thickness from 1 cm to 10 cm. Furthermore, it is well known that dose differs for different breast thicknesses. A more complex, but representative approach might be to establish DRLs for groups of standard-sized breasts.

While DRLs have been established for mammography in many countries around the world;[17–22] the Australian breast screening programmes are into their third decade; to date, no patient-based DRLs are available, nonetheless, phantom-based DRLs were established in 2011 for Queensland hospitals.[23] However, Phantom-based DRLs may not reflect the clinical environment; hence, this study aims to propose patient-based DRLs for screening mammography in New South Wales, and to explore whether compressed breast thickness should be taken into account when determining DRLs.

Methods

This study was performed retrospectively using a patient data sample from 50 BreastScreen NSW centres and mobile units, ethical approval was granted by the Cancer Institute Human Research Ethics Committee (No.2014/08/552). In total, data were obtained from 63 mammography units. Radiation dose and supplementary data were assembled from 12,034 patient cases (52,405 mammograms).

Data relating to the patient and required for dose calculations were extracted from the Digital Imaging and Communication in Medicine (DICOM) headers (Table 1) and exported to a CSV format file using third party software (YAKAMI DICOM Tools ver. 1.4.1.0, Kyoto University, Japan).

Table 1. Information extracted from the DICOM headers of digital images

Information	DICOM tag
Patient age	0019,1052
Body part thickness	0018,11A0
Implant present	0028,1300
Patient orientation	0020,0020
Image laterality	0020,0062
Tube voltage (kVp)	0018,0060
Exposure (mAs)	0018,1152
Anode target material	0018,1191
Filter material	0018,7050
Exposure control mode	0018,7060
Detector ID	0018,700A
Manufacturer's model name	0008,1090
Manufacturer	0008,0070

Dose calculation also required data from the annual medical physics quality assurance (QA) reports for each centre; these data included tube output and HVL for all kVps and anode/filter combinations available for each mammography unit.

Based on the information gathered, exclusion criteria were applied thus removing from the study mammograms involving breast implants (1337 images), and incomplete or unavailable QA data (1662 images), as well as images with compressed breast thickness not within 20–110 mm (82 images). Data were then imported into an excel sheet with macros developed in-house that calculates MGD for each acquired image using the methods described by Dance *et al.*[24–26]

For each image, MGDs were calculated using the following equation:

$$\mathrm{MGD} = K_{gcs}$$

where K is the incident air kerma (IAK) at the upper surface of the breast without backscatter, calculated from mAs, kVp and the tube output corrected using the inverse square law. The g factor is the IAK to MGD conversion factor for breasts with 50% glandularity and an anode/filter combination of Mo/Mo. The c factor corrects for any difference in breast glandularity from 50% for different thickness breasts and is available for two ranges of age, 40–49 and 50–64, women aged over 64 were included in the 50–64 range table, we have moderately assumed here that the breast density of women over the age of 64 will behave in a similar way that the density of women aged 50–64; this is an estimation that will be investigated in future studies. The s factor corrects for any difference in the types of anode/filter combination used other than Mo/Mo.[24–26]

Note: Both *g* and *c* factors are tabulated as functions of breast thickness and half-value layer (HVL) of the x-ray beam. The HVL for each system was obtained from concurrent QA data.

Table 2. Manufacturer, model, technology, Anode/ filter combinations and number of mammography units included in the dose audit from BreastScreen centres in NSW/Australia

Manufacturer	Model	Technology	Anode/Filter	Unit number
General Electric (GE)	Senographe Essential ADS_54.11	DR	Mo/Mo, Mo/Rh, Rh/Rh	1–14
	Senographe Essential ADS_54.10	DR	Mo/Mo, Rh/Rh	15
	Senographe Essential ADS_53.40	DR	Mo/Mo, Mo/Rh, Rh/Rh	16
	Senographe DS ADS_54.11	DR	Mo/Mo, Mo/Rh, Rh/Rh	17, 18
	Senographe DS ADS_53.40	DR	Mo/Mo, Rh/Rh	19
	Senographe 2000D ADS_17.4.5	DR	Mo/Mo, Mo/Rh, Rh/Rh	20
Hologic	Selenia Dimensions	DR	W/Ag, W/Rh	21–41
Philips (Sectra)	L30	DR	W/AL	42–52
Fuji Film	Amulet	DR	W/Rh	53
		CR	Mo/Mo, Mo/Rh	54–61

DR, digital radiography; CR, computed radiography; Mo, molybdenum; Rh, rhodium; W, tungsten; Ag, silver; Al, aluminium.

For each woman and mammographic unit, the MGD median was found per image and examination, the median examination MGD was found by summing image MGDs for each examination and dividing the result by two; this is to average for one breast.

To determine DRLs, the 75th and 95th percentiles were calculated across the median image MGDs per mammography unit. Then values for each mammography unit were categorized according to their compressed breast thickness to ranges of 10 mm thicknesses and median image MGDs per mammography unit were calculated for each thickness range, an ANOVA with a Tukey post hoc test was used to analyse the significance of the differences between the median image MGDs for each thickness range. The 75th and 95th percentiles were determined for each thickness range.

Results

Summary of data

The final data set included 11,029 women with a mean age of 60 years and a total of 45,054 images (DR: 40,033 images and CR: 5,021 images). Forty-eight BreastScreen centres (Sixty-one digital mammography units) were involved, (two centres were disqualified due to missing QA data) consisting of 53 DR and 8 CR units as shown in Table 2; it is worth highlighting here that Rhodium (Rh) anodes were unavailable or disabled in the CR units included for this study during the period in question. Image sets included in the analysis comprised of the standard 4 view examinations (MLO and CC for left and right breasts) and extra projections, the latter representing <6% of all examinations.

The histogram of compressed breast thicknesses for the study showed a normal distribution with a mean of 58 mm (Fig. 1), while image MGDs showed a skewed distribution that ranged from 0.19 mGy to 10.00 mGy with a mean and a median of 1.51 mGy and 1.39 mGy respectively (Fig. 2). An overall summary of the background data for each unit is shown in Table 3.

Radiation doses and percentile values

Median image MGD across all patients for each MLO and CC image were 1.43 and 1.36 mGy, respectively, with individual doses per image ranging from 0.32 to 10.00 mGy for the MLO and 0.19 to 7.45 mGy for the CC. Also, the lowest and highest median image MGD per mammography unit, respectively, were 0.67 and 2.43 mGy for MLO, 0.66 and 2.24 mGy for CC.

Median MGD per examination for all women was 2.84 mGy with the smallest and highest dose being delivered being 0.68 and 21.9 mGy respectively. Furthermore, the lowest and highest median examination MGD per mammography unit were 1.40 and 4.42 mGy in units 51 and 54 respectively.

Median MGD per image, view (MLO, CC) and examination as well as mean patient age, compressed breast thickness, kVp, mAs for each mammography unit are displayed in Table 3. The 75th and 95th percentiles across all units' median image MGD for 60 $\pm$ 5 mm compressed breast thicknesses were 2.06 and 2.69 mGy respectively (Fig. 3). Percentile values and proposed DRLs are also presented for each of the nine compressed breast thickness ranges and for the three different detector technologies (Table 4), Tukey's post hoc test showed statistically significant differences between median image MGDs for each 10 mm compressed breast thickness range examined ($p < 0.05$).

Discussion

DRLs have been shown to be an effective method for dose optimization of protection in medical exposure of patients for diagnostics and interventional procedures. DRLs work by minimizing the wide variations in dose demonstrated across centres for the same examination for groups of standard-sized patients.[27] Centres delivering the highest doses are identified using the percentile method. A 75th percentile which is often used for general X-ray examinations, identifies the 25% of centres that are giving higher doses and encourages them to optimize

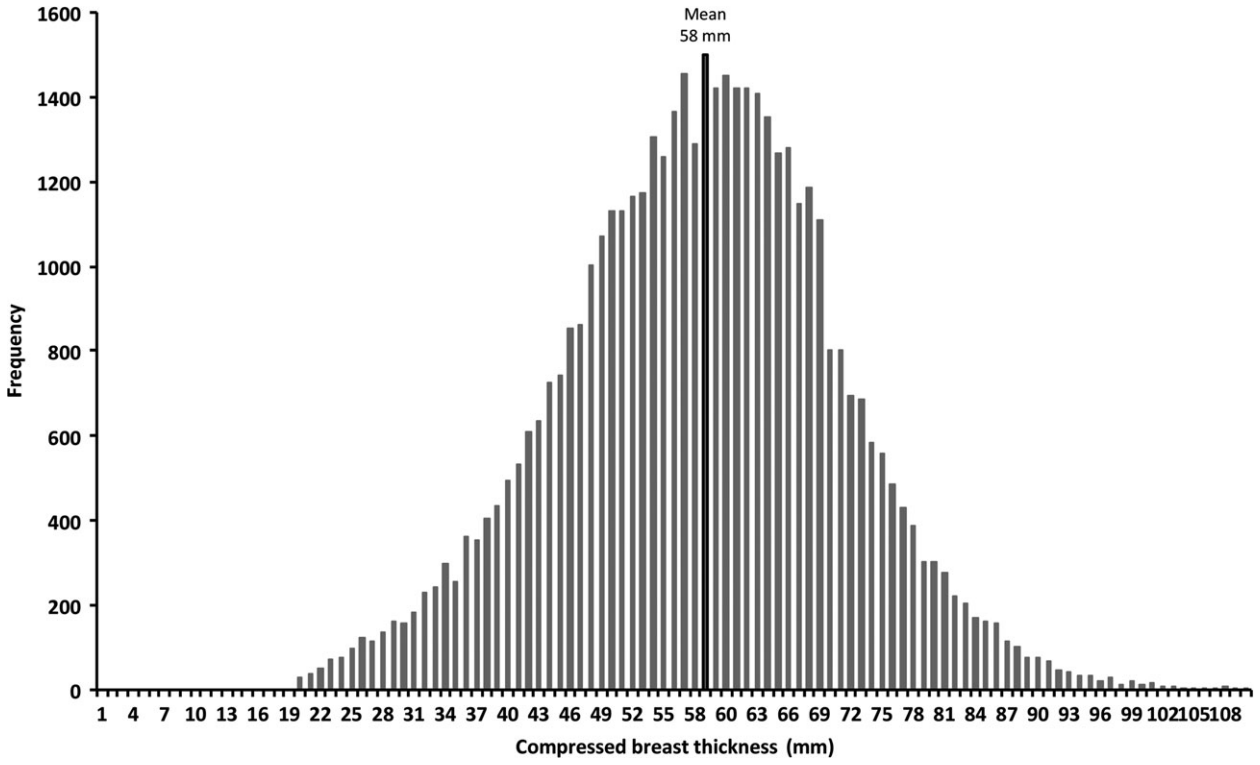

Fig. 1. Distribution of compressed breast thickness for 45,054 mammography images.

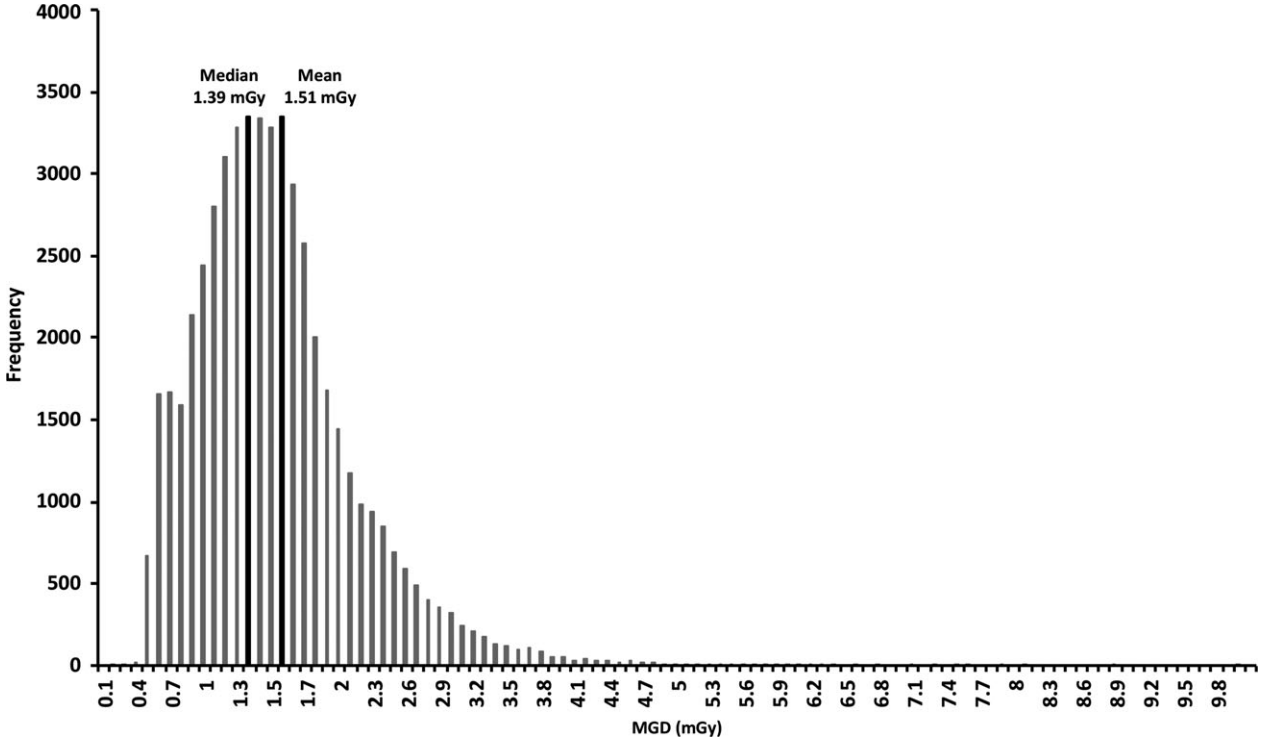

Fig 2. Distribution of image mean glandular dose (MGD) for 45,054 mammography images.

Table 3. Number of images/examinations per mammography unit, exposure parameters means, median entrance surface air kerma and median mean glandular dose per view, image and case, for 45,054 mammograms across 61 mammography units

Unit	No. of images	No. of cases	Mean age (SD)	Mean thickness (SD)	Mean kVp (SD)	Mean mAs (SD)	Median ESAK (IQR)	Mean image MGD/View						Median Image MGD (IQR)	Median Examination MGD (IQR)
								CC			MLO				
								R	L	All	R	L	All		
1	812	200	61.81 (7.88)	53.79 (12.10)	28.66 (1.27)	55.68 (13.54)	5.69 (2.53)	1.31	1.35	1.33	1.57	1.59	1.58	1.46 (0.45)	**2.98 (1.30)**
2	721	175	56.36 (7.67)	60.12 (12.62)	28.96 (0.83)	67.56 (16.74)	6.03 (2.32)	1.37	1.38	1.37	1.41	1.44	1.43	1.40 (0.34)	**2.85 (1.33)**
3	744	192	58.87 (7.17)	62.63 (10.89)	29.09 (0.71)	65.33 (14.64)	6.97 (2.56)	1.44	1.48	1.46	1.54	1.55	1.54	1.51 (0.39)	**2.98 (1.69)**
4	775	200	60.11 (7.72)	60.67 (10.26)	29.01 (0.64)	59.26 (14.56)	6.09 (2.18)	1.37	1.39	1.38	1.40	1.40	1.40	1.39 (0.35)	**2.77 (1.42)**
5	960	219	59.44 (7.82)	59.09 (12.67)	28.64 (0.96)	57.07 (12.87)	5.87 (2.39)	1.29	1.27	1.29	1.33	1.36	1.34	1.32 (0.35)	**2.75 (1.81)**
6	680	172	60.20 (8.04)	63.07 (11.11)	29.00 (0.66)	59.43 (15.91)	6.22 (2.23)	1.29	1.31	1.30	1.45	1.41	1.44	1.36 (0.35)	**2.74 (1.61)**
7	770	203	60.06 (7.50)	61.52 (11.86)	28.96 (0.78)	57.65 (12.48)	5.41 (2.09)	1.17	1.19	1.18	1.22	1.24	1.23	1.21 (0.32)	**2.43 (1.25)**
8	926	233	59.60 (6.53)	65.65 (11.10)	29.21 (0.69)	63.10 (15.16)	6.56 (2.18)	1.37	1.34	1.36	1.46	1.43	1.45	1.39 (0.37)	**2.83 (1.41)**
9	844	208	58.20 (6.85)	60.59 (15.52)	29.31 (1.10)	61.68 (22.66)	6.30 (2.63)	1.30	1.34	1.32	1.49	1.57	1.53	1.43 (0.35)	**2.91 (1.19)**
10	828	184	59.81 (6.70)	65.83 (10.93)	29.15 (0.56)	69.83 (19.05)	7.21 (2.62)	1.44	1.46	1.45	1.56	1.59	1.57	1.50 (0.38)	**3.25 (2.73)**
11	826	187	58.90 (6.79)	60.45 (11.74)	28.85 (0.82)	65.20 (13.77)	6.37 (2.49)	1.43	1.43	1.43	1.48	1.48	1.48	1.46 (0.32)	**3.05 (1.77)**
12	881	202	59.65 (8.13)	61.68 (13.43)	28.88 (0.91)	65.20 (13.57)	7.05 (2.99)	1.48	1.52	1.50	1.56	1.57	1.57	1.54 (0.37)	**3.21 (1.94)**
13	651	174	60.07 (7.69)	58.43 (12.05)	29.58 (0.73)	73.91 (19.50)	7.17 (2.44)	1.64	1.66	1.65	1.80	1.76	1.77	1.71 (0.35)	**3.44 (1.60)**
14	848	194	58.51 (7.34)	61.73 (13.21)	28.96 (0.88)	60.22 (13.57)	6.11 (2.36)	1.33	1.35	1.34	1.37	1.41	1.39	1.37 (0.33)	**2.80 (1.56)**
15	746	192	59.84 (8.26)	63.90 (11.67)	29.17 (0.84)	61.15 (14.06)	6.28 (2.39)	1.37	1.35	1.36	1.46	1.45	1.45	1.39 (0.38)	**2.81 (1.75)**
16	1057	242	59.55 (8.07)	58.61 (13.73)	28.76 (0.94)	55.75 (11.64)	5.70 (2.57)	1.32	1.32	1.32	1.31	1.37	1.34	1.33 (0.33)	**2.78 (1.60)**
17	915	195	62.15 (7.38)	57.89 (13.50)	28.86 (0.98)	46.44 (12.51)	4.84 (2.15)	1.08	1.07	1.08	1.12	1.14	1.14	1.10 (0.35)	**2.35 (1.66)**
18	574	137	59.65 (6.58)	59.13 (11.14)	29.11 (0.71)	50.77 (11.90)	5.17 (1.79)	1.24	1.20	1.21	1.27	1.28	1.27	1.25 (0.28)	**2.56 (1.82)**
19	721	166	61.02 (7.30)	61.80 (11.39)	29.02 (0.74)	58.86 (13.09)	6.02 (2.24)	1.29	1.30	1.30	1.36	1.34	1.34	1.33 (0.31)	**2.74 (1.89)**
20	589	116	62.67 (6.83)	56.83 (12.57)	28.87 (1.45)	67.75 (18.39)	6.76 (2.58)	1.51	1.47	1.50	1.62	1.62	1.62	1.56 (0.46)	**3.59 (2.92)**
21	787	188	60.07 (7.96)	59.37 (12.83)	29.96 (1.65)	139.43 (38.92)	7.09 (4.10)	1.90	1.83	1.85	2.16	2.13	2.14	2.00 (0.88)	**4.13 (3.29)**
22	734	178	58.26 (9.12)	65.00 (12.20)	28.54 (1.16)	199.27 (71.79)	7.63 (4.73)	1.72	1.71	1.72	2.22	2.08	2.14	1.94 (0.92)	**3.95 (3.75)**
23	587	167	63.81 (8.32)	54.73 (9.96)	29.68 (1.68)	137.04 (36.57)	6.04 (3.67)	1.70	1.71	1.70	1.83	1.85	1.84	1.75 (0.88)	**3.12 (3.24)**
24	636	181	59.45 (9.07)	54.83 (9.61)	29.71 (1.62)	133.45 (38.44)	6.04 (3.70)	1.73	1.77	1.76	1.83	1.92	1.84	1.80 (0.90)	**3.22 (3.56)**
25	812	192	60.27 (8.28)	59.25 (13.36)	29.91 (1.71)	171.09 (53.05)	6.81 (3.59)	1.97	1.97	1.97	1.98	1.89	1.94	1.95 (0.83)	**3.98 (3.68)**
26	845	202	59.61 (7.24)	54.46 (14.49)	29.36 (1.95)	175.42 (85.60)	5.41 (5.30)	1.80	1.77	1.78	1.63	1.70	1.68	1.72 (1.28)	**3.57 (5.40)**
27	575	163	60.52 (8.23)	54.03 (9.59)	29.57 (1.64)	131.55 (37.04)	5.74 (3.50)	1.82	1.72	1.76	1.71	1.80	1.73	1.75 (0.88)	**3.17 (2.90)**
28	815	189	58.60 (7.18)	55.00 (13.05)	29.42 (1.75)	159.72 (52.66)	6.29 (4.38)	1.81	1.76	1.80	1.91	1.92	1.91	1.86 (1.09)	**3.98 (4.58)**
29	909	206	58.60 (7.18)	60.22 (13.75)	30.02 (1.75)	156.72 (49.99)	7.03 (4.09)	1.86	1.93	1.89	2.13	2.02	2.08	1.98 (0.90)	**4.27 (3.97)**
30	578	170	60.43 (8.76)	55.39 (10.04)	29.85 (1.73)	115.45 (34.23)	5.95 (3.45)	1.65	1.68	1.66	1.79	1.85	1.84	1.71 (0.82)	**3.05 (3.11)**
31	344	99	60.48 (9.28)	55.75 (9.73)	29.92 (1.61)	126.10 (40.56)	6.03 (3.42)	1.72	1.75	1.73	1.83	1.79	1.82	1.76 (0.85)	**3.12 (3.56)**
32	530	157	61.57 (9.28)	56.87 (8.83)	30.06 (1.55)	123.59 (35.75)	6.18 (3.36)	1.72	1.73	1.72	1.86	1.84	1.84	1.76 (0.82)	**3.00 (3.76)**
33	536	156	60.26 (10.43)	55.57 (10.37)	29.87 (1.73)	121.67 (35.45)	5.75 (3.73)	1.67	1.71	1.70	1.68	1.68	1.68	1.69 (0.91)	**2.88 (3.37)**
34	509	143	59.56 (8.05)	56.02 (9.28)	29.91 (1.60)	129.63 (41.12)	5.85 (3.90)	1.72	1.75	1.74	1.72	1.66	1.69	1.72 (0.94)	**3.10 (3.77)**
35	577	162	61.65 (7.96)	53.37 (10.84)	29.49 (1.78)	116.21 (34.92)	6.25 (4.37)	1.81	1.84	1.84	1.85	1.72	1.77	1.81 (0.97)	**3.26 (3.25)**
36	844	203	59.89 (7.67)	51.65 (11.94)	29.07 (1.71)	138.38 (42.00)	5.20 (3.57)	1.70	1.72	1.71	1.69	1.46	1.63	1.67 (0.87)	**3.37 (3.47)**
37	846	205	60.63 (8.09)	55.13 (13.92)	29.46 (1.86)	137.89 (45.41)	5.82 (4.25)	1.68	1.70	1.69	1.67	1.74	1.71	1.70 (0.99)	**3.56 (3.97)**
38	830	185	58.77 (6.63)	57.20 (14.10)	29.68 (1.85)	151.77 (52.47)	6.22 (4.18)	1.76	1.79	1.77	1.85	1.90	1.87	1.83 (0.96)	**4.09 (4.57)**
39	310	98	63.05 (7.39)	56.18 (9.12)	29.95 (1.60)	108.82 (28.41)	5.49 (3.32)	1.54	1.58	1.55	1.59	1.54	1.55	1.55 (0.81)	**2.44 (2.80)**

Table 3. (continued)

Unit	No. of images	No. of cases	Mean age (SD)	Mean thickness (SD)	Mean kVp (SD)	Mean mAs (SD)	Median ESAK (IQR)	Mean image MGD/View						Median Image MGD (IQR)	Median Examination MGD (IQR)
								CC			MLO				
								R	L	All	R	L	All		
40	634	195	61.08 (9.18)	56.94 (9.53)	30.10 (1.66)	128.68 (40.11)	7.13 (5.35)	2.00	1.97	1.98	1.98	2.06	2.01	2.00 (1.29)	**3.14 (4.03)**
41	826	201	60.54 (8.10)	56.77 (13.50)	29.70 (1.81)	137.95 (39.37)	6.55 (4.07)	1.81	1.78	1.80	2.01	2.05	2.03	1.91 (0.93)	**3.93 (3.42)**
42	876	188	59.23 (7.52)	59.02 (13.11)	33.31 (2.04)	14.52 (3.41)	3.18 (1.85)	0.69	0.71	0.70	0.81	0.84	0.82	0.77 (0.34)	**1.72 (1.61)**
43	1320	299	58.78 (7.23)	62.89 (14.36)	34.03 (2.18)	14.47 (3.27)	3.22 (1.89)	0.73	0.72	0.73	0.81	0.81	0.81	0.77 (0.33)	**1.65 (1.37)**
44	346	79	58.10 (6.91)	59.65 (13.36)	34.02 (2.17)	14.37 (2.96)	2.86 (1.51)	0.69	0.67	0.68	0.76	0.78	0.78	0.73 (0.27)	**1.53 (1.31)**
45	949	203	60.49 (7.98)	58.97 (12.67)	33.68 (2.33)	14.61 (2.96)	2.93 (1.66)	0.71	0.69	0.69	0.75	0.75	0.75	0.72 (0.29)	**1.55 (1.47)**
46	559	132	59.89 (7.65)	59.29 (13.34)	33.07 (1.73)	14.41 (3.52)	2.96 (1.87)	0.70	0.69	0.70	0.70	0.73	0.72	0.71 (0.32)	**1.45 (1.16)**
47	774	180	62.02 (6.21)	62.97 (13.48)	33.20 (1.73)	14.42 (3.23)	3.26 (1.72)	0.66	0.65	0.66	0.79	0.81	0.80	0.74 (0.27)	**1.50 (1.21)**
48	825	198	60.46 (9.50)	63.16 (12.53)	34.89 (2.33)	15.38 (3.36)	3.43 (1.89)	0.82	0.79	0.81	0.96	0.94	0.95	0.87 (0.39)	**1.83 (1.38)**
49	952	240	60.34 (9.47)	62.40 (13.34)	34.85 (2.41)	15.36 (3.08)	3.99 (3.78)	0.92	0.94	0.93	1.02	1.03	1.03	0.97 (0.84)	**2.07 (2.85)**
50	921	197	59.38 (7.42)	60.89 (13.26)	33.57 (1.95)	15.18 (3.42)	3.61 (1.95)	0.84	0.84	0.84	0.88	0.86	0.88	0.86 (0.34)	**1.82 (2.01)**
51	556	136	61.69 (7.08)	55.45 (13.88)	33.42 (2.23)	13.88 (2.92)	2.69 (1.45)	0.68	0.69	0.69	0.71	0.70	0.71	0.70 (0.25)	**1.40 (0.96)**
52	786	186	58.94 (7.75)	55.32 (13.99)	33.07 (2.15)	14.76 (3.48)	2.61 (1.84)	0.70	0.70	0.70	0.65	0.69	0.67	0.69 (0.32)	**1.41 (1.38)**
53	1237	280	58.42 (8.09)	55.64 (13.47)	29.20 (1.46)	77.24 (29.96)	2.84 (1.94)	0.83	0.82	0.82	0.96	0.99	0.96	0.89 (0.45)	**1.92 (2.21)**
54	723	192	61.54 (6.58)	48.92 (10.39)	27.28 (0.82)	110.62 (45.98)	9.70 (5.27)	2.15	2.07	2.09	2.42	2.46	2.43	2.26 (1.01)	**4.41 (5.62)**
55	638	162	63.74 (7.68)	56.63 (11.96)	27.09 (0.29)	86.00 (55.34)	5.82 (5.30)	1.16	1.22	1.18	1.43	1.40	1.40	1.26 (0.88)	**2.53 (3.26)**
56	527	145	61.93 (8.69)	55.66 (12.06)	27.32 (0.66)	88.34 (47.40)	8.06 (6.15)	1.62	1.66	1.64	1.84	1.85	1.85	1.72 (0.94)	**3.20 (4.18)**
57	863	204	61.72 (7.68)	51.45 (12.31)	28.24 (0.65)	80.92 (43.81)	9.43 (6.56)	1.81	1.84	1.82	1.96	2.13	2.05	1.91 (0.98)	**3.95 (4.13)**
58	590	145	62.01 (6.79)	48.38 (11.92)	27.94 (0.76)	88.96 (43.58)	9.08 (7.46)	1.85	1.80	1.84	1.96	2.00	1.98	1.90 (1.17)	**3.85 (4.86)**
59	731	192	56.70 (7.58)	45.63 (11.63)	27.41 (0.83)	80.11 (36.53)	7.56 (4.07)	1.77	1.80	1.79	1.77	1.70	1.74	1.77 (0.74)	**3.37 (3.18)**
60	169	44	61.51 (6.83)	46.75 (10.79)	27.91 (0.65)	79.60 (39.38)	9.95 (7.22)	2.08	2.28	2.24	1.91	1.98	1.97	2.09 (1.23)	**4.21 (5.30)**
61	780	197	60.05 (6.92)	46.82 (11.93)	28.22 (1.01)	79.14 (37.04)	8.88 (5.71)	1.96	1.89	1.94	1.98	2.06	2.02	1.97 (0.90)	**3.51 (4.38)**
Overall	**45054**	**11030**	**60.03 (7.88)**	**58.01 (13.19)**	**30.00 (2.49)**	**80.97 (58.77)**	**5.62 (3.75)**	**1.36**	**1.37**	**1.36**	**1.43**	**1.43**	**1.43**	**1.39 (0.78)**	**2.84 (3.29)**

SD, standard deviation; Thickness: compressed breast thickness; kVp: X-ray tube potential; mAs: X-ray tube current time product; IQR, interquartile range; MGD, mean glandular dose; ESAK, entrance surface air kerma; CC: Craniocaudal view; MLO, mediolateral oblique view; R, right breast; L, left breast.

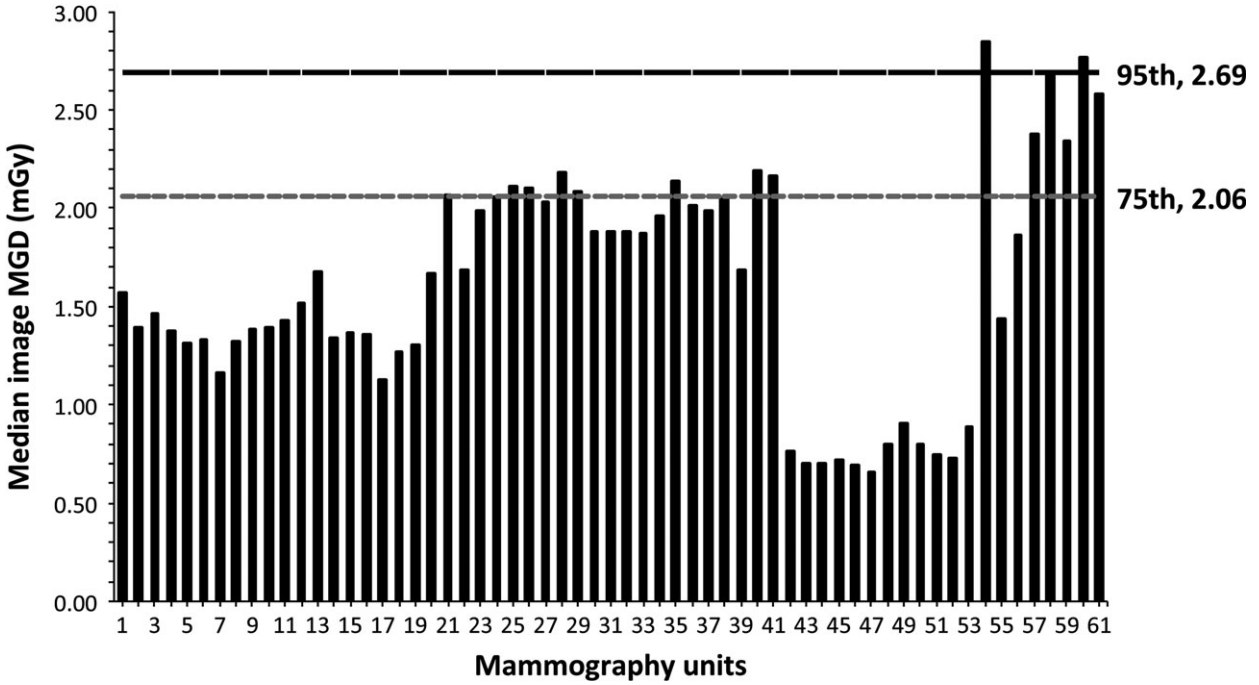

Fig. 3. A histogram plot of the median image MGD for a compressed breast thickness of 60 ± 5 mm is indicated for each mammography unit, the 75th and 95th percentile values are indicated by the horizontal lines.

Table 4. 75th and 95th percentiles for different compressed breast thickness ranges and three different detector technologies, representing 45,054 mammograms from 61 BreastScreen units (Proposed DRLs for 60 ± 5 mm breast thickness are in **bold**).

Breast thickness range	All Units		CR		DR		Photon counting	
	75th % (mGy)	95th % (mGy)	75th % (mGy)	95th % (mGy)	75th % (mGy)	95th % (mGy)	75th % (mGy)	95th % (mGy)
20–29	0.97	1.19	1.17	1.26	0.97	1.11	0.58	0.63
30–39	1.13	1.50	1.50	1.52	1.12	1.22	0.60	0.65
40–49	1.31	1.86	1.92	2.08	1.30	1.41	0.58	0.65
50–59	1.67	2.38	2.48	2.58	1.65	1.80	0.65	0.69
60–69	2.37	3.00	3.08	3.21	2.35	2.57	0.88	0.99
70–79	2.23	4.38	4.41	4.46	2.08	2.67	1.08	1.56
80–89	2.48	6.24	6.39	6.74	2.34	3.07	1.12	1.52
90–99	2.89	7.75	7.84	7.85	2.63	3.48	0.99	1.39
100–110	3.24	5.97	6.26	6.26	3.31	5.38	0.91	0.92
DRLs 60 ± 5	**2.06**		**2.22**		**2.04**		**0.79**	

CR, computed radiography; DR, digital radiography.

exposures, thus making DRLs a dynamic and changing value. Often in mammography, however, a 95th percentile is used due to rigorous quality assurance procedures and tight dose variations.[28] However, in the current work, the long tail exhibited in Figure 2 would suggest that at this time a 75th percentile maybe more prudent across the state from which our measurements are obtained.

Examination of the data in Table 3 demonstrates minimal differences in dose between left and right breasts and between the CC and MLO projections compared with the inter-centre differences, hence and in alignment with previous authors, the *median image MGD* will be used throughout this discussion.[17,29,30] Examination of the median image MGD, demonstrated that the lowest values belong to the Philips L30 (Sectra) units (units 51 and 52), with all of the Philips units reporting median MGDs below the 20th percentile. The low dose associated with these units is in line with other studies in the literature,[19,31] and is likely linked to the effective utilization of

tightly collimated scanning slot beam of X-rays and a detector technology that employs photon counting with energy discrimination, so scattered photons are rejected from the image. This means that a grid is not required and consequently, doses are lower. The highest median image MGD and case MGD were delivered in CR units (Fujifilm Corporation) in a mobile setting with five of the eight CR units reporting an overall median image MGD that was over the 75th percentile for all compressed breast thickness ranges. It is interesting to note that all Hologic units reported median image MGDs higher than the 50th percentile while 11 out of the 20 GE units reported median image MGDs less than or equal to the 50th percentile. These data emphasize the impact of technology on reported dose variations. It should be stressed, however, that drawing conclusions regarding technology, based on dose values alone without a full consideration of diagnostic efficacy must be treated with caution.

While it is important to acknowledge the variations shown in Figure 3 and to focus on existing units/centres that are responsible for the higher doses, it is important to put these inter-unit or inter-centre dose variations into context. The variations in dose values represented in the long tailed distribution in Figure 2 are similar to the distribution reported in an earlier large UK study.[32] In addition, the level of difference between the highest and the lowest dose units/centres reported here are not dissimilar from that expressed in other countries with other work demonstrating marginally less,[20,28,33] comparable[18,19] or higher variations.[34] It should be acknowledged that the higher doses in this study as discussed above, mainly relate to CR units, which at the time of writing have generally now been replaced and the next round of DRL surveys should reflect this. Overall, when taking into consideration the reported compressed breast thicknesses by other international studies, it was found that our reported dose medians and percentiles were less than most of patient studies reviewed by Suleiman *et al.* in 2014.[16]

The median MGD and 75th percentile for compressed breast thicknesses of 60 ± 5 mm were 1.62 and 2.06 mGy respectively (Mean compressed breast thickness for the study is 58 mm), while, for comparison reasons, the median MGD and 75th percentile for compressed breast thicknesses of 50 ± 5 mm were 1.35 and 1.50 mGy respectively. These values are lower than the 1.88 and 2.1 mGy reported in a Spanish study in 2005, which used similar methods to estimate the dose, albeit with a lower overall mean compressed breast thickness of 52 mm.[35] The higher doses reported in the Spanish work are most likely due to possibly different technology and the study's focus on diagnostic mammography (symptomatic women). With regard to this last point, O'Leary *et al.* suggested that the higher mean dose received by symptomatic women could be explained by the inclusion of younger women with denser breasts and the less strict mammographic educational requirements for radiographers compared with those involved in the breast screening services.[28] More recent studies in Ireland and Malta reporting a closer overall mean compressed breast thicknesses (57.5 and 54.7 mm respectively) to our findings indicated lower mean MGDs (1.07 and 1.33 mGy respectively) and 75th percentiles (1.11 and 1.5 mGy respectively) than those reported here.[28,36] While differences in technology and subtle differences in compressed breast thickness may contribute to the higher doses reported here, the results suggest some potential for optimization of the units or practices included in this study.

It is important to revisit the interpretation of DRL definitions, particularly since these have been available and employed for 20 years. In particular, the term 'representative patient' has often been translated in mammography to mean average compressed breast thickness of the study sample. However, some authors have calculated DRLs for groups of standard compressed breast thickness in order to facilitate national and international comparisons.[28] Differences in compressed breast thicknesses are clearly responsible for at least some of the statistically significant MGD variations displayed in our work. If we use a standard-sized group of patients with compressed breast thickness 60 ± 5 mm to represent the overall population, the 75th percentile at this value is more than double and almost half that of the lowest and highest compressed breast thickness categories respectively. These results alongside the compressed breast thickness-dependent dose variations demonstrated elsewhere highlight the importance of clearly identifying standard-sized groups of compressed breast thicknesses when specifying DRLs.[16] Although to date, this is not often seen, such stratification would extend the translation of a '*representative patient*' from average compressed breast thickness to ranges of compressed breast thicknesses that are more representative of the population of women. In addition, such a compressed breast thickness specific approach if used universally would facilitate useful and accurate national and international comparisons.

Finally, it is important to acknowledge that this paper is limited to radiation dose values. It should be stressed that similar to almost all previous DRL work, comparing dose data does not factor in image quality variations, therefore the potential for highest dose locations offering best diagnostic efficacy cannot be out-ruled. Equally, however, currently there is no evidence here or elsewhere that those centres or units with the lowest dose are offering less accurate diagnoses than elsewhere. This is an area of research that requires much more attention.

In conclusion, patient-based DRL values for different compressed breast thickness ranges and different image detector technology have been proposed for the first time in Australia, providing valuable insights into the radiation dose status of screening mammography in

NSW. DRL values in mammography should be specific to breast thickness and image detector technology, as large variations between compressed breast thickness ranges and different image detector technologies were shown.

References

1. Tabar L, Vitak B, Chen TH *et al.* Swedish two-county trial: impact of mammographic screening on breast cancer mortality during 3 decades. *Radiology* 2011; **260**: 658–63.
2. AIHW. BreastScreen Australia Monitoring Report 2010–2011. Canberra: AIHW, 2013 2013. Report No.: 77.
3. ICRP. Radiological protection and safety in medicine. ICRP Publication 73. 1996; ICRP Publication 73. Ann. ICRP 26 (2).(2):1–47.
4. Boag JW, Stacey AJ, Davis R. Radiation exposure to the patient in xeroradiography. *Br J Radiol* 1976; **49**: 253–61.
5. Breslow L, Thomas LB, Upton AC. Final reports of the National Cancer Institute ad hoc Working Groups on Mammography in Screening for Breast Cancer and a summary report of their joint findings and recommendations. *J Natl Cancer Inst* 1977; **59**: 467–541.
6. Jensen JE, Butler PF. Breast exposure: nationwide trends; a mammographic quality assurance program–results to date. *Radiol Technol* 1978; **50**: 251–7.
7. Fitzgerald M, White DR, White E, Young J. Mammographic practice and dosimetry in Britain. *Br J Radiol* 1981; **54**: 212–20.
8. Karlsson M, Nygren K, Wickman G, Hettinger G. Absorbed dose in mammary radiography. *Acta Radiol Ther Phys Biol* 1976; **15**: 252–8.
9. ICRP. Protection of the Patient in Nuclear Medicine (and Statement from the 1987 Como Meeting of ICRP). ICRP Publication 52. 1987;Ann. ICRP 17(4).
10. NCRP. Mammography - a user's guide. Bethesda: National Council on Radiation Protection and Measurements, 1986.
11. IPEM. Guidance on the Establishment and Use of Diagnostic Reference Levels for Medical X-ray Examinations. Institute of Physics and Engineering in Medicine, 2004.
12. Perry N, Broeders M, De Wolf C *et al.* European guidelines for quality assurance in breast cancer screening and diagnosis Fourth Edition. Luxembourg office for official publications of the European Communities. 2006.
13. Perry N, Schouten J. European guidelines for quality assurance in mammography screening: Office for official publications of the European communities; 2001.
14. Zoetelief J, Fitzgerald M, Leitz W, Säbel M. European protocol on dosimetry in mammography. Publication EUR. 1996; 16263.
15. IAEA. Dosimetry in diagnostic radiology: an international code of practice. Vienna: International Atomic Energy Agency; 2007. Available from URL: http://www-pub.iaea.org/MTCD/publications/PDF/TRS457_web.pdf.
16. Suleiman ME, Brennan PC, McEntee MF. Diagnostic reference levels in digital mammography: a systematic review. *Radiat Prot Dosimetry* 2015; **167**: 608–19.
17. Asada Y, Suzuki S, Minami K, Shirakawa S. Results of a 2011 national questionnaire for investigation of mean glandular dose from mammography in Japan. *J Radiol Prot* 2014; **34**: 125–32.
18. Baldelli P, McCullagh J, Phelan N, Flanagan F. Comprehensive dose survey of breast screening in Ireland. *Radiat Prot Dosimetry* 2011; **145**: 52–60.
19. Hauge IHR, Bredholt K, Olerud HM. New diagnostic reference level for full-field digital mammography units. *Radiat Prot Dosimetry* 2013; **157**: 181–92.
20. Smans K. Towards a proposition of a diagnostic (dose) reference level for mammographic acquisitions in breast screening measurements in Belgium. *Radiat Prot Dosimetry* 2006; **117**: 321–6.
21. Vassileva J, Dimov A, Slavchev A, Karadjov A. Bulgarian experience in the establishment of reference dose levels and implementation of a quality control system in diagnostic radiology. *Radiat Prot Dosimetry* 2006; **117**: 131–4.
22. Zdesar U. Reference levels for image quality in mammography. *Radiat Prot Dosimetry* 2008; **129**: 170–2.
23. Thiele DL, Irvine M, Want D, Bernardo M. Diagnostic reference levels for mammography in BreastScreen Queensland. *Australas Phys Eng Sci Med* 2011; **34**: 415–8.
24. Dance D. Monte-Carlo calculation of conversion factors for the estimation of mean glandular breast dose. *Phys Med Biol* 1990; **35**: 1211.
25. Dance DR, Skinner CL, Young KC, Beckett JR, Kotre CJ. Additional factors for the estimation of mean glandular breast dose using the UK mammography dosimetry protocol. *Phys Med Biol* 2000; **45**: 3225–40.
26. Dance DR, Young KC, van Engen RE. Further factors for the estimation of mean glandular dose using the United Kingdom, European and IAEA breast dosimetry protocols. *Phys Med Biol* 2009; **54**: 4361–72.
27. Seeram E, Brennan PC. Diagnostic reference levels in radiology. *Radiol Technol* 2006; **77**: 373–84.
28. O'Leary D, Rainford L. A comparison of mean glandular dose diagnostic reference levels within the all-digital Irish National Breast Screening Programme and the Irish Symptomatic Breast Services. *Radiat Prot Dosimetry* 2013; **153**: 300–8.
29. Geeraert N, Klausza R, Mullera S, editors. Breast characteristics and dosimetric data in X-ray mammography A large sample worldwide survey. Bonn: IAEA conference; 2012.
30. Michielsen K, Jacobs J, Lemmens K *et al.* Results of a European dose survey for mammography. *Radiat Prot Dosimetry* 2008; **129**: 199–203.

31. Hemdal B, Herrnsdorf L, Andersson I, Bengtsson G, Heddson B, Olsson M. Average glandular dose in routine mammography screening using a Sectra MicroDose Mammography unit. *Radiat Prot Dosimetry* 2005; **114**: 436–43.
32. Young KC, Burch A, Oduko JM. Radiation doses received in the UK Breast Screening Programme in 2001 and 2002. *Br J Radiol* 2005; **78**: 207–18.
33. Chevalier M, Moran P, Ten JI, Soto JMF, Cepeda T, Vano E. Patient dose in digital mammography. *Med Phys* 2004; **31**: 2471–9.
34. Bor D, Akyol O, Olgar T. Performance measurements of mammographic systems. *Radiat Prot Dosimetry* 2008; **129**: 165–9.
35. Moran P, Chevalier M, Ten JI, Sot JMF, Vano E. A survey of patient dose and clinical factors in a full-field digital mammography system. *Radiat Prot Dosimetry* 2005; **114**: 375–9.
36. Borg M, Badr I, Royle GJ. Mammography equipment performance, image quality and mean glandular dose in Malta. *Radiat Prot Dosimetry* 2013; **156**: 168–83.

DICOM organ dose does not accurately represent calculated dose in mammography

Moayyad E. Suleiman*, Patrick C. Brennan, Mark F. McEntee

Faculty of Health Sciences, The University of Sydney, M205, Cumberland Campus, 75 East St, Lidcombe, NSW 2141, Australia

* msul1801@uni.sydney.edu.au

ABSTRACT

This study aims to analyze the agreement between the mean glandular dose estimated by the mammography unit (organ dose) and mean glandular dose calculated using Dance et al published method (calculated dose). Anonymised digital mammograms from 50 BreastScreen NSW centers were downloaded and exposure information required for the calculation of dose was extracted from the DICOM header along with the organ dose estimated by the system. Data from quality assurance annual tests for the included centers were collected and used to calculate the mean glandular dose for each mammogram. Bland-Altman analysis and a two-tailed paired t-test were used to study the agreement between calculated and organ dose and the significance of any differences. A total of 27,869 dose points from 40 centers were included in the study, mean calculated dose and mean organ dose (± standard deviation) were 1.47 (±0.66) and 1.38 (±0.56) mGy respectively. A statistically significant 0.09 mGy bias ($t = 69.25$; $p<0.0001$) with 95% limits of agreement between calculated and organ doses ranging from -0.34 and 0.52 were shown by Bland-Altman analysis, which indicates a small yet highly significant difference between the two means. The use of organ dose for dose audits is done at the risk of over or underestimating the calculated dose, hence, further work is needed to identify the causal agents for differences between organ and calculated doses and to generate a correction factor for organ dose.

Keywords: Mean Glandular dose, Breast, Screening, Radiation.

Medical Imaging 2016: Physics of Medical Imaging, edited by Despina Kontos, Thomas G. Flohr, Joseph Y. Luo,
Proc. of SPIE Vol. 9783, 97832L · © 2016 SPIE · CCC code: 1605-7422/16/$18 · doi: 10.1117/12.2216698

1. INTRODUCTION

Screening mammography invites healthy women for an x-ray examination of the breast, with the aim of early detection of breast cancer. The benefits of screening mammography have been scientifically examined and it has been shown, on the basis of randomized controlled trials [1-3], that screening mammography reduces breast cancer mortality by up to 25% [4]. This evidence was revisited in 2015 to find out if it still valid today, the International Agency for Research on Cancer conducted a review of all published peer reviewed literature through which they concluded that mammography screening is still effective in reducing breast cancer mortality [5].

The use of ionizing radiation in screening mammography is associated with a risk of radiation induced cancer to fibroglandular tissues of the breast [6], and possibly other exposed organs, as very few research studies examine the dose absorbed by other body parts [7]. Thus monitoring the dose is vital to ensure unnecessarily high doses do not occur.

Breast absorbed dose has been calculated using different methods throughout the years, mean glandular dose (MGD) is now the adopted method of estimating breast absorbed dose and is calculated using conversion factors established by monte-carlo simulations. The conditions underlying monte-carlo simulation employed by different authors can impact the estimated dose by up to 19% [8]. Dance et al [9-11], Wu et al [12, 13] and Boone et al [14-16] have established conversion factors that are widely used to estimate MGD. The three models differ slightly in the simulation method but all reported conversion factors depend on breast thickness, glandularity, x-ray spectra, and beam quality.

There are three main principles of radiation protection: justification, optimization and dose limitation, hence strict quality assurance (QA) policies are applied to keep the dose "as low as reasonably achievable", known as the ALARA principle [17]. Diagnostic reference levels (DRLs) are a method of dose optimization. Protocols have been proposed to attempt to standardize how DRLs are established around the world, although these protocols differ in methods such as calculation of dose, average breast density, and standard breast thickness [18-21]. Such differences have been proven to make international comparisons difficult [22].

Current QA practices are reported on a local level to make sure mammography units are operating within internationally approved guidelines, such practices use a limited range of phantoms that do not reflect the population of women attending screening, and do not identify operator errors. Thus a more clinically aligned method of measuring the dose is needed to account for variation in the breasts of the patient population.

The introduction of digital mammography and the readily available estimation of MGD displayed by the digital systems provides a digital indication of the breast dose named organ dose, as well as information on radiographic technique and the performance of the imaging system. However, this estimated organ dose needs to be validated against other calculation methods before it can be used as an alternative approach to dose surveys for QA purposes and perhaps establishing DRLs. Therefore, this study aims to analyze the agreement between organ dose estimated by digital mammography units and calculated dose values for the same exposures using methods published by Dance et al [9-11].

2. MATERIALS AND METHODS

Data collection

Ethical approval was granted by the Human Research Ethics Committee (HREC) of the Cancer Institute of NSW (No.2014/08/552). The dose audit included 61 mammography units from 50 BreastScreen centers and mobile vans throughout the state of NSW Australia. 52,405 (12,034 women) anonymised mammograms were downloaded from the Picture Archiving and Communication System located at the Cancer institute of NSW .

The following information was extracted from the Digital Imaging and Communication in Medicine (DICOM) headers using a third party software (YAKAMI DICOM Tools ver. 1.4.1.0, Kyoto University, Japan), namely: age, study date, compressed breast thickness (CBT), presence of implants, view, laterality, tube voltage (kVp), tube current exposure time product (mAs), target material, filter material, exposure control mode, organ dose, detector ID and mammographic unit model. Further quality assurance (QA) data required for the calculation of mean glandular dose (MGD) were collected from the annual QA medical physics reports of participating centers through the Cancer Institute of NSW, these reports consisted of dose measurements on 20 mm, 42 mm (ACR), and 60 mm phantom thicknesses for different anode/filter combinations. It should be noted here that some estimations have been made to calculate the output and HVL using the QA reports for certain systems, also different dosimeters utilized to measure the output may have slight differences which could carry up to 5% error in calibration.

Data preparation and analysis

Only mammograms for women with no breast implant, aged 40-64 and a compressed breast thickness (CBT) 20-110 mm were included as the MGD calculation method utilized is limited to these criteria. Any exposure information with manual exposure settings, no organ dose in DICOM header, or missing QA data was excluded due to the lack of exposure information to calculate MGD. For each mammogram, MGD was calculated using an in-house developed excel workbook utilizing the methods published by Dance et al [9-11], using the following equation:

$$\mathbf{MGD = Kgcs}$$

Where: K is the incident air kerma (IAK) at the upper surface of the breast. g converts IAK to MGD for a breast with 50% glandularity. c corrects for differences in glandularity other than the 50% and is given for two age groups 40-49 and 50-64 years. g and c are dependent on HVL and compressed breast thickness. s is spectra dependent, it corrects for different types of spectra where s = 1 for Mo/Mo anode/filter combination and changes for other combinations.

A Bland-Altman analysis was used to study the level of agreement between organ dose and calculated dose, this graphical method is used to compare two measurement techniques where the differences between the two methods are plotted against the means of the two methods [23]. On the plot a reference line is drawn at the average difference between the methods, this is called the bias, it describes the average discrepancy between the methods and its value is interpreted clinically, to determine whether the bias is large enough to be considered clinically important. Another output for the Bland-Altman analysis is the limits of agreement. Wider limits of agreement would mean ambiguous results. A two-tailed paired t-test was also used to determine the significance of differences. Linear regression analysis was used to study the correlation between the two methods of dose estimation and find the best-fit equation.

3. RESULTS

The final data set included 27,869 mammograms from 40 BreastScreen centers and mobile vans (53 digital mammography units). Both calculated and organ dose showed skewed distributions that ranged from 0.31 mGy to 8.05 mGy and 0.29 mGy to 7.40 mGy with means (±SD) of 1.47 (±0.66) mGy and 1.38 (±0.56) mGy respectively. The Bland-Altman analysis revealed that the organ dose underestimates the calculated dose by a significant bias of 0.09 mGy ($t = 69.25$; $p<0.001$) with 95% limits of agreement between calculated and organ dose that ranged from -0.336 and 0.517 mGy (Figure 1). Linear regression showed high correlation between the calculated and organ dose ($R= 0.95$) with statistically significant regression model ($R^2 = 0.9038$, $p < 0.005$) (Figure 2).

Table 1 demonstrates the number of systems included, number of images, mean calculated dose, mean organ dose, bias, and limits of agreement per model. The average calculated and average organ dose per exposure for each type of mammography unit in the study ranged from 0.83 mGy to 1.97 mGy and from 0.86 mGy to 1.73 mGy respectively. The differences between organ dose and calculated dose, although very small, were statistically significant ($p<0.001$ for all systems). The highest bias belonged to the Hologic Selenia Dimensions, where the organ dose is overestimating the calculated dose by a bias of 0.24 mGy.

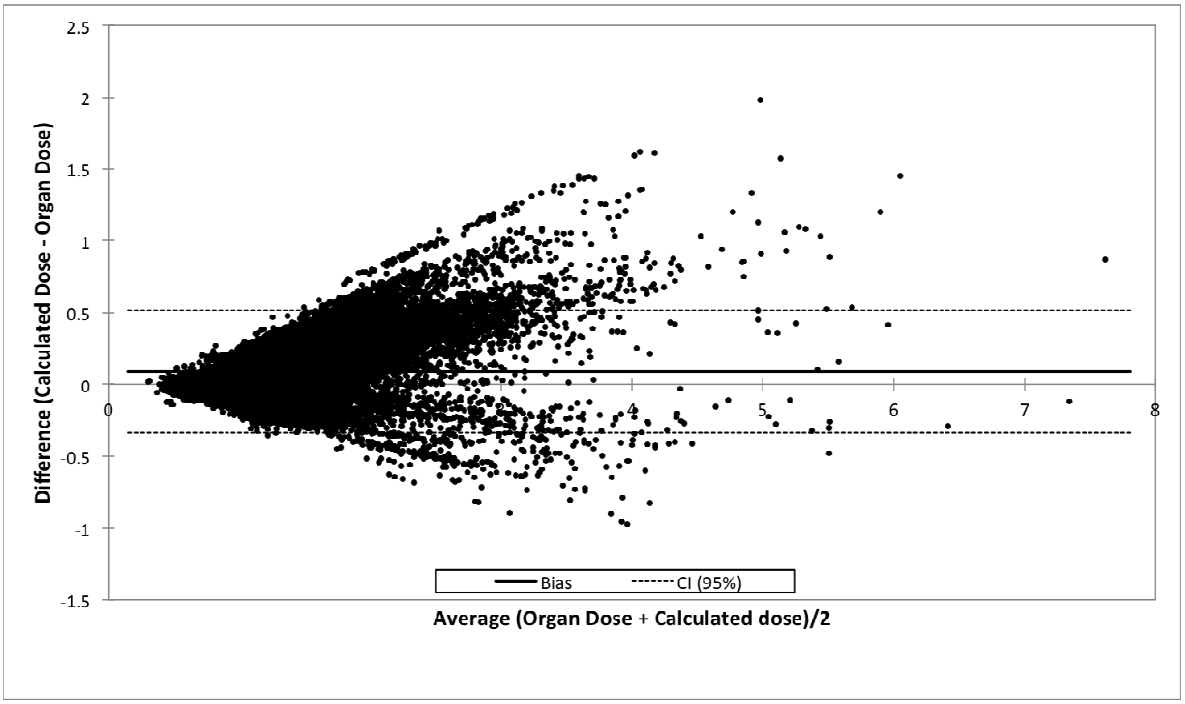

Figure 1: Bland-Altman plot for calculated and organ mean glandular dose (MGD) for 27,869 digital mammography images.

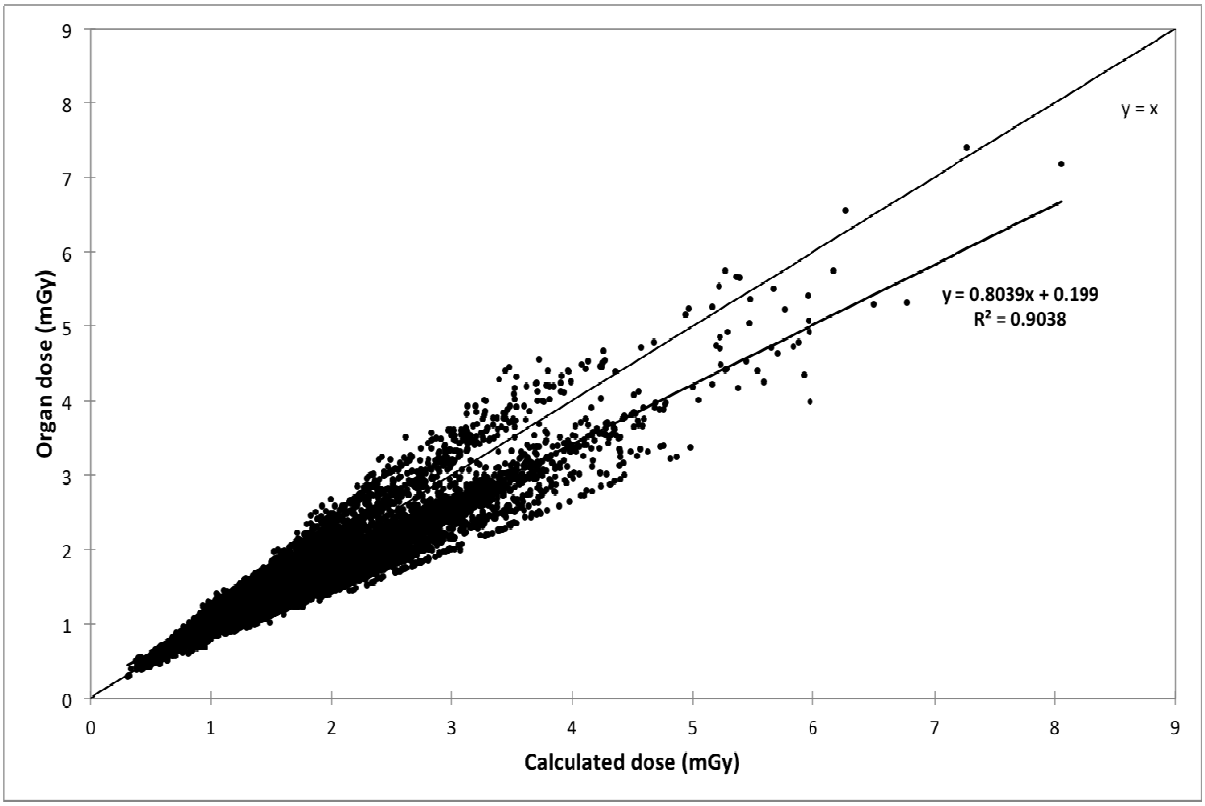

Figure 2: Scatter plot showing the calculated versus organ dose and the regression line for 27,869 digital mammography images.

Table 1: Calculated and organ average mean glandular dose (MGD) with 95% confidence interval (CI) and their Bias for different mammography unit models from 27,869 digital mammography images.

Make	Model	Systems	Images	Mean calculated dose (mGy) ± 95% CI	Mean organ dose (mGy) ± 95% CI	Bias (mGy)	p value	Lower, upper 95% Limits of agreement (mGy)
GE MEDICAL SYSTEMS	Senographe Essential VERSION ADS_54.11	14	8282	1.48 ± 0.01	1.45 ± 0.01	0.03	<0.001	-0.35, 0.29
	Senographe Essential VERSION ADS_54.10	1	488	1.43 ± 0.02	1.46 ± 0.02	-0.03	<0.001	-0.22, 0.27
	Senographe Essential VERSION ADS_53.40	1	727	1.34 ± 0.02	1.26 ± 0.02	0.08	<0.001	-0.29, 0.13
	Senograph DS VERSION ADS_54.11	2	982	1.23 ± 0.02	1.16 ± 0.02	0.07	<0.001	-0.30, 0.17
	Senograph DS VERSION ADS_53.40	1	454	1.38 ± 0.02	1.52 ± 0.03	-0.13	<0.001	-0.16, 0.43
	Senograph 2000D ADS_17.4.5	1	316	1.64 ± 0.04	1.54 ± 0.04	0.10	<0.001	-0.37, 0.17
	All GE Systems	20	11249	1.45 ± 0.01	1.42 ± 0.01	0.03	<0.001	-0.28, 0.34
HOLOGIC	Selenia Dimensions	21	9504	1.97 ± 0.01	1.73 ± 0.01	0.24	<0.001	-0.27, 0.74
Philips	L30	11	6210	0.83 ± 0.01	0.86 ± 0.01	-0.03	<0.001	-0.21, 0.15
Fujifilm	Amulet	1	906	1.01 ± 0.03	0.93 ± 0.02	0.09	<0.001	-0.18, 0.35
Overall		53	27869	1.47 ± 0.01	1.38± 0.01	0.09	<0.001	-0.34, 0.52

4. DISCUSSION

Worldwide mammography QA protocols that govern establishing DRLs have a similar goal, which is keeping the dose as low as reasonably achievable. Nonetheless, it has been shown that the methods through which DRLs are established differ from one country to the other, as does the tolerance to variations in dose values, making useful international comparisons difficult [22]. An internationally accepted protocol needs to be established before accurate international comparisons can be made. The same issue exists for the organ dose displayed by the imaging system, where different vendors are using different methods to estimate the organ dose. For example Philips systems and Fujifilm Amulet use Dance et al conversion factors to estimate the dose while GE systems use Wu et al conversion factors and Hologic uses Boone et al calculation method, although its important to emphasize here that the calculation methods employed by different vendors are not clear. Organ dose displayed by the system could be used as a robust method to evaluate the dose for a wide range of breast thicknesses, systems, and bigger sample size, yet this needs to be validated against other dose calculation methods before it can be implemented. This study examined the agreement and correlation between calculated dose and organ dose. Results overall showed statistically significant bias between the two methods, demonstrating that if the organ dose were to be used to calculate DRLs it would under or over estimate in comparison to the calculated dose depending on the vendor.

The Philips systems showed a statistically significant bias indicating the organ dose is overestimating the calculated dose by an average of 0.030 mGy with 0.153 mGy and -0.213 mGy upper and lower 95% limits of agreement respectively. On the other hand the Bland-Altman graph for the Philips systems revealed a group of dose points that have a higher difference between organ and calculated dose, these belonged to one system and may be due to an error in the QA data collection for that system or an error in the system calibration; once that system was removed from the analysis, the bias became -0.047 with a narrower upper and lower 95% limits of agreement (-0.152, 0.057). A scatter plot with the outliers removed shows the dose points aligned towards the origin line with possible agreement even if the bias was statistically significant (Figure 1).

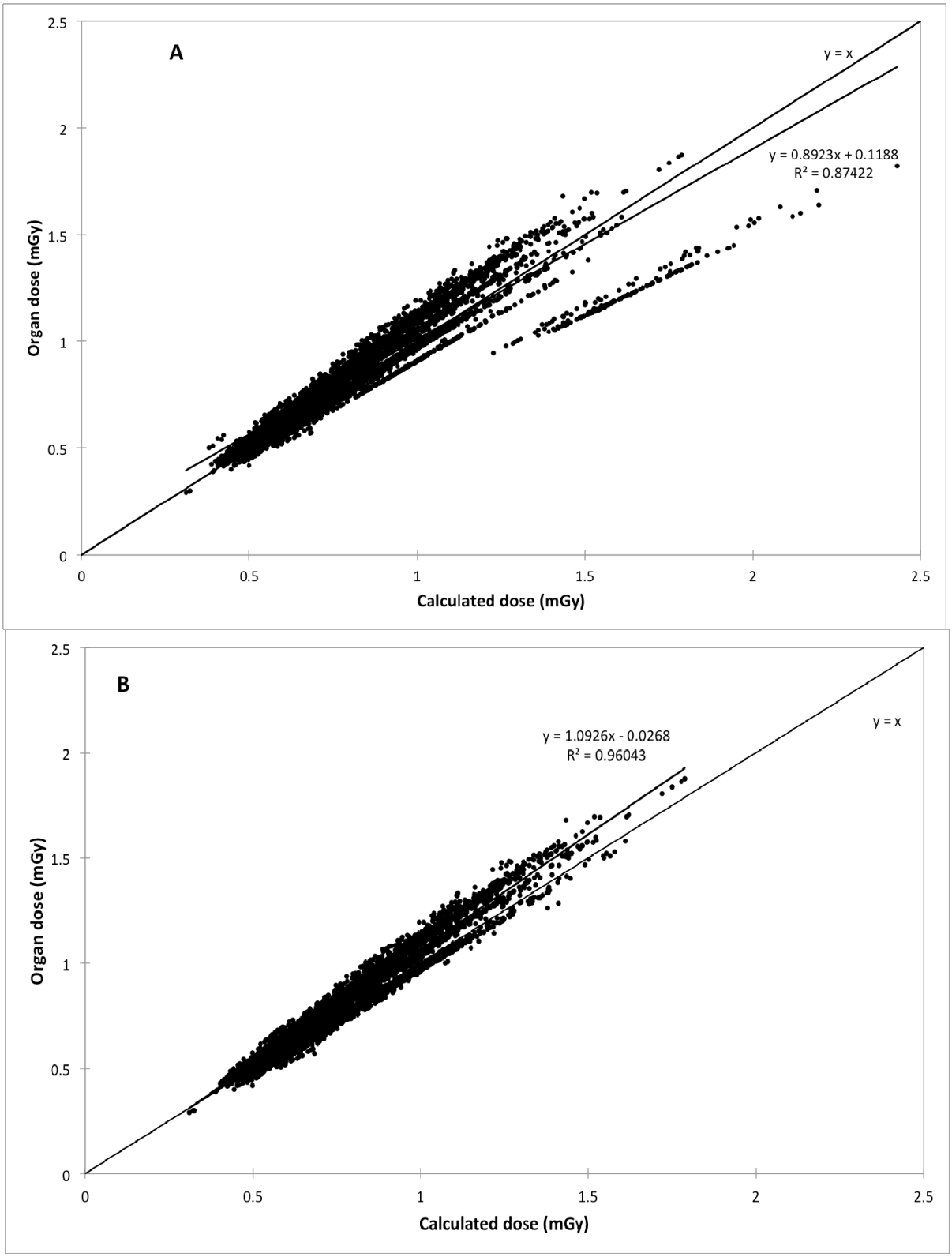

Figure 3: Scatter plot showing calculated versus Organ dose for Philips systems (6,210 mammography images) also showing the origin line and regression line with R^2 value. A. Showing one problematic unit, B. Problematic unit excluded.

GE systems varied in performance depending on the model and version; in total though, they showed on average an under estimation of 0.03 mGy with 0.34 and -0.28 upper and lower 95% limits of agreement, a few units had higher or lower bias one of which overestimated the calculated dose by an average of 0.13 mGy, but removing them from the analysis did not have any significant change to the result. It is important to state here that it has been reported that GE systems utilize a different method for the calculation of dose (Wu et al). Hence, further work is needed to investigate the agreement between organ dose and dose calculated using Wu et al calculation method.

The highest bias reported belonged to Hologic systems (0.24 mGy) with 0.74 mGy, -0.27 mGy upper and lower 95% limits of agreement, this shows a difference of up to 0.74 mGy which is clinically unacceptable as it represents the complete absorbed dose for small breast thicknesses. Nonetheless it is important to mention that Boone method was reported to have up to 19% difference in results from Dance et al method, which would explain some of the difference.

Only one Fujifilm amulet unit was included in this survey, this unit showed average results underestimating the calculated dose by a bias of 0.09 mGy.

It is crucial to understand that MGD calculation methods are all estimates; they inherit systematic errors throughout the measurements and calculations. Earlier methods of measuring the entrance dose using TLDs, although difficult, time consuming and having smaller sample sizes, offered more accurate measurements with higher accepted error of 25% for the entrance dose. The bias reported here for some systems was 3-12% and is still within the error value that is considered clinically acceptable. Nonetheless choosing the use of organ dose may risk underestimating the dose by up to an average of 0.09 mGy this is a level of bias that could include clinically important discrepancies of up to 0.74 mGy. Considering that the European protocol DRL for a 53 mm breast thickness is 2.0 mGy [18-21], this could have significant implications for the reporting of doses locally and nationally.

5. CONCLUSION

Organ dose is potentially beneficial for rapid dose audits and DRLs, however conclusions drawn based on the Organ dose have a risk of over or underestimating the calculated dose to the patient and this error should be included in any reported results. Further investigation is needed to study the correlation, if any, between the two methods. Further work is needed to identify the causal agents for the difference and to possibly generate a correction factor for Organ dose.

REFERENCES

[1] Chu, K. C., Smart, C. R., and Tarone, R. E., "Analysis of Breast Cancer Mortality and Stage Distribution by Age for the Health Insurance Plan Clinical Trial," Journal of the National Cancer Institute, 80(14), 1125-1132 (1988).

[2] Miller, A. B., Baines, C. J., To, T. *et al.*, "Canadian National Breast Screening Study: 2. Breast cancer detection and death rates among women aged 50 to 59 years," CMAJ: Canadian Medical Association Journal, 147(10), 1477-1488 (1992).

[3] Nyström, L., Wall, S., Rutqvist, L. E. *et al.*, "Breast cancer screening with mammography: overview of Swedish randomised trials," The Lancet, 341(8851), 973-978 (1993).

[4] Vainio, H., and Bianchini, F., "Breast cancer screening, IARC handbooks of cancer prevention," IARC, Lyon, 157-170 (2002).

[5] Lauby-Secretan, B., Scoccianti, C., Loomis, D. *et al.*, "Breast-cancer screening—viewpoint of the IARC Working Group," New England Journal of Medicine, 372(24), 2353-2358 (2015).

[6] Yaffe, M. J., and Mainprize, J. G., "Risk of Radiation-induced Breast Cancer from Mammographic Screening," Radiology, 258(1), 98-105 (2011).

[7] M. Ali, R., England, A., McEntee, M. F. *et al.*, "A method for calculating effective lifetime risk of radiation-induced cancer from screening mammography," Radiography, 21(4), 298-303 (2015).

[8] Zoetelief, J., and Jansen, J. T. M., "Calculation of Air Kerma to Average Glandular Tissue Dose Conversion Factors for Mammography," Radiation Protection Dosimetry, 57(1-4), 397-400 (1995).

[9] Dance, D., "Monte-Carlo calculation of conversion factors for the estimation of mean glandular breast dose," Physics in medicine and biology, 35(9), 1211 (1990).

[10] Dance, D. R., Skinner, C. L., Young, K. C. *et al.*, "Additional factors for the estimation of mean glandular breast dose using the UK mammography dosimetry protocol," Physics in Medicine and Biology, 45(11), 3225-3240 (2000).

[11] Dance, D. R., Young, K. C., and van Engen, R. E., "Further factors for the estimation of mean glandular dose using the United Kingdom, European and IAEA breast dosimetry protocols," Phys Med Biol, 54(14), 4361-72 (2009).

[12] Sobol, W. T., and Wu, X., "Parametrization of mammography normalized average glandular dose tables," Med Phys, 24(4), 547-54 (1997).

[13] Wu, X., Gingold, E. L., Barnes, G. T. *et al.*, "Normalized average glandular dose in molybdenum target-rhodium filter and rhodium target-rhodium filter mammography," Radiology, 193(1), 83-89 (1994).

[14] Boone, J. M., "Glandular breast dose for monoenergetic and high-energy X-ray beams: Monte Carlo assessment," Radiology, 213(1), 23-37 (1999).

[15] Boone, J. M., "Normalized glandular dose (DgN) coefficients for arbitrary X-ray spectra in mammography: computer-fit values of Monte Carlo derived data," Med Phys, 29(5), 869-75 (2002).

[16] Boone, J. M., Fewell, T. R., and Jennings, R. J., "Molybdenum, rhodium, and tungsten anode spectral models using interpolating polynomials with application to mammography," Med Phys, 24(12), 1863-74 (1997).

[17] ICRP, "Radiological protection and safety in medicine," ICRP Publication 73, ICRP Publication 73. Ann. ICRP 26 (2).(2), 1-47 (1996).

[18] Hendrick, R., Bassett, L., Botsco, M. *et al.*, "Mammography quality control manual," Reston, Va: American College of Radiology, (1999).

[19] IAEA, [Quality Assurance Programme for Digital Mammography. Human Health Series. No. 17] IAEA, Vienna(2011).

[20] Moore, A. C., and Physics, D. B. S. Q. A. C. G. f., [The Commissioning and Routine Testing of Mammographic X-ray Systems: A Protocol Produced by a Working Party of the Diagnostic Breast Screening Quality Assurance Coordinating Group for Physics] Institute of Physics and Engineering in Medicine, (2005).

[21] Perry, N., Broeders, M., De Wolf, C. *et al.*, "European guidelines for quality assurance in breast cancer screening and diagnosis Fourth Edition," Luxembourg office for official publications of the European Communities, (2006).

[22] Suleiman, M. E., Brennan, P. C., and McEntee, M. F., "Diagnostic reference levels in digital mammography: A systematic review," Radiat Prot Dosimetry, ncu365 (2014).

[23] Bland, J. M., and Altman, D. G., "Statistical methods for assessing agreement between two methods of clinical measurement," Lancet, 1(8476), 307-10 (1986).

Journal of Medical Imaging

MedicalImaging.SPIEDigitalLibrary.org

Mean glandular dose in digital mammography: a dose calculation method comparison

Moayyad E. Suleiman
Patrick C. Brennan
Mark F. McEntee

SPIE.

Moayyad E. Suleiman, Patrick C. Brennan, Mark F. McEntee, "Mean glandular dose in digital mammography: a dose calculation method comparison," *J. Med. Imag.* **4**(1), 013502 (2017), doi: 10.1117/1.JMI.4.1.013502.

Mean glandular dose in digital mammography: a dose calculation method comparison

Moayyad E. Suleiman,* Patrick C. Brennan, and Mark F. McEntee
The University of Sydney, Faculty of Health Sciences, M205, Cumberland Campus, 75 East Street, Lidcombe, New South Wales 2141, Australia

Abstract. Our objective was to analyze the agreement between organ dose estimated by different digital mammography units and calculated dose for clinical data. Digital Imaging and Communication in Medicine header information was extracted from 52,405 anonymized mammograms. Data were filtered to include images with no breast implants, breast thicknesses 20 to 110 mm, and complete exposure and quality assurance data. Mean glandular dose was calculated using methods by Dance et al., Wu et al., and Boone et al. Bland–Altman analysis and regression were used to study the agreement and correlation between organ and calculated doses. Bland–Altman showed statistically significant bias between organ and calculated doses. The bias differed for different unit makes and models; Philips had the lowest bias, overestimating Dance method by 0.03 mGy, while general electric had the highest bias, overestimating Wu method by 0.20 mGy, the Hologic organ dose underestimated Boone method by 0.07 mGy, and the Fujifilm organ dose underestimated Dance method by 0.09 mGy. Organ dose was found to disagree with our calculated dose, yet organ dose is potentially beneficial for rapid dose audits. Conclusions drawn based on the organ dose alone come with a risk of over or underestimating the calculated dose to the patient and this error should be considered in any reported results. [DOI: 10.1117/1.JMI.4.1.013502]

Keywords: dosimetry; screening mammography; radiation; organ dose.

Paper 16146PRR received Jul. 17, 2016; accepted for publication Dec. 27, 2016; published online Jan. 24, 2017.

1 Introduction

Screening mammography invites healthy women for an x-ray examination of the breast, with the aim of early detection of breast cancer. The benefits of screening mammography have been scientifically examined and it has been shown, on the basis of randomized controlled trials, that screening mammography reduces breast cancer mortality by up to 25%.[1–4] This evidence was revisited in 2015 to find out if it is still valid today. The International Agency for Research on Cancer conducted a review of all published peer-reviewed literature through which they concluded that mammography screening is still effective in reducing breast cancer mortality.[5]

Mammography efficacy in detecting breast cancer in early stages comes with a small but nonnegligible risk of radiation-induced cancer to the fibroglandular tissues of the breast[6] and possibly other exposed organs.[7] Monitoring the breast-absorbed dose is thus vital to ensure unnecessarily high doses do not occur; therefore, many quality assurance (QA) protocols have included breast dose assessments to govern the diagnostic adequacy of the imaging techniques in mammography.[8–11]

Mean glandular dose (MGD) is the main descriptor of absorbed dose to the breast. MGD is calculated using conversion factors established by Monte-Carlo simulations. Dance et al.,[12–14] Sobol and Wu,[15] Wu et al.,[16] and Boone et al.[17–19] have established conversion factors that are widely used to estimate MGD. The three models differ slightly in the simulation method, but all reported conversion factors dependent on breast thickness, glandularity, x-ray spectra, and beam quality. The conditions underlying Monte-Carlo simulation employed by different authors can impact the estimated dose by up to 19%.[20]

The estimation of MGD is dependent on the values of half value layer (HVL) and output, while these values are also dependent on the measurement methods and can change substantially depending on the dosimeters and how they are used.[21] Furthermore, MGD is estimated using Monte-Carlo simulations, which utilize a computer model of the breast to simulate photon absorption in the glandular tissue of the breast, hence making MGD a dose to a breast model rather than a dose to the breast. This makes the estimation of MGD prone to errors regardless of the method used, hence, it is important to highlight that MGD is and will always be an estimation as it is not possible to measure the dose absorbed by the glandular tissue directly as well as the differences in density distribution of the glandular tissue that also depend on the thickness of the breast and age of women.

Modern technology and the introduction of digital mammography provide valuable utility to easily collect data required to facilitate dose audits. The readily available estimation of MGD displayed by the digital systems provides a digital indication of the breast dose named organ dose, as well as information on radiographic technique and the performance of the imaging system. However, this estimated organ dose needs to be validated against other calculation methods before it can be used for dose audits or as an alternative approach to establish diagnostic reference levels (DRLs). Borg et al.[22] studied two mammography units [General Electric (GE) Essential and Hologic Selenia] to establish the correlation between organ dose and the dose calculated for different thickness phantoms using the three Monte-Carlo estimations mentioned earlier. The authors concluded that

*Address all correspondence to: Moayyad E. Suleiman, E-mail: msul1801@uni.sydney.edu.au

organ dose compares well with the Monte-Carlo estimations within small to medium phantom thicknesses and differs slightly with thicker phantoms.

This study aims to analyze the agreement and correlation between organ dose displayed by four types of digital mammography units and calculated dose values for clinical data with a wide range of breast thicknesses using methods published by Dance et al.,[12–14] Sobol and Wu,[15] Wu et al.,[16] and Boone et al.[17–19]

2 Materials and Methods

2.1 *Data Collection*

Ethical approval was granted by the Human Research Ethics Committee of the Cancer Institute of NSW (No. 2014/08/552). The dose assessment included 61 mammography units from 50 BreastScreen centers and mobile vans throughout the state of NSW Australia. 52,405 (12,034 women) anonymized mammograms were downloaded from the Picture Archiving and Communication System located at the Cancer institute of NSW.

The following information was extracted from the Digital Imaging and Communication in Medicine (DICOM) headers using a third party software (YAKAMI DICOM Tools ver. 1.4.1.0, Kyoto University, Japan), namely: age, study date, compressed breast thickness (CBT), presence of implants, view, laterality, tube voltage (kVp), tube current exposure time product (mAs), target material, filter material, exposure control mode, organ dose, detector ID, and mammographic unit model. Further QA data required for the calculation of MGD were collected from the annual QA medical physics reports of participating centers through the Cancer Institute of NSW. These reports consisted of dose measurements on 20, 42 American College of Radiology (ACR) mammography accreditation phantom, and 60 mm phantom thicknesses for different anode/filter combinations. It should be noted here that as QA reports vary in detail given, some estimation is necessitated to calculate the output and HVL. The normal QA practice for mammography units is made on three different phantoms, hence, different sets of data (HVL, output, and mAs) were provided for different anode/filter combinations. Extrapolation was used to estimate the HVL for mammograms taken by anode/filter combinations that had one set of QA data using the method published by Robson et al.[23] and expanded by Borg et al.[22] Different dosimeters utilized to measure the output may have slight differences some of which are stated in the calibration certificates provided from the manufacturers and could carry up to 5% error in calibration.[24,25]

2.2 *Data Preparation*

Only mammograms for women with no breast implants, aged 40 to 64 and a CBT 20 to 110 mm, were included. Any exposure information with manual exposure settings, no organ dose in DICOM header, or missing QA data were excluded due to the lack of exposure information to calculate MGD. The final data set included 27,869 mammograms from 40 BreastScreen centers and mobile vans (53 digital mammography units).

2.3 *Mean Glandular Dose Estimation*

Mammography system vendors utilize different methods for the estimation of organ dose displayed by the imaging systems. Philips (Sectra) and Fujifilm utilize Dance method, while Hologic utilize Boone method and GE utilizes Wu method[26] (it is important to stress here that the calculation methods are not clear) (Table 1). Hence, for each mammogram, MGD was calculated using an in-house developed excel workbook utilizing the three methods published by Dance et al.,[12–14] Sobol and Wu,[15] and Boone et al.[17–19]

Table 1 Calculation methods and glandularities known to be used by each system included in this study for the estimation of displayed organ dose (vendor Method).

	Displayed organ dose	
Manufacturer	Calculation method	Glandularity
Philips (Sectra)	Dance	Unknown
GE Medical systems	Wu	Proprietary measure
Hologic	Boone	Unknown
Fujifilm	Dance	Unknown

2.3.1 *Dance's method*

Dance et al. method utilizes the following equation to calculate MGD:

$$\mathrm{MGD} = Kgcs,$$

where K is the incident air kerma (IAK) at the upper surface of the breast. g converts IAK to MGD for a breast with 50% glandularity. This method incorporates an estimation of glandularity provided as the c factor, which corrects for differences in glandularity other than the 50% and is given for two age groups 40 to 49 and 50 to 64 years. g and c are dependent on HVL and CBT. s is spectra dependent, it corrects for different types of spectra where $s = 1$ for Mo/Mo anode/filter combination and changes for other combinations.

2.3.2 *Wu's method*

Wu's method utilizes the following equation:

$$\mathrm{MGD} = K \times \mathrm{DgN},$$

where K is the IAK at the upper surface of the breast and DgN is the normalized glandular dose per unit IAK. This method was applied using the paper published by Sobol and Wu,[15] which provides parameterization equations to calculate DgN for different anode/ filter combinations and different glandularities. The parameterization equations were implemented into our excel workbook using 50% glandularity. Wu's method is limited to three spectra namely Mo/Mo, Mo/Rh, and Rh/Rh, hence it could only be applied on the GE units.

2.3.3 *Boone et al. method*

Boone's method[17–19] utilizes Wu's equation to calculate the MGD with data tables having an extended utility to include more anode/filter combinations (W/Rh and W/Ag) and thicker breasts. Boone data tables are provided for 0%, 50%, and 100% glaundularities and those tables were used to calculate the MGD with the assumption of 50% glandularity.

Table 2 Average MGD for system displayed dose, three dose calculation methods and their SD for 27,869 digital mammography images from four different mammography unit makes.

Make	Model	Images	Average MGD (mGy), SD			
			System	Dance	Wu	Boone
Philips (Sectra)	L30	6210	0.86, 0.25	0.83, 0.26	N/A	0.95, 0.27
GE Medical systems	All	11249	1.42, 0.31	1.45, 0.34	1.22, 0.26	1.60, 0.41
Hologic	Selenia dimensions	9504	1.73, 0.66	1.97, 0.74	N/A	1.80, 0.68
Fujifilm	Amulet	906	0.93, 0.32	1.01, 0.42	N/A	0.91, 0.41

2.4 *Data Analysis*

Bland–Altman analysis was used to study the agreement between organ dose and each of the three other calculation methods. Multiple regression analysis was performed to study the correlation between organ dose and each calculation method (SPSS v22, Excel 2011).

3 Results

Table 2 shows the average MGD values and standard deviation (SD) for the organ dose and the three calculation methods. The Bland–Altman analysis revealed statistically significant bias between organ dose and the three calculation methods with bias values, 95% limits of agreements (LOA), and p values shown in Table 3. Linear regression models for each mammography unit make are shown in Figs. 1(a), 2(a), 3, and 4.

4 Discussion

The variation in methods used to estimate MGD makes international comparisons difficult.[27] The same issue exists for the organ dose displayed by the imaging system, where different

Table 3 Bland–Altman bias and 95% LOA to study the agreement between organ dose (displayed by the digital mammography unit) and dose calculated using three Monte-Carlo methods (Dance et al., Wu et al., and Boone et al.) for different mammography unit models from 27,869 digital mammography images.

Make	Model	Systems	Images	Organ versus Dance			Organ versus Wu			Organ versus Boone		
				Bias (mGy)	LOAs (mGy)	p value	Bias (mGy)	LOAs (mGy)	p value	Bias (mGy)	LOAs (mGy)	p value
Philips (Sectra)	L30	11	6210	0.03	−0.15, 0.21	<0.001	N/A	N/A	<0.001	−0.09	−0.33, 0.15	<0.001
GE Medical Systems	Senographe Essential ADS_54.11	14	8282	−0.03	−0.29, 0.35	<0.001	0.21	−0.13, 0.54	<0.001	−0.20	−0.68, 0.28	<0.001
	Senographe Essential ADS_54.10	1	488	0.03	−0.27, 0.22	<0.001	0.26	0.00, 0.53	<0.001	−0.14	−0.54, 0.26	<0.001
	Senographe Essential ADS_53.40	1	727	−0.08	−0.13, 0.29	<0.001	0.13	−0.13, 0.38	<0.001	−0.22	−0.54, 0.10	<0.001
	Senograph DS ADS_54.11	2	982	−0.07	−0.17, 0.30	<0.001	0.12	−0.17, 0.42	<0.001	−0.14	−0.50, 0.23	<0.001
	Senograph DS ADS_53.40	1	454	0.13	−0.16, 0.43	<0.001	0.36	0.01, 0.71	<0.001	−0.04	−0.44, 0.37	<0.001
	Senograph 2000D ADS_17.4.5	1	316	−0.10	−0.37, 0.17	<0.001	0.17	−0.47, 0.126	<0.001	−0.04	−0.43, 0.35	<0.001
	GE Systems	20	11249	−0.03	−0.34, 0.28	<0.001	0.20	−0.14, 0.54	<0.001	−0.18	−0.64, 0.28	<0.001
	GE Systems with gladularity	20	11249	−0.03	−0.34, 0.28	<0.001	0.03	−0.14, 0.21	<0.001	−0.18	−0.64, 0.28	<0.001
Hologic	Selenia dimensions	21	9504	−0.24	−0.74, 0.27	<0.001	N/A	N/A	<0.001	−0.07	−0.67, 0.53	<0.001
Fujifilm	Amulet	1	906	−0.09	−0.35, 0.18	<0.001	N/A	N/A	<0.001	0.01	−0.28, 0.30	<0.001
Overall		53	27869	−0.09	−0.52, 0.34	<0.001	N/A	N/A	<0.001	−0.12	−0.60, 0.37	<0.001

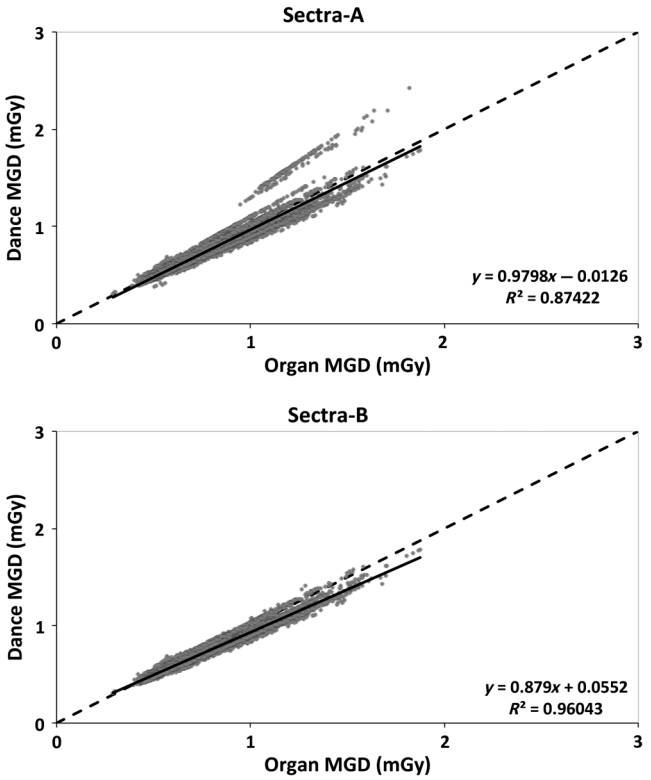

Fig. 1 Linear regression scatter plots showing the line of best-fit between MGD calculated using Dance method and organ dose displayed by Philips (Sectra) units for 6210 digital mammograms: (a) full data and (b) data after removing a problematic unit. (Philips systems utilize Dance method for the estimation of organ dose).

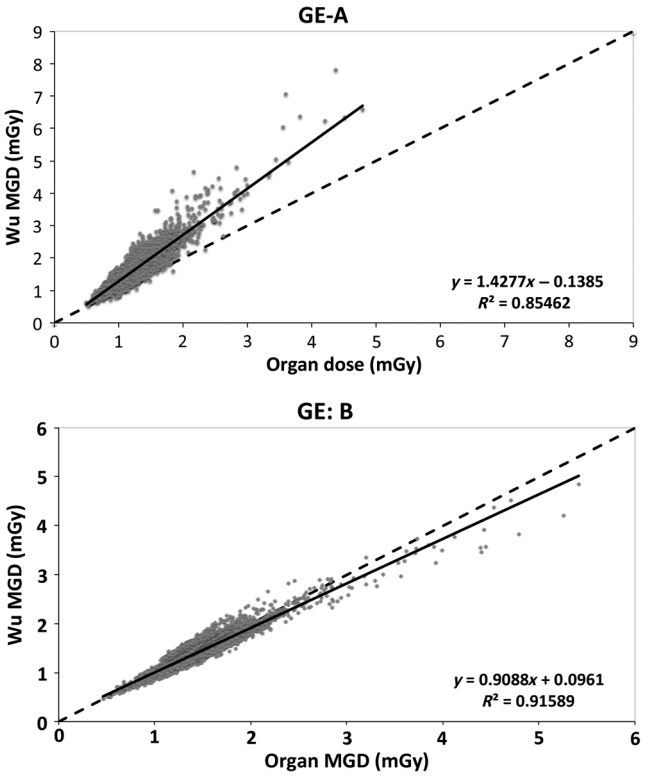

Fig. 2 Linear regression scatter plots showing the line of best-fit between (a) MGD calculated using Wu method assuming 50% glandularity and organ dose displayed by GE units and (b) MGD calculated using Wu method and using the DICOM glandularity (0040,0310 comments on radiation dose) and organ dose displayed by GE units for 11,249 digital mammograms. (GE systems utilize Wu method for the estimation of organ dose).

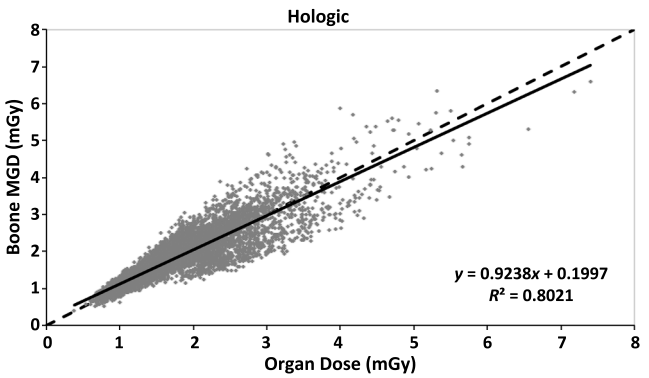

Fig. 3 Linear regression scatter plot that shows the line of best-fit between MGD calculated using Boone method and organ dose displayed by Hologic units for 9504 digital mammograms. (Hologic systems utilize Boone method for the estimation of organ dose).

vendors are using different methods to estimate the organ dose, although it is important to emphasize here that the calculation methods employed by different vendors are not clear. Organ dose displayed by the system could be used as a robust method to evaluate the dose for a wide range of breast thicknesses and systems, as well as facilitating larger sample sizes. However, the use of organ dose needs to be validated against other dose calculation methods before it can be implemented. This study examined the agreement and correlation between MGDs calculated using three Monte-Carlo methods and the organ dose displayed by the mammography systems.

Philips systems showed a statistically significant bias indicating the displayed organ dose is overestimating Dance MGD by an average of 0.03 mGy, while Boone MGD under estimated the organ dose by a higher bias (Table 3). This is expected as the Philips (Sectra) systems employ Dance conversion factors for the organ dose estimation. On the other hand, the scatter plot for the Philips systems revealed a group of dose points that have a higher difference between the organ and Dance MGD [Fig. 1(a)]. These belonged to one system and are due to an error in the QA data collection for that system or an error in the system calibration. A scatter plot with those dose points removed shows a higher correlation increasing from $R^2 = 0.87$ to $R^2 = 0.96$ [Fig. 1(b)]. Removing that system from the analysis increased the bias from 0.03 to 0.047 mGy. Therefore, as the bias is small in comparison to the clinical dose of 2.0 mGy, and there is a narrow upper and lower 95% LOA (Table 3), we can conclude that the calculated and organ doses are in agreement.

GE systems varied in performance depending on the model and version; in total though, they showed an average bias overestimated the organ dose by a 0.20 mGy, a few units had higher or lower bias, one of which overestimated the calculated dose by an average of 0.36 mGy. Figure 2(a) shows the correlation between calculated dose (Wu method) and the organ dose with $R^2 = 0.85$. Due to the higher bias, further investigation was carried out and it was discovered that GE systems utilize a proprietary measure of glandularity and they enter this into the DICOM header at tag 0040,0310 "Comments on radiation dose." It was also found that the glandularity estimation

was set to 50% in some centers and many mammograms had 0% or 100% estimations, regardless of the breast thickness. Neither the glandularity estimation method nor its accuracy is described in the literature. Nonetheless, once the calculations were adjusted to account for the proprietary glandularity estimation the bias was substantially reduced (Table 3) and showed a much better correlation with an $R^2 = 0.92$ [Fig. 2(b)]. Although the GE organ dose had a higher level of agreement with the Wu method after the inclusion of the proprietary glandularity estimation, these 0% glandularity estimations in many of the GE systems mean that these organ doses cannot reflect the calculated MGD correctly as they do not account for any glandularity.

Hologic system's organ dose reported a small bias (Table 3) underestimating the Boone calculated MGD, nonetheless, it shows a difference of up to 0.67 mGy, which represents the complete absorbed dose for small breast thicknesses. The correlation between calculated dose (Boone method) and organ dose show an $R^2 = 0.8$, which although good, is the lowest correlation out of the four vendors. We can conclude that in our study the Hologic system organ dose did not accurately reflect our calculated dose.

Fujifilm constitutes less than 4% of the total sample. Only one Fujifilm amulet unit was included in this survey, hence no intrasystem comparison was possible. Other Fujifilm units were computed radiography (CR) systems that did not record organ dose. The Fijifilm amulet unit showed average results underestimating Dance MGD with a small positive bias of 0.09 mGy. Linear regression showed an excellent correlation with $R^2 = 0.94$ (Fig. 4).

Organ dose from the four systems showed a statistically significant bias when compared to the calculated dose. It has been reported that the statistical significance of the bias in the Bland–Altman method should not be the only value considered; the clinical significance of that value and the LOA should be considered as well. In this study, the bias reported for Philips (Sectra), Hologic, and Fujifilm are considered clinically insignificant, being much smaller than the clinical dose. Nonetheless, when considering how wide the LOA are, it can be concluded that a disagreement between organ and calculated doses was found. Furthermore, it should be stressed that vendors using different methods of estimating the organ dose make reporting the dose across systems unreliable, as the dose reported by the three methods differ by up to 19%. Nonetheless, with vendors using various algorithms, some of which are not particularly well defined, there is a need for further work to establish a benchmark and allow comparison of doses between systems.

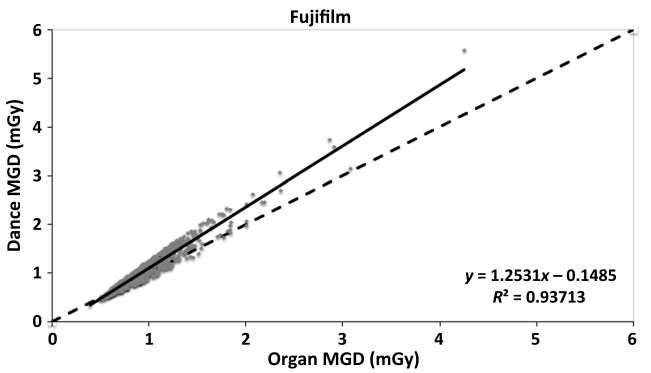

Fig. 4 Linear regression scatter plot that shows the line of best-fit between MGD calculated using Dance method and organ dose displayed by Fujifilm units for 906 digital mammograms. (Fujifilm systems utilize Dance method for the estimation of organ dose).

MGD calculation methods are all estimates; they are prone to systematic errors throughout measurement and calculation. Earlier methods of measuring the entrance dose using TLDs, although difficult, time consuming, and having smaller sample sizes, offered more accurate measurements. The bias reported here for some systems was 0.36 mGy, which is 18% of the acceptable dose level of 2.00 mGy reported by the European commission for a 4.5-mm breast thickness.[11] This is still within the error value that is reported for the dose calculation methods. However, choosing to use organ dose may risk underestimating the dose by up to an overall average of 0.09 mGy with a range from −0.52 to 0.34 mGy. This range of bias could result in a clinically important discrepancy between calculated and organ dose of up to 0.52 mGy. Considering that the European protocol DRL for a 45-mm breast thickness is 2.0 mGy,[11] this could have important implications for reporting doses locally and nationally. Further work might examine actual air kerma using TLDs on select phantoms, such as the ACR phantom and phantoms with different thicknesses.

5 Conclusion

Organ dose was found to disagree with calculated dose, with a bias ranging from −0.24 to 0.36 mGy. However, organ dose is potentially beneficial for rapid dose audits in centers using mammography units of the same make. Conclusions drawn based on the organ dose alone, whether to establish DRLs or for dose audits, come with a risk of over or underestimating the calculated dose to the patient by up to 18% for a standard breast and this error should be considered in any reported results.

Disclosures

The authors have nothing to disclose.

References

1. H. Vainio and F. Bianchini, "Breast cancer screening, IARC handbooks of cancer prevention," in *IARC*, Lyon, pp. 157–170 (2002).
2. K. C. Chu, C. R. Smart, and R. E. Tarone, "Analysis of breast cancer mortality and stage distribution by age for the health insurance plan clinical trial," *J. Natl. Cancer Inst.* **80**(14), 1125–1132 (1988).
3. A. B. Miller et al., "Canadian National Breast Screening Study: 2. breast cancer detection and death rates among women aged 50 to 59 years," *CMAJ* **147**(10), 1477–1488 (1992).
4. L. Nyström et al., "Breast cancer screening with mammography: overview of Swedish randomised trials," *Lancet* **341**(8851), 973–978 (1993).
5. B. Lauby-Secretan et al., "Breast-cancer screening—viewpoint of the IARC Working Group," *N. Engl. J. Med.* **372**(24), 2353–2358 (2015).
6. M. J. Yaffe and J. G. Mainprize, "Risk of radiation-induced breast cancer from mammographic screening," *Radiology* **258**(1), 98–105 (2011).
7. R. M. Ali et al., "A method for calculating effective lifetime risk of radiation-induced cancer from screening mammography," *Radiography* **21**(4), 298–303 (2015).
8. R. Hendrick et al., *Mammography Quality Control Manual*, American College of Radiology, Reston, Virginia (1999).
9. IAEA, *Quality Assurance Programme for Digital Mammography*, Human Health Series. No. 17, IAEA, Vienna (2011).
10. A. Moore, The Commissioning and Routine Testing of Mammographic X-ray Systems: A Protocol Produced by a Working Party of the Diagnostic Breast Screening Quality Assurance Coordinating Group for Physics, Institute of Physics and Engineering in Medicine (2005).
11. N. Perry et al., *European Guidelines for Quality Assurance in Breast Cancer Screening and Diagnosis*, 4th ed., Luxembourg office for

official publications of the European Communities, Luxembourg (2006).
12. D. Dance, "Monte-Carlo calculation of conversion factors for the estimation of mean glandular breast dose," *Phys. Med. Biol.* **35**(9), 1211–1220 (1990).
13. D. R. Dance et al., "Additional factors for the estimation of mean glandular breast dose using the UK mammography dosimetry protocol," *Phys. Med. Biol.* **45**(11), 3225–3240 (2000).
14. D. R. Dance, K. C. Young, and R. E. van Engen, "Further factors for the estimation of mean glandular dose using the United Kingdom, European and IAEA breast dosimetry protocols," *Phys. Med. Biol.* **54**(14), 4361–4372 (2009).
15. W. T. Sobol and X. Wu, "Parametrization of mammography normalized average glandular dose tables," *Med. Phys.* **24**(4), 547–554 (1997).
16. X. Wu et al., "Normalized average glandular dose in molybdenum target-rhodium filter and rhodium target-rhodium filter mammography," *Radiology* **193**(1), 83–89 (1994).
17. J. M. Boone, "Glandular breast dose for monoenergetic and high-energy X-ray beams: Monte Carlo assessment," *Radiology* **213**(1), 23–37 (1999).
18. J. M. Boone, "Normalized glandular dose (DgN) coefficients for arbitrary X-ray spectra in mammography: computer-fit values of Monte Carlo derived data," *Med. Phys.* **29**(5), 869–875 (2002).
19. J. M. Boone, T. R. Fewell, and R. J. Jennings, "Molybdenum, rhodium, and tungsten anode spectral models using interpolating polynomials with application to mammography," *Med. Phys.* **24**(12), 1863–1874 (1997).
20. J. Zoetelief and J. T. M. Jansen, "Calculation of air kerma to average glandular tissue dose conversion factors for mammography," *Radiat. Prot. Dosim.* **57**(1–4), 397–400 (1995).
21. S. Avramova-Cholakova et al., "An estimate of the influence of the measurement procedure on patient and phantom doses in breast imaging," *Radiat. Prot. Dosim.* **129**(1–3), 150–154 (2008).
22. M. Borg, I. Badr, and G. J. Royle, "A study to determine the differences between the displayed dose values for two full-field digital mammography units and values calculated using a range of Monte-Carlo-based techniques: a phantom study," *Radiat. Prot. Dosim.* **154**(2), 217–228 (2012).
23. K. J. Robson, "A parametric method for determining mammographic X-ray tube output and half value layer," *Br. J. Radiol.* **74**(880), 335–340 (2001).
24. RaySafe, "RaySafe Xi classic specifications," 2015, http://mediabank.raysafe.com/A/RaySafe+Media+Bank/1599?encoding=UTF-8 (10 October 2016).
25. RTIgroup, "Piranha specification," 2016, http://rtigroup.com/content/downloads/brochures/Specifications_Piranha.pdf (10 October 2016).
26. J. B. McCullagh, P. Baldelli, and N. Phelan, "Clinical dose performance of full field digital mammography in a breast screening programme," *Br. J. Radiol.* **84**(1007), 1027–1033 (2011).
27. M. E. Suleiman, P. C. Brennan, and M. F. McEntee, "Diagnostic reference levels in digital mammography: a systematic review," *Radiat. Prot. Dosim.* **167**(4), 608–619 (2015).

Biographies for the authors are not available.

BJR

https://doi.org/10.1259/bjr.20180032

Received: 01 January 2018 | Revised: 30 January 2018 | Accepted: 31 January 2018

Cite this article as:
Suleiman ME, Brennan PC, Ekpo E, Kench P, McEntee MF. Integrating mammographic breast density in glandular dose calculation. *Br J Radiol* 2018; **91**: 20180032.

FULL PAPER

Integrating mammographic breast density in glandular dose calculation

MOAYYAD E SULEIMAN, MSc, PATRICK C BRENNAN, PhD, ERNEST EKPO, PhD, PETER KENCH, PhD and MARK F MCENTEE, BSc (Hons), PhD

Medical Radiation Sciences, The University of Sydney, Faculty of Health Sciences, Cumberland Campus, Lidcombe, NSW, Australia

Address correspondence to: Mr Moayyad E Suleiman
E-mail: *msul1801@uni.sydney.edu.au*

Objective: This work proposes the use of mammographic breast density (MBD) to estimate actual glandular dose (AGD), and assesses how AGD compares to mean glandular dose (MGD) estimated using Dance et al method.
Methods: A retrospective sample of anonymised mammograms (52,405) was retrieved from a central database. Technical parameters and patient characteristics were exported from the Digital Imaging and Communication in Medicine (DICOM) header using third party software. LIBRA (Laboratory for Individualized Breast Radiodensity Assessment) software package (University of Pennsylvania, Philadelphia, USA) was used to estimate MBDs for each mammogram included in the data set. MGD was estimated using Dance et al method, while AGD was calculated by replacing Dance et al standard glandularities with LIBRA estimated MBDs. A linear regression analysis was used to assess the association between MGD and AGD, and a Bland-Altman analysis was performed to assess their mean difference.
Results: The final data set included 31,097 mammograms from 7728 females. MGD, AGD, and MBD medians were 1.53 , 1.62 mGy and 8% respectively. When stratified per breast thickness ranges, median MBDs were lower than Dance's standard glandularities. There was a strong positive correlation (R^2 = 0.987, p < 0.0001) between MGD and AGD although the Bland-Altman analysis revealed a small statistically significant bias of 0.087 mGy between MGD and AGD (p < 0.001).
Conclusion: AGD estimated from MBD is highly correlated to MGD from Dance method, albeit the Dance method underestimates dose at smaller CBTs.
Advances in knowledge: Our work should provide a stepping-stone towards an individualised dose estimation using automated clinical measures of MBD.

INTRODUCTION

Screening mammography is an effective tool for the early detection of breast cancer, and has been shown to reduce cancer mortality by 25–40%.[1–3] Since screening mammography was first instigated at a national level in Sweden in 1977, there has been continuous debate about the extent of benefits and the nature of the risk.[4] The risks arising from screening mammography are two-fold: risk from radiologist's errors such as false positives, false negatives and over diagnosis;[5] radiation-induced cancer risk arising from the high radiosensitivity of rapidly dividing epithelial cells in the fibroglandular tissues.[6] Therefore, it is increasingly important to appropriately account for the effect of radiation when assessing the risk *vs* benefit of screening mammography.[5] The relative risk of radiation-induced cancer from mammography is quantified by the mean glandular dose (MGD).

MGD is an estimate of the energy deposited per unit mass of glandular tissue averaged over all glandular tissue in the breast.[7] MGD is estimated using conversion factors derived from Monte-Carlo simulations.[8–10] All estimates use assumptions and the available MGD estimation methods operate on the assumption that the breast is 50% glandular and 50% fatty (50:50 model)[11] or that glandularity is proportional to compressed breast thickness.[12,13] The 50:50 model proposed by Hammerstein et al[11] was based on a phantom with homogeneous distribution of glandular tissue and the authors suggested that the 50:50 model can be used for comparing mammography doses delivered using different techniques and equipment. MGD calculation models such as Wu et al[10,14] and Boone et al[8,15,16] are based on the 50:50 model. However, it is well known that the breast composition is not homogeneous.[17] Additionally, it has been shown, in a volumetric breast density study, that about 80% of females have breasts with less than 27% fibroglandular tissue.[18] Thus, the assumptions made in the 50:50 model are clearly not true for all breasts, and do not represent the glandularity of the population. To address these limitations, another model was established by Dance

et al.[12,13] To account for the increased cancer risk in glandular tissue, this model incorporates estimates of breast glandularity taking into consideration patient age and compressed breast thickness (CBT).

Although the incorporation of glandularity and CBT in the Dance et al model is logical, this approach to estimation of glandularity has some limitations. First, the Dance et al method estimates changes in glandularity using CBT and age. However, breast composition differs across females within age groups and CBTs. Second, breasts with similar CBT can have different glandular compositions. Third, females of the same age and CBT can have different amount of glandular tissues. Thus, it is increasingly relevant to explore alternative models that account for a female's actual breast composition when estimating glandularity. Also, breast density, which is the amount of fibroglandular tissue in the breast, is a determinant of X-ray attenuation and risk of cancer.[19] The fibroglandular tissue contains high concentrations of primitive epithelial cells, the most susceptible to radiation damage, and from which 80% of cancers arise.[20] As the proportion of dense breast influences susceptibility to cancer, it is important that we should be exploring mammographic breast density (MBD) data when estimating radiation-induced risk from mammography. This makes individualised MBD a promising alternative to the 50:50 and Dance models for estimating glandularity and patient-specific dose estimates.

MBD is a representation of the fibroglandular tissue of the breast as seen by the X-ray attenuation patterns on a mammogram. MBD can be assessed qualitatively (visual grading) and quantitatively (area-based (2D) or volumetric (3D) methods).[21,22] However, qualitative visual methods are prone to intra- and inter-reader variability,[23] suggesting a need to automate MBD measurement for dose calculation. The automated use of MBD for dose assessment has been developed[24] and a white paper by Highnam et al[24] was the first to report MGD using MBD. This approach has now been incorporated into Volpara™ software (Volpara Health Technologies Limited) to propose Volpara Dose for patient-specific MGD estimation from mammography unit firmware.[24] Although Volpara Dose is robust and automated, it has a hardware and software cost, it requires networked systems and needs to be supported by the mammography equipment vendors. Furthermore, Volpara Dose only works on the "Raw Projection" data. These challenges limit its applicability for low-resource facilities and countries, and highlight the need for less costly, accessible and versatile automated alternative. Automated area-based methods utilise computer-assisted interactive thresholding techniques to measure the percentage area covered by the dense tissue on a radiograph and uses this as a proxy for fibroglandular tissue. The Laboratory for Individualized Breast Radiodensity Assessment (LIBRA) software for MBD estimation uses post-processed images, can do batch processing, is freely available and is therefore a possible low cost and low man-power alternative. LIBRA is freely available, fully automated software for the estimation of MBD. It estimates MBD on both "raw projection" data and "post processed" images, and has been validated for GE and Hologic digital mammography systems.[25]

The current work proposes the use of a female's automatically generated actual MBD to estimate the actual glandular dose (AGD) to the breast. This work explores the use of MBD measured by LIBRA to estimate AGD. It also assesses whether the AGD estimated using MBD compares to MGD estimates from Dance et al method.

METHODS AND MATERIALS

The work involved a retrospective sample of screening mammograms. A total of 52,405 mammograms from 12,034 females were used. Mammograms were acquired on 63 mammography units across 50 Breast Screen centres in New South Wales, Australia between September and October 2014. The data were retrieved from the Cancer Institute of New South Wales Picture Archiving and Communication System, following ethics approval (HREC2014/08/552) from the Cancer Institute Human Research Ethics Committee.

Patient-related information such as mammographic projections, age and breast thickness, exposure parameters, and mammography unit information (make, model) were exported from the Digital Imaging and Communication in Medicine (DICOM) image header to MS Excel using a third party software (YAKAMI DICOM Tools v. 1.4.1.0, Kyoto University, Japan).[26] Medical physics annual reports were also obtained from participating centres, as the calculation of MGD requires these data.

MBD was estimated for the data set using LIBRA software.[27] LIBRA uses a thresholding technique to detect the boundaries of the breast and the pectoral muscle on the mammogram. An "adaptive multi-class fuzzy c-means" algorithm is then applied to partition the mammographic breast tissue into clusters of similar intensity. These clusters are then aggregated to a dense tissue area. The software package then generates quantitative estimates of breast area, dense tissue area, and calculates MBD by dividing the dense area by the total breast area.[27,28]

LIBRA has only been validated for GE and Hologic mammography units.[25] Therefore, mammograms obtained using Philips and Fujifilm units (14,065 mammograms) were excluded in the current work. Further exclusion criteria related to the calculation method were applied on the data. These included mammograms reported to have 0% glandularity by LIBRA (180 mammograms) which were considered as an indicative of measurement error, mammograms with breast implants (1337 mammograms), mammograms not within 20–110 mm CBT (39 mammograms), incomplete calculation data (1971 mammograms). The final data set was imported to an excel workbook developed in-house which calculated MGD and our proposed AGD.

The calculation of MGD in our study followed the methods described by Dance et al.[9,12,13] This method calculates MGD using entrance air kerma and three conversion factors that depend on age, CBT, half value layer (HVL), and anode/filter combination. A full explanation of the methodology has been previously described[29] (Figure 1). AGD in our work was calculated by replacing the original *c* factor values (6 in Figure 1) with

Figure 1. Dance calculation method: input information that needs to be available for the calculation of MGD, the steps taken to calculate MGD for a mammogram and the equations utilised for that process. MGD, mean glandular dose.

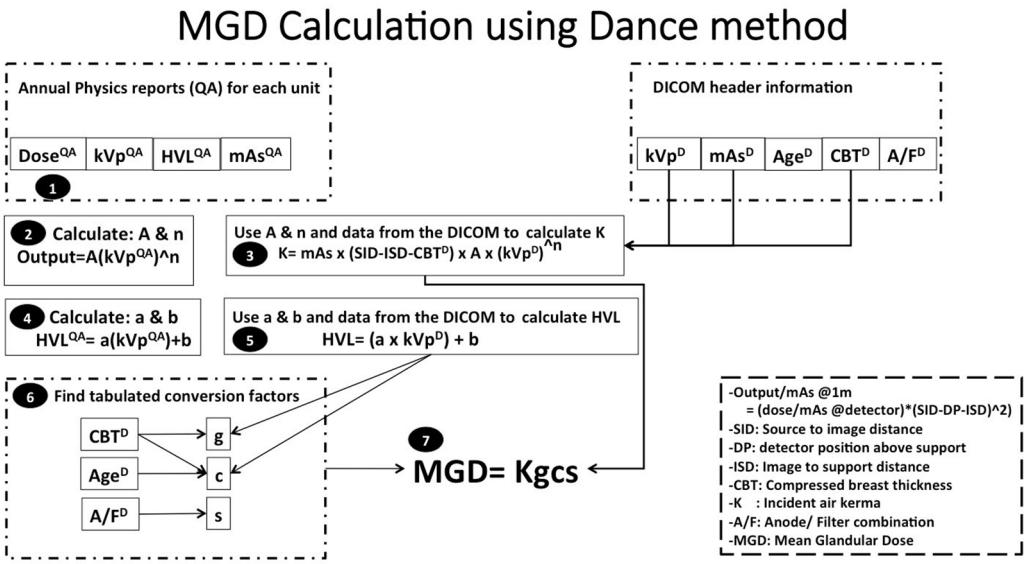

a look-up table of interpolated *c* values for MBDs ranging from 1 to 100%.

The data were stratified by age (40–49 and 50–64) and CBT (20–110 in 10 mm increments). For each age group, our estimated median MBD was compared to Dance's glandularity for each CBT (Figure 2). The distribution of the data was assessed using a D'Agostino & Pearson normality test, and a non-parametric Spearman's correlation was used to assess the relationship between median MBD and age.

MGD and AGD medians were calculated per mammogram. The median MGD and AGD were compared across different breast thicknesses (Figure 3). Bland-Altman analysis was performed to show the mean difference between the two dose estimation methods. Bland-Altman analysis also provided a measure of the bias and 95% limits of agreement (LOA) between MGD and AGD.[30] A linear regression analysis was performed to assess the linear correlation between MGD and AGD. AGDs and MGDs were stratified by CBT, and the median differences between AGD and MGD as well as their 95% confidence intervals were calculated for each range of CBTs.

RESULTS

A further 3716 mammograms failed LIBRA analysis, and the final data set comprised of 31,097 mammograms (7728 females) from 48 Breast screen centres. Table 1 provides a descriptive summary of the data set, including the minimum, maximum, 1st and 3rd quartiles, median, mean, variance, and standard deviation for age, CBT, MBD, MGD, and AGD. Both MGD and AGD

Figure 2. Median glandularity *vs* breast thickness for 31,097 mammograms, glandularity estimated using LIBRA, and compared to Dance method typical glandularities for two age groups (40–49, 50–64). LIBRA, Laboratory for Individualized Breast Radiodensity Assessment.

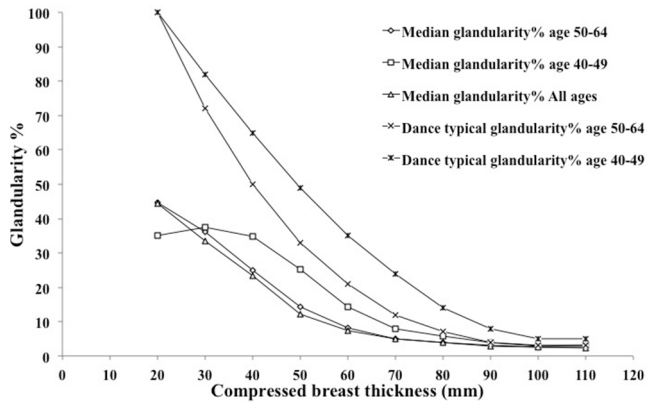

Figure 3. MGD and AGD variation with different CBT. The difference between median AGD and MGD for different CBT ranges becomes insignificant at CBTs greater than 80 mm. AGD, actual glandular dose; CBT, compressed breast thickness; MBD, mammographic breast density.

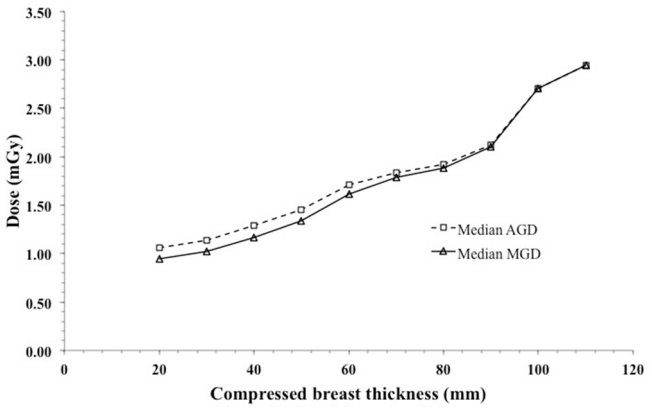

Table 1. Statistical description of the included data set (31,097 mammograms)

Statistic	Age	CBT1	MBD	MGD	AGD
Minimum	40	20	0.01	0.37	0.40
Maximum	89	110	0.99	14.53	13.93
1st quartile	54	50	0.04	1.27	1.37
Median	60	59	0.08	1.53	1.62
Mean	60	59	0.13	1.71	1.80
3rd quartile	66	68	0.17	1.96	2.03
Variance (n-1)	63	175	0.02	0.58	0.55
SD (n-1)	8	13	0.13	0.76	0.74

AGD, actual glandular dose; CBT, compressed breast thickness; MBD, mammographic breast density; MGD, mean glandular dose; SD, standard deviation.

showed skewed distributions with medians of 1.53 and 1.62 mGy respectively. MBD showed a skewed distribution with a median and a mean of 8 and 13% respectively.

Findings show that the median MBD decreased at higher CBTs but were lower than the Dance method at corresponding phantom CBTs for all age groups (Figure 2). There was a direct relationship between dose and compressed breast thickness. The AGD calculated using MBD followed a similar trend as the MGD estimated using Dance Method. However, the Dance method MGD underestimated dose at lower CBTs (below 80 mm) compared to AGD (Figure 3). Further analysis showed that the 95% confidence interval of the difference between median AGD and MGD for different CBT ranges becomes insignificant at CBTs greater than 80 mm (Figure 4).

Bland-Altman analysis revealed a small yet statistically significant bias of 0.087 mGy between MGD and AGD (Figure 5), with 95% confidence intervals and p value of −0.08–0.26 and <0.0001 respectively. Linear regression analysis demonstrated a strong positive correlation (R^2 = 0.987, p < 0.001) between MGD and AGD.

Figure 4. Median difference between AGD and MGD at different CBTs and the 95% confidence intervals (shown in bars). AGD, actual glandular dose; CBT, compressed breast thickness; MBD, mammographic breast density.

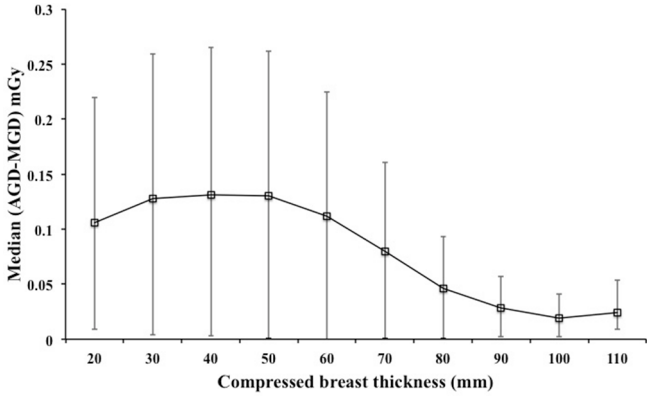

DISCUSSION

Previous studies estimating radiation risk from mammography made assumptions that are not necessarily true for all breast compositions. Given that the breast is infrequently 50% glandular, and that breasts with the same CBT and age vary in glandularity, the current work argues the importance of integrating actual measures of glandularity in dose calculation. The current work proposes the use of MBD to quantify individual's glandularity for the purpose of patient-specific dose estimation during mammography. Our work demonstrates that MBD is inversely related to CBT, with our median MBDs being lower than the glandularity estimated by Dance et al[12,13] at corresponding CBTs for all age groups. Findings also demonstrated a direct association between CBT and AGD as well as MGD. MGD was lower than AGD at smaller CBTs, with the difference becoming insignificant at higher CBTs (>80 mm). Bland-Altman analysis showed a small yet statistically significant bias between MGD and AGD.

The median breast glandular tissue content in our data set was 8%, with a mean of 13%, similar to that previously reported (17.4–27%) elsewhere[18,31] and for Australian females (8.1%).[32] These values are substantially lower than the 50% glandularity

Figure 5. Bland-Altman plot for MGD and AGD showing a Bias of 0.087 and 95% LOA of −0.08, 0.26 for 31,097 digital mammography images. AGD, actual glandular dose; MBD, mammographic breast density.

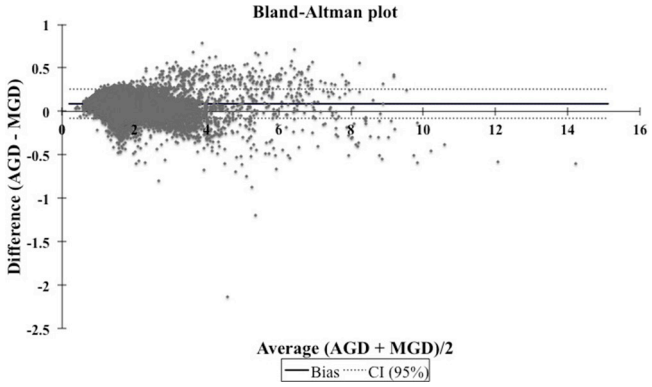

used in the standard breast composition model for mammography dose optimisation. These findings suggest that the 50:50 model overestimates glandularity and that there is in reality the same dose going to less glandular tissue. Therefore the mean glandular dose is actually higher than estimated by the 50:50 model. This same finding is explained by Dance et al[12] in a different way; they indicate that "The increase of the c-factor with decreasing glandularity is due to the increased percentage depth dose for fattier breasts". In other words, fattier breasts allow more photon penetration. Therefore, underestimating the dose absorbed per 1 gm of fibroglandular tissue, leading to an underestimation of radiation risk from mammography. Similarly, in comparison to the current work, the Dance et al method, which accounted for variation in breast composition using CBT, overestimated glandularity at smaller CBTs for all ages. We found that the glandularity estimated using the Dance method was almost double the actual glandularity at smaller CBTs, suggesting an overestimation of glandularity in small breasts. Such overestimation may result in an underestimation of dose and risk to patients undergoing mammography procedures, limiting the applicability of Dance model for patient-specific dose estimation, particularly for small breasts.

Further analysis demonstrated a linear increase in AGD and MGD with CBT. MGD was consistently significantly lower (6% difference; $p < 0.001$) than AGD at CBTs <80 mm. However, Bland-Altman analysis, revealed a small but significant positive bias towards AGD and a narrow LOA. Although the bias was statistically significant, it represents less than 5% of the average dose to the standard breast described by the European protocol.[33] Nonetheless, when females were stratified into different CBTs, the differences in MBD for smaller CBTs resulted in a higher difference (10%) between MGD and AGD, while larger CBTs (over 80 mm) demonstrated under a 2% difference, with narrower 95% confidence intervals (Figure 4). Smaller breast may have lesser fibroglandular content than larger ones but demonstrate higher percentage glandularity. This is perhaps the reason why AGD was higher in smaller breast when individuals' MBDs were accounted for. This finding implies that Dance et al model may not be suitable for dose calculation in smaller breasts. The high correlation between AGD and MGD reported in the current work may be due to the use of a similar methodology for estimating both parameters.

The 2–10% difference in AGD and MGD at different CBTs has implications for risk and lifetime effective risk, as MGD contributes to 98% of effective lifetime risk, while the other body parts (irradiated during mammography) such as contralateral breast, thyroid and lungs contribute to only 2%.[34] Furthermore, according to the Linear Non-Threshold (LNT) model, which is often used for radiation-induced risk assessment, cancer risk from radiation exposure increases linearly with dose. This suggests that underestimation of dose using MGD will result in an underestimation of risk. Although the LNT model is still being debated due to the lack of drop-off effect from death at higher doses and the paucity of data at lower doses, it is still used to quantify risk. There are contentions about the effects of radiation at low doses. While one theory suggests that the processes by which our cells repair damage (hormesis) and destroy unrepairable cells (apoptosis) occur at low doses[35] another asserts that cells are hypersensitive to low level doses.[36] Importantly, it has been shown that radiation-induced genetic effects vary between individuals.[37] These individual differences in risk emphasise the need to personalise glandularity and dose measurements in order to provide patient-specific estimates of radiation-induced risk.

The overestimation of glandularity at lower CBTs and underestimation of dose by Dance et al model highlights the limitations in the current mammography dosimetry approaches. The current work provides a more objective clinical approach to patient-specific mammography dose estimate. Although the difference between AGD and MGD was small (2–10%), it constitutes a significant difference in terms of risk according to the LNT model, and should be considered when estimating radiation-induced risk from mammography.

Another factor supporting individualized dose and risk estimation is the fact that risk from radiation and DNA repair differ between individuals even at similar dose levels.[36] For example, females with BRCA1 &2 mutations as well as those with single nucleotide polymorphisms (SNPs) are less likely to successfully repair and more likely to develop breast cancer.[38,39] Unfortunately, because 45–65% of females with BRCA mutations will develop breast cancer by the age of 70,[40] they are targeted for more regular screening. Cancer risk will also vary between individuals due to difference glandular content. Therefore, it is important to take into consideration these differences when estimating risk from mammography.

Although doses from medical procedures are relatively small, the effect of medical exposure to radiation is well established. A longitudinal study has reported an overall 24% increase in cancer incidence in individuals exposed to low doses compared to unexposed individuals.[41] Evidence also shows that oncogenecity in younger females may be higher at low mammography doses compared to higher doses.[36] A significant relationship has also been established between low doses and cell repair.[42] Therefore, one cannot definitely say that low doses are beneficial, harmful or have no effect, as radiation effects may vary between individuals.

The uncertainty of radiation effects at all doses suggests a conservative risk strategy should be adopted, and that actual measures of the radiosensitive fibroglandular tissues be included in dose calculation models for individualised dose estimation. Thus, AGD may be a better dosimetric parameter, as it accounts for the actual glandular content at risk. Importantly, advances in technology and automation of MBD measurement should facilitate easier estimation of breast glandular tissue content and AGD. This will provide actual measures of dose received by each patient and the potential risk from screening mammography.

The current work is limited in that only images retrieved from two mammography vendors were used. LIBRA is currently being tested on mammography units from different vendors, and may become more versatile in the future. Future work will explore AGD with LIBRA MBD measures from Philips (Sectra), Fuji,

and Siemens systems. The strengths of our work include the use of clinical images rather than phantoms for dose calculation as well as a large sample. Furthermore, the use of an automated MBD measurement software package (LIBRA) eliminates the variability associated with subjective human assessment. It does not, however, deal with heterogeneous glandular tissue distribution in the breast. Using a voxel phantom Dance et al[43] found that accounting for different glandular distributions in the breast could give up to 48% error in the conversion factors estimated using simple homogenous phantoms. He concluded, "For accurate breast dosimetry, it is therefore very important to take the distribution of glandular tissues into account". Therefore the MBD proposed in the current work, although not yet accounting for heterogeneity, is a reasonable alternative. Our work should provide a stepping-stone towards an individualised dose estimation using automated clinical measures of MBD.

CONCLUSION

The use of MGD underestimates dose from screening mammography compared to AGD. There are inconsistent differences between AGD and MGD at different CBTs, with larger differences seen in smaller breasts. This inconsistency may result in the underestimation of radiation risk during mammography for females with smaller CBTs.

REFERENCES

1. Glasziou P, Houssami N. The evidence base for breast cancer screening. *Prev Med* 2011; **53**: 100–2. doi: https://doi.org/10.1016/j.ypmed.2011.05.011
2. Lauby-Secretan B, Scoccianti C, Loomis D, Benbrahim-Tallaa L, Bouvard V, Bianchini F, et al. Breast-cancer screening--viewpoint of the IARC Working Group. *N Engl J Med* 2015; **372**: 2353–8. doi: https://doi.org/10.1056/NEJMsr1504363
3. Njor S, Nyström L, Moss S, Paci E, Broeders M, Segnan N, et al. Breast cancer mortality in mammographic screening in Europe: a review of incidence-based mortality studies. *J Med Screen* 2012; **19**(Suppl 1): 33–41. doi: https://doi.org/10.1258/jms.2012.012080
4. Beckett JR, Kotre CJ, Michaelson JS. Analysis of benefit:risk ratio and mortality reduction for the UK breast screening programme. *Br J Radiol* 2003; **76**: 309–20. doi: https://doi.org/10.1259/bjr/64009424
5. Jin J. JAMA patient page. Breast cancer screening: benefits and harms. *JAMA* 2014; **312**: 2585–85. doi: https://doi.org/10.1001/jama.2014.13195
6. Yaffe MJ, Mainprize JG. Risk of radiation-induced breast cancer from mammographic screening. *Radiology* 2011; **258**: 98–105. doi: https://doi.org/10.1148/radiol.10100655
7. Hendrick R, Bassett L, Botsco M, Deibel D, Feig S, Gray J. *Mammography quality control manual*. Reston, VA: American College of Radiology; 1999.
8. Boone JM, Fewell TR, Jennings RJ. Molybdenum, rhodium, and tungsten anode spectral models using interpolating polynomials with application to mammography. *Med Phys* 1997; **24**: 1863–74. doi: https://doi.org/10.1118/1.598100
9. Dance DR. Monte Carlo calculation of conversion factors for the estimation of mean glandular breast dose. *Phys Med Biol* 1990; **35**: 1211–20. doi: https://doi.org/10.1088/0031-9155/35/9/002
10. Wu X, Gingold EL, Barnes GT, Tucker DM. Normalized average glandular dose in molybdenum target-rhodium filter and rhodium target-rhodium filter mammography. *Radiology* 1994; **193**: 83–9. doi: https://doi.org/10.1148/radiology.193.1.8090926
11. Hammerstein GR, Miller DW, White DR, Masterson ME, Woodard HQ, Laughlin JS. Absorbed radiation dose in mammography. *Radiology* 1979; **130**: 485–91. doi: https://doi.org/10.1148/130.2.485
12. Dance DR, Skinner CL, Young KC, Beckett JR, Kotre CJ. Additional factors for the estimation of mean glandular breast dose using the UK mammography dosimetry protocol. *Phys Med Biol* 2000; **45**: 3225–40. doi: https://doi.org/10.1088/0031-9155/45/11/308
13. Dance DR, Young KC, van Engen RE. Further factors for the estimation of mean glandular dose using the United Kingdom, European and IAEA breast dosimetry protocols. *Phys Med Biol* 2009; **54**: 4361–72. doi: https://doi.org/10.1088/0031-9155/54/14/002
14. Sobol WT, Wu X. Parametrization of mammography normalized average glandular dose tables. *Med Phys* 1997; **24**: 547–54. doi: https://doi.org/10.1118/1.597937
15. Boone JM. Glandular breast dose for monoenergetic and high-energy X-ray beams: Monte Carlo assessment. *Radiology* 1999; **213**: 23–37. doi: https://doi.org/10.1148/radiology.213.1.r99oc3923
16. Boone JM. Normalized glandular dose (DgN) coefficients for arbitrary X-ray spectra in mammography: computer-fit values of Monte Carlo derived data. *Med Phys* 2002; **29**: 869–75. doi: https://doi.org/10.1118/1.1472499
17. McCormack VA, dos Santos Silva I. Breast density and parenchymal patterns as markers of breast cancer risk: a meta-analysis. *Cancer Epidemiol Biomarkers Prev* 2006; **15**: 1159–69. doi: https://doi.org/10.1158/1055-9965.EPI-06-0034
18. Yaffe MJ, Boone JM, Packard N, Alonzo-Proulx O, Huang SY, Peressotti CL, et al. The myth of the 50-50 breast. *Med Phys* 2009; **36**: 5437–43. doi: https://doi.org/10.1118/1.3250863
19. Yaffe MJ. Mammographic density. Measurement of mammographic density. *Breast Cancer Res* 2008; **10**: 209. doi: https://doi.org/10.1186/bcr2102
20. Dimri G, Band H, Band V. Mammary epithelial cell transformation: insights from cell culture and mouse models. *Breast Cancer Res* 2005; **7**: 171. doi: https://doi.org/10.1186/bcr1275
21. Ekpo EU, Hogg P, Highnam R, McEntee MF. Breast composition: measurement and clinical use. *Radiography* 2015; **21**: 324–33. doi: https://doi.org/10.1016/j.radi.2015.06.006
22. Ekpo EU, McEntee MF. Measurement of breast density with digital breast tomosynthesis--a systematic review. *Br J Radiol* 2014; **87**: 20140460. doi: https://doi.org/10.1259/bjr.20140460
23. Ekpo EU, Ujong UP, Mello-Thoms C, McEntee MF. Assessment of interradiologist agreement regarding mammographic breast density classification using the fifth edition of the BI-RADS atlas. *AJR Am J Roentgenol* 2016; **206**: 1119–23. doi: https://doi.org/10.2214/AJR.15.15049
24. Highnam R, Solutions V. *Patient-Specific Radiation Dose Estimation in Breast Cancer Screening*.

25. CBIGLIBRA. University of Pennsylvania: Section for Biomedical Image Analysis (SBIA) | Perelman School of Medicine at the University of Pennsylvania. 2017. Available from: http://www.med.upenn.edu/sbia/libra.html [cited 2017 27 October].
26. Yakami M. Japan: department of diagnostic imaging and nuclear medicine, Kyoto University. 2014YAKAMI DICOM Tools (Free DICOM Viewer/Converter/etc.). Available from: http://www.kuhp.kyoto-u.ac.jp/~diag_rad/intro/tech/dicom_tools.html [updated on 21 Jan 2014; cited 2015 20 February].
27. Keller BM, Nathan DL, Wang Y, Zheng Y, Gee JC, Conant EF, et al. Estimation of breast percent density in raw and processed full field digital mammography images via adaptive fuzzy c-means clustering and support vector machine segmentation. *Med Phys* 2012; **39**: 4903–17. doi: https://doi.org/10.1118/1.4736530
28. Keller B, Nathan D, Wang Y, Zheng Y, Gee J, Conant E, et al. Adaptive multi-cluster fuzzy C-means segmentation of breast parenchymal tissue in digital mammography. *Med Image Comput Comput Assist Interv* 2011; **14**(Pt 3): 562–9.
29. Suleiman ME, McEntee MF, Cartwright L, Diffey J, Brennan PC. Diagnostic reference levels for digital mammography in New South Wales. *J Med Imaging Radiat Oncol* 2017; **61**: 48–57. doi: https://doi.org/10.1111/1754-9485.12540
30. Myles PS, Cui J. Using the Bland-Altman method to measure agreement with repeated measures. *Br J Anaesth* 2007; **99**: 309–11. doi: https://doi.org/10.1093/bja/aem214
31. Olgar T, Kahn T, Gosch D. Average glandular dose in digital mammography and breast tomosynthesis. *Rofo* 2012; **184**: 911–8. doi: https://doi.org/10.1055/s-0032-1312877
32. Hill M. *Large variation in mammography compression internationally 2016*: European Congress of Radiology; 2017. http://dx.doi.org/10.1594/ecr2017/C-2133.
33. Perry N, Broeders M, De Wolf C, Törnberg S, Holland R, Von Karsa L. *European guidelines for quality assurance in breast cancer screening and diagnosis*. 4th Ed. Luxembourg: office for official publications of the European Communities; 2006.
34. M Ali RMK, England A, Mercer C, Tootell A, Walton L, Schaake W, et al. Mathematical modelling of radiation-induced cancer risk from breast screening by mammography. *Eur J Radiol* 2017; **96**: 98–103. doi: https://doi.org/10.1016/j.ejrad.2017.10.003
35. Baldwin J, Grantham V. Radiation Hormesis: Historical and Current Perspectives. *J Nucl Med Technol* 2015; **43**: 242–6. doi: https://doi.org/10.2967/jnmt.115.166074
36. Heyes GJ, Mill AJ, Charles MW. Mammography-oncogenecity at low doses. *J Radiol Prot* 2009; **29**: 2A: A123–A132. doi: https://doi.org/10.1088/0952-4746/29/2A/S08
37. Nguyen PK, Lee WH, Li YF, Hong WX, Hu S, Chan C, et al. Assessment of the radiation effects of cardiac CT angiography using protein and genetic biomarkers. *JACC Cardiovasc Imaging* 2015; **8**: 873–84. doi: https://doi.org/10.1016/j.jcmg.2015.04.016
38. Yue W, Yager JD, Wang JP, Jupe ER, Santen RJ. Estrogen receptor-dependent and independent mechanisms of breast cancer carcinogenesis. *Steroids* 2013; **78**: 161–70. doi: https://doi.org/10.1016/j.steroids.2012.11.001
39. Pijpe A, Andrieu N, Easton DF, Kesminiene A, Cardis E, Noguès C, et al. Exposure to diagnostic radiation and risk of breast cancer among carriers of BRCA1/2 mutations: retrospective cohort study (GENE-RAD-RISK). *BMJ* 2012; **345**: e5660. doi: https://doi.org/10.1136/bmj.e5660
40. Antoniou A, Pharoah PD, Narod S, Risch HA, Eyfjord JE, Hopper JL, et al. Average risks of breast and ovarian cancer associated with BRCA1 or BRCA2 mutations detected in case Series unselected for family history: a combined analysis of 22 studies. *Am J Hum Genet* 2003; **72**: 1117–30. doi: https://doi.org/10.1086/375033
41. Mathews JD, Forsythe AV, Brady Z, Butler MW, Goergen SK, Byrnes GB, et al. Cancer risk in 680,000 people exposed to computed tomography scans in childhood or adolescence: data linkage study of 11 million Australians. *BMJ* 2013; **346**: f2360. doi: https://doi.org/10.1136/bmj.f2360
42. Jeggo P. The role of the DNA damage response mechanisms after low-dose radiation exposure and a consideration of potentially sensitive individuals. *Radiat Res* 2010; **174**: 825–32. doi: https://doi.org/10.1667/RR1844.1
43. Dance DR, Hunt RA, Bakic PR, Maidment AD, Sandborg M, Ullman G, et al. Breast dosimetry using high-resolution voxel phantoms. *Radiat Prot Dosimetry* 2005; **114**: 1-3: 359–63. doi: https://doi.org/10.1093/rpd/nch510

Subject: Re: Copy right permission
Date: Thursday, 7 June 2018 at 4:50:56 am Australian Eastern Standard Time
From: Ralph Highnam
To: Mo'ayyad Suleiman
CC: Ernest Usang Ekpo, Mark McEntee
Attachments: Outlook-nq00430y.png

All good.

--
Ralph P. Highnam, PhD.
Chief Executive Officer
ralph.highnam@volparasolutions.com
Phone: +64-21-149-0541

volparasolutions™

Breast Imaging Analytics
www.volparasolutions.com

Follow us: Facebook Twitter LinkedIn

From: Mo'ayyad Suleiman <moe.suleiman@sydney.edu.au>
Sent: Thursday, 7 June 2018 1:34:25 AM
To: Ralph Highnam
Cc: Ernest Usang Ekpo; Mark McEntee
Subject: Copy right permission

Dear Ralph,
Hope this email finds you well.
I wish to ask your permission to use Figure 3. “Illustration of how breast density can be under- or over-estimated by visual/area-based approaches. “ from your paper titled: Breast composition: Measurement and clinical use.
You are a co-author with Ernest, Peter and Mark, however Mark told me that the figure is originally yours and that I should seek your permission to use it in my thesis.
I trust you will give me your careful consideration, thank you for your time.

Best regards,
Moe

Mo’ayyad E. Suleiman | Postdoc
MSc. IT, BSc. Applied Physics
BreastScreen Reader Assessment Strategy (BREAST)
Discipline of Medical Radiation Sciences
Faculty of Health Sciences

THE UNIVERSITY OF SYDNEY
M513 Cumberland Campus | 75 East St Lidcombe | NSW2141
T +61 2 9351 9465 | **M** +61 405033029

of individual, can never be long injurious to the cause of truth. It may, at a particular time, retard its progress for a while, but it repays the transitory injury by a benefit as permanent as the duration of the truth to which it is opposed!”*

Babbage, Bridgewater treatise, 1837, p28